A STUDY OF DIVIDING STEAM-WATER FLOW IN T-JUNCTIONS: EXPERIMENTS AND ANALYSES

By

Fei Peng, M.Eng.

A Thesis

Submitted to the School of Graduate Studies

in Partial Fulfilment of the Requirements

for the Degree

Doctor of Philosophy

McMaster University

Hamilton, Ontario, Canada

A STUDY OF DIVIDING STEAM-WATER FLOW IN T-JUNCTIONS: EXPERIMENTS AND ANALYSES

DOCTOR OF PHILOSOPHY (1994) McMASTER UNIVERSITY

(Mechanical Engineering) Hamilton, Ontario, Canada

TITLE: A Study of Dividing Steam-Water Flow In T-Junctions: Experiments and Analyses

AUTHOR: Fei Peng, M.Eng.

SUPERVISOR: Dr. M. Shoukri

NUMBER OF PAGES: xxi, 235

ABSTRACT

Phase redistribution is a complicated physical phenomenon which occurs in dividing two-phase flow in T-junctions. In this study detailed experimental data of phase redistribution and associated pressure changes in T-junctions having horizontal inlet are presented for both annular and stratified inlet flows. Two phenomenological phase redistribution models for annular and stratified flows were developed. The objectives of the study are enriching the available data bank on the subject through the experimental measurements and enhancing current understanding of the phenomenon through model development and analysis.

Two-phase redistribution in T-junctions was found to be significantly affected by the inlet flow conditions, i.e. inlet flow pattern, inlet quality and inlet flow rates. The phase redistribution phenomenon also depends on the junction geometry, i.e. branch orientation and diameter. The experimental results showed that for annular flow in horizontal T-junctions an increase of inlet quality reduces the degree of phase redistribution while the inlet mass flux was found to be less significant. However, in stratified flow the increase of either the inlet superficial vapour or liquid velocities increases the degree of phase separation. The experimental results also showed that decreasing the branch diameter will increase the degree of phase separation. Moreover, downward orientation of the branch can reduce the branch flow quality significantly.

The pressure changes in T-junctions were correlated using simple momentum and energy balances for the run and branch respectively using measured void fractions. The run momentum correction factor was found to be independent of inlet flow conditions but was dependent on the junction geometry. The branch two-phase multiplier was found to depend on both the inlet flow conditions and junction geometry. Comparison of the present data on pressure changes in T-junctions with some available models showed that those models which account for phase redistribution effects were better than the others in correlating the present data, confirming the strong interdependence between the pressure changes and phase redistribution.

A general phenomenological phase redistribution model was derived based on the analysis of available models. This general model was extended to two phenomenological models for annular flow and stratified inlet flows. Each of the models included two sub-models to account for two phase distribution in the inlet tube and phase redistribution in the junction. Comparisons of the present experimental data and some available models were made and the results indicate that most of the available models can predict 70% of annular flow data and 80% of stratified flow data within $\pm 40\%$ of the measurements. The newly developed models in this study can predict 90% of the data within $\pm 40\%$ for both annular and stratified flows.

ACKNOWLEDGEMENTS

I would like to express my sincere appreciation to Dr. M. Shoukri for providing the opportunity of this study and for his continuous encouragement and interest throughout the phases of this research. I would also like to thank Drs. A.M.C. Chan, J.S. Chang and G.F. Round for serving on my supervisory committee and for their encouragement and constructive criticism.

Many thanks to the technical staff of Department of Mechanical Engineering; R. Lodewyks, D. Shick and J. Verhaeghe for their fruitful advices and assistance on technical issues. I am indebted to B. Diacon, from the Department of Engineering Physics, for the loan of the ultrasonic instrument and valuable discussions on the measurements.

I am grateful for the financial support provided by the Natural Sciences and Engineering Research Council of Canada through the research and graduate scholarship programs.

Finally I would like to acknowledge my wife Lien for her encouragement and understanding over the years and my son Frank for his sacrificing the time which belongs to him. Without their love and patience this work could have never been completed.

TABLE OF CONTENTS

NOMENCLATURE

A	area	[m^2]
c	sound velocity	[m/s]
C	empirical coefficient	
D	pipe diameter	[m]
DLX	run development length	[m]
DLY	branch development length	[m]
E	entrainment fraction of liquid	
g	gravitational acceleration	[m/s^2]
G	mass flux	[$kg/m^2.s$]
h	liquid film thickness, enthalpy	[m], [kJ/kg]
H	dimensionless liquid height	
k	turbulent kinetic energy	[N.m/kg]
K	empirical coefficient	
$\dot{m}$	mass flow rate	[kg/s]
M	mass flux of liquid droplet	[$kg/m^2.s$]
N	photon count of gamma densitometer	[count/s]
P	pressure	[kPa]
ΔP	pressure drop	[kPa]

R, r	radius	[m]
s	slip ratio, perimeter	[m]
T	temperature	[°c]
u	velocity in x direction	[m/s]
v	velocity in y direction	[m/s]
W	liquid film velocity	[m/s]
x	thermodynamic quality	
X	Martinelli parameter	

Greek Symbols

α	void fraction	
β	branch orientation angle	
Γ	circumferential flow rate per length	[kg/m.s]
ϵ	eddy diffusivity	[m^2/s]
ϵ	dissipation rate of turbulent kinetic energy	[N.m/kg.s]
δ	location of dividing streamline	[m]
θ	angle of liquid film distribution	[rad]
μ	dynamic viscosity	[$N.s/m^2$]
ν	kinematic viscosity	[m^2/s]
ρ	density	[kg/m^3

σ	surface tension, turbulent Plandtl number	[N/m]
τ	shear stress	[N/m^2]
Φ	two-phase multiplier	

Subscripts

1	inlet
2	run
3	branch
b	branch
c	condensate
cw	cooling water
d	deposition
e	energy weighted, entrainment
f	liquid film
g	vapour phase
gs	superficial gas
h	homogeneous flow
i	inlet, interface
irr	irreversible component
L	liquid phase

Ls	superficial liquid
m	momentum weighted, mixer
o	outlet
r	run
rev	reversible component
s	separated flow
t	test section
tp	two-phase flow
tt	turbulent-turbulent
w	tube wall

LIST OF FIGURES

LIST OF TABLES

CHAPTER 1

INTRODUCTION

T-junctions are commonly used components in piping systems. The behaviour of dividing two-phase flow in a T-junction is critical in the design of two-phase flow piping systems. When two-phase flow is divided in T-junctions, the branch and run qualities will, in general, differ from the inlet quality due to the significant difference of the axial momentum fluxes of the two phases. This phenomenon of phase redistribution has profound effect on system operation downstream of the junction. The knowledge of phase redistribution and associated pressure changes in T-junctions is of primary importance in many industrial applications. Examples are gas network distribution systems, where condensation takes place, oil production systems when steam injection is used for enhanced oil recovery and nuclear power stations in connection with the loss of coolant accident (LOCA).

Due to the large number of flow and geometrical parameters involved in the process, both the available experimental data bank and analytical models are incomplete. Driven by this point, the objectives of the present research are: (i) to obtain experimental data at ranges of test conditions not examined before to complement the available data bank and, (ii) to develop phenomenological phase redistribution models to enhance the current understanding of the physical phenomenon and provide tools for predicting this

phenomenon.

In Chapter 2, a critical literature review is presented. The effects of inlet flow conditions and junction geometry are surveyed and summarized. The available models for phase redistribution and pressure changes are discussed as well. Chapter 3 deals with the experimental facilities and experimental uncertainties. The experimental data for annular flow is presented in Chapter 4. The effect of branch orientation under annular inlet flow conditions is discussed in detail. In Chapter 5 the experimental data on stratified flow is presented. The effects of inlet flow conditions, branch diameter and orientation, and system pressure are analyzed. Chapter 6 is devoted to the model development. A general phase redistribution model is derived based on the analysis of available models. This general model is then further developed to obtain two phenomenological models for annular and stratified flows. Finally the predictions of the newly developed models and some available models are compared with experimental data. In Chapter 7, the main findings and conclusions from this study and the recommendations for future research are discussed.

CHAPTER 2

LITERATURE REVIEW

Prior to commencing the following literature review we first define the terminology conventions used throughout the thesis. Fig.2.1 shows schematically the relevant flow and geometrical parameters involved in the process of dividing two-phase flow in a T-junction with horizontal inlet. These are the mass fluxes and qualities in the inlet, run and branch (G_1, G_2, G_3, x_1, x_2, and x_3), the diameters of the inlet, run and branch (D_1, D_2, and D_3) and the branch orientation θ. To be consistent with the literature, subscripts 1, 2 and 3 refer to the inlet, run and branch respectively.

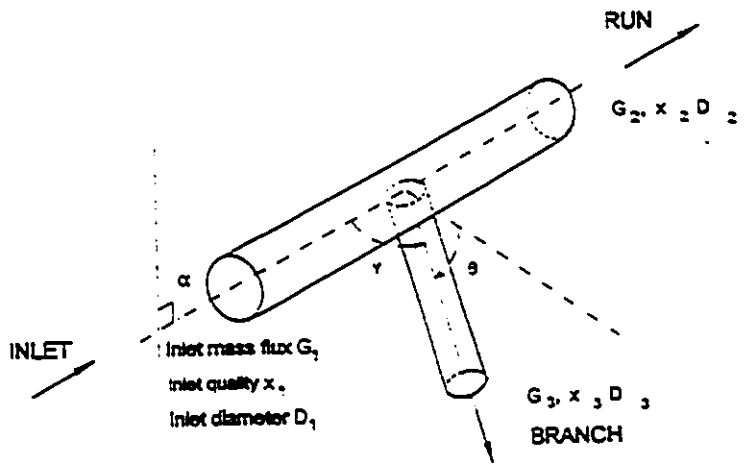

Fig.2.1 Flow and geometrical parameters of a T-junction

Fig.2.2 shows an approach to present phase redistribution data. The extent of phase redistribution is represented by the branch to inlet flow quality ratio x_3/x_1 which is plotted against branch flow split ratio $\dot{m}_3/\dot{m}_1$. The experimental data will fall in the range of ABCDEF. The limiting case of only liquid entering branch, i.e. $x_3=0$, is represented by the horizontal line AF. Line BE represents an even phase distribution, i.e. $x_3=x_1$, and line CD represents gas only extracted to the branch or $x_3=1$. At point D all the gas phase in the inlet is extracted to the branch. Starting at point D is another limiting case of total gas extraction represented by the curve DE, i.e. $x_3/x_1=\dot{m}_1/\dot{m}_3$. At point E ($\dot{m}_3/\dot{m}_1=1.0$) the quality ratio x_3/x_1 reduces to 1.0.

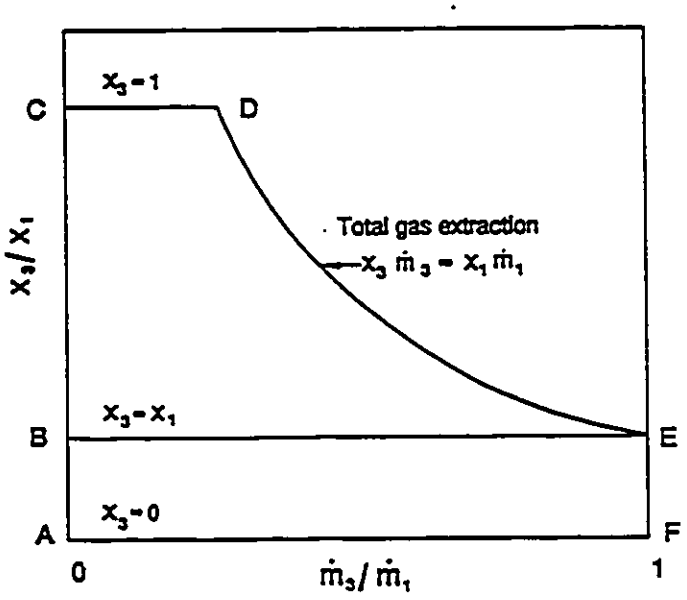

Fig.2.2 The method to present phase separation data x_3/x_1 vs. $\dot{m}_3/\dot{m}_1$

Another approach to present the phase redistribution data, whereby the fraction

of gas removed through the branch F_{BG}, i.e. $\dot{m}_3x_3/\dot{m}_1x_1$, is plotted against the fraction of liquid removed F_{BL}, i.e. $\dot{m}_3(1-x_3)/\dot{m}_1(1-x_1)$, is shown in Fig.2.3 with corresponding points ABCDEF. The limiting cases of liquid or gas only entering the branch (line AF or CD) is represented by $F_{BG}=0$ or $F_{BL}=0$. Total gas extraction DE corresponds to $F_{BG}=1.0$, while the conditions of even phase separation $x_3=x_1$ are represented by diagonal BE.

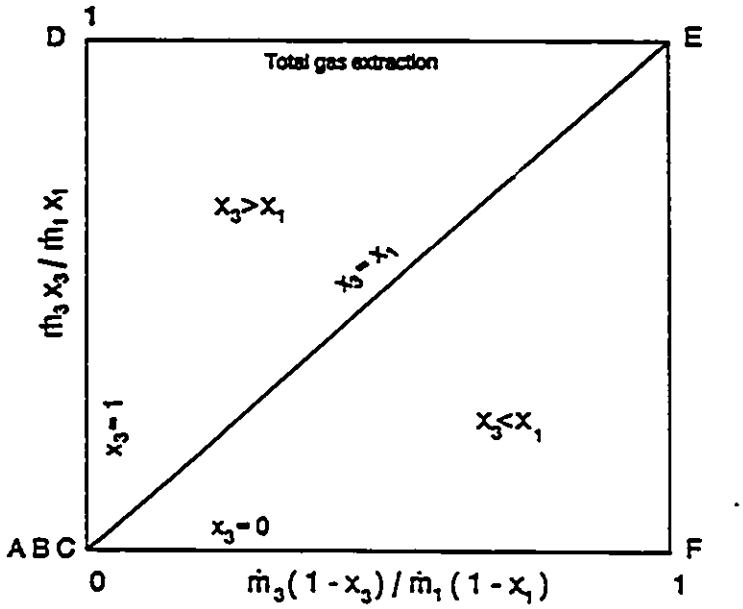

Fig.2.3 The method to present phase separation data F_{BG} vs. F_{BL}

The term "pressure changes" refers to the pseudo axial pressure rise $\Delta P_{2\text{-}1}$ and branch pressure drop $\Delta P_{1\text{-}3}$ in the T-junction. The frictional effect of these pressure changes is isolated by extrapolating the fully developed pressure profiles in each leg to the centre of the junction as shown in Fig.2.4.

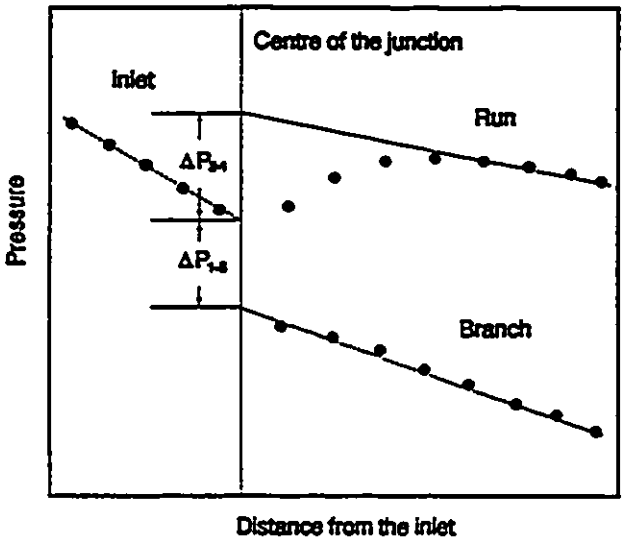

Fig.2.4 Method to present pressure changes

2.1. Experiments on Phase Redistribution

Due to the importance of dividing two-phase flow in piping junctions, tremendous efforts have been devoted to experimental studies on the subject. Dividing two-phase flow in a T-junction with a horizontal main inlet tube is a more complex phenomenon than that with a vertical main inlet. The difficulty arises from the effect of gravity, causing asymmetric distribution of the phases in the inlet tube. The following review focuses on the experimental works on T-junctions with horizontal main inlet tube. Previous research

evidence has shown that the phase redistribution phenomenon and associated pressure changes in T-junctions are extremely complicated, and are affected by inlet flow parameters, fluid properties and junction geometry. Due to the large number of variables involved in the process, study of the effect of each parameter was usually obtained by isolating the effects of other parameters. The following literature review surveys the parametric trends of available data and a brief summary is given based on the survey for the effect of each parameter.

2.1.1. Studies on the effect of inlet flow parameters

Collier (1976) presented air-water flow data in a 37.6 mm diameter inlet T-junction with a horizontal 25.4 mm diameter branch. The mass flux was fixed at 136 $kg/m^2.s$ and the inlet quality varied between 0.021 and 0.5, which led to both stratified and annular flow in the inlet tube. The majority of his data showed that gas was preferentially extracted into the branch. The effect of inlet quality on phase redistribution appeared in a complex manner. The level of phase redistribution x_3/x_1 first increased with increasing inlet quality when $x_1 < 0.25$ and then decreased as the inlet quality increased above 0.25. This reversed trend is probably caused by the effect of flow regime transition from stratified to annular flow. Therefore Collier's data not only showed the influence of inlet quality but also indicated the effect of inlet flow regime on two-phase redistribution.

Henry (1981) performed air-water experiments in a T-junction having a 100 mm diameter inlet and a 20 mm diameter branch. The inlet conditions covered mass flux range of $200 < G_1 < 850$ kg/m^2.s and quality range of $0.1 < x_1 < 0.6$, which gave rise to annular flow. The data only covered a limited range of branch flow split ratio, $G_3/G_1 < 0.06$. His measurements indicated that at a fixed inlet quality, the branch quality x_3 increases with increasing branch flow split ratio and eventually reaches a plateau. The data also indicated that an even phase distribution was more likely to occur at high inlet mass fluxes. A low mass flux, on the other hand, resulted in severe maldistribution of the two phases. The data exhibited similar trends to those presented by Collier (1976).

Saba and Lahey (1984) presented air-water data of both phase redistribution and pressure changes in a horizontal T-junction with $D_1=D_2=D_3=38$ mm. Three mass fluxes were used 1353, 2041 and 2711 kg/m^2.s. The inlet quality was less than 0.01, which led to bubbly flow and slug flow in the inlet tube. It was found that even for these low inlet qualities the degree of phase redistribution was quite pronounced with the gas phase preferentially separating into the branch. In their test conditions they also found that the inlet mass flux had little effect on phase redistribution.

Seeger et al. (1986) published a detailed study on phase redistribution and pressure changes for air-water and steam-water flows in dividing T-junctions with different branch orientations. The experiments were performed in a 50 mm equal diameter T-junction with horizontal, upward and downward branches. The inlet mass flux and quality covered wide ranges; $500 < G_1 < 7500$ kg/m^2.s and $0.002 < x_1 < 0.33$, which

led to the observation of bubbly, slug and annular flow. With a horizontal branch, they found that the degree of phase redistribution x_3/x_1 increased rapidly with increasing branch flow split ratio, peaking near the flow split ratio $G_3/G_1 = 0.3$, after which total phase separation occurred. The data also indicated that for a fixed inlet superficial liquid velocity, x_3/x_1 decreased as the inlet superficial gas velocity increased. This trend was consistent with the observations of Collier (1976) and Henry (1981) in the annular flow regime.

Shoham et al. (1987) performed air-water experiments in a 51 mm diameter T-junction. The data were collected at fixed inlet superficial gas velocities of 2.5, 6.1 and 26 m/s, while superficial liquid velocity varied from 0.0029 to 0.059 m/s for each gas velocity, thus giving rise to stratified and annular flow. In stratified flow they found that, in all conditions tested, at very low branch flow split no liquid flowed into the branch. The liquid phase was extracted into the branch only after a higher portion of gas was diverted into the branch. This phenomenon was not reported in previous research. The data also showed that with an increase of inlet superficial liquid velocity, the fraction of liquid extracted into the branch decreased, indicating an increase in the degree of phase separation. This was consistent with the data trend of Collier (1976) at $x_1 < 0.25$. In most of the experiments relating to annular flow they observed that the liquid phase tended to be extracted preferentially into the branch at low extraction rate. Furthermore, the annular data showed that, when the inlet superficial liquid velocity increased, the liquid fraction in the branch decreased or the extent of phase separation x_3/x_1 increased.

Ballyk et al. (1988) studied steam-water annular flow phase redistribution and pressure changes in a 25 mm diameter horizontal T-junction. These experiments were particularly interesting since the measurements included the void fraction profiles in the three legs of the junction, and the data were collected at a higher range of inlet mass flux $450 < G_1 < 1200$ kg/m^2.s, not previously tested. The inlet quality covered the range of $0.02 < x_1 < 0.15$. They reported that the branch quality was higher than inlet quality over most of the flow split range, and only at low flow split was the branch quality less than that of the inlet. The maximum value of x_3/x_1 occurred at branch flow split ratio around 0.2. It is interesting to note that this result differs from that of Shoham et al. (1987) in which liquid tended to be extracted preferentially into the branch for most of the test conditions. These different trends are probably caused by the large difference of inlet mass flux used by the different authors (2.9 to 59 kg/m^2.s by Shoham et al. and 450 to 1200 kg/m^2.s by Ballyk et al.). Higher inlet liquid velocity increases the axial momentum flux of the liquid phase, and furthermore, generates higher entrainment of liquid droplets which have the largest momentum flux and the largest resistance to being diverted to the branch. The data of Ballyk et al. (1988) also showed that an increase in inlet quality resulted in reducing the peak and the degree of the phase separation, x_3/x_1, and increasing the flow split ratio G_3/G_1 at which complete vapour extraction took place. The inlet mass flux, however, was found to have little effect on phase redistribution under their test conditions.

Rubel et al. (1988) performed steam-water experiments in a 37.6 mm equal

diameter T-junction. The inlet mass flux and quality covered the ranges: $16.1 < G_1 < 50.3$ kg/m^2.s and $0.21 < x_1 < 0.87$ respectively, which resulted mostly in stratified, stratified wavy and semi-annular flow regime. Their data showed that the inlet mass flux did not have significant effect on the phase redistribution. However, when the inlet quality x_1 increased the degree of phase separation x_3/x_1 decreased in the semi-annular flow and increased in stratified flow. These results are consistent with the observation of Collier (1976). This indicates the complexity of dividing two-phase flow in the junction and also that the parametric trend could be totally reversed depending on the inlet flow pattern.

Reimann et al. (1988) presented detailed air-water results which complemented Seeger et al.'s data (1986). The data were collected in T-junctions having 50 mm inlet diameter with different branch diameters and orientations. The experiments covered a wide range of inlet superficial gas and liquid velocities, $1 < u_{gs} < 40$ m/s and $0.05 < u_{Ls} < 6.0$ m/s respectively. The unique feature of this study is that the data was collected in a high pressure system, where most of the system pressures were between 0.4 to 0.8 MPa. In equal diameter T-junction, the data showed that the quality ratio x_3/x_1 was very close to unity at low inlet mass flux conditions, indicating even phase redistribution in the junction. With increased inlet superficial gas velocity u_{gs} the degree of phase redistribution x_3/x_1 decreased slightly, but the effect was insignificant. The flow patterns were not reported in these tests since it was not visually observed in the experiments.

Azzopardi et al. (1988) reported data on air-water in annular, wavy and stratified

flows in a 38 mm diameter T-junction. The ranges of inlet mass flux and quality were: $30 < G_1 < 145$ kg/m^2.s and $0.05 < x_1 < 0.90$ respectively. The data showed that an increase of inlet liquid flow rate increased branch quality x_3 in both stratified and annular flows. The data also indicated that an increase of the inlet gas flow rate in annular flow resulted in decreasing x_3/x_1, while in stratified flow resulted in increasing x_3/x_1. The parametric trends were in agreement with other researchers, e.g. Collier (1976), Ballyk et al. (1988) and Rubel et al. (1988).

Buell et al. (1993) reported their air-water data of phase redistribution and pressure changes in a 37.6 mm T-junction. Inlet superficial gas and liquid velocities covered the ranges of $2 < u_{gs} < 40$ m/s and $0.002 < u_{Ls} < 0.2$ m/s respectively, which led to observation of stratified, wavy, annular and slug flows. In the annular flow regime at fixed superficial gas velocity u_{gs}=40 m/s, an increase of superficial liquid velocity resulted in increasing branch quality x_3, which was consistent with the observation of Azzopardi et al. (1988). However, the effect of inlet superficial gas velocity was flow regime dependent. In slug flow at fixed u_{Ls}=0.18 m/s, the effect was insignificant. In stratified flow at low liquid velocity u_{Ls}=0.0021 m/s, an increase of u_{gs} decreased branch quality, while at u_{Ls}=0.04 m/s increasing u_{gs} increased branch quality and then the trend was reversed as the inlet gas flow rate was continuously increased. This change of the data trend is probably due to the flow regime transition from stratified flow to annular flow.

The above survey of parametric trends indicates that the inlet flow rate and phase

distribution, i.e. flow regime in the inlet tube, have significant effect on phase redistribution in the junction. The trends pertinent to the effect of inlet flow rate and quality are dependent on inlet flow regime. Even in the same inlet flow regime, varying the flow velocities, can change the parametric trends totally, e.g. in annular flow, an increase of inlet liquid flow rate may increase the extent of phase separation in low inlet mass flux flow but decrease it in high mass flux flow. Distribution of the two phases in the main inlet tube, e.g. the liquid level in stratified flow, the entrainment of liquid droplet and asymmetrical distribution of liquid film in annular flow, are no doubt directly correlated with the phase redistribution in the downstream junction. However, phase distribution in the inlet tube was not measured in the previous studies. A variation of inlet flow rates may change inlet flow regimes and the distribution of the two phases, and consequently affect the phase redistribution in the junction.

2.1.2. Studies on the effect of branch diameter

Azzopardi and Whalley (1982) studied the effect of branch diameter on phase separation in a 32 mm main inlet T-junction with branch diameters of 6.35, 12.7 and 19 mm, giving branch-to-inlet diameter ratios of 0.2, 0.4 and 0.6 respectively. Azzopardi (1984) extended the study to the diameter ratio of 0.8 and 1.0. The experiments were performed at $G_1 = 152$ kg/m^2.s and $x_1 = 0.56$. The results indicated a systematic influence of branch diameter on phase redistribution although the trend was not always clear at

lower inlet mass flux conditions. It was found that the smaller the branch diameter the higher the quality ratio x_3/x_1. Azzopardi et al. (1988) extended the study to stratified flow and obtained the same parametric trend.

Shoham et al. (1989) performed experiments on a T-junction with a branch-to-inlet diameter ratio of 0.5 and compared the data with their previous study with a diameter ratio of 1.0 (1987). The measurements implied that under stratified flow condition much less liquid was extracted in the reduced size branch than in a regular T-junction at the same inlet flow conditions. This influence is more significant for higher liquid flow rate tests. The effect of branch diameter in annular flow, however, was not significant under their test conditions, which supported the observation of Azzopardi (1984).

Ballyk et al. (1987) examined the effect of branch-to-inlet diameter ratio in annular flow with inlet diameter of 25 mm and branch diameter of 12.5 mm, giving the diameter ratio of 0.5, and extended the work to the diameter ratio of 0.82 (Ballyk, 1992). He showed a clear trend that the smaller branch experienced more severe phase maldistribution. It was also shown that the flow split ratio, at which complete vapour extraction occurred, was reduced in a smaller size branch junction. Ballyk also found that the degree of maldistribution associated with the smaller branch size appeared to be higher than that of other reports. The reason for the larger influence of branch size was probably contributed by the high inlet mass flux used.

Reimann et al. (1988) studied the effect of branch diameters by using various

branch-to-inlet diameter ratios of 1.0, 0.52, 0.2 and 0.08 under high system pressures. The data showed that in slug flow, the flow quality ratio x_3/x_1 increased when the diameter ratio d_3/d_1 decreased at the same inlet flow conditions, but this data trend was reversed when very small branch diameter was used.

In general, a smaller size branch experiences a more severe phase maldistribution in the junction, however, the extent of this influence greatly depends upon the inlet flow conditions i.e. mass flux, quality and flow regime.

2.1.3. Studies on the effect of branch orientation

Hong (1978) performed air-water experiments in a T-junction of equal diameters (9.5 mm). The main pipe was horizontal while the branch was oriented vertically upwards, horizontally and vertically downwards. His data were obtained at the inlet conditions of $15 < G_1 < 80$ kg/m^2.s and $0.25 < x_1 < 0.97$, which led to observation of stratified wavy and annular flows. Hong reported that as the branch position varied from top to bottom of the main tube, the amount of liquid in branch increased significantly.

Azzopardi and Whalley (1982) studied the effect of branch orientation in a T-junction with branch-to-inlet diameter ratio of 0.4 (12.7 mm/32 mm). The inlet condition was $G_1 = 156$ kg/m^2.s and $x_1 = 0.56$, thus generating annular flow in the inlet tube. Their results showed the same trend observed by Hong (1978), i.e. the branch quality x_3 decreased dramatically in junctions with the downwardly orientated branch.

Seeger et al. (1986) examined the effect of branch orientation on phase redistribution in slug and bubbly flow using upward, horizontal and downward orientated branches. Compared with the horizontal branch T-junction, it was observed that more gas was extracted into the upward branch and more water was extracted into the downward branch.

Reimann et al. (1988) tested the influence of branch orientation on T-junctions with branch-to-inlet diameter ratios of 1.0, 0.52, 0.2 and 0.08. The data from this large data bank supported the general trend of the effect of branch orientation. Due to the effect of gravity, water was scarcely diverted into an upward branch and was easily extracted into a downward branch.

In relation to the asymmetrical distribution of the two phases in horizontal inlet tubes, the orientation of the branch has significant effect on phase redistribution in the T-junction. However, the inlet phase distributions depend on the flow conditions, e.g. in high inlet flow rate annular flow the liquid film becomes more uniform, and therefore, gravity has less effect on phase redistribution.

2.1.4. Studies on the effect of fluid properties

Hong (1978) studied the effect of liquid viscosity on phase redistribution. Liquid viscosities of 1 centipoise for water, and 5 and 10 centipoise for water plus hydroxyethyl cellulose were tested. The degree of phase redistribution x_3/x_1 was found to decreased

as liquid viscosity increased.

Seeger et al. (1986) examined the effect of system pressure on phase redistribution in slug flow. They varied the system pressure in a wide range from 0.7 to 10 MPa and used the same horizontal T-junction with equal diameter for both air-water and steam-water flows. Under their test conditions, the effect of system pressure was insignificant.

Reimann et al. (1988) compared their high pressure data with Hong (1978) and Shoham et al. (1987) low pressure data at the same inlet flow and geometry conditions. The results showed that the value of phase redistribution x_3/x_1 was generally higher in low system pressure tests.

The effect of fluid properties on phase redistribution in a T-junction has not been addressed adequately by previous researchers owing to the difficulty of performing the experiments and the complexity of the required test facility. The changing of system pressure will significantly vary the density of the vapour phase, and accordingly change the vapour axial momentum flux. An increase of system pressure will increase vapour density and hence increase vapour axial momentum flux. As a result, it is expected to reduce the degree of phase redistribution.

2.1.5. Summary of the experiments on phase redistribution in T-junctions

Dividing two-phase flow in a horizontal piping junction is a complex physical phenomenon and significant experimental efforts have been devoted on the subject over

the past two decades. A summary of available experimental data for two-phase flow in T-junctions with horizontal inlet is given in Table 2.1. Previous experimental results have revealed that phase redistribution in the junction is influenced by inlet flow and junction geometrical parameters. Inlet flow conditions have been tested by many researchers but, due to the complexity of the problem and the limited data base, the phenomenon is still poorly understood. The parametric trends were found to be dependent on the inlet flow regime. This is attributed to the inlet phase distribution and the variation of this distribution due to the change of inlet flow conditions. Even in the same flow regime, e.g. annular flow, the parametric trends may change depending on the film thickness distribution and the amount of liquid entrainment in the gas core. The characteristic parameters of inlet flow pattern, i.e. asymmetric liquid film thickness and entrainment fraction in annular flow and liquid level in stratified flow directly affect two phase redistribution in the downstream junction. Unfortunately these important characteristic parameters were not included in previous measurements of phase redistribution.

The effects of junction geometry has been studied by few researchers and the data base available is very small. More detailed investigations on a variety of junction geometries is needed to enhance the understanding of the phenomenon.

It should be also noted that although available results show the strong interrelationship between phase redistribution, pressure changes and phase concentration in the legs of the junction, most of the reported experiments did not include measurement of void fraction and some did not include the pressure distribution in the junction, see

Table 2.1. Lack of such measurements may reduce the effectiveness of these data as basis for model development.

2.2. Phase Redistribution Models

Dividing two-phase flow in piping junctions is a complex physical phenomenon by virtue of the large number of variables involved in the process. Three approaches have been used by previous researchers to model phase redistribution in T-junctions. They are: (1) complete empirical correlations e.g. Henry (1981), Seeger et al. (1986), (2) phenomenological analysis e.g. Azzopardi and Whalley (1982), Shoham et al. (1987), Hwang et al. (1988), Ballyk and Shoukri (1990), McCreery and Banerjee (1990) and Lemonnier and Hervieu (1991), (3) two-fluid numerical simulations e.g. Lahey (1990) and Issa and Oliveira (1991). The current state-of-the-art is far from obtaining an accurate prediction of two-phase redistribution phenomenon in T-junctions. No model is available with general applicability to varied inlet flow regimes and junction geometries.

2.2.1. Empirical correlations

Henry (1981) developed an empirical correlation for predicting branch flow quality. The correlation generated was based on the flow conditions of $200 < G_1 < 850$ kg/m^2.s and $0.04 < x_1 < 0.5$, but the branch flow split G_3/G_1 was smaller than 0.06. This

Table 2.1 Important experiments on T-junction with horizontal inlet

Authors	G_i kg/m².s	x_i %	G_2/G_1	D_i mm	P_i bar	Inlet Flow Regime	Pressure measurement	Void fraction measurement
Collier, 1976	136	2-50	0-0.95	38	2.5	annular, stratified	no	no
Hong, 1978	2.3-47	0.25-1.0	0-1	9.5	1.5	annular, stratified	no	no
Henry, 1981	200-850	10-60	0-0.06	100	1.5	annular	no	no
Azzopardi & Whalley, 1982	152	56	0-1	32	2.5	annular	no	no
Saba & Lahey, 1984	1350-2700	0.3-0.7	0.3-0.7	38	1.0	intermittent	yes	no
Seeger et al. 1986	500-7500	0.2-35	0-1	50	4.0-10	annular, intermittent, dispersed bubble	yes	no
Katsaounis et al., 1987	30-1700	0-0.16	0-1	45, 203	1.5	intermittent, stratified	no	no
Shoham et al. [...] 1989	19-230	22-98	0-1	51	3.0	annular, stratified	no	no
Hwang & Lahey, 1987	1350-2700	0.2-0.4	0-0.35	38	1.5	intermittent	yes	no
Ballyk et al. 1988, 1992	400-1200	2-15	0-1	26	0.1-1.5	annular	yes	yes
Reimann et al. 1988	50-6130	0.4-77	0-1	50	4.0-10	annular, stratified, intermittent, dispersed bubble	yes	no
Rebel et al. 1988	15-50	20-90	0.15-0.8	38	1.0-2.5	annular, stratified	no	no
Azzopardi et al. 1988, 1992	30-145	5-90	0-1	38	1.5-3.0	annular, stratified	no	no
Buel et al 1993	5-200	1-96	0-1	38	1.5	annular, stratified, intermittent	yes	no

empirical model was reported to predict the data of Henry (1981) and Collier (1976) quite well in the annular flow regime but was less successful in predicting the data in the stratified wavy flow regime. Due to the limited data base used this empirical correlation has not been examined by other researchers.

Seeger et al. (1986) developed several empirical correlations based on a large data bank covering the ranges of $500 < G_1 < 7500$ kg/m^2.s, $0.002 < X_1 < 0.33$, $0.1 < P_1 < 10$ MPa. They recommended empirical correlations for different branch orientations, i.e. horizontal, vertically upward and vertically downward.

For horizontal branch T-junction:

$$\frac{x_3}{x_1} = 5\eta - 6\eta^2 + 2\eta^3 + a\eta(1-\eta)^b \tag{2.1}$$

$$\eta = \frac{G_3}{G_1} \tag{2.2}$$

$$b = 4 \tag{2.3}$$

for bubbly flow $$a = 14.6 \tag{2.4}$$

for other flow $$a = 13.9[(\frac{\rho_g}{\rho_L} S_1^2)^{-0.26} - 1] \tag{2.5}$$

$$S_1 = \frac{\rho_L}{1-x_1}[\frac{1+0.12(1-x_1)}{\rho_{kl}} + \frac{W_{rel}}{G_1} - \frac{x_1}{\rho_g}] \tag{2.6}$$

$$\rho_{hl}=[\frac{x_1}{\rho_g}+\frac{1-x_1}{\rho_L}]^{-1} \tag{2.7}$$

$$W_{rel}=\frac{1.18}{\rho_L^{0.5}}[g\sigma(\rho_L-\rho_g)^{0.25}] \tag{2.8}$$

For the vertical downward branch T-junction:

$$\frac{x_3}{x_1}=5\eta-6\eta^2+2\eta^3+a\eta(1-\eta)^b \tag{2.9}$$

$$\eta=\frac{(\frac{G_3}{G_1}-\frac{G_{3max,x=0}}{G_1})}{(1-\frac{G_{3max,x=0}}{G_1})} \tag{2.10}$$

$$G_{3max,x=0}=0.52\rho_L^{0.5}[\sigma g(\rho_L-\rho_g)]^{0.25} \tag{2.11}$$

For the vertical upward branch T-junction:

$$\frac{x_3}{x_1}=(\frac{G_3}{G_1})^{-0.8} \tag{2.12}$$

These correlations were generated based on experiments in equal diameter T-junctions (d=50 mm) with different branch orientations (horizontal, vertical upward and vertical downward). Both air-water and steam-water two-phase flow were examined under different inlet flow regimes. Rubel et al. (1988) compared this correlation with their data in stratified wavy and annular steam-water flow under the conditions $16<G_1<50\,kg/m^2.s$, $0.21<X_1<0.87$, $0.11<P_1<0.23\,MPa$. Good agreement was found

for the branch split ratio $G_3/G_1>0.3$. Satisfactory performance of Seeger et al.'s correlation was also reported by Timmerman et al. (1992) in high pressure steam-water experiments in large diameter pipes. However, Ballyk et al. (1988) found this correlation to underpredict their data in annular steam-water flow under the flow conditions of $400<G_1<1200$ kg/m^2.s, $0.02<X_1<0.08$, $0.1<P_1<0.2$ MPa.

2.2.2. Phenomenological models

The phenomenological models are based on the assumption of the existence of "zones of influence" in the inlet tube from which liquid and gas are diverted into the branch. The concept of "zone of influence" came from the experimental observation of single-phase flow by McNown (1954) and was extended to two-phase flow by Azzopardi and Whalley (1982). This concept was commonly accepted and further developed by other researchers, e.g. McCreery and Banerjee (1990) and Lemonnier and Hervieu (1991) for dispersed flow regimes and Shoham et al. (1987), Hwang et al. (1988) and Ballyk and Shoukri (1990) for the separated flow regimes.

Azzopardi and Whalley (1982) developed a simple geometric model for vertical annular flow. In this model they defined one "zone of influence" for both liquid and gas. The authors assumed that liquid and gas were extracted from the same "zone of influence" to the branch, i.e. the dividing streamlines for liquid and gas are coincident. Gas and liquid fractions from the inlet to the branch are completely governed by

geometrical relations between the phase distribution in the main inlet tube and the "zone of influence" characterized by angle θ as shown in Fig.2.5.

The fraction of gas phase extracted to the branch can be defined as:

$$\frac{\dot{m}_3 x_3}{\dot{m}_1 x_1} = \frac{\theta - \sin\theta}{2\pi} \tag{2.13}$$

where $\dot{m}_i$ and x_i (i=1, 3) are flow rates and qualities in the inlet and branch. The angle θ is related to the liquid film flow rate by the following expression:

$$\frac{\theta}{2\pi} = \frac{\dot{m}_3(1-x_3)}{\dot{m}_1(1-x_1)(1-E)} \tag{2.14}$$

where E is the fraction of liquid entrainment. Combining Eqns.(2.13) and (2.14) gives:

$$\frac{x_3}{x_1} = \frac{\dot{m}_1}{\dot{m}_3 2\pi}\left\{\frac{2\pi\dot{m}_3(1-x_3)}{\dot{m}_1(1-x_1)(1-E)} - \sin\left[\frac{2\pi\dot{m}_3(1-x_3)}{\dot{m}_1(1-x_1)(1-E)}\right]\right\} \tag{2.15}$$

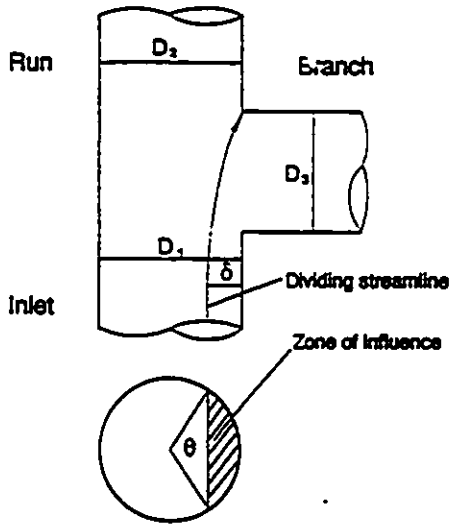

Fig.2.5 Zone of influence defined by Azzopardi and Whalley (1982)

If the inlet mass flow rate $\dot{m}_1$, quality x_1, branch flow rate $\dot{m}_3$ and fraction of liquid entrainment E are known, the branch quality x_3 can be evaluated with Eqn.(2.15) by an iterative method.

This simple geometrical model was extended by Azzopardi (1984) to take into account the effect of branch diameter by adding an empirical correlation into Eqn.(2.14)

$$\frac{\theta}{2\pi} = \frac{\dot{m}_3(1-x_3)}{1.2(\frac{d_3}{d_1})^{0.4}\dot{m}_1(1-x_1)(1-E)} \qquad (2.16)$$

Saba and Lahey (1984) derived a model based on five equations to describe phase redistribution in the junction, namely, mixture continuity equation, vapour-phase continuity equation, mixture linear momentum equation for the run and mixture linear momentum equation for the branch. By integrating the vapour linear momentum equation along branch streamlines with several relationships based on the "drift flux model" for bubbly flow they obtained the fifth equation as the closure for the equation set. The model was reported to be in reasonable agreement with their experimental data.

Shoham et al. (1987) developed a model for predicting phase redistribution in T-junction with horizontal equal diameter branch in stratified and annular flow. The model was based on the existence of two different "zones of influence" for liquid and gas respectively. Phase redistribution in the junction is assumed to be governed by competing inertial and centrifugal forces. In annular flow it is assumed that no liquid droplets are entrained in the gas core and that the liquid film has a uniform thickness distribution

along the circumferential direction of the main inlet tube.

The gas dividing streamline is assumed to form a circular arc as shown in Fig.2.6. The radius of the arc can be determined as:

$$r_0 = \frac{d_1^2+\delta_g^2}{2\delta_g} \tag{2.17}$$

The movement of the liquid phase in the radial direction is assumed to be controlled by the balance of inertia, centripetal and damping forces through an ordinary differential equation:

$$\frac{d^2r}{dt^2} = f_c - k\frac{dr}{dt} \tag{2.18}$$

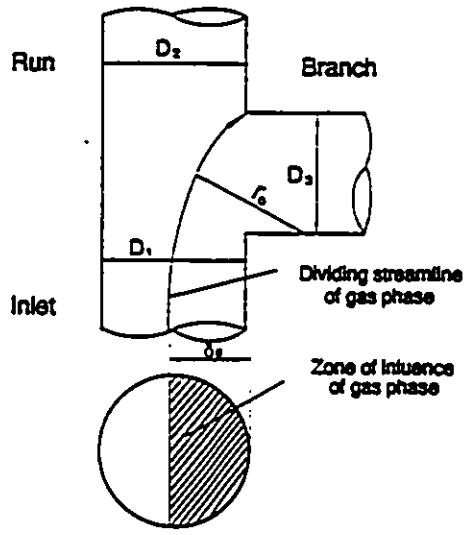

Fig.2.6 Dividing streamline defined by Shohaim et al. (1987)

The centripetal force f_c acting on the liquid phase (per unit mass) is:

$$f_c = \frac{\rho_L u_L^2 - \rho_g u_g^2}{\rho_L r_0} \tag{2.19}$$

The damping coefficient is given by:

$$k = \frac{3\mu_L}{\rho_L h} \tag{2.20}$$

where h represents the liquid hight in stratified flow and mean film thickness in annular flow.

The solution of Eqn.(2.18) yields the radial movement of the liquid as follows:

$$\Delta r = \frac{f_c}{k}[t - \frac{1}{k}(1 - e^{-kt})] \tag{2.21}$$

where t is the liquid transit time along the circular arc,

$$t = \frac{r_0 \sin^{-1}(\frac{d_1}{r_0})}{u_L} \tag{2.22}$$

The position of the liquid dividing streamline can be determined as:

$$\delta_L = \delta_g - \Delta r \tag{2.23}$$

The prediction of this model was compared by the authors with their own experimental data with reasonable agreement. Recently, the model was examined by Timmerman et al. (1992) and relatively good results were reported.

Hwang et al. (1988) developed a phenomenological model for horizontal equal

diameter T-junctions based on the hypothesis that there are different dividing streamlines for liquid and gas which separate the inlet flow into branch and run flow as shown in Fig.2.7. The model traces the dividing streamlines' path based on the balance between the centrifugal and interfacial drag forces acting on each phase. For the separated two-phase flow, i.e. stratified and annular flows, it was found that the influence of the interfacial drag force is relatively small and can be neglected. The model is then simplified to a balance between centrifugal forces of the two phases:

$$\frac{\rho_g u_g^2}{R_g} = \frac{\rho_L u_L^2}{R_L} \tag{2.24}$$

where R_g and R_L are the radii of curvature of gas and liquid dividing streamlines which are assumed to satisfy the following relation:

$$\frac{R_g}{R_L} = \frac{(\frac{\delta_L}{d_1})^{n_L}}{(\frac{\delta_g}{d_1})^{n_g}} \tag{2.25}$$

The exponent n_i in the above equation is determined empirically as:

$$n_k = 5+20\ \exp[-53(\frac{\delta_k}{d_1})] \qquad k=g,\ L \tag{2.26}$$

Combining Eqns.(2.24) and (2.25) gives the relationship between the positions of gas and liquid dividing streamlines δ_g and δ_l in terms of inlet parameters:

$$\frac{(\frac{\delta_l}{d_1})^{n_l}}{(\frac{\delta_g}{d_1})^{n_g}} = (\frac{1-\alpha_1}{\alpha_1})^2(\frac{x_1}{1-x_1})^2\frac{\rho_l}{\rho_g} \qquad (2.27)$$

where α_1 and x_1 represent inlet flow void fraction and quality.

The comparisons between this model and the available data corresponding to different flow regimes, system pressure, fluid properties, inlet flow rates and qualities were made by the authors. Good results were reported with the accuracy of the predictions within 25% of the experimental data. The model was also reported to be capable of predicting the steam-water data of Rubel et al. (1986) and Timmerman et al. (1992).

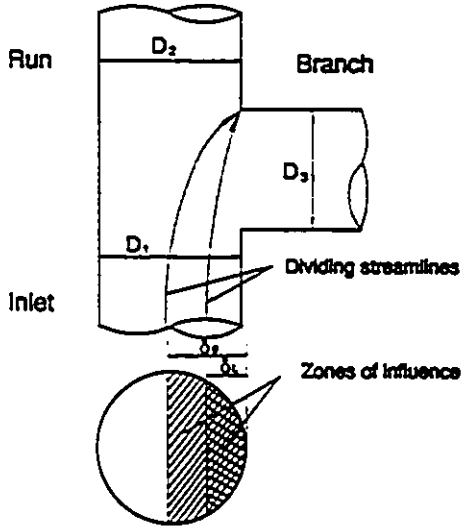

Fig.2.7 Dividing streamlines defined by Hwang et al. (1988)

Ballyk and Shoukri (1990) developed a more detailed phase redistribution model for horizontal annular flow. They determined the positions of the liquid and gas dividing streamlines by calculating the path of fluid particles via the free streamline theory in potential flow. The unique feature of this model is that the locations of the dividing streamlines are dependent on the height in the cross section of the main inlet tube as shown in Fig.2.8. This approach partially account of the 3-D effects.

The authors included the effect of pressure changes in the model. The inertia and pressure forces were assumed to dominate phase redistribution in the junction. Furthermore, the effect of the asymmetrical liquid film distribution in horizontal annular flow was taken into account. This made it possible to extend the model to allow for the effect of branch orientation on phase redistribution. This model is further developed in this study and discussed in detail in Chapter 6.

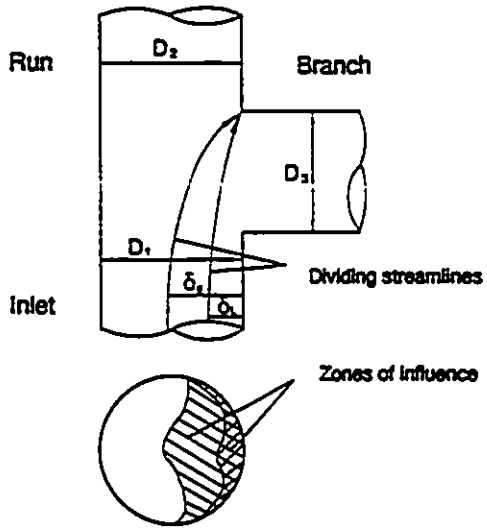

Fig.2.8 Dividing streamline defined by Ballyk and Shoukri (1990)

For the highly dispersed two-phase flows, i.e. annular mist and bubbly flow, McCreery and Banerjee (1990) and Lemonnier and Hervieu (1991) assumed weak interaction between the dispersed and continuous phases. The flow field of the continuous phase was first determined by using numerical or conformal mapping methods on the basis of potential flow. Consequently, the bubble trajectories were evaluated within a known pressure and velocity field. Once the "dividing trajectory" is determined from the information of the size and distribution of droplets or bubbles, the corresponding fractions of each phase in the branch and run can be determined. Since the present study is limited to separated flow regimes, i.e. stratified flow and annular flow, these models are not discussed in detail.

2.2.3. Two-fluid models

The state-of-the-art of computational fluid dynamics has made it possible to simulate complicated two-phase flow phenomenon with sophisticated codes. In theory, the two-fluid continuity and momentum conservation equations can be solved numerically together with the interfacial transfer constitutive relations which attempt to reintroduce some physics lost during the averaging process. The difficulties in applying the two fluid model is typically the availability of appropriate interfacial constitutive relations. The two-fluid model has the potential of predicting the phase redistribution and the pressure changes in T-junctions. It has been successfully used for one-dimensional transient two-

phase flow in nuclear reactor safety analysis. Its application for multi-dimensional flow has been limited because of the lack of appropriate constitutive relations for the interfacial interaction between the two phases. Most available interfacial relations are flow regime dependent and have been verified for one-dimensional flow. In applying a multi-dimensional two-fluid flow model for two-phase flow in a T-junction, the problem becomes more completed because flow regime changes can take place in the junction. Two attempts have been reported in the literature on the application of two-fluid model for two-phase flow in T-junctions.

Lahey (1990) used a two-fluid formulation to model phase redistribution in T-junctions with stratified flow. The unique features of this work is the 3-D nature of the simulation. Most importantly, the information on pressure changes was numerically obtained. Two-fluid continuity and momentum equations were simultaneously solved by PHOENICS, a well known CFD code. A stratified wavy correlation developed by Andritsos and Hanratty (1987) was used as a constitutive relation for interfacial momentum transfer. The authors noted that the two-fluid model used to analyze phase distribution in the inlet tube should also be applicable to model phase redistribution in the junction. Different orientations of the T-junction were treated as boundary conditions. The simulation results were very encouraging and indicated the versatility and capability of a properly formulated two-fluid model. Both the phase redistribution and pressure changes were well predicted.

Issa and Oliveira (1991) reported their 3-D two-fluid model numerical results in

vertical rectangular cross-section T-junction for bubbly flow. The procedure was based on the numerical solution of transport equations of continuity and momentum for each phase together with additional equations pertaining to the k-ϵ turbulence model. Finite-volume representation of T-junction geometries was facilitated by using block-structured computational meshes and an indirect addressing technique. The authors compared their numerical simulation with the data of Popp and Sallet (1983) and found their results were in agreement with the experimental data.

2.2.4. Summary of the models on phase redistribution

The completely empirical correlations are typically valid in the range of conditions of the experimental data used in their development. Consequently, when extended to the conditions outside the ranges from which they were developed, great care should be taken. The available empirical correlations were developed based on limited data. The present significantly enlarged data bank can be used for developing empirical design correlations for future use.

The phenomenological models are based on the assumption that there are "Zones of influence" in the junction from which liquid and vapour are diverted into the branch. The "Zones of influence" are directly related with the phase distribution in the main inlet tube and junction geometry. To distinguish the different "Zones of influence" of the liquid and vapour phases a variety of approaches and assumptions have been used by

previous researchers. Phenomenological models provide a simple and practical approach to analyze the complicated two phase redistribution phenomenon in T-junctions. These models are flow regime and junction geometry dependent. However, since more or less the principles of fluid mechanics have been involved in the modelling process some of the phenomenological models could be expected to be applicable to the other geometrical configurations.

A multi-dimensional two-fluid model has, in principle, the potential to predict both phase redistribution and pressure changes in T-junctions as long as appropriate interfacial constitutive relations are available. The two-fluid model has the potential to predict the 3-D effects on phase redistribution in the junctions. Proper application of the model can, in theory, also provide the phase distribution information in the inlet pipe upstream of the junctions. The success of the prediction relies greatly on the correctness of the interfacial constitutive relations developed for different flow regimes. Limited attempts to use the two-fluid model have been reported and further work in this direction is certainly needed.

The available phase redistribution models in T-junction are shown in Table 2.2.

2.3. Experiments and Models on Pressure changes

The present approaches for two-phase pressure changes are, in general, direct extensions of the methods used in single-phase flow. The commonly accepted procedure

Table 2.2 Available models of phase redistribution in T-junction

Authors	Nature of Model	$D_3/D3_1$	Branch Orientation θ	Inlet Flow Regime
Zetzman, 1982	empirical correlations	1:1, 1:2	horizontal (vertical inlet)	annular
Azzopardi & Whalley, 1982	phenomenological model	1:1	horizontal	annular
Saba & Lahey, 1984	phenomenological model	1:1	horizontal	intermittent
Seeger et al. 1986	empirical correlations	1:1	upward, horizontal, downward	annular, stratified, intermittent
Shoham et al. 1987	phenomenological model	1:1	horizontal	annular, stratified
Hwang et al. 1988	phenomenological model	1:1	horizontal	annular, stratified, intermittent
Ballyk & Shoukri, 1990	phenomenological model	1:1	horizontal	annular
McMreey & Banerjee, 1990	phenomenological model	1:1, rectangular tube	horizontal	annular mist
Lahey, 1990	two-fluid model formulation	1:1	upward, horizontal, downward	stratified
Lemonnier & Hervieu, 1991	phenomenological model	1:1	horizontal	intermittent
Issa & Oliveira, 1991	two-fluid model formulation	1:1, rectangular tube	horizontal (vertical inlet)	intermittent

is to use loss coefficients determined in single-phase flow and modify the correlations by a two-phase multiplier determined from two-phase flow experiments.

2.3.1. Pressure drop in the branch

Based on the existence of a recirculation zone in the branch, Fouda and Rhodes (1974) modelled the branch pressure drop by treating the vena contracta as an orifice. The orifice equation gave the branch pressure drop as:

$$\dot{m}_3 = C_{tp} A_3 [2\rho_{h3} \Delta P_{1\text{-}3}]^{\frac{1}{2}} \tag{2.28}$$

where the subscript 3 refers to the branch conditions. C_{tp} is a homogeneous discharge coefficient determined from the experiments.

Saba and Lahey's model (1982) was based on single-phase flow approach which divided the branch pressure change $\Delta P_{1\text{-}3}$ into reversible and irreversible components. Assuming separated flow and using mechanical energy balance between the inlet and the branch the authors obtained,

$$\Delta P_{1\text{-}3} = \frac{\rho_{h3}}{2}\left(\frac{G_3^2}{\rho_{e3}^2} - \frac{G_1^2}{\rho_{e1}^2}\right) + K_{13}\frac{G_1^2}{2\rho_{m1}} \tag{2.29}$$

where k_{13} is the empirical single-phase energy loss coefficient based on the same flow split G_3/G_1, the energy, momentum and homogeneous densities ρ_e, ρ_m and ρ_h respectively are defined as:

$$\rho_e = \left[\frac{x^3}{\alpha^2\rho_g^2} + \frac{(1-x)^3}{(1-\alpha)^2\rho_L^2}\right]^{-0.5} \tag{2.30}$$

$$\rho_m = \left[\frac{x^2}{\alpha\rho_g} + \frac{(1-x)^2}{(1-\alpha)\rho_L}\right]^{-1} \tag{2.31}$$

$$\rho_h = \left[\frac{x}{\rho_g} + \frac{(1-x)}{\rho_L}\right]^{-1} \tag{2.32}$$

In homogeneous flow all the above densities reduce to the homogeneous density and Eqn.(2.29) becomes:

$$\Delta P_{1\text{-}3} = \frac{\rho_{k3}}{2}\left(\frac{G_3^2}{\rho_{k3}^2} - \frac{G_1^2}{\rho_{k1}^2}\right) + K_{13}\frac{G_1^2}{2\rho_{k1}} \tag{2.33}$$

Reimann and Seeger (1986) found that the prediction of branch pressure drop from a homogeneous model was in better agreement with their experimental data. This model can be expressed as:

$$\Delta P_{1\text{-}3} = \frac{\rho_{k3}}{2}\left(\frac{G_3^2}{\rho_{k3}^2} - \frac{G_1^2}{\rho_{k1}^2}\right) + K_{13}\frac{G_1^2}{2\rho_{k1}}\frac{\rho_{k3}}{\rho_{k1}} \tag{2.34}$$

Ballyk et al. (1988) suggested an annular flow model based on the mechanical energy equation:

$$\Delta P_{1\text{-}3} = \frac{\rho_{k3}}{2}\left(\frac{G_3^2}{\rho_{e3}^2} - \frac{G_1^2}{\rho_1^{*2}}\right) + K_{13}\frac{\rho_{k3}G_1^2}{2\rho_1^{*2}}\phi_{tp} \tag{2.35}$$

where Φ_{tp} is a two-phase multiplier determined by the experiments, ρ_1^* is an equivalent inlet density defined as:

$$\rho_1^* = \left[\frac{x_1^2 x_3}{\alpha_1^2 \rho_g^2} + \frac{(1-x_1)^2(1-x_3)}{(1-\alpha_1)^2 \rho_L^2}\right]^{-0.5} \tag{2.36}$$

Ballyk (1992) extended this model to T-junctions with smaller diameter branch. He found that the two-phase multiplier Φ_{tp} was a unique function of the branch flow split ratio, independent of both inlet mass flux and quality but with strong dependence on the junction geometry. In annular flow, the author recommended three correlations for horizontal orientated branches with branch/inlet diameter of 1.0, 0.82 and 0.5.

$$\phi_{tp} = -1.28+22.61\left(\frac{\dot{m}_3}{\dot{m}_1}\right)-15.21\left(\frac{\dot{m}_3}{\dot{m}_1}\right)^2 \qquad for\ \frac{D_3}{D_1}=1.0 \tag{2.37}$$

$$\phi_{tp} = -1.85+36.06\left(\frac{\dot{m}_3}{\dot{m}_1}\right)-26.00\left(\frac{\dot{m}_3}{\dot{m}_1}\right)^2 \qquad for\ \frac{D_3}{D_1}=0.82 \tag{2.38}$$

$$\phi_{tp} = -16.05+297.02\left(\frac{\dot{m}_3}{\dot{m}_1}\right)-249.38\left(\frac{\dot{m}_3}{\dot{m}_1}\right)^2 \qquad for\ \frac{D_3}{D_1}=0.5 \tag{2.39}$$

All above mentioned models are 1-D simple models. Recently more detailed analysis of the pressure changes in the junction have been published. These analyses of the pressure changes were based on the detailed study of flow structure in the junction. Boulanger and Lemonnier (1992) performed a 2-D analysis of two-phase pressure changes in T-junction for dispersed flow. Lahey (1990) published 3-D numerical simulation for T-junction with different branch orientations in stratified flow. Encouraging results have been reported by these authors. However these multi-dimensional models are strongly flow regime dependent since the models rely on detailed

constitutive relations which dependent on the interfacial momentum transfer between the two phases.

2.3.2. Pressure recovery in the run

When a flow is divided in a T-junction the deceleration of the fluid causes a reversible pressure rise in the branch and run due to the Bernoullis' effect. There are also irreversible energy losses generated by turning the flow direction and enlarging the flow channel. It should be noted that in the 1-D mechanical energy equation the kinetic energy correction factor was assumed as unity, i.e. the velocity is assumed uniform on the cross section of the tube. The 2-D effect of the velocity profiles in the branch and run was ignored. Furthermore, the effect of the interfacial momentum transfer on the dividing surface between the two flows (branch and run flows) is ignored due to the lack of understanding of the local flow mechanics. These simplifications have no significant effect on the model of branch pressure drop, due to the high irreversible energy losses corresponding to the turning of flow direction. However, the irreversible energy losses between the inlet and run are very small, the model of run pressure recovery is much more sensitive to these simplifications.

Correlating the pressure recovery in the run using mechanical energy balance, as shown for the pressure drop in the branch, was found to be unsatisfactory by many researchers, for example, Reimann and Seeger (1986), Ballyk et al. (1988). This is

mainly because the irreversible pressure loss in the run is very small. Accordingly, when the run pressure recovery data are reduced using mechanical energy balance, negative values of energy loss coefficients may obtained, which is physically incorrect.

Alternatively, a simple momentum balance was used by earlier investigators to correlate the pressure recovery in the run. This was driven by the success of the momentum balance approach in correlating the pressure recovery data in a sudden enlargement in flow channel.

A comprehensive survey of the open literatures indicated that the run pressure recovery were modelled by the axial momentum balance as shown, for example, by Madden and St. Pierre (1969), Fouda and Rhodes (1974), Collier (1976), Saba and Lahey (1984) and Ballyk et al. (1988). Assuming separated flow, the momentum balance in axial direction yields:

$$\Delta P_{2-1} = P_2 - P_1 = K_{12s}\left(\frac{G_1^2}{\rho_{m1}} - \frac{G_2^2}{\rho_{m2}}\right) \qquad (2.40)$$

where K_{12s} is the two-phase separated momentum correction factor which is empirically determined and ρ_m is the momentum density. Several separated two-phase momentum correction factors have been suggested by different researchers for T-junctions with horizontal branch. Fouda and Rhodes (1974) recommended that $K_{12s}=0.533$. Madden and St. Pierre (1969) and Ballyk (1992) showed that $K_{12s}=1.0$ under annular inlet flow conditions. The two-phase momentum correction factor K_{12s} was found by Ballyk (1992) to be independent of the inlet mass flux and quality, the branch flow split and the

junction geometry.

For homogeneous flow Saba and Lahey (1984) reduced the axial pressure rise data in terms of a homogeneous momentum equation:

$$\Delta P_{2-1} = P_2 - P_1 = K_{12}\left(\frac{G_1^2}{\rho_{h1}} - \frac{G_2^2}{\rho_{h2}}\right) \tag{2.41}$$

where K_{12} is the single-phase momentum correction factor and ρ_h is the homogeneous density. The authors reported that good agreement between the model and experimental data was obtained.

Reimann and Seeger (1986) used both mechanical energy balance and simplified momentum balance to model run pressure recovery:

$$\Delta P_{2-1} = \Delta P_{1-c2} + \Delta P_{c2-2} \tag{2.42}$$

$$\Delta P_{1-c2} = \frac{\rho_{h2}}{2\rho_L^2}\left\{\frac{G_2^2}{C_2^2}\left[x_2\left(\frac{\rho_L}{\rho_g}\right)+(1-x_2)\right]^2 - G_1^2\left[x_1\left(\frac{\rho_L}{\rho_g}\right)+S_1(1-x_1)\right]^2\left[x_2+\frac{1-x_2}{S_1^2}\right]\right\} \tag{2.43}$$

$$\Delta P_{c2-2} = \frac{G_2^2}{\rho_L}\left\{\left[x_2\left(\frac{\rho_L}{\rho_g}\right)+S_2(1-x_2)\right]\left[x_2+\frac{1-x_2}{S_2}\right] - \frac{1}{C_2}\left[x_2\left(\frac{\rho_L}{\rho_g}\right)+(1-x_2)\right]\right\} \tag{2.44}$$

where S is the slip ratio, the contraction coefficient C_2 is derived based on the single-phase flow at the same volumetric flow split:

$$C_2 = \left[1+\left(\frac{\rho_{h1}}{\rho_{h2}}\right)^{0.5}\frac{V_1}{V_2}\sqrt{k_{1-2}}\right]^{-1} \tag{2.45}$$

where V_1 and V_2 are the inlet and run volumetric flow rates and k_{1-2} is the single-phase

energy loss coefficient. The authors recommended Rouhani's correlations (1969) to evaluate slip ratios.

2.3.3. Summary of pressure changes

When two-phase flow is divided in a piping junction, the resulting pressure changes and phase redistribution are closely interdependent. Current correlations are developed based on simple application of mechanical energy and momentum balances, which, in general, do not reflect the interdependence of pressure changes and phase redistribution.

CHAPTER 3

EXPERIMENTAL ARRANGEMENTS

3.1. Experimental Facility

3.1.1. Steam-Water two-phase flow loop

The steam-water two-phase flow loop used for the experimental investigation is schematically shown in Fig.3.1. Hot water supplied from a 450 L reservoir to the progressive cavity pump was controlled by the valves of the main water line and the loop bypass. The water flow first passed through a 6 kW preheater to increase the water enthalpy and the flow rate and temperature were measured by the turbine flow meter and thermocouple before entering the two-phase mixer where it was mixed with superheated steam.

Steam taken from the main supply at approximately 7 bar was throttled to the desired pressure through a pressure regulator. The steam line is equipped with an inverted bucket steam trap to collect any condensate that may be present. The steam flow rate was measured by an orifice meter and controlled by a valve on the steam line. The steam pressure and temperature were measured before entering the two-phase mixer.

The hot water and superheated steam were well mixed in the two-phase mixer and

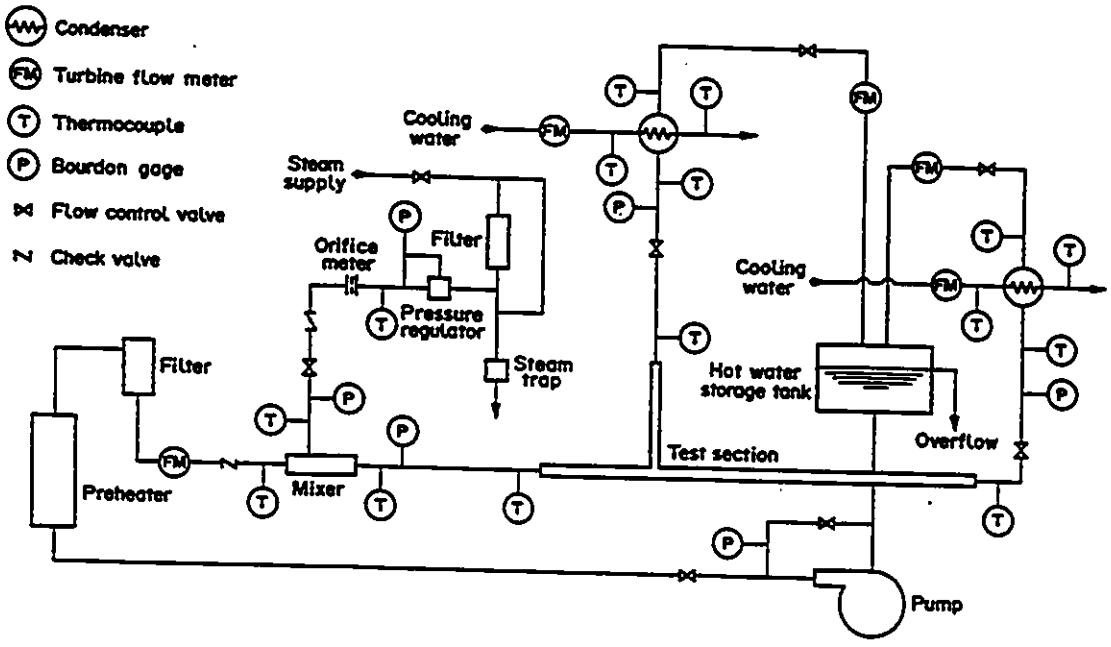

Fig.3.1 Experimental loop (reproduced from Ballyk, 1992)

the two-phase mixture passed through a 3.6 m long pipe to reach fully developed flow and attain thermal equilibrium before entering the inlet of the test section. The pressure and temperature of the two-phase mixture at the inlet of test section were measured. The quality of the inlet flow was evaluated by energy balance at the two-phase mixer based on the measurement of flow rates and temperatures.

The two-phase flow was divided in the T-junction into two streams, i.e. run flow and branch flow. At the outlet of the each leg the temperature and the pressure of the two-phase mixture were measured and the steam-water flow entered a 50 kW shell-tube condenser exiting as single-phase water. The flow split ratio was controlled by the valves located at the upstream and downstream of condensers. The condensate flow rate in each leg was metered by a turbine flow meter. The qualities of run and branch flow were evaluated by energy balance on the condensers. The condensate from each condenser was then delivered back to the hot water reservoir. The entire loop and the reservoir were insulated to minimize heat losses. The detailed description of the design and construction of the major components of the loop was given by Ballyk (1992).

3.1.2. Test sections

In the annular flow experiments the T-junctions were constructed of 25 mm I.D stainless steel tubing with equal diameters of inlet, run and branch. The inlet and branch conduits were the same length, 610 mm, with five pressure taps on each leg while the

run conduit was extended to 2300 mm with 15 pressure taps due to slower flow development. Two test sections were used in the annular flow experiments. Each had a horizontal inlet and the branches were downwardly inclined by 45° or 90° respectively. They were identical to the completely horizontal junction used by Ballyk (1992) and accordingly the results compliment his data. The detailed design and construction of the test sections can be found in the thesis of Ballyk (1992).

In the stratified flow experiments two T-junctions were used. One was made of equal diameters of 76 mm I.D. stainless steel tubing, another was constructed of 76 mm I.D. of inlet with 26 mm I.D. of branch giving a branch-to-inlet diameter ratio of 0.33. The equal diameter test section was mounted horizontally to study the effect of inlet flow conditions on the junction phase redistribution and pressure changes. The reduced size branch test section was mounted either horizontally to study the effect of branch diameter or downwardly to study the effect of branch orientation. A schematic diagram of the test section with a branch to inlet diameter ratio of 1.0 is shown in Fig.3.2. For both T-junctions the inlet, run and branch conduits were 610 mm, 920 mm and 1830 mm in length respectively. Five pressure taps were made on the inlet and branch while six taps were on the run. Each tap contained a 1.6 mm hole drilled through the tube wall and carefully filed to ensure no burrs protruded in the flow area. Host nipple fittings were soldered onto the outside of the tube wall to facilitate the connection of the taps to the pressure transducers.

To observe the flow patterns, three transparent sections were mounted at the inlet,

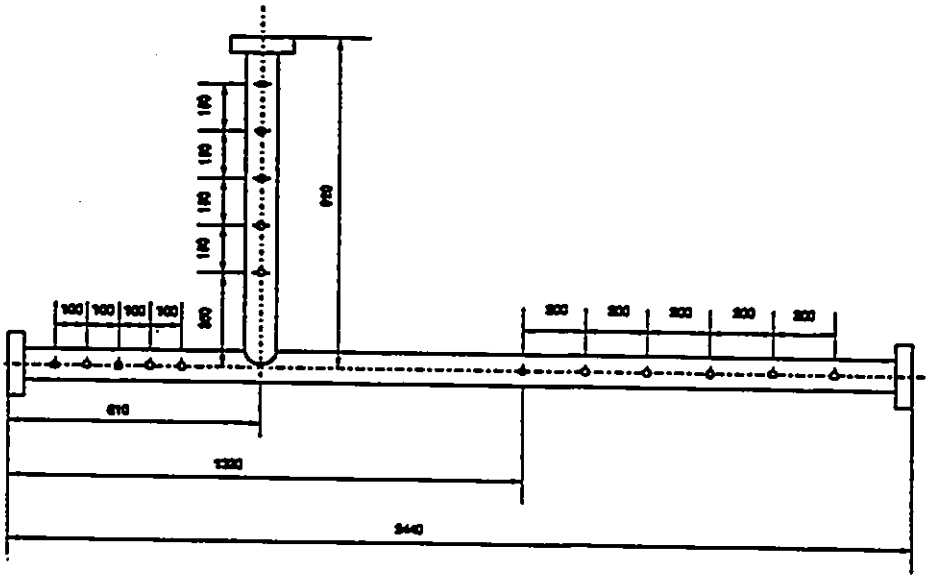

Fig.3.2 Test section

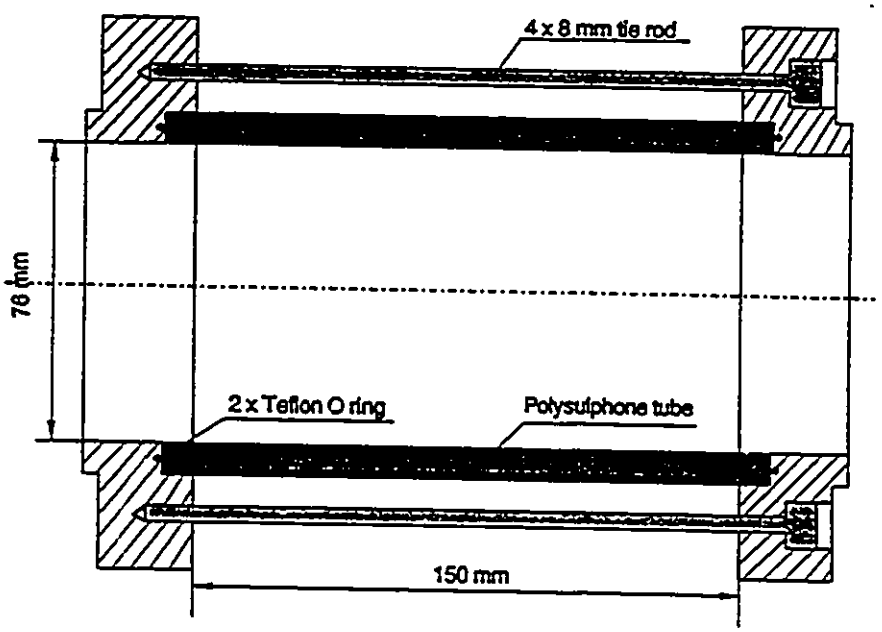

Fig.3.3 Transparent part of test section

run and branch. The transparent sections were constructed of polysuphone, 150 mm in length, connected to the loop using specially machined flanges as shown in Fig.3.3. The design of the polysuphone tube and the flanges were such that the inside diameter were identical to those of inlet, run and branch to eliminate any disturbance to the flow. In assembling each transparent section extreme care was taken to ensure the alignment and coaxiality between the polysuphone tube and test section tubing.

3.2. Measurements and Calibration

In the present steam-water flow experiments thermodynamic qualities of the inlet, run and branch flows were evaluated using the energy balance on the two-phase mixer and condensers. The measured parameters to determine the qualities included the temperatures, flow rates and pressures of the water and steam flows. Void fraction in each leg of the T-junctions were measured to facilitate the calculation of two-phase flow momentum and energy densities. All data measured were collected by a computerized acquisition system Taurus One through appropriate transducers. The flow condition was monitored on-line by the acquisition system throughout the experiments using specially written programs.

3.2.1. Temperatures measurements

Temperatures were measured at 15 different locations throughout the loop using standard E type thermocouples as following:

1. Hot water temperature at the inlet of two-phase mixer
2. Steam temperature at the inlet of two-phase mixer
3. Two-phase mixture temperature at the exit of mixer
4. Inlet temperature of the test section
5. Branch temperature of the test section
6. Run temperature of the test section
7. Inlet temperature of the branch condenser
8. Outlet temperature of the branch condenser
9. Cooling water inlet temperature of the branch condenser
10. Cooling water outlet temperature of the branch condenser
11. Inlet temperature of the run condenser
12. Outlet temperature of the run condenser
13. Cooling water inlet temperature of the run condenser
14. Cooling water outlet temperature of the run condenser
15. Steam temperature at the exit of the pressure regulator

Temperature measurements were referenced to 0 °C through ice-water bath. The

analog signals from the thermocouples were fed to the I/O module T-3732T of acquisition system which provided 32 channels of direct DC signal inputs. Module T-3732T is a 12 bit ADC which converts analog signals to digital numbers. The temperatures were periodically scanned during the experiments and the readings were converted to degree centigrade using the following correlation generated from the table of E type thermocouple:

$$T = 0.0433 + 17.0378\ mv - 0.2205\ mv^2 + 0.0045\ mv^3 \qquad (3.1)$$

The temperature measurement system was calibrated using water bath with a precision mercury thermometer. The calibrated temperatures varied from 0° to 100° at 1 atm. The results showed that the resultant error of the measurement system was within ±1%.

3.2.2. Measurements of flow rates

Water flow rates were measured at five locations using turbine flow meters as listed below:

Inlet of the mixer (ITT Barton 8086, 0.15-1.8 L/s)

Outlet of the run condenser (ITT Barton 8086, 0.15-1.8 L/s)

Outlet of the branch condenser (FT-8N10, 0.06-0.6 L/s)

(FT-8N5, 0.03-0.3 L/s)

Inlet of the run cooling water (FT-8N10, 0.06-0.6 L/s)

inlet of the branch cooling water (FT-8N10, 0.06-0.6 L/s)

For the low branch flow split a lower range flow meter FT-8N5 was used to improve the accuracy of the measurement. The turbine meters were equipped with magnetic pick-up coils and the output frequency signals were directed to the I/O module T-10470 of the data acquisition system. The T-10470 module provided a mixture of pulse or event counting and frequency measurement. Included were seven 16 bit counter blocks, three were used as event counters in the measurements of void fraction discussed later, the other four were set up through software commands as counters to measure the outlet frequency signals of the turbine flow meters. Since there were six turbine flow meters used in the measurement of water flow rates, the branch condensate meters of different ranges and the cooling water meters of the run and branch were sharing the same counters using switches. Calibration of the turbine flow meters was provided by the manufacturers, which indicated that the expected error of the ITT series was within $\pm 1\%$ and FT series was $\pm 0.5\%$ of reading over the entire flow range. As a check, the meters were calibrated on-line by examining the mass balance between the inlet and outlets (run and branch) of the test section. Single phase water calibration results showed that the maximum deviation was within $\pm 1\%$.

Steam flow rate was measured by the orifice meter installed at the downstream of the pressure regulator with different orifice plates for a wide range of measurement.

The pressure difference of the orifice meter was sensored by a differential pressure transducer Validyne DP15-36 (0-35 kPa). The transducer was excited by a carrier demodulator CDC 101. The unit demodulates the transducer output providing a ± 10 volt DC signal which was fed to the I/O module T-3732T of the data acquisition system. The uncertainty of the pressure transducer was provided by the manufacturer as $\pm 0.5\%$. The calibration of the orifice meter was performed on-line by direct weighting the condensates at different upstream pressures, i.e. 450 kPa for the experiments of annular flow and 150 kPa for the experiments of stratified flow. The calibration results indicated that the deviations were within $\pm 2\%$.

3.2.3. Pressure measurement

System pressures in five different locations throughout the loop were monitored by Bourdon pressure gages as shown in Fig.3.1. The pressure profiles along the inlet, run and branch were measured to determine the pressure changes in the T-junctions. The first station of the pressure was used to measure the inlet pressure of the test section to determine the saturated state of the two-phase flow. This inlet pressure was measured by a differential pressure transducer Validyne DP15-46 (0-350 kPa) between the first pressure tap and the atmosphere. The inlet pressure was also used as the reference for measuring the pressure profiles in each leg of the junction by connecting the first pressure tap to the high side of a bank of two differential pressure transducers, one high

rang and one low range. The other pressure taps were connected to the low side of the transducer bank through a 24 channel switching valve (Scanivalve WO2). Accordingly, the pressure differences between the inlet and each station along the test section were subsequently sensed. The detailed design of the pressure measurement system was given by Ballyk (1992). During the experimental study the pressure lines from the taps to the transducer bank were periodically purged to ensure no air remained in the system. The high range differential pressure transducer used was Validyne DP15-38 (0-55 kPa). The low range transducer used was DP103 series with different diaphragms for various measurement purposes, i.e. DP103-10 (0-0.086 kPa) and DP103-20 (0-0.55 kPa) for the experiments of stratified flow and DP103-28 (0-5.5 kPa) for the experiments of annular flow. This selection of the diaphragms makes accurate measurement in the entire pressure range of 0-55 kPa. All the transducers were exited at 5 volts 5 kHz by the carrier demodulators, the output signals were fed to the I/O module T-3732T of the acquisition system. The uncertainties of the differential pressure transducers were provided by the manufacturer as $\pm 0.5\%$. The differential pressure transducers were calibrated using micromanometer and U-tube manometer. The calibration results were found to be very linear for all the transducers.

3.2.4. Void fraction measurement

In the annular flow, the void fraction was measured in the run and branch only

while the inlet void fraction was determined by the empirical correlation recommended by Baroczy (1970). The correlation was chosen based on the comparison of five void fraction relationships discussed by Butterworth (1975) with the data of Ballyk et al. (1988), which was measured in the same facility and the same inlet tube. It was found that the Baroczy correlation predicted the data within the error of $\pm 6\%$. In the stratified flow experiments, the inlet void fraction was measured using the ultrasonic pulse-echo technique discussed in Chapter 5. The ultrasonic device was used to obtain the liquid level from which the void fraction was calculated. The average void fractions at the exit of the run and branch were measured using single beam gamma densitometer. In the annular flow experiments the gamma source used was a Cobalt-57 line source while in the stratified flow experiments a Barium-133 line source was used. Lead collimators were used on both sides of the pipe to define the line gamma beam as a thin rectangular beam corresponding to the appropriate pipe diameter. The collimators were installed so that the gamma rays were perpendicular to the liquid-vapour interface in stratified flow. The gamma flux from the line source was detected using a 76.2 mm cubic NaI(TI) scintillator. Standard pulse counting signal processing system was used to provide the output signal. The signal processing system consisted of a pre-amplifier (Harshaw NB-11), a linear amplifier (Harshaw NA-17), a high voltage power supply (Harshaw NV-15A) and a single channel analyzer (Harshaw NC-22). A window was set using the single channel analyzer to count the photons at the range of gamma energy of interest. The output signal from the single channel analyzer was directed to two cascaded counters in

the I/O module T-10470 of Taurus One data acquisition system. The module T-10470 provided three counters which can be set as event counters through software commands.

The sensitivity of the gamma beam S can be defined as:

$$S = \frac{N_{\alpha=1} - N_{\alpha=0}}{\frac{1}{2}(N_{\alpha=1} + N_{\alpha=0})} \tag{3.2}$$

were $N_{\alpha=1}$ and $N_{\alpha=0}$ are the counting rates when the test section is completely filled with steam or water respectively. Under the present test arrangements the sensitivities of the gamma densitometers were evaluated as 0.26 for the Cobalt-57 source and 0.32 for the Barium-133 source. The statistical error of the counting was defined by Chan and Banerjee (1981) as:

$$\varepsilon_\alpha = \frac{1}{S\sqrt{N_\alpha}} \tag{3.3}$$

In the annular flow experiments (Cobalt-57 source) a counting period of 60 seconds gave the statistical error of 1.22%, while in the stratified flow experiments (Barium-133 source) a counting period of 10 seconds provided a statistical error of 0.32%. The gamma densitometers were calibrated using specially machined lucite tube to simulate annular and stratified flow conditions. The deviations were found within ±8%.

3.2.5. Computerized data acquisition system

The signals of the thermocouples, turbine flow meters, pressure transducers and gamma densitometer were fed to Taurus One Date Acquisition System through I/O modules T-3732T and T-10470. The heart of the Taurus One system is a single board microcomputer T-200 based on Z80A microprocessor. The acquisition system has its own firmware based operation system and an I/O bus for plugging a variety of I/O modules. The command messages of the data acquisition were sent to the Taurus One from its host IBM-PC computer through communication port. The I/O modules of T-3732T and T-10470 provide 32 analog channels, 4 frequency channels and 3 event counters for the measurements of temperatures, pressures, steam and water flow rates and void fractions. Specially functioned computer programs were written to monitor test conditions, data acquisition and reduction.

3.2.6. Measurement procedure

The experiments started by circulating single-phase water in the loop. The required mass flux was adjusted by the main water line valves and system bypass. Water was preheated to approximately 45 °C, before the superheated steam was injected into the two-phase mixer. During the preheating process the temperatures throughout the loop were carefully monitored by the data acquisition system. When the water temperature at

the inlet of two-phase mixer reached approximately 70 °C, the water and steam flow rates and the branch flow split ratio were adjusted according to the test condition. The system typically required three to four hours of continuous adjustments to achieve the thermodynamic equilibrium and the required test conditions. The variation of the temperatures, flow rates and pressures during the adjustments were scanned by the Taurus One system using a specially written monitoring program. The program was written in order that the mass fluxes and qualities in each leg of the junction, the branch flow split ratio and the deviation of the mass and energy balance between the inlet and exits could be read directly on the screen of the computer monitor. Once the designed conditions were obtained the system was allowed to run for approximately 30 minutes to ensure that a steady state was reached.

A special measurement program was written in which the test was monitored and recorded by sweeping the flow conditions and averaging the latest values to the old sweeps. This sweep averaging process was continuously carried out throughout the pressure and phase redistribution measurements. Void fractions were measured before and after the measurement of the pressure profile in the junction. In the pressure measurements it was found that a 30 seconds time period at a rate of 100 samples per seconds was good enough to obtain stable pressure readings in annular flow while a 200 seconds of time period at a rate of 100 samples per second was suitable to achieve reasonable reading in stratified flow, a further increase of the sampling rate was limited by the speed of the host computers. The pressure distributions in the three legs of the

junction were measured station by station in order. Phase redistribution data, i.e. the ratio of branch-to-inlet flow qualities was obtained from the final recording of averaged values of flow conditions. The test conditions, void fractions, pressures and phase redistribution data were saved in a data file for further reductions.

3.3. Data Reduction and Experimental uncertainties

3.3.1. Data reduction

The data collected from the experiments were reduced to determine eight parameters of interest, i.e. the mass flow rates $\dot{m}_1$, $\dot{m}_2$, $\dot{m}_3$, the flow qualities x_1, x_2, x_3 and the pressure changes in the T-junction ΔP_{2-1} and ΔP_{1-3}.

The inlet mass flow rate $\dot{m}_1$ was determined by the sum of inlet water flow rate $\dot{m}_{Lm}$ and inlet steam flow rate $\dot{m}_{gm}$ of the two-phase mixer:

$$\dot{m}_1 = \dot{m}_{Lm} + \dot{m}_{gm} \tag{3.4}$$

The run and branch mass flow rate $\dot{m}_2$ and $\dot{m}_3$ were directly determined from the measurement of the condensates of the appropriate condensers.

The thermodynamic qualities of x_1, x_2 and x_3 were determined by the energy balances on the mixer and condensers:

$$x_1 = \frac{\dot{m}_{gm}h_{gm}+\dot{m}_{Lm}h_{Lm}-\dot{m}_1h_{Li}}{\dot{m}_1(h_{gi}-h_{Li})} \tag{3.5}$$

$$x_2 = \frac{\dot{m}_2h_{c2}+[\dot{m}_{cw}(h_{cwo}-h_{cwi}]_2-\dot{m}_2h_{Lr}}{\dot{m}_2(h_{gr}-h_{Lr})} \tag{3.6}$$

$$x_3 = \frac{\dot{m}_3h_{c3}+[\dot{m}_{cw}(h_{cwo}-h_{cwi}]_3-\dot{m}_3h_{Lb}}{\dot{m}_3(h_{gb}-h_{Lb})} \tag{3.7}$$

where the inlet steam enthalpy h_{gm} was determined from the superheated steam table according to the inlet steam temperature and pressure, other enthalpies were determined by the empirical correlations generated from saturated water tables based on measured temperatures and pressures. The correlations of thermodynamic properties of the water and steam were given by Ballyk (1992).

The validity of the determined mass flow rates and qualities were checked on-line by the mass and energy balances.

$$\dot{m}_1 = \dot{m}_2+\dot{m}_3 \tag{3.8}$$

$$\dot{m}_1x_1 = \dot{m}_2x_2+\dot{m}_3x_3 \tag{3.9}$$

$$\dot{m}_1(1-x_1) = \dot{m}_2(1-x_2)+\dot{m}_3(1-x_3) \tag{3.10}$$

$$\dot{E}_1 = \dot{E}_2+\dot{E}_3 \tag{3.11}$$

where the inlet and the outlet energies were determined as:

$$\dot{E}_1 = \dot{m}_{gm}h_{gm}+\dot{m}_{Lm}h_{Lm} \tag{3.12}$$

$$\dot{E}_2 = \dot{m}_2h_{c2}+[\dot{m}_{cw}(h_{cwo}-h_{cwi})]_2 \tag{3.13}$$

$$\dot{E}_3 = \dot{m}_3h_{c3}+[\dot{m}_{cw}(h_{cwo}-h_{cwi})]_3 \tag{3.14}$$

The errors of mass and energy balances were monitored throughout the test period. In most of the test runs the balances exhibited very good results, except for the low branch flow split runs in which relatively large errors of steam mass balance were observed. For the experimental data list in Appendix A, 90% of the data satisfied the total mass balance within $\pm 4\%$ and total energy balance within $\pm 5\%$, water balance within $\pm 4\%$ and steam balance within $\pm 8.5\%$.

The pressure changes of the T-junction $\Delta P_{2\text{-}1}$ and $\Delta P_{1\text{-}3}$ were determined by extrapolating the fully developed pressure profile in the inlet, run and branch to the centre of the junction. The pressure profile in each leg of the T-junction was obtained by the least squares method. This approach is commonly accepted by previous researchers as shown in Fig.2.4.

3.3.2. Experimental uncertainties

The uncertainties of measurement of temperatures, flow rates, flow qualities, void fractions and the pressure changes were evaluated. The detailed calculation can be found

in Appendix B. The results of the experimental uncertainties are summarized in Table 3.1.

Table 3.1 Experimental uncertainties

Variables	Uncertainty
Temperatures T	±1.00%
Inlet water mass flow rate $\dot{m}_{Lm}$	±1.00%
Inlet steam mass flow rate $\dot{m}_{gm}$	±2.00%
Inlet two-phase mass flow rate $\dot{m}_1$	±0.93%
Branch mass flow rate $\dot{m}_3$	±1.00%
Run mass flow rate $\dot{m}_2$	±1.00%
Branch flow split ratio $\dot{m}_3/\dot{m}_1$	±1.37%
Inlet quality x_1	±7.22%
Branch quality x_3	±6.07%
Run quality x_2	±5.73%
Branch to inlet quality ratio x_3/x_1	±9.43%
Void fractions α	±5.00%
Branch pressure drop ΔP_{1-3}	±14.86%
Run pressure recovery ΔP_{2-1}	±13.23%

3.4. Test Conditions

In the annular flow experiments the inlet mass flux G_1 covered the range of 600 to 900 kg/m^2.s and inlet quality covered the range of 2% to 8%. The branch flow split ratio in the present study was varied from 0.1 to 1.0. The inlet pressure was less than 250 kPa in all the experiments. The tests were carried out in two junctions having horizontal inlet and branch downward inclination of 45° and 90°. The above test conditions are identical to those covered by Ballyk (1992) who used a horizontal junction in the same facility. Accordingly, direct comparison with his data on the effect of branch orientation is possible.

In the stratified flow experiments the test condition covered the range of:

inlet mass flux	$50 < G_1 < 90$ kg/m^2.s
inlet quality	$1.5\% < x_1 < 7.0\%$
branch flow split ratio	$0.2 < \dot{m}_3/\dot{m}_1 < 1.0$
branch-to-inlet diameter ratio	$D_3/D_1 = 1.0, 0.33$
branch orientation	$\theta = 0°$ (horizontal) and 90° (vertically downward)

Other stratified flow data were reported by Azzopardi et al. (1988), Reimann et al. (1988) and Shoham et al. (1987), who used the superficial liquid and gas velocities to identify their test condition. For comparison purpose, the present test conditions in terms of superficial velocities are:

superficial vapour velocity	$1.5 < u_{g_s} < 5.0$ m/s
superficial liquid velocity	$0.05 < u_{L_s} < 0.09$ m/s

The data ranges were plotted onto the flow regime map as shown in Fig.3.4. Some major experimental ranges of previous research are also shown in the figure. The inlet flow regimes were identified by visual observation in the present study as annular flow and stratified wavy flows. Smooth stratified flow was never observed in the present test conditions although the experimental range was defined as smooth stratified flow using the flow map of Mandhane et al. (1974).

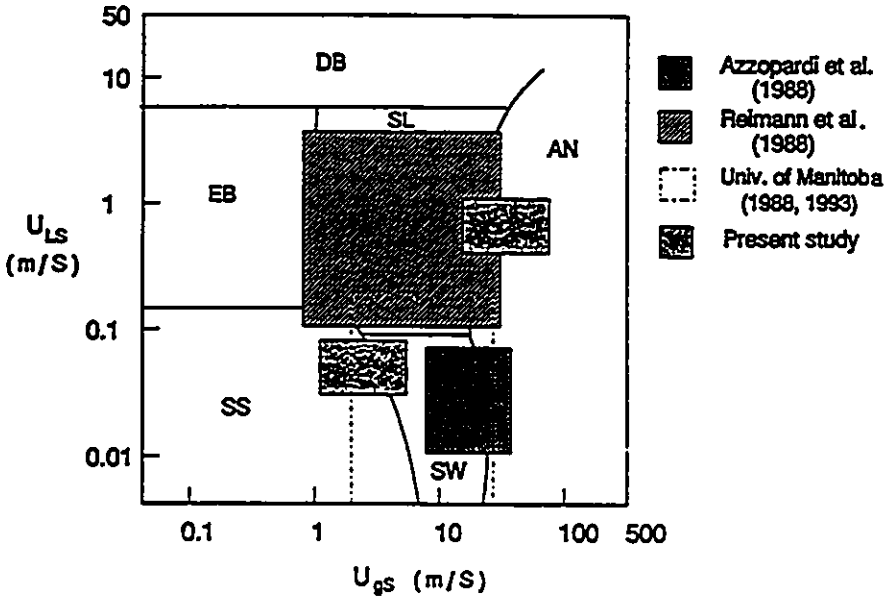

Fig.3.4 Test ranges on the flow map

CHAPTER 4

ANNULAR FLOW EXPERIMENTS

4.1. Introduction

Annular flow is the two-phase flow regime encountered at high gas velocity in a wide range of liquid velocity. As the inlet gas velocity increases, the flow regime in a horizontal tube change from stratified flow at low inlet liquid velocities, or from slug flow at high inlet liquid velocities, to annular flow. In annular flow, most of the liquid flows as liquid film along the tube wall. Part of the liquid phase flows in the form of droplets entrained in the gas core. In horizontal annular flow, since the gravity acts normal to the flow direction, the liquid phase tends to be preferentially distributed towards the bottom of the tube. The extent of the asymmetrical distribution of liquid phase may be offset by wave formation, turbulent mixing and secondary gas flow depending on the inlet velocities of the two phases. Reported experimental and analytical studies have shown that for annular inlet flow the phase redistribution and pressure distribution in T-junctions are complex functions of inlet quality, inlet mass flux, branch flow split ratio, junction geometry etc. Important experimental investigations on the subject of annular flow are due to Collier (1976), Hong (1978), Henry (1981), Azzopardi and his colleagues (1982, 1984, 1988, 1992), Saba and Lahey (1984), Seeger et al.

(1986), Shoham et al. (1987, 1988), Reimann et al. (1988), Ballyk et al. (1988, 1992) and Rubel et al. (1988). Comprehensive reviews of the topic are available by Azzopardi (1986), Lahey (1986) and recently by Müller and Reimann (1991). However, the data base and our understanding of the subject remain incomplete. Most of the existing experimental data were obtained from low pressure and low inlet mass flux air-water annular flow divided in horizontal branches, focusing on the study of the effects of inlet flow conditions. The effects of the junction geometry, e.g. the orientation of the branch, were studied only by a few researchers in limited inlet flow conditions. Recently, experiments on the effect of branch orientation were reported by Azzopardi et al. (1988, 1992) and Reimman et al. (1988) for annular and stratified air-water flows.

The present annular flow work is an extension of that of Ballyk (1992) in which high inlet mass flux annular flow divided in horizontal junctions was studied in detail. The effects of inlet flow conditions and branch diameters were studied separately. This work, however, focuses on the effect of branch orientation on phase redistribution and pressure changes in T-junctions under the same inlet flow conditions. The experiments were performed under test conditions at which the effect of branch orientation was not examined before. The present experiments also included the measurements of void fraction and pressure changes in the junction. Accordingly, it can enhance the current understanding of the phenomenon and contribute to the existing data base on the subject. Moreover, the data obtained in this work are among a few sets of data in which the void fraction in each leg was measured.

4.2. Measurements of Junction Phase Redistribution and Pressure Changes

4.2.1. Phase redistribution in the junction

A substantial part of the liquid in annular flow flows as a thin liquid film along the tube wall. It is, therefore, expected that the liquid film in the main tube segment intercepted by the branch conduit will be the first component to be extracted into the branch. At low branch flow split, most of the branching flow is removed from the liquid film. Accordingly, under such conditions, the branch quality is expected to be below that of the inlet flow. Increasing the branch flow, which corresponds to decreasing the branch downstream pressure, causes more vapour to be extracted through the branch due to its lower axial momentum flux, and thus increasing branch quality. It should be noted that increasing the branch flow split is associated with a pressure rise through the junction run due to flow expansion. This adverse pressure rise yields an additional force which tends to drive the flow through the branch. Since the vapour phase in the inlet tube has a lower axial momentum than the liquid phase, it tends to respond more readily to the decreasing pressure through the branch and the increasing pressure through the run. Accordingly, increasing the branch flow tends to result in an increase in the branch flow quality. At a certain branch flow split ratio, almost all of the inlet vapour will be extracted through the branch. The critical branch flow split ratio, at which almost all the vapour is

extracted through the branch, depends upon the inlet quality, the inlet mass flux and the branch diameter as shown by Ballyk et al. (1988) .

4.2.1.1. Effect of Branch Orientation

Under horizontal annular flow conditions, the orientation of the branch has a significant influence on the redistribution of the two phases in the T-junction due to the non-uniform distribution of the liquid film caused by the gravity force. Unlike vertical annular inlet flow in which uniform angular distribution of the liquid film is expected, in horizontal annular flow the liquid film is expected to drain toward the bottom of the pipe under the influence of gravitational forces, resulting in a thicker film at the bottom. The liquid film, however, is expected to be symmetrically distributed about a vertical plane passing through the axis of the tube.

Typical results showing the effect of branch orientation on phase redistribution are presented in Figs.4.1 to 4.4. The branch quality and mass flux are normalized with respect to inlet conditions, i.e. x_3/x_1 vs. G_3/G_1. Equal phase distribution is represented by horizontal line $x_3/x_1 = 1$, while complete vapour extraction is represented by curve $x_3/x_1 = G_1/G_3$. The results of three branch orientations, i.e. horizontal (Ballyk 1992), 45° downward and 90° downward (present work), under various inlet flow conditions are presented. Within the range of this study, the results show the significant effect of branch orientation on phase redistribution. It is clear that the horizontal branch causes

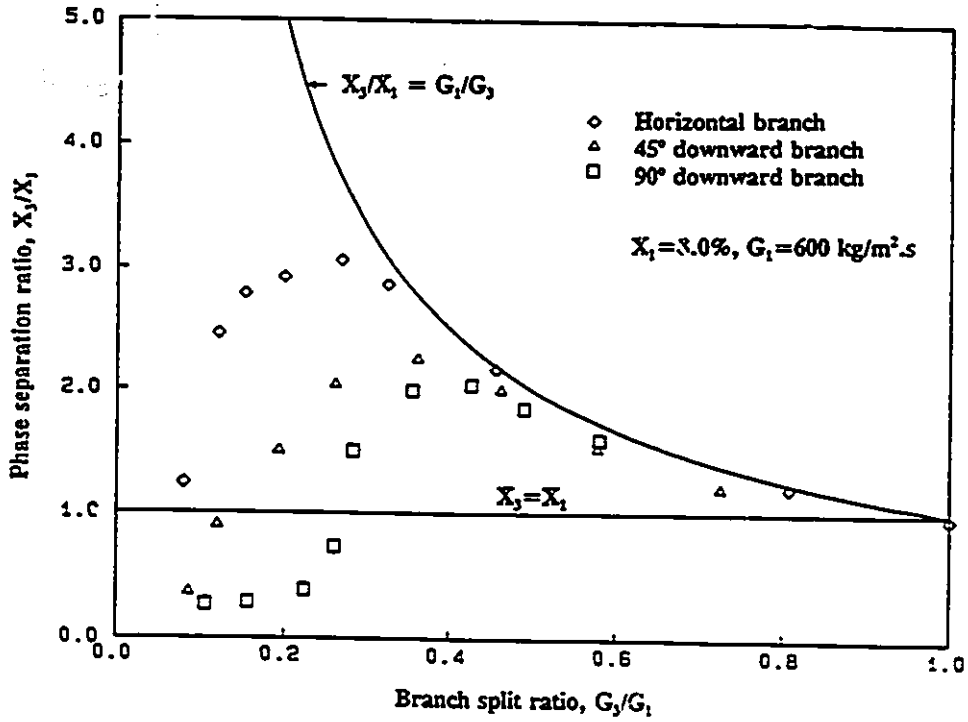

Fig.4.1 Effect of branch orientation (G_1=600 kg/m².s, X_1=8.0%)

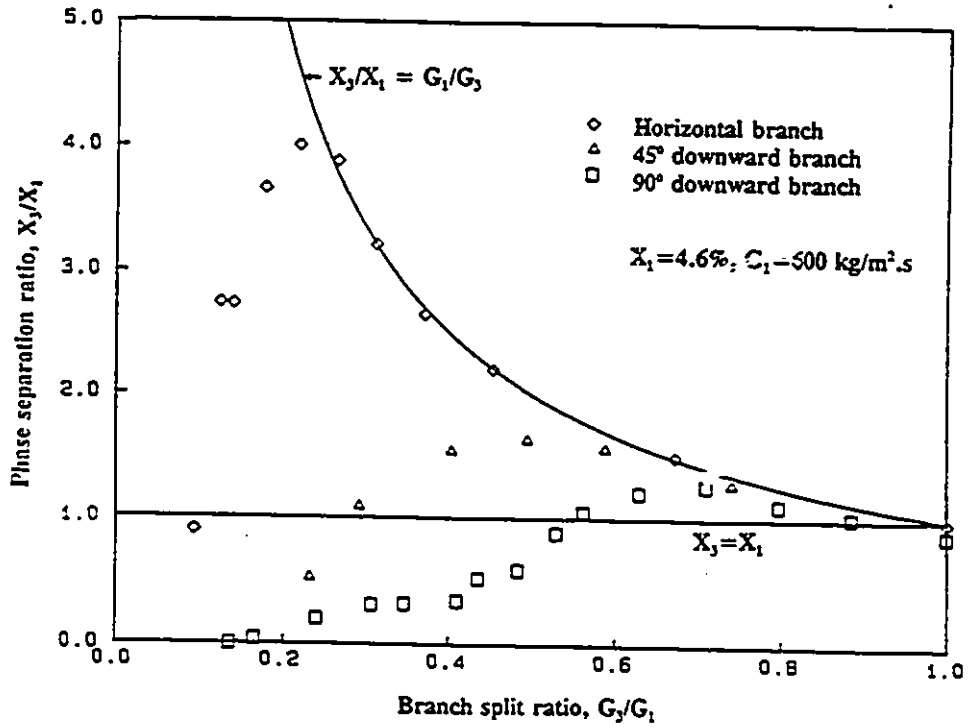

Fig.4.2 Effect of branch orientation (G_1=600 kg/m².s, X_1=4.6%)

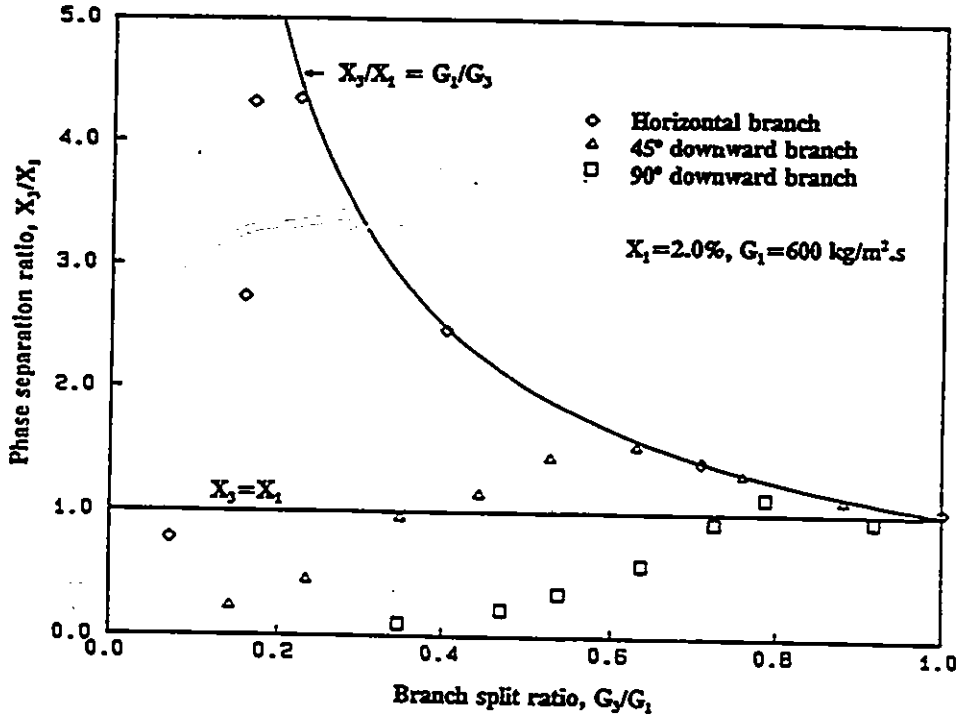

Fig.4.3 Effect of branch orientation (G_1=600 kg/m².s, X_1=2.0%)

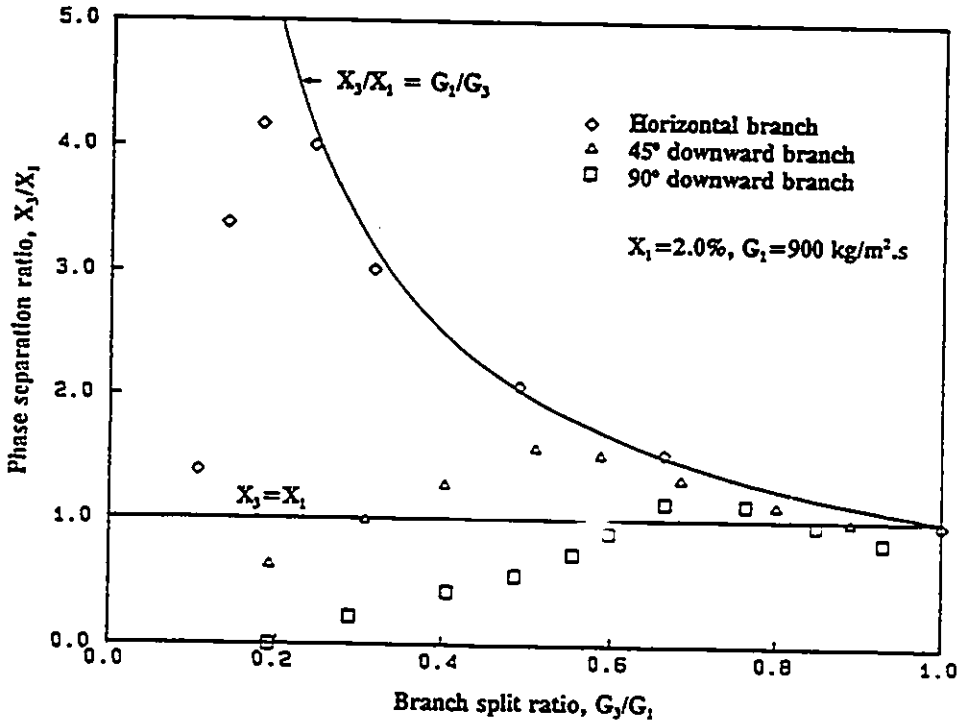

Fig.4.4 Effect of branch orientation (G_1=900 kg/m².s, X_1=2.0%)

the most severe phase redistribution. For the same inlet condition, the results show that rotating the branch downwardly from the horizontal orientation results in reducing the branch quality x_3 through the entire range of flow split ratio. The maximum normalized branch quality is also reduced. Moreover, the flow split ratio at which equal phase distribution and complete vapour extraction occur is moved to a higher value by increasing the downward rotation of the branch.

The trends observed are explained in terms of asymmetrical distribution of the liquid film in the annular inlet flow, having a very thin film at the top with increasing thickness toward the bottom of the tube. By downward rotation of the branch, more liquid becomes readily available for extraction, resulting in higher liquid content in the branch flow at any given flow split ratio. The recent results of Azzopardi and Smith (1992) for upward branches appear as a natural extension of the trends described above for downwardly inclined branches. Azzopardi and Smith (1992) showed that for an upward branch, the branch quality increased significantly over that for a horizontal branch under the same inlet annular flow conditions. However, direct comparison with the present results cannot be carried out since their results were obtained for air-water annular flow at low inlet mass flux, $G_1 < 100$ kg/m^2.s, and high inlet quality $0.60 < x_1 < 0.90$.

It is interesting to note that the asymmetrical distribution of the liquid film thickness depends on the inlet quality and mass flux. For high quality annular flow a more uniform liquid film may be generated, and one would expect the effect of the

branch orientation on the junction phase separation may reduce or diminish at such inlet conditions.

4.2.1.2 Effect of Inlet Mass Flux and Quality

Fig.4.5 and 4.6 show the effect of inlet mass flux on phase redistribution in the T-junction with downward branches. The results clearly showed that, independent of the branch orientation, the inlet mass flux had little effect on the phase redistribution phenomenon. Higher inlet mass flux caused the degree of phase redistribution to increase slightly. It is believed that this effect is generated because of the increase of liquid axial momentum flux. The trend is consistent with those observed by other researchers, e.g. Azzopardi et al. (1988) in low inlet mass flux annular flow conditions.

It is also interesting to note that the effect of inlet quality on phase redistribution is greatly dependent on branch orientation. This effect is seen from the data presented in Figs.4.7 to 4.9 where at a fixed inlet mass flux $G_1 = 600$ kg/m^2.s, the effect of inlet quality is shown for the horizontal, 45° downward and 90° downward branches respectively. The data for the horizontal branch are reproduced from the work of Ballyk (1992) and are shown in Fig.4.7. It can be seen that an increase of inlet quality results in reducing the extent of the phase redistribution and increasing the flow split ratio at which complete phase redistribution is encountered. This is caused by the increase in the thickness of the liquid film available for extraction as the liquid film tends to be more

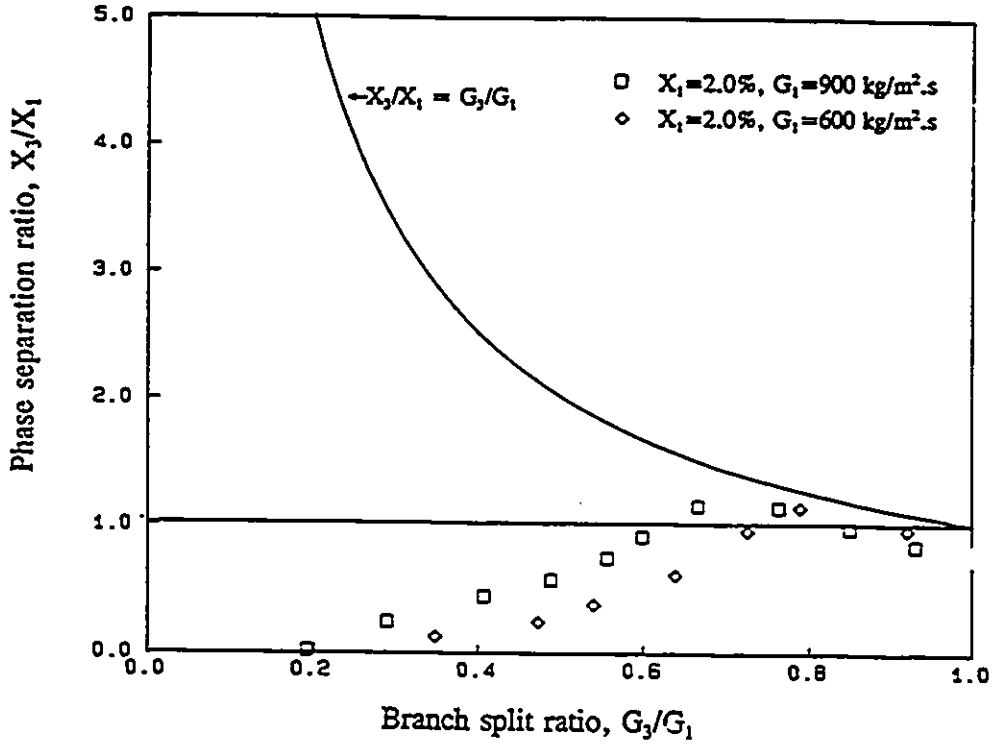

Fig.4.5 Effect of inlet mass flux (X_1=0.02, θ=90°)

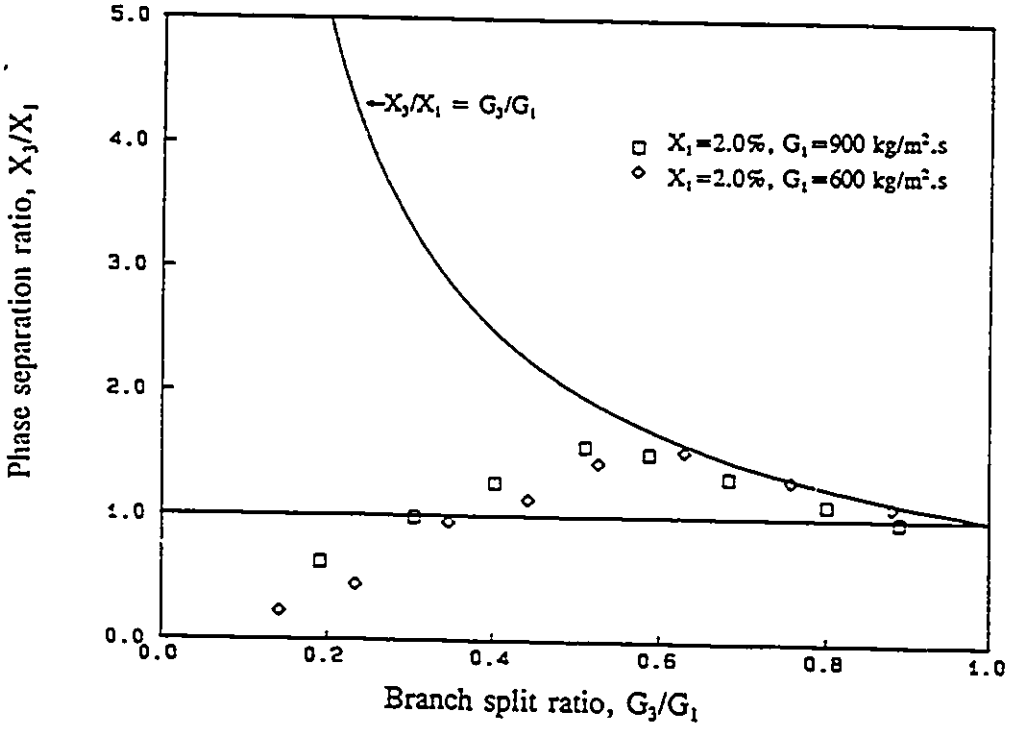

Fig.4.6 Effect of inlet mass flux (X_1=0.02, θ=45°)

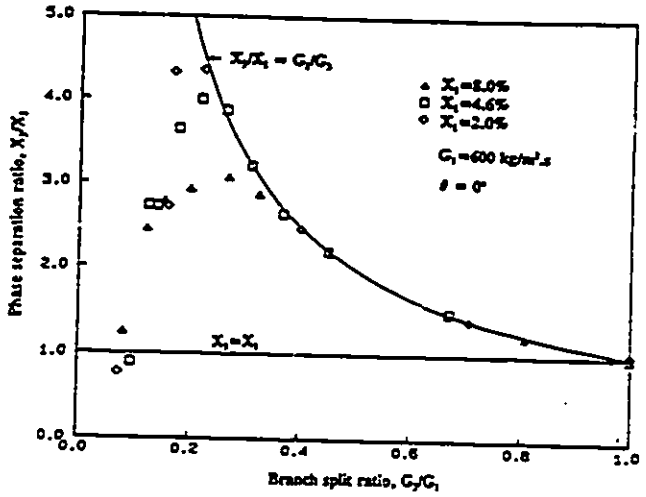

Fig.4.7 Effect of inlet quality (G_l=600 kg/m².s, θ=0°)

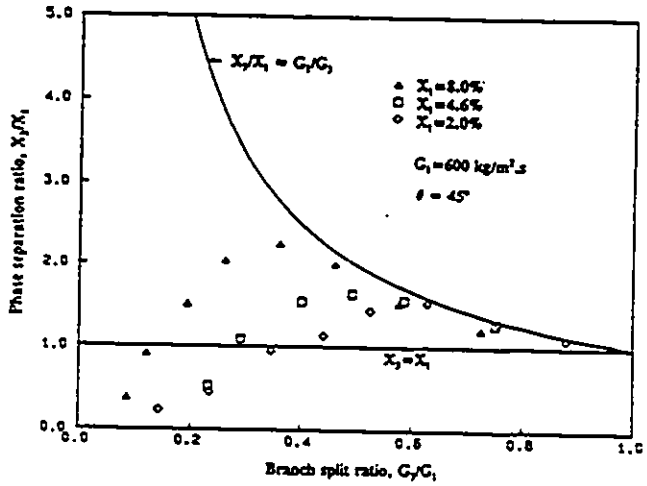

Fig.4.8 Effect of inlet quality (G_l=600 kg/m².s, θ=45°)

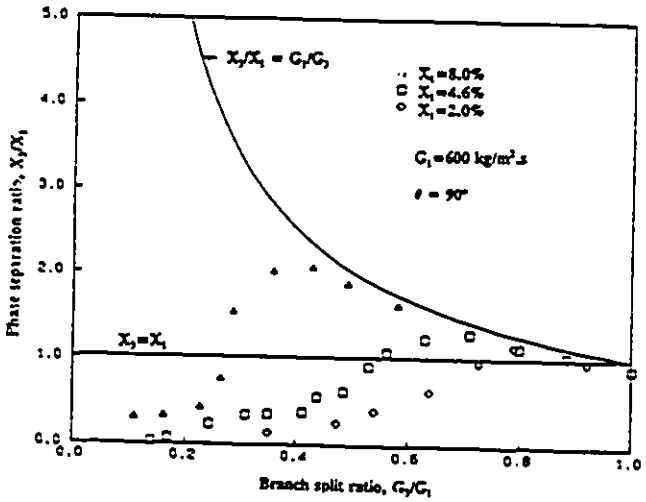

Fig.4.9 Effect of inlet quality (G_l=600 kg/m².s, θ=90°)

uniform with increasing vapour velocity, i.e. increasing inlet quality. However, this increase of inlet quality which corresponds to a more uniform liquid film, causes the film thickness at the bottom to decrease. As a result, less liquid becomes available for extraction to the downwardly inclined branches. Accordingly, the effect of inlet quality is reversed in the 90° downward branch as shown in Fig.4.9, i.e. the degree of phase separation increases with increasing inlet quality. The same effect is observed, but to a less extent, in the 45° inclined branch as shown in Fig.4.8.

4.2.2. Pressure changes in the junction

The pressure changes in the T-junction are normally modelled by both momentum and mechanical energy balances. When a flow is divided in a T-junction the deceleration of the fluid causes a reversible pressure rise in the run and branch due to the Bernoulli effect. Previous studies have shown that the irreversible pressure drop is much lower than the Bernoulli type reversible pressure recovery in the run. As a result, there is a net pressure rise in the run and the axial pressure recovery is usually based on a momentum balance model. Studies also indicated that the irreversible pressure drop is much higher than the reversible pressure rise in the branch. Accordingly, there is a net pressure drop in the branch which is typically modelled based on a mechanical energy balance. Using these models, the data are usually reduced to obtain the required empirical coefficients. In these simple models, it is assumed that the static pressure across any flow channel is

uniform and the velocities are parallel to the conduit walls, therefore, the momentum flux and kinetic energy correction factors are equal to one.

4.2.2.1. Single-phase flow

By applying the momentum and mechanical energy equations to model the run pressure rise and the branch pressure drop respectively, it can be shown that for single-phase flow:

$$\Delta P_{2\text{-}1} = K_{12}\rho(u_1^2 - u_2^2) \tag{4.1}$$

$$\Delta P_{1\text{-}3} = \frac{\rho}{2}(u_3^2 - u_1^2) + K_{13}\frac{\rho u_1^2}{2} \tag{4.2}$$

where $\Delta P_{2\text{-}1}$ and $\Delta P_{1\text{-}3}$ are the run pressure rise and branch pressure drop respectively. K_{12} is known as the run momentum correction factor, which accounts for the indeterminant axial momentum carried out of the control volume by the branching flow. K_{13} is the mechanical energy loss coefficient due to the dissipation in the T-junction. The experimental measurements of $\Delta P_{2\text{-}1}$ and $\Delta P_{3\text{-}1}$ are obtained by extrapolating the fully developed pressure profile in the conduits to the junction centre line. The single phase run momentum correction factor K_{12} and branch energy loss coefficient K_{13} were obtained in the present 90° downward branch using Eqns.(4.1) and (4.2) and were shown in Figs.4.10 and 4.11 respectively. They were found to agree with the following

correlations suggested by Ballyk et al. (1988) for the horizontal branch,

$$K_{12} = 0.704 - 0.320 \left(\frac{G_3}{G_1}\right) - 0.028 \left(\frac{G_3}{G_1}\right)^2 \qquad (4.3)$$

$$K_{13} = 1.081 - 0.914 \left(\frac{G_3}{G_1}\right) + 1.050 \left(\frac{G_3}{G_1}\right)^2 \qquad (4.4)$$

It indicates that there is no effect of branch orientation on single-phase empirical coefficients K_{12} and K_{13}.

4.2.2.2. Two-phase flow

Simplification of the momentum and mechanical energy equations of two-phase flow in the T-junction can be achieved by assuming homogeneous or phase-separated flow. Besides the assumptions applied to single-phase flow, the following additional assumptions are applied to two-phase flow in the junction.

i. thermal equilibrium exists between the phases,

ii. the pressure changes in the junction are small relative to the absolute pressure of the system, and

iii. uniform void fraction is present across the piping conduits.

A typical two-phase flow pressure distribution obtained in the inlet, run and branch is presented in Fig.4.12.

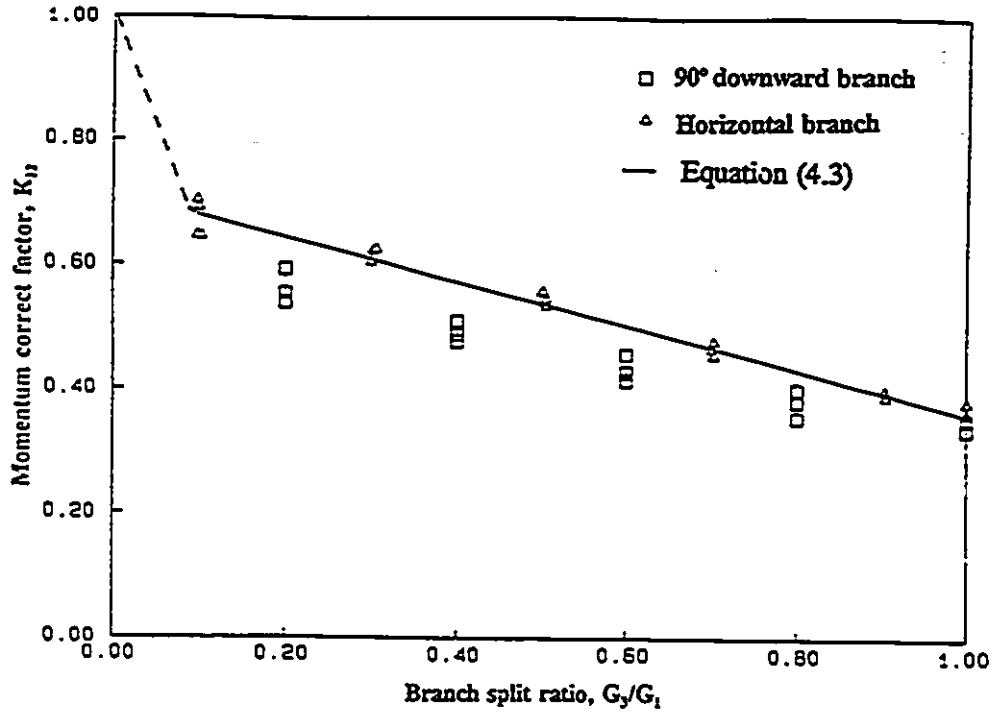

Fig.4.10 Single-phase run momentum correction factor

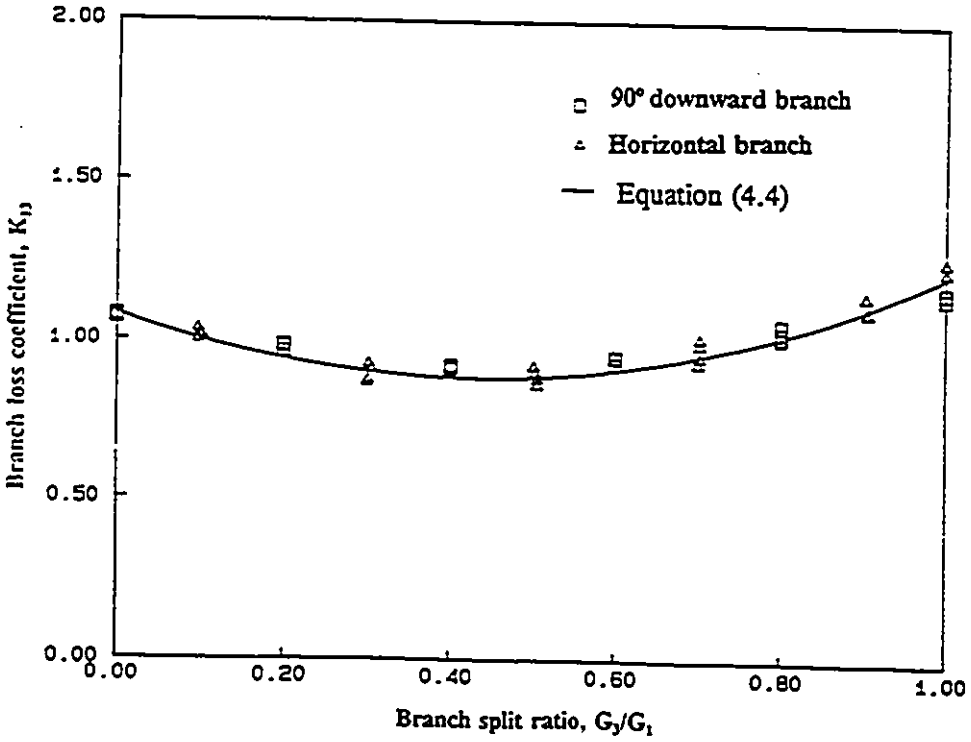

Fig.4.11 Single-phase branch energy loss coefficient

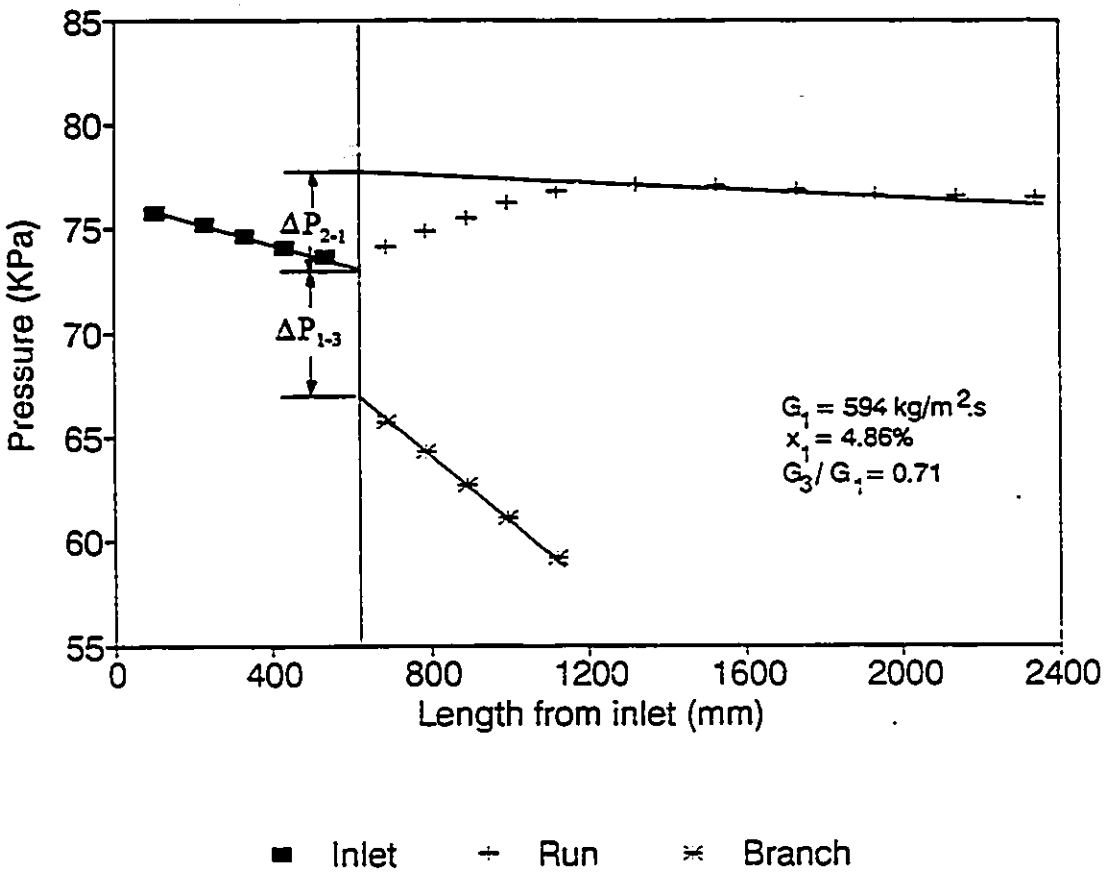

Fig.4.12 Typical pressure distributions in the inlet, run and branch (90° downward branch)

4.2.2.2.1. Run Pressure Recovery

Most available models for two-phase pressure changes in T-junction are simple extensions of Eqns. (4.1) and (4.2). As summary of the methods suggested in the literature for modelling the pressure recovery in the run was given in Section 2.3.2, Chapter 2. The correlations suggested were based on data obtained for a horizontal branch. Their applicability to junctions with downwardly inclined branches with inlet annular flow are tested here.

Saba and Lahey (1984) suggested the use of axial momentum balance in which the homogeneous density is used to represent the mixture density and the single phase run momentum correction factor is employed, i.e.

$$\Delta P_{2\text{-}1} = P_2 - P_1 = K_{12} \left(\frac{G_1^2}{\rho_{h1}} - \frac{G_2^2}{\rho_{h2}}\right) \tag{4.5}$$

The present results, together with those of Ballyk (1992), for annular flow in T-junctions, are compared with the predictions of the above equation in figure 4.13.

Assuming separated flow, the axial momentum balance yields:

$$\Delta P_{2\text{-}1} = P_2 - P_1 = K_{12s} \left(\frac{G_1^2}{\rho_{m1}} - \frac{G_2^2}{\rho_{m2}}\right) \tag{4.6}$$

where K_{12s} is the two-phase momentum correction factor and ρ_m is the momentum density.

Several two-phase momentum correction factors have been suggested by various researchers for the T-junction with a horizontal branch. Fouda and Rhodes (1974) recommended that $K_{12s} = 0.533$. Madden and St. Pierre (1969) and Ballyk et al. (1988) showed that $K_{12s} = 1.0$ under annular inlet flow conditions. The work of Ballyk et al. (1988) was the only one in which the momentum density was calculated using measured void fractions. Other researchers used empirical void fraction correlations for calculating the densities of the mixture.

The two-phase momentum correction factor K_{12s} was evaluated from the present data, based on the measured void fractions, for the T-junctions with the branch downwardly inclined by 90° and 45°. Physically, K_{12s} is the correction factor which accounts for the axial momentum flux taken off by the branch flow. For a horizontal branch, Ballyk et al. (1988) showed that K_{12s} equals to unity, which indicates that the axial momentum flux carried by the branch is insignificant. In the case of downwardly oriented branches, more water is extracted into the branch because of the gravitational forces. As the water film has a higher axial momentum than the vapour phase, due to its high density, more axial momentum flux will be taken from the control volume. Consequently, the axial momentum correction factor should be smaller than that of horizontal branch junction. This study shows that K_{12s} can be approximated by 0.78 and 0.42 for the 45° and 90° downward branches respectively. Using the measured void fractions the present data, together with those of Ballyk(1992) obtained from horizontal branch, are used to evaluate the model represented by equation (4.6) in figure 4.14.

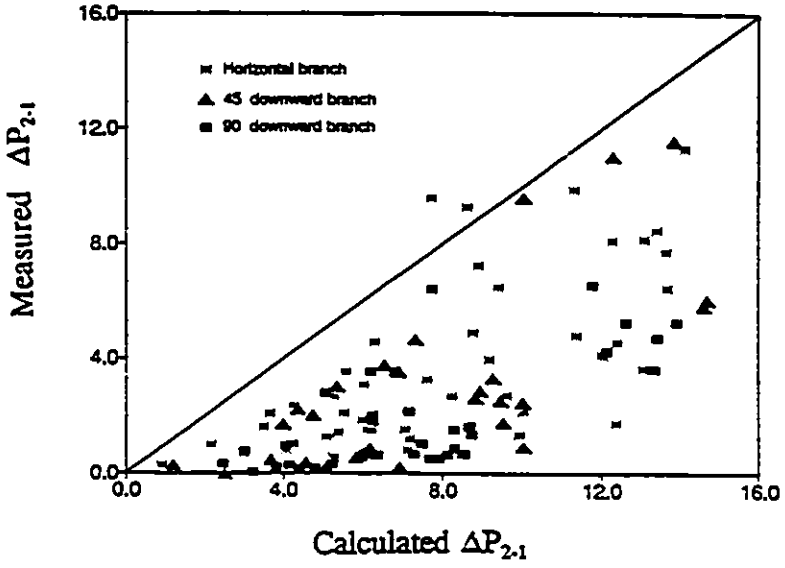

Fig.4.13 Comparison of Saba and Lahey (1984) correlation

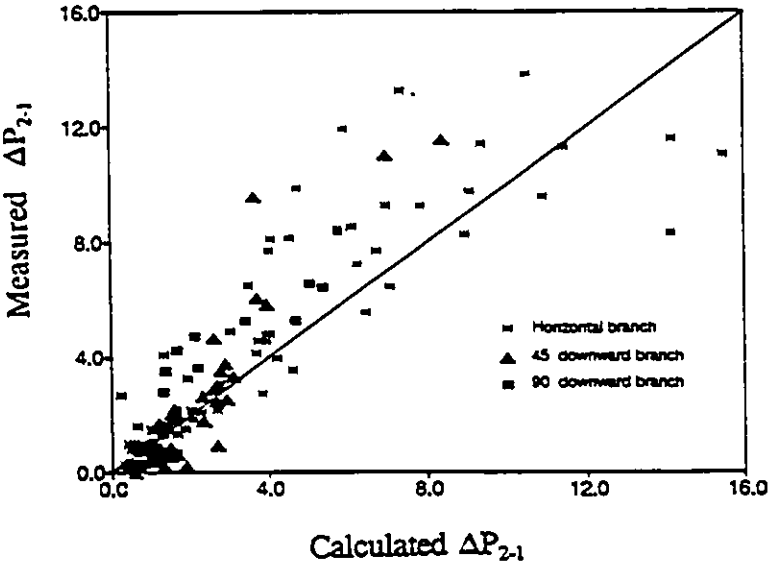

Fig.4.14 Comparison of separated flow correlation

4.2.2.2.2. Branch pressure drop

The models used for two-phase pressure drop in the branch are also extensions of the single phase case, and can generally be written in the mechanical energy balance form,

$$\Delta P_{1\text{-}3} = P_1 - P_3 = \frac{\rho_{h3}}{2}\left(\frac{G_3^2}{\rho_3^2} - \frac{G_1^2}{\rho_1^2}\right) + K_{13}\,\frac{G_1^2}{2\rho_L}\bar{\phi}_{tp} \qquad (4.7)$$

here K_{13} is the single-phase energy loss factor and $\bar{\phi}_{tp}$ is a two-phase multiplier. Available models differ in their definitions of the densities, ρ_1 and ρ_3, and the multiplier $\bar{\phi}_{tp}$.

Saba and Lahey (1984) and Reimann and Seeger (1986) recommended the use of the homogeneous density ρ_h given by:

$$\rho_{hi} = \left[\frac{x_i}{\rho_g} + \frac{(1-x_i)}{\rho_L}\right]^{-1}, \quad i = 1, 3 \qquad (4.8)$$

With the homogeneous model, Saba and Lahey (1984) correlated the two-phase multiplier by, $\bar{\phi}_{tp}=\rho_L/\rho_{h1}$ for homogeneous flow model, while Reimann and Seeger (1986) suggested that $\bar{\phi}_{tp}=\rho_L\rho_{h3}/\rho^2_{h1}$.

Saba and Lahey (1984) recommended also that if the momentum density was used for ρ_1 and ρ_3 in equation (4.7) then the two-phase multiplier for this separated flow model should be defined by $\bar{\phi}_{tp}=\rho_L/\rho_{m1}$.

The predictions of the above three correlations are compared with the present data for downwardly inclined branches in Figures 4.15 to 4.17. All the models appear to predict the data well in the range of high branch split ratio, $G_3/G_1 > 0.6$. In the lower range of branch split ratio, the models are inadequate, although Reimann and Seeger's model appears to be somewhat better.

Through a consistent application of the mechanical energy balance, Ballyk at al. (1988) derived an equation for the branch pressure drop similar to Eqn. (4.7). However, the branch and inlet densities were defined by

$$\rho_3 = \rho_{e3} = \left[\frac{x_3^3}{\alpha_3^2\rho_g^2} + \frac{(1-x_3)^3}{(1-\alpha_3)^2\rho_L^2}\right]^{-0.5} \tag{4.9}$$

and

$$\rho_1 = \rho^* = \left[\frac{x_1^2 x_3}{\alpha_1^2\rho_g^2} + \frac{(1-x_1)^2(1-x_3)}{(1-\alpha_1)^2\rho_L^2}\right]^{-0.5} \tag{4.10}$$

Moreover, Ballyk et al. (1988) defined the multiplier $\bar{\phi}_{tp}$ by,

$$\bar{\phi}_{tp} = \frac{\rho_L\rho_{h3}}{\rho^{*2}}\phi_{tp} \tag{4.11}$$

where ϕ_{tp} was experimentally determined for horizontal T-junctions. It is interesting to note that the above model and that of Reimann and Seeger (1986) include characteristics of phase redistribution in pressure drop term. This was shown by Ballyk et al. (1988) to

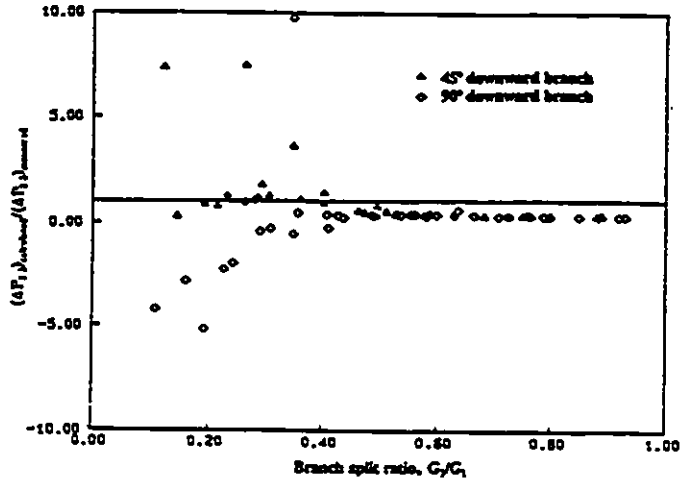

Fig.4.15 Comparison of Saba and Lahey (1984) separated model

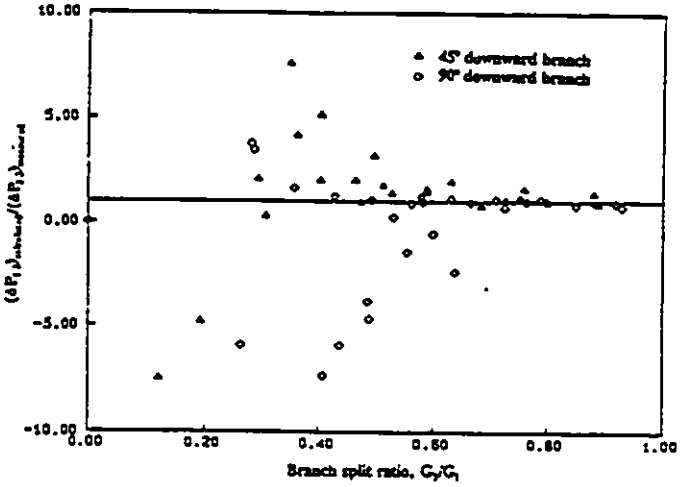

Fig.4.16 Comparison of Saba and Lahey (1984) homogeneous model

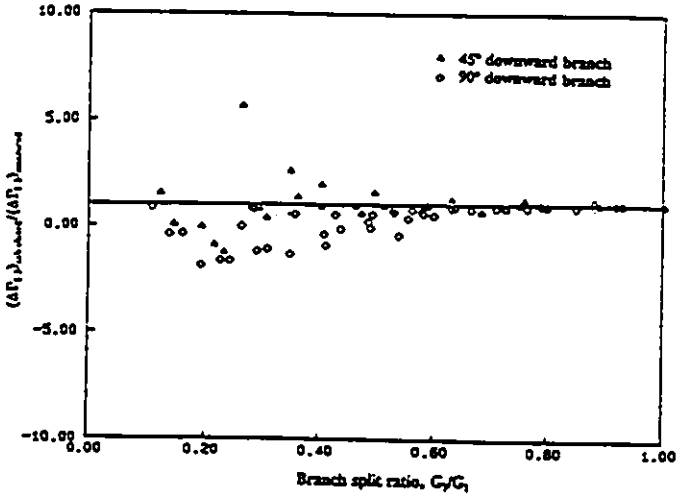

Fig.4.17 Comparison of Reimann and Seeger (1986) homogeneous

be consistent with the mechanical energy balance assumptions.

The present data were used to calculate the multiplier ϕ_{tp} using Eqns. (4.7), (4.9), (4.10) and (4.11). The results were empirically correlated, independent of branch orientation, by the following expression as shown in Fig. 4.18,

$$\phi_{tp} = 0.603+3.193(\frac{G_3}{G_1})+14.210(\frac{G_3}{G_1})^2+10.354(\frac{G_3}{G_1})^3-20.730(\frac{G_3}{G_1})^4 \quad (4.12)$$

The comparison between the branch pressure drop calculated by this correlation and the experimental measurements is presented in Fig. 4.19 where 75% of the data lies within $\pm$50% of the predictions. Although this may not be very good, it is far superior than available correlations. Eqn. (4.12) is an updated correlation from that presented earlier by Ballyk et al. (1988).

4.3. Conclusion

Detailed experimental data on dividing steam-water annular flow in T-junctions having horizontal inlet and downwardly inclined branches were obtained. The branch orientation was found to be a significant parameter affecting phase redistribution under horizontal annular inlet flow condition. The effect of branch orientation on phase redistribution is mainly caused by the non-uniform thickness distribution of the liquid film in the inlet tube, typical of horizontal annular flow. The results showed that, in general, downward rotation of the branch results in less vapour extraction as the liquid

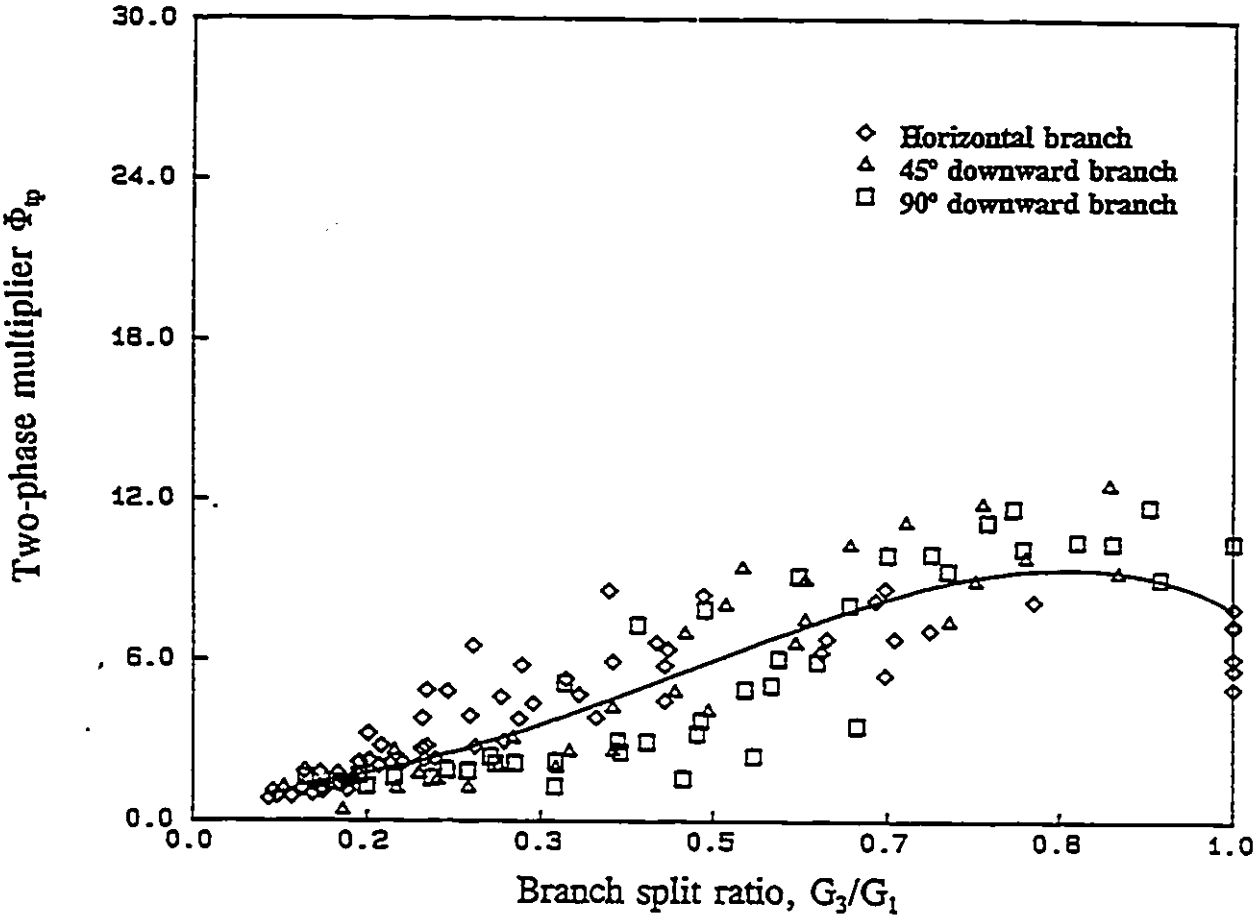

Fig.4.18 Annular two-phase multiplier

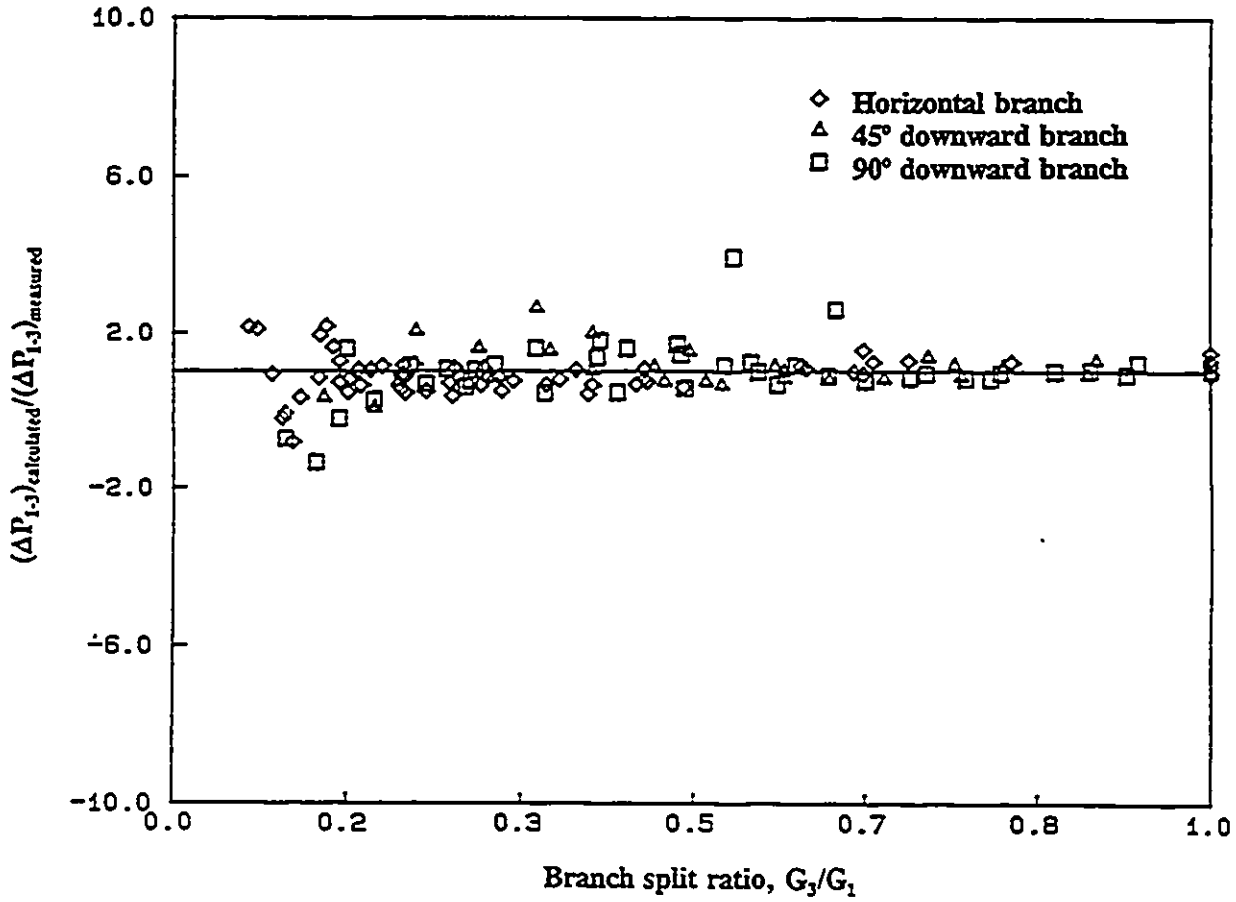

Fig.4.19 Comparison of Ballyk and Shoukri (1988) correlation with present experimental data

film available for extraction is thicker. The inlet mass flux was found not to have significant effect on the phase redistribution phenomenon under the present test conditions. However, the inlet quality has a pronounced effect. Changing the inlet quality affects the liquid film thickness distribution and accordingly affects the phase redistribution phenomenon.

The data on pressure changes through the junction were correlated using simple models based on momentum and mechanical energy balances. The run pressure recovery data was correlated using a momentum balance model. The momentum correction factor was found to depend on branch orientation. The branch pressure drop was correlated using a mechanical energy model and the two-phase multiplier which was found to be independent of branch orientation. The subject of correlating the pressure changes in T-junctions still requires additional efforts. Current methods are seen yet unsatisfactory.

CHAPTER 5

EXPERIMENTS OF STRATIFIED FLOW

5.1. Introduction

Most of the existing experimental data on two-phase flow in T-junctions were collected in annular or bubbly flow regimes. The available data on phase redistribution in stratified flow came from Collier (1976), Hong (1978), Rubel et al. (1988), Shoham et al. (1987,1989), Reimann et al. (1988) and recently from Azzopardi and Smith (1992) and Buell et al. (1993). Phase redistribution in the stratified flow regime and especially the associated pressure characteristics have received less attention by previous researchers as compared to annular flow. The void fraction and the pressure changes in the junction were not measured in most of the above mentioned works. The present work focuses on the stratified flow regime at a range of test conditions which has not been examined before, to study the effects of inlet flow conditions and junction geometries on both phase redistribution and pressure changes in the T-junction. Accordingly this work complements the available data bank on the subject and enhances the understanding of the phenomena. The data collected in this study are also benchmark data for the development of a phase redistribution model for stratified flow in Chapter 6.

5.2. Measurements of Inlet Liquid Level

Stratified two-phase flow in a horizontal pipe is encountered at low flow rates of the two phases due to the effect of gravity. In stratified flow, the liquid flows on the bottom of the tube while vapour flows co-currently above the liquid layer. The height of the liquid layer is a characteristic parameter of the structure of stratified flow. Earlier data on stratified flow in T-junctions indicated that the height of liquid layer in the inlet main tube would significantly affect phase redistribution downstream of the T-junction. The knowledge of liquid level, as a function of inlet flow conditions is of great importance to improve the understanding of phase redistribution in the T-junction. However measurement of liquid level has never been taken in the previous studies of stratified flow in T-junctions. To improve the understanding of the phenomenon, the liquid level of inlet flow was measured in this study by an ultrasonic pulse-echo technique and compared with some models of stratified flow. These measurements are the complementary information for the analysis of the phase redistribution data.

5.2.1 Ultrasonic pulse-echo technique

The ultrasonic pulse-echo technique has been used successfully to determine the transient liquid level in stratified flow by Chang et al. (1990). An ultrasonic wave is propagated through vibration of the particles in the medium. When an ultrasonic wave

is incident normally to the interface between two media, the reflection coefficient R is defined as:

$$R=\frac{I_r}{I_i}\left[\frac{\rho_2 c_2-\rho_1 c_1}{\rho_2 c_2+\rho_1 c_1}\right] \qquad (5.1)$$

where I_i and I_r are the intensities of the incident and reflected waves, ρ is the density and c is the sound speed in the medium of transmission. The product of ρc is also called the characteristic acoustic impedance. Due to the large difference of the characteristic acoustic impedance between the liquid and vapour phases, almost 99 % of the incident wave will be reflected back from liquid-vapour interface. This phenomenon is the basis of the application of the ultrasonic pulse-echo technique in two-phase flow research. The liquid level can be determined by measuring the time-of-flight of the reflected wave relative to the incident wave.

5.2.2. Determination of the liquid level

The measurements of the liquid level in the inlet tube were performed using a commercial ultrasonic analyzer (Panametrics 5052PR) and a contact transducer (Panametrics A104, 2.25 MHz). Panametrics 5052PR is a broadband ultrasonic pulser/receiver unit which provides continuous repetitional pulse over the range of 200 to 5000 Hz. The transducer was mounted on the bottom outside wall of the transparent section of the inlet tube. This transparent part of the test section was made of

polysulphone which makes it possible to visually observe the inlet flow pattern. A block diagram of the measurement is shown in Fig.5.1a. The first echo, as show in Fig.5.1b, is reflected by the interface between the liquid and solid wall, the second echo is reflected by the interface between the liquid and vapour phases. The time-of-flight of the echoes T_i can be measured either analogically by an oscilloscope or digitally by a logic circuit via a computer. The instantaneous liquid level h(t) is evaluated as:

$$h(t)=\frac{1}{N}\sum_{i=1}^{N}\frac{1}{2}cT_i \qquad (5.2)$$

where c is sound velocity in the water, T_i is the measured time-of-flight by oscilloscope or computer and N is the number of measurements. For the stratified wavy flow the repetition frequency generated by the ultrasonic analyzer is much higher than the movement frequency of the wave, therefore, the sampling rate is fast enough to capture the dynamic characteristics of the moving interface. However, for higher superficial vapour velocity tests, the averaged echo flight time was difficult to determine by the oscilloscope due to the high fluctuation of the signal. A logic circuit was designed to obtain the average echo flight time. The basic design of this logic circuit was a modification of the work of Chang et al. (1990). A 10 Mhz 16 bit counter was used to measure the echo time-of-flight. A 0.1 microsecond time resolution is achieved and a maximum of 4.9 m height of water level can be detected for a steam-water system. A signal logic schematic and block diagram of this specially designed circuit is shown in Figs.5.2 and 5.3.

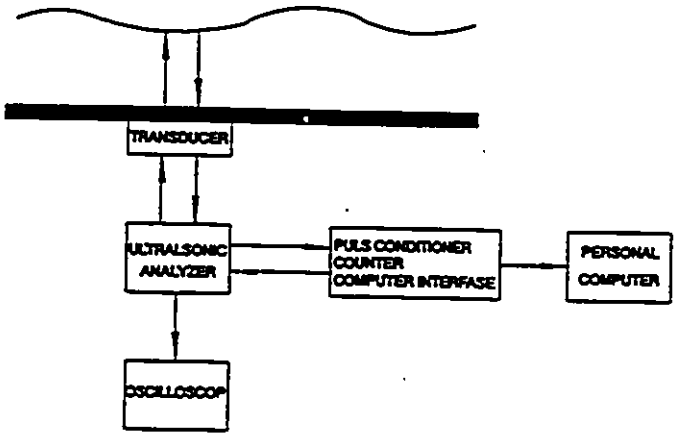

Fig.5.1a Ultrasonic measurement block diagram

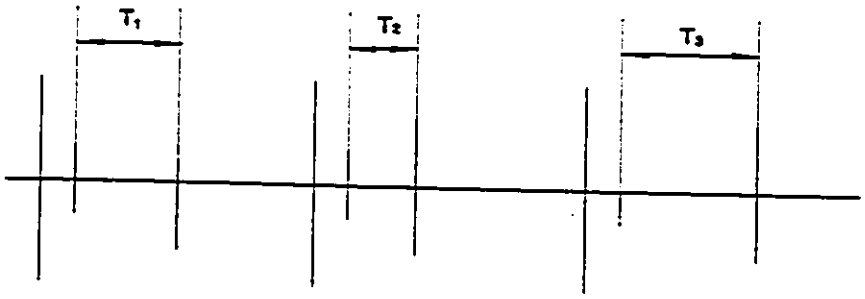

Fig.5.1b Ultrasonic echo signals

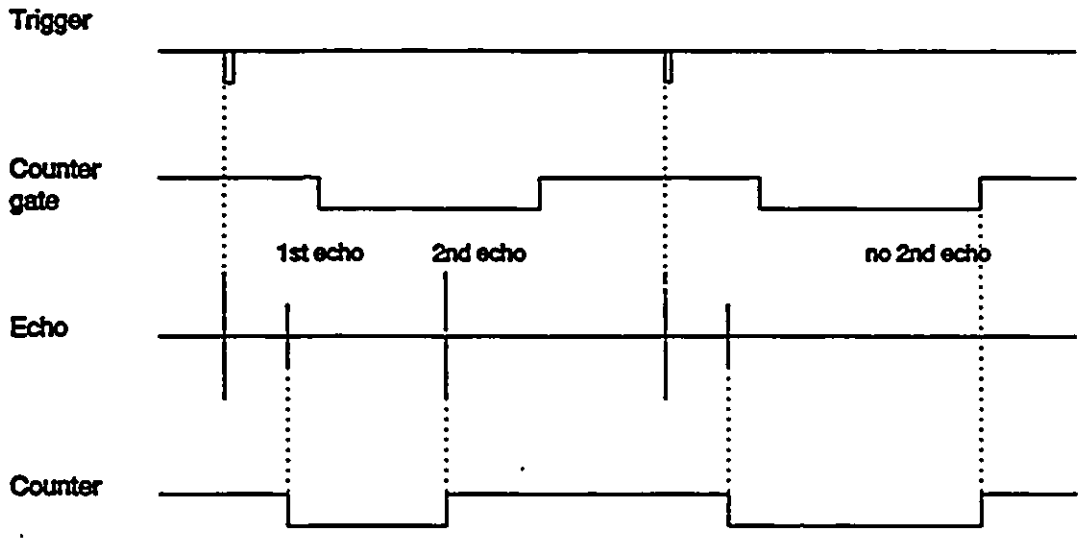

Fig.5.2 Signal logic schematic

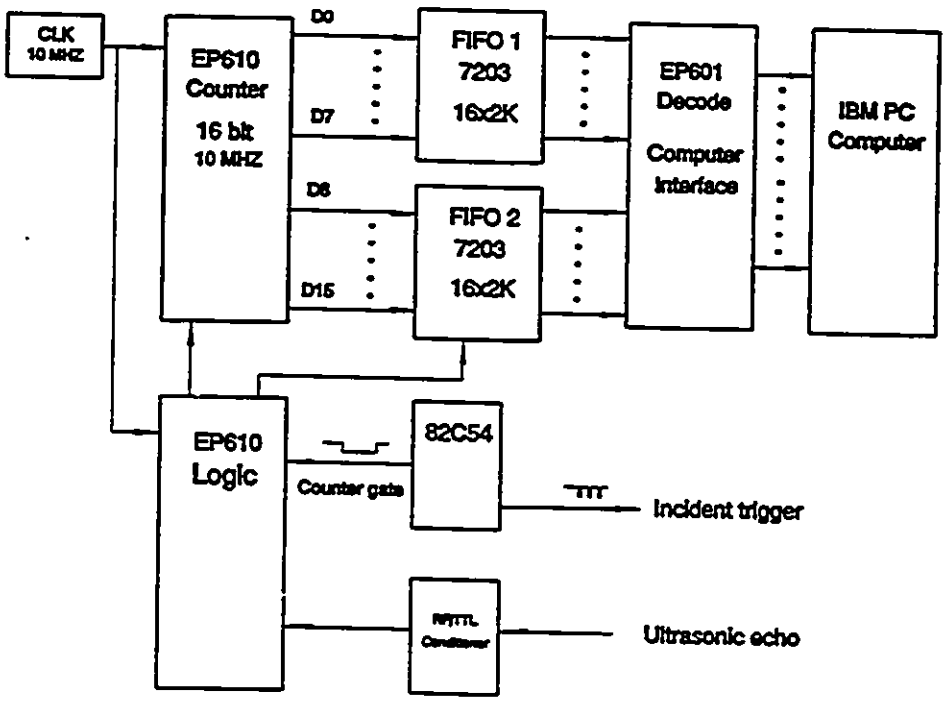

Fig.5.3 Digital circuit of signal conditioner

The incident trigger is generated by a programmable timer 82C54 via the external trigger connector of the ultrasonic analyzer Panametrics 5052PR. After a short time delay ($0.2\mu s$) the counter is enabled by the timer 82C54. A counter gate is also generated by the timer 82C54 which is programmable by the software to meet different requirements of the flow structure. The 16 bit counter is created by a programmable logic array EP610 with a 10 Mhz clock. When the first echo pulse, reflected by the liquid-wall boundary, is received by the ultrasonic analyzer, it is channelled through a pulse echo conditioner to convert to transistor-transistor logic (TTL) standards and is used to start the counter. The second echo signal, which is the reflection of the liquid-vapour boundary, is used to stop the counter. The binary count is then written to a 16 bit 4K high density First-In First-Out (FIFO) memory. The strength of the return echo signal is dependent upon the reflective area of the interface assuming that the attenuation in the fluid is negligible and the reflection coefficient R of the interface is high. It was found that for very wavy stratified flow the amplitude of the signal was much smaller than that of stationary stratified flow. Certain signals may be missed if a large amplitude roll wave comes. To solve this problem, one bit of the FIFO serves as the status bit. If the second echo is received, it is written as 0, if no second echo is detected the counter is stopped at the rising edge of the counter gate generated by the timer 82C54 (see Fig.5.2) and the status bit is written to 1. The data saved in the FIFO are transferred to a PC computer via an interface. The averaged liquid level is then evaluated by Eqn.(5.2).

Sound speed c in the water was determined by measuring the averaged time-of-

flight of the pulse echo in the test section of 76 mm diameter filled with water. The effect of water temperature on the sound speed was first examined within the temperature range of 20 to 80 ℃ and no temperature effect was found under these conditions. Fig.5.4 shows typical signals observed on the oscilloscope screen at a fixed superficial liquid velocity of 0.07 m/s with various superficial vapour velocities of 0, 1.5, 2.5 and 5.0 m/s. In single-phase water flow, the detected time period of the echo pulse is 98.4 μs, indicating that the sound speed in water is 1545 m/s in the present test conditions. Fig.5.4 also shows that, with increasing superficial vapour velocity at a fixed liquid velocity, the level of the liquid decreases.

5.2.3. Stratified liquid level results

The experimental data obtained on the stratified liquid level in terms of the superficial liquid and vapour velocities are shown in Figure 5.5. The dimensionless liquid level h/D is given as a function of the Martinelli parameter X_{tt} for three different liquid velocities. The Martinelli parameter is defined by:

$$X_{tt}=\left(\frac{\nu_l}{\nu_g}\right)^{0.2}\left(\frac{\rho_g}{\rho_l}\right)^{0.8}\left(\frac{1-x}{x}\right)^{1.8} \tag{5.3}$$

The data shows a sudden drop in the measured h/D values at X_{tt} value of about 1.0. It should be noted that for a given value of the superficial liquid velocity a decrease in X_{tt} implies increasing the vapour velocity. As shown for high X_{tt} values, i.e. low

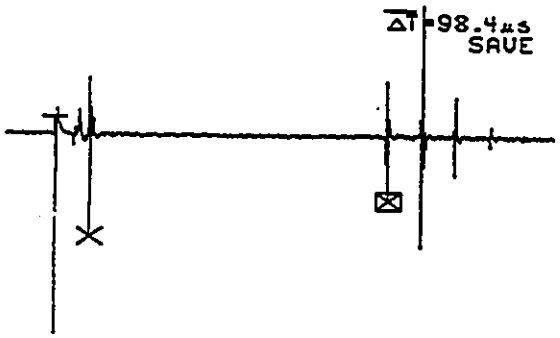

u_{Ls} = 0.07 m/s
u_{gs} = 0.00 m/s

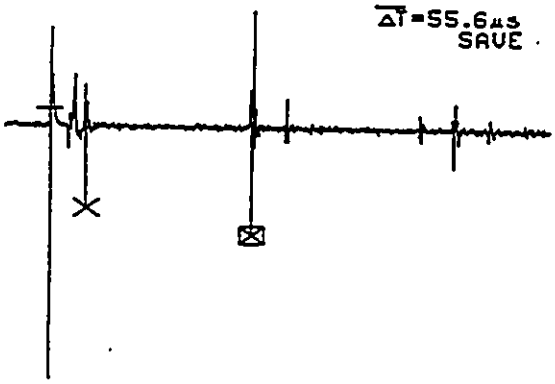

u_{Ls} = 0.07 m/s
u_{gs} = 1.50 m/s

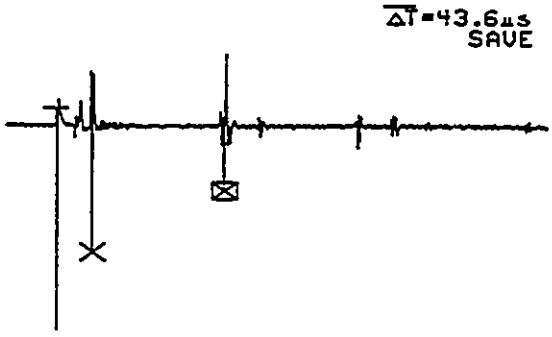

u_{Ls} = 0.07 m/s
u_{gs} = 2.50 m/s

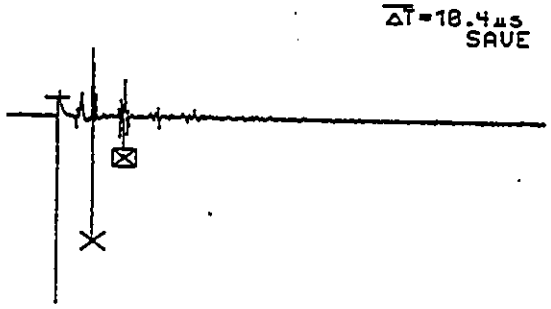

u_{Ls} = 0.07 m/s
u_{gs} = 5.00 m/s

Fig.5.4 Typical signals from the oscilloscope

vapour velocity, the data shows consistent decrease of h/D with increasing the vapour velocity, i.e. decreasing X_{tt}. This is expected to be due to the increase in interfacial friction between the two phases. The sudden drop in the measured values of h/D was associated with the formation of large amplitude roll waves. This observation is consistent with the measurements reported by Andritsos and Hanratty (1987) and Shi and Kocamustaogullari (1993).

There are several theoretical stratified flow models available which can be used to evaluate the liquid level in the inlet tube. One of the best known models was developed by Taitel and Dukler (1976). This model is tested using the results obtained in this section. In the Taitel and Dukler model, the dimensionless liquid level h/D_i was expressed as a function of the turbulent Martinelli parameter X_{tt}. The predictions of this model are compared with the present results in Fig.5.5.

As shown in Fig.5.5, the Taitel and Dukler model can predict the liquid level well when the Martinelli parameter is higher than 1.0. However, for the low Martinelli parameters ($X_{tt} < 1.0$) the Taitel-Dukler model failed to predict the correct liquid level. The deviation of the prediction is believed to be due to the simplification of the model as the liquid-vapour interface is assumed to be smooth and the interfacial friction factor f_i is equal to the vapour phase friction factor f_g. In high quality two-phase flows represented by lower Martinelli parameters, this assumption is no longer valid due to the generation of large amplitude roll waves. In this situation the interfacial friction factor f_i increases rapidly and a more sophisticated model should be used. The deviation of the

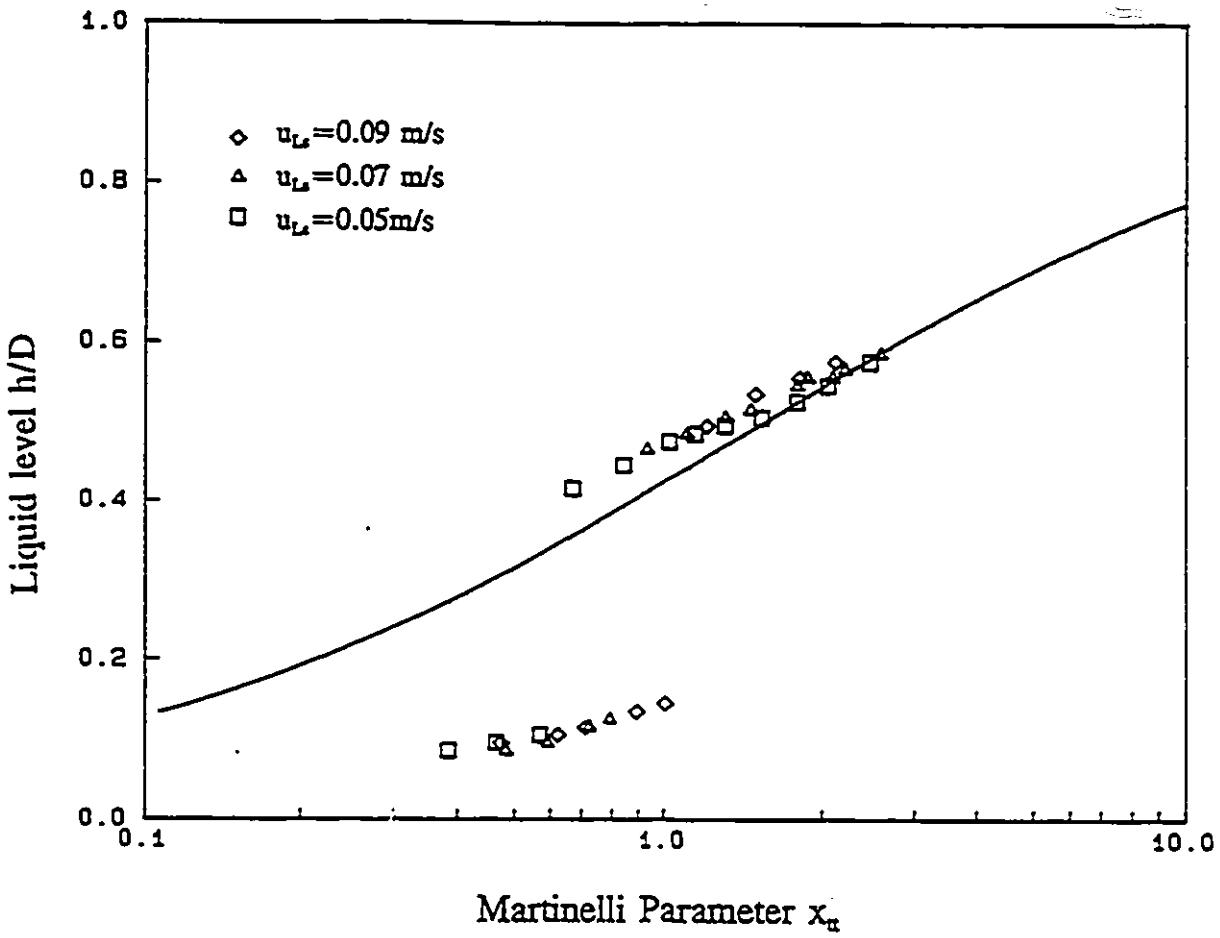

Fig.5.5 Comparison the measurement with Taitel-Dukler model (1976)

model at low Martinelli parameter range was also reported by other researchers, e.g. Andritsos and Hanratty (1987) and recently Shi and Kocamustafaogullari (1993).

Andritsos and Hanratty (1987) developed a more accurate air-water stratified flow mode. This model is similar to that of Taitel and Dukler except that the interfacial friction factor f_i was modified after a critical gas superficial velocity u_{gt}. The authors made an estimate of u_{gt} to be 5 m/s for air-water stratified flow. In the present steam-water experiments, a lower critical vapour superficial velocity of 3 m/s at which the large amplitude roll waves were generated, was observed. A comparison of the present data with Andritsos and Hanratty's model (1987), using 3 m/s as critical vapour superficial velocity, is shown in Figs.5.6 to 5.8.

As shown in these figures Andritsos and Hanratty's model (1987) can predict the present data quite well. Recently this model was also examined by Shi and Kocamustafaogullari (1993) and good results were achieved as well.

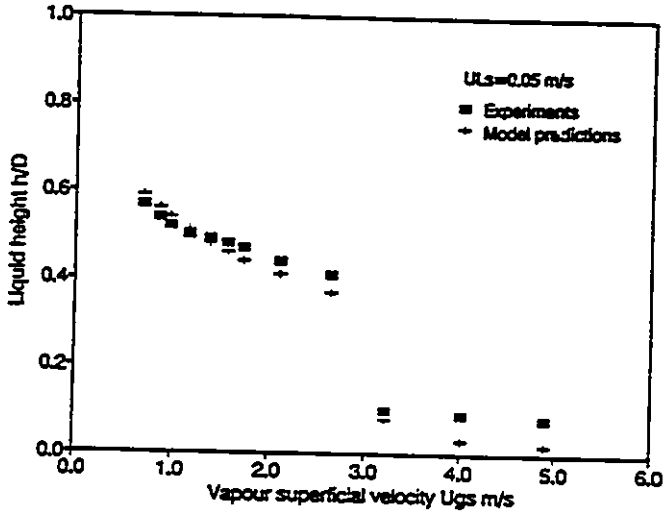

Fig. 5.6 Comparison the measurement with Andritsos and Hanratty model (1987) (u_{Ls}=0.05 m/s)

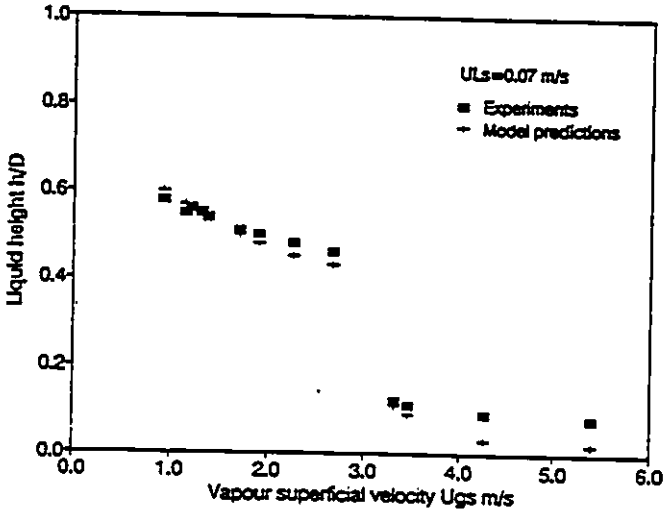

Fig. 5.7 Comparison the measurement with Andritsos and Hanratty model (1987) (u_{Ls}=0.07 m/s)

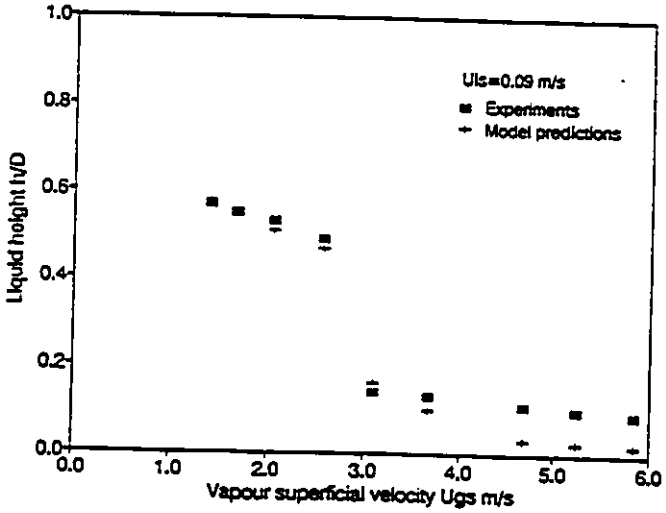

Fig. 5.8 Comparison the measurement with Andritsos and Hanratty model (1987) (u_{Ls}=0.09 m/s)

5.3. Measurements of Junction Phase Redistribution and Pressure Changes

5.3.1. Phase redistribution in the junction

As discussed earlier, the phases are redistributed in the junction such that the phase distribution and quality in the downstream legs may be different from each other and those of the inlet flow. This phase redistribution process is affected not only by the inlet flow conditions but also by the junction geometry. Previous experimental studies of stratified flow in T-junctions have shown that the most significant inlet flow and junction geometrical parameters are the superficial velocities and densities of inlet two phases and the branch orientation and diameter. Intuitively it makes sense that the phase redistribution under stratified flow conditions significantly differs from that of annular flow. In annular flow, a substantial amount of liquid flows as a liquid film along the tube wall, therefore, the first phase extracted to the branch is the liquid film flowing in the main tube segment intercepted by the branch. In stratified flow, however, liquid is flowing on the bottom of the tube and usually its axial momentum flux $\rho_L u_L^2$ has a much higher value than the vapour phase $\rho_g u_g^2$. Depending on the liquid level in the inlet tube and the branch size and orientation, one can see that at lower branch flow split conditions the vapour phase with lower momentum flux is expected to be diverted preferentially into the branch since there is no water film formed in stratified flow. This indicates that a

high branch quality, or a high degree of phase separation, may occur. Increasing the branch flow split ratio, which corresponds to increasing the pressure difference between the inlet and the branch, water begins to be extracted through the branch and the branch flow quality will drop rapidly. For a given branch size and orientation, the onset of the water extraction depends on the liquid level in the inlet conduit of the junctions. A higher liquid level, which typically corresponds to a lower averaged water velocity, needs lower branch flow split to divert water into the branch. If the inlet flow quality is low the liquid level may be high enough, such that, the momentum fluxes of the two phases are comparable and water is expected to be extracted with the vapour, resulting in a more even phase distribution in the junction.

5.3.1.1. Effect of inlet vapour superficial velocity

Sixty-four experimental runs were carried out in the horizontal T-junction with branch-to-inlet diameter ratio of 1.0 under the present stratified flow conditions. Strong effect of vapour superficial velocity was observed in the experiments and typical results are shown in Figs.5.9 to 5.11. The abscissa and the ordinate in the figures are the branch flow split ratio $\dot{m}_3/\dot{m}_1$ and the branch-to-inlet quality ratio x_3/x_1 respectively. The even phase separation was represented by the horizontal line $x_3/x_1=1.0$. In Figs.5.9 to 5.11 the data were presented at fixed liquid superficial velocities of 0.05, 0.07 and 0.09 m/s respectively with varied vapour superficial velocities of 1.5, 2.5, and 5.0 m/s. As shown,

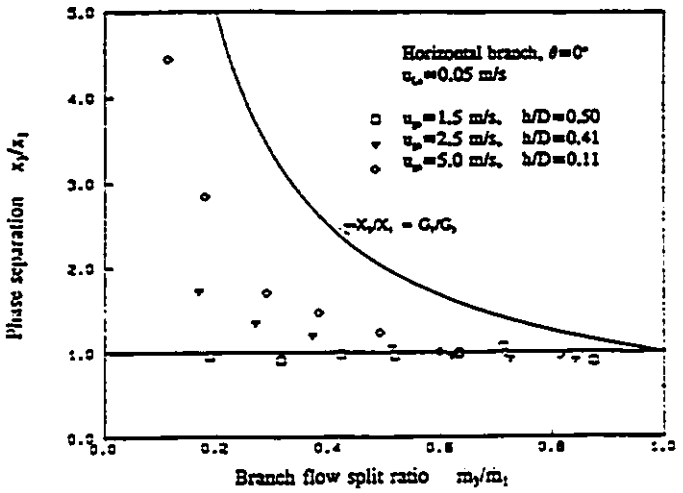

Fig.5.9 Effect of inlet superficial vapour velocity ($D_3/D_1=1.0$, $u_{Ls}=0.05$ m/s)

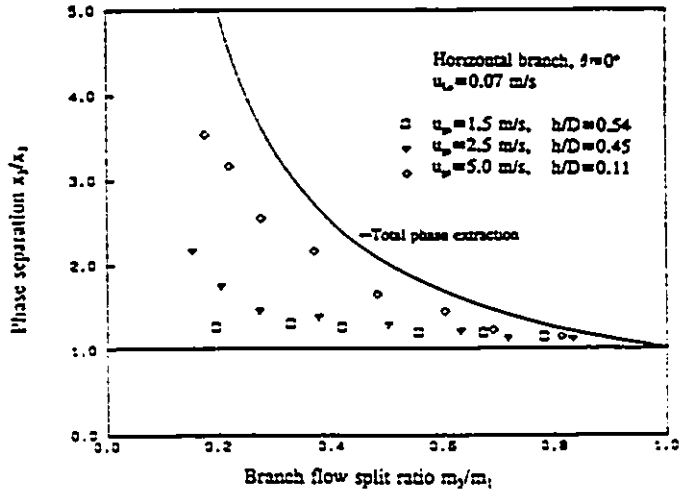

Fig.5.10 Effect of inlet superficial vapour velocity ($D_3/D_1=1.0$, $u_{Ls}=0.07$ m/s)

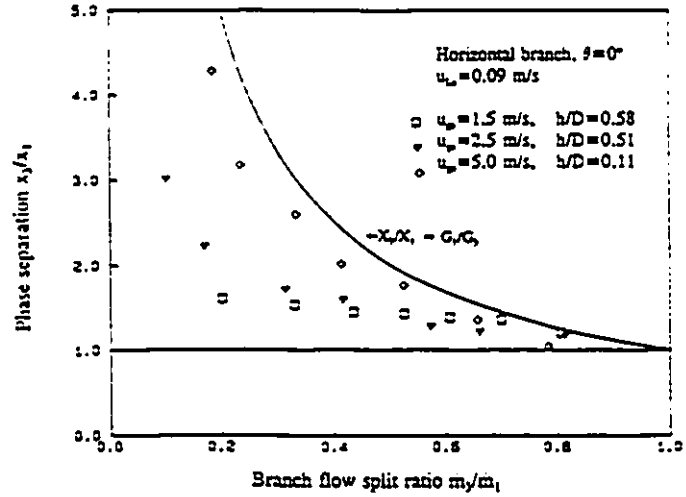

Fig.5.11 Effect of inlet superficial vapour velocity ($D_3/D_1=1.0$, $u_{Ls}=0.09$ m/s)

at small branch split flow rates the quality of branch flow becomes very high, especially in the higher inlet superficial vapour velocity runs, e.g. u_{g1}=5 m/s, corresponding to the dimensionless liquid level $H=h/D_1=0.1$. The same phenomenon was reported by Hong (1978) and Shoham et al. (1987). Increasing branch flow split results in reducing the branch flow quality rapidly, indicating liquid phase being extracted into the branch and the quality ratio x_3/x_1 tends to approach unity. Under the present test conditions, no evidence was observed where the liquid phase was preferentially diverted into the branch. In low superficial liquid and vapour velocity runs, e.g. u_{L1}=0.05 m/s, u_{g1}=1.5 m/s, corresponding to the liquid level $h/D_1=0.5$, the data closely followed the equal phase distribution line $x_3/x_1=1.0$, indicating an even phase redistribution. In the range of the present test conditions, the data indicates that the increase of vapour superficial velocity results in an increase of the degree of phase separation. This trend is consistent with the observation of Collier (1976) and Rubel et al. (1988) for stratified flow. It should be noted that in Collier's measurements, the effect of inlet quality on phase separation appeared in a complex manner. The degree of phase separation first increased and then decreased as the inlet flow quality increased. Same phenomenon was observed by Buell et al. (1993). These trends were caused by the flow regime transition from stratified wavy to annular flow with increasing superficial vapour velocity.

The characteristics of phase redistribution in stratified flow exhibited in Figs.5.9 to 5.11 can be explained in the terms of the variation of liquid level when the inlet vapour superficial velocity is varied. The measurements of liquid level, using the

ultrasonic pulse-echo technique, indicated that the dimensionless liquid level $H=h/D_1$, under the above test conditions, were approximately 0.5, 0.4 and 0.1 for the vapour superficial velocities of 1.5, 2.5 and 5.0 m/s respectively. The effect of liquid superficial velocity on the liquid level was rather insignificant. Due to the reduction of the liquid flow area, with increasing inlet superficial velocity, the liquid axial momentum flux increases dramatically and, therefore, the possibility of the extraction through the branch is decreased. Calculations on the ratio of axial momentum fluxes of liquid-to-vapour indicate that $\rho_L u_L^2/\rho_g u_g^2$ increases as the superficial vapour velocity is increased. For a fixed superficial liquid velocity u_{L_s} of 0.09 m/s, the ratio of axial momentum fluxes of $\rho_L u_L^2/\rho_g u_g^2$ increases from 3.84 to 21.5 as inlet superficial vapour velocity u_{g_s} increases from 1.5 m/s to 5.0 m/s, indicating the degree of phase separation in the junction will increase.

5.3.1.2. Effect of inlet liquid superficial velocity

The effect of inlet superficial liquid velocity on the phase redistribution can be seen in Figs.5.12 to 5.14. In these figures the vapour superficial velocities were fixed at 1.5, 2.5 and 5.0 m/s while the liquid superficial velocities were varied at 0.05, 0.07 and 0.09 m/s. It can be seen that an increase of inlet superficial liquid velocity results in an increase of phase separation. The present experimental results are consistent with the data trends obtained by Shoham et al. (1987) and Azzopardi et al. (1988). These

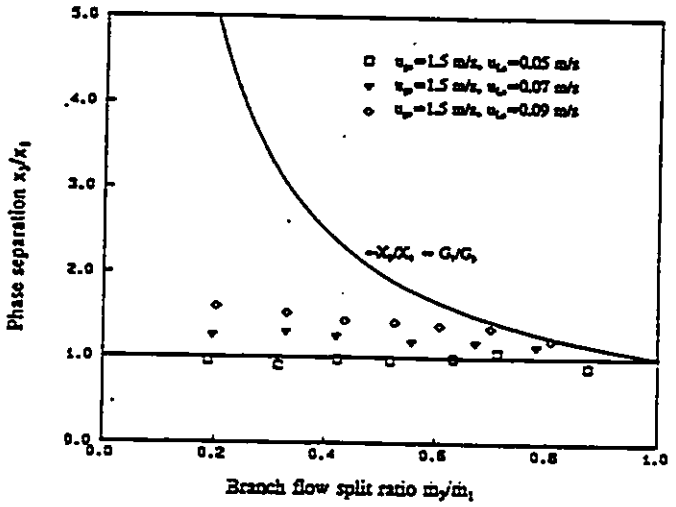

Fig.5.12 Effect of inlet superficial liquid velocity (D_3/D_1=1.0, u_{gs}=1.5 m/s)

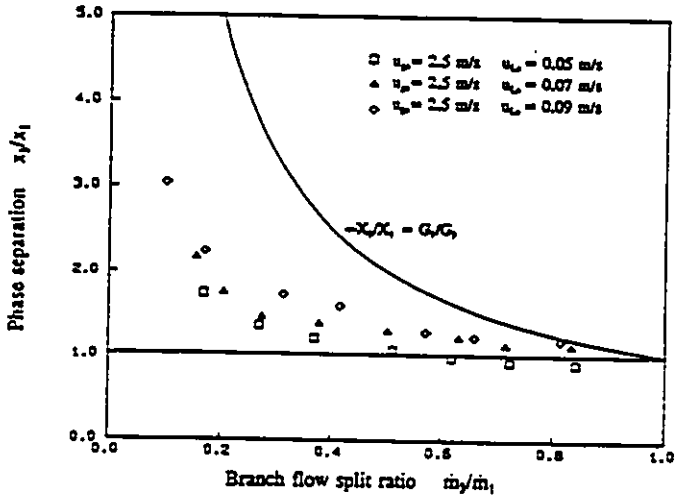

Fig.5.13 Effect of inlet superficial liquid velocity (D_3/D_1=1.0, u_{gs}=2.5 m/s)

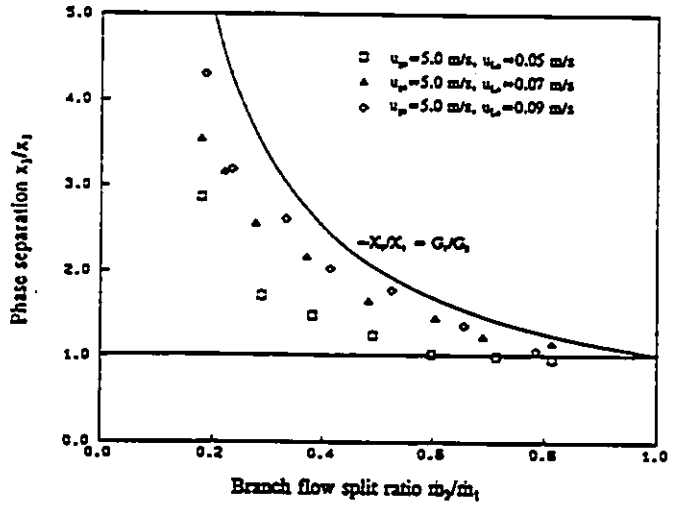

Fig.5.14 Effect of inlet superficial liquid velocity (D_3/D_1=1.0, u_{gs}=5.0 m/s)

results may be explained in the terms of the increase of liquid momentum flux as liquid superficial velocity increases. In liquid level measurements, only small differences of the elevation of liquid level was observed when the inlet liquid superficial velocity was changed at a fixed vapour superficial velocity. Calculations show that the ratio of liquid to vapour momentum flux $\rho_L u_L^2/\rho_g u_g^2$ increases as inlet liquid superficial velocity increases. For a fixed inlet superficial vapour velocity u_{g_s} of 5.0 m/s, the ratio of liquid to vapour momentum flux $\rho_L u_L^2/\rho_g u_g^2$ increases from 6.64 to 21.5 as the inlet superficial liquid velocity u_{L_s} increases from 0.05 m/s to 0.09 m/s. Consequently the liquid phase is more difficult to divert to the branch due to its increased axial momentum flux.

5.3.1.3. Effect of branch diameter

The effect of branch diameter on phase redistribution and pressure changes in the T-junction were studied using 76 mm diameter main tube with 25 mm diameter branch giving a branch-to-inlet diameter ratio of 0.33. Thirty-two runs were performed for examining the phase redistributions in the reduced branch diameter horizontal T-junction. The effects of vapour and liquid superficial velocities are shown in Figs.5.15 and 5.16 respectively. The data trends of this reduced branch configuration are similar to that of regular T-junction with a branch-to-inlet diameter ratio of 1.0. The parametric trends indicate that increasing in either inlet vapour or liquid flow rates will reduce the intake of the liquid phase in the branch or increase the degree of phase separation. The analyses

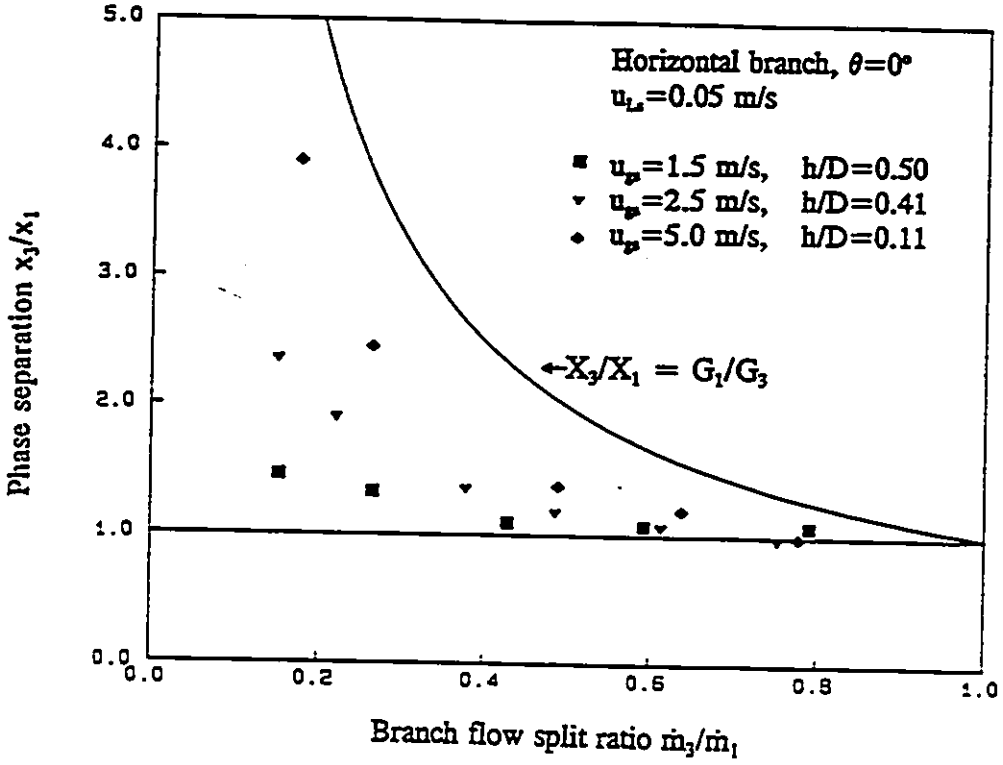

Fig.5.15 Effect of inlet superficial vapour velocity (D_3/D_1=0.33, u_{Ls}=0.05 m/s)

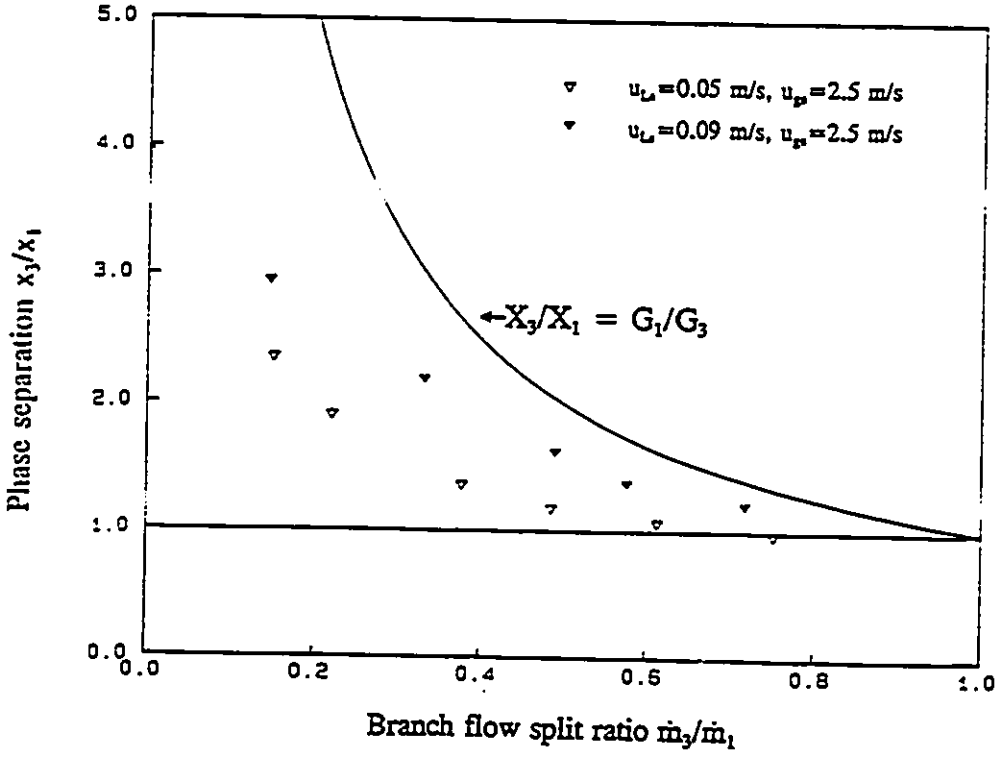

Fig.5.16 Effect of inlet superficial liquid velocity (D_3/D_1=0.33, u_{gs}=2.5 m/s)

discussed in the previous sections for the regular T-junction is applicable to this reduced branch configuration.

In Figs.5.17 to 5.19 the data measured from the reduced branch diameter junction are compared with the regular T-junction under the same inlet flow conditions. It can be seen that less liquid was diverted into the reduced branch, represented by a higher degree of phase separation. The same data trend was observed by Shoham et. al (1989), Azzopardi et al. (1988) and Reimann et al. (1988). A reduced size branch has a shorter axial length over which branch flow extraction may occur, therefore, flow has less chance of being diverted. When the branch diameter is smaller than the inlet diameter, the liquid flowing along the bottom of the main tube cannot move directly into the branch but has to climb along the tube wall before entering the branch, obviously, more effort is needed to extract the same amount of liquid to the reduced size branch junction. The transverse pressure difference between the inlet and branch, on the other hand, is much higher when the same amount of mass flow is diverted in a reduced diameter, as a result, more vapour is extracted into the branch to respond the larger transverse pressure difference due to its low axial momentum flux. This increase of the degree of phase separation by reduced size branch was observed to be much more pronounced in high inlet mass flux annular flow tests, e.g. Ballyk et al. (1987).

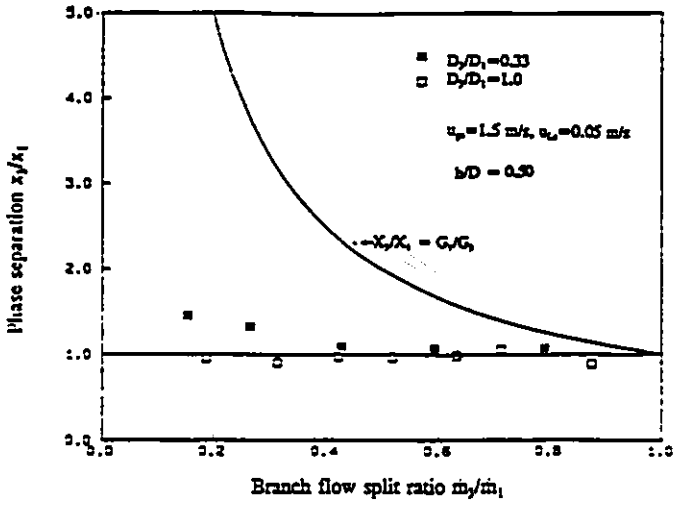

Fig.5.17 Effect of branch diameter (u_{Ls}=0.05 m/s, u_{gs}=1.5 m/s)

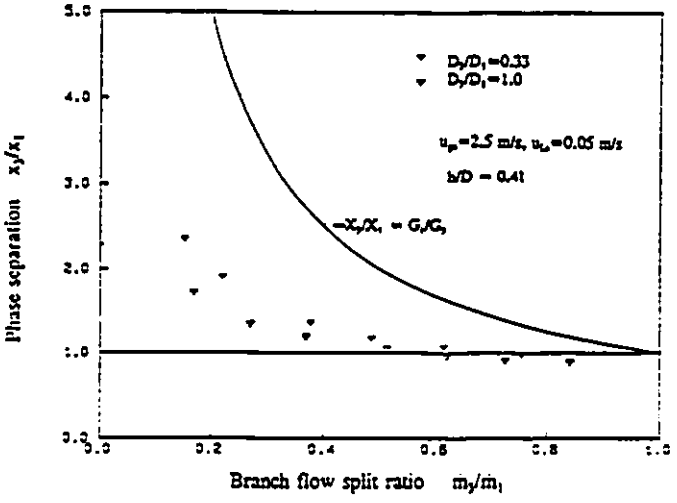

Fig.5.18 Effect of branch diameter (u_{Ls}=0.05 m/s, u_{gs}=2.5 m/s)

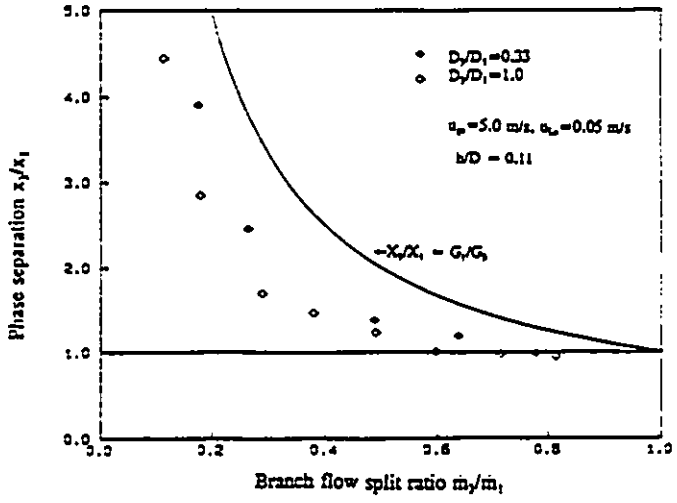

Fig.5.19 Effect of branch diameter (u_{Ls}=0.05 m/s, u_{gs}=5.0 m/s)

5.3.1.4. Effect of branch orientation

The effect of branch orientation on phase redistribution and pressure changes was studied using a T-junction of 76 mm diameter horizontal main inlet tube with a 25 mm diameter 90° downward branch. The inlet flow conditions were similar to that of the horizontal branch T-junction. Figs.5.20 and 5.21 present the effect of branch orientation on phase redistribution at fixed inlet superficial liquid velocities of 0.05 m/s and 0.09 m/s respectively. As one may expect, the liquid phase was preferentially extracted in the downward branch resulting in lower qualities in the downward branch as compared to the horizontal branch. As shown, the parametric trends are consistent with the effect of various parameters on the liquid level. For example, the inlet parametric trends did not change with downward branch configuration, i.e. an increase of inlet superficial vapour velocity, which are associated with reduction of the liquid level, resulted in a decrease of the amount of the liquid extracted into the branch. In the present test conditions, it was also observed that in low branch flow split only water was extracted through the downward branch, the vapour phase was diverted into the branch only at higher branch flow splits. This onset of vapour extraction was closely related with inlet superficial velocities of the two phases, more significantly affected by the vapour velocity. The present data indicates that an increase of the inlet superficial vapour velocity will reduce the branch flow split ratio at which the onset of vapour extraction occurred. In stratified flow, vapour flows on the top of the liquid layer, therefore, in a downward branch T-

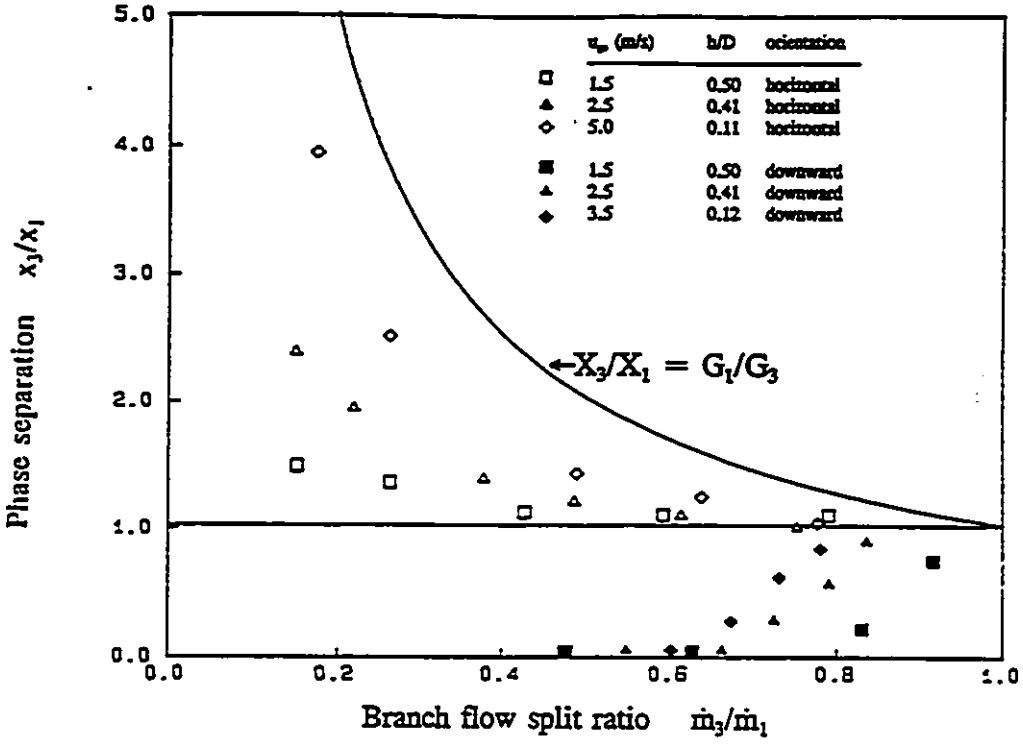

Fig.5.20 Effect of branch orientation (D_3/D_1=0.33, u_{Ls}=0.05 m/s)

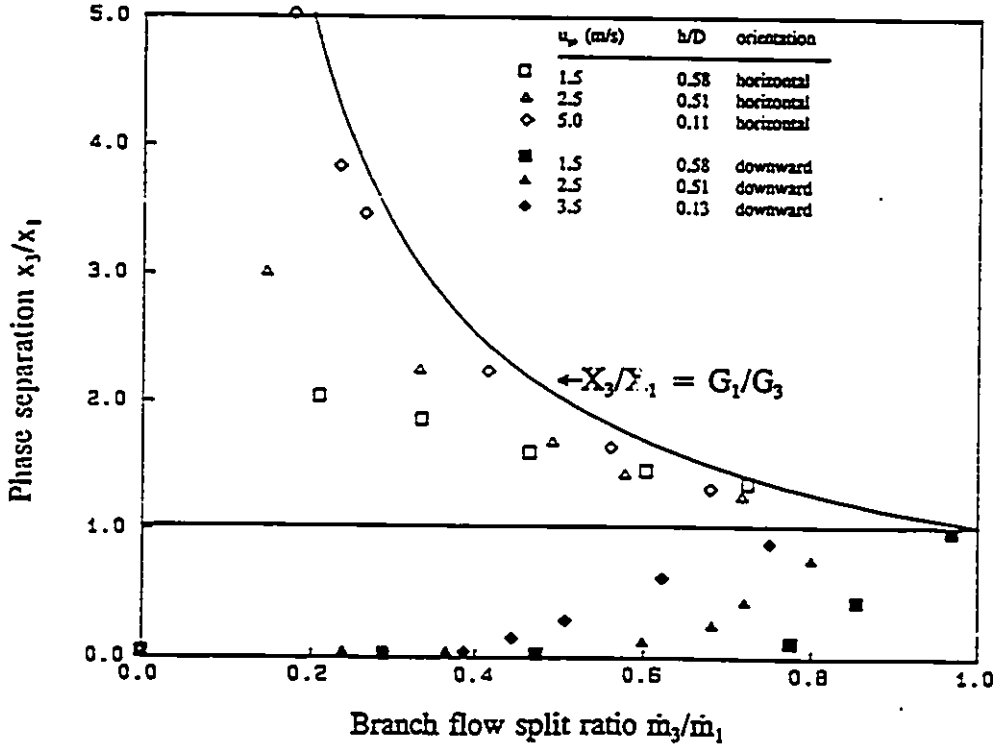

Fig.5.21 Effect of branch orientation (D_3/D_1=0.33, u_{Ls}=0.09 m/s)

junction, vapour can be extracted through the branch only when the effect of gravity and pressure difference between inlet and branch is large enough to overcome the resistance of the liquid flow layer. As a result, it is expected that at a higher vapour superficial velocity, which corresponds to a thinner liquid layer, the onset of vapour extraction occurs earlier, i.e. at lower flow split ratio. Figs.5.20 and 5.21 show that in the horizontal T-junction, vapour is extracted to the branch first at very low branch flow split and the quality of branch flow x_3 can be very high under the conditions of high inlet superficial velocity. However, in downward branch configuration, the branch quality remains zero, indicating only water is extracted in the branch over some range of flow split. The effect of branch orientation on phase redistribution in T-junctions is clearly seen in the figures.

It is expected that for an upwardly orientated branch T-junction the vapour will be first extracted through the branch in a wide range of branch flow split. At high branch flow splits the onset of liquid extraction will occur. The onset of the vapour and liquid pull-through in downward or upward branches depend on inlet flow rates and densities of the two phases and junction geometries. A detailed study of this phenomenon needs more measurement and is beyond the scale of this research. Research work on the onset of vapour or liquid pull-through in downward or upward branches should be performed in more detail in future studies since the phenomena greatly affects the behaviours of phase redistribution in T-junctions.

5.3.1.5. Effect of system pressure

The effect of system pressure on the phase redistribution for stratified flow in T-junctions was less studied by previous researchers due to the difficulty of the measurements and the need for a complex test facility. Available high pressure data can be found in the work of Reimann et al. (1988) obtained at Kernforschungszentrum Karlsruhe, Germany. The changing of system pressure will significantly vary the density of the vapour phase, accordingly change the vapour axial momentum flux. An increase of system pressure will increase the vapour density and hence increase the vapour axial momentum flux, as a results, it is expected that the increase of system pressure will reduce the degree of phase separation. Figs.5.22 and 5.23 show the effect of system pressure on phase separation. Data from present measurements is compared with the data obtained for the same inlet flow condition but at higher system pressure (P=5.0 bar) and a smaller branch-to-inlet diameter ratio (D_3/D_1=0.2) by Reimman et al. (1988). Under such a high system pressure the vapour axial momentum flux is approximately four times larger than that of present work. As expected, the degree of phase separation observed in the high pressure system is lower than that of in our low pressure system.

5.3.2. Pressure changes in the junction

Little data has been published on pressure changes of dividing stratified flow in

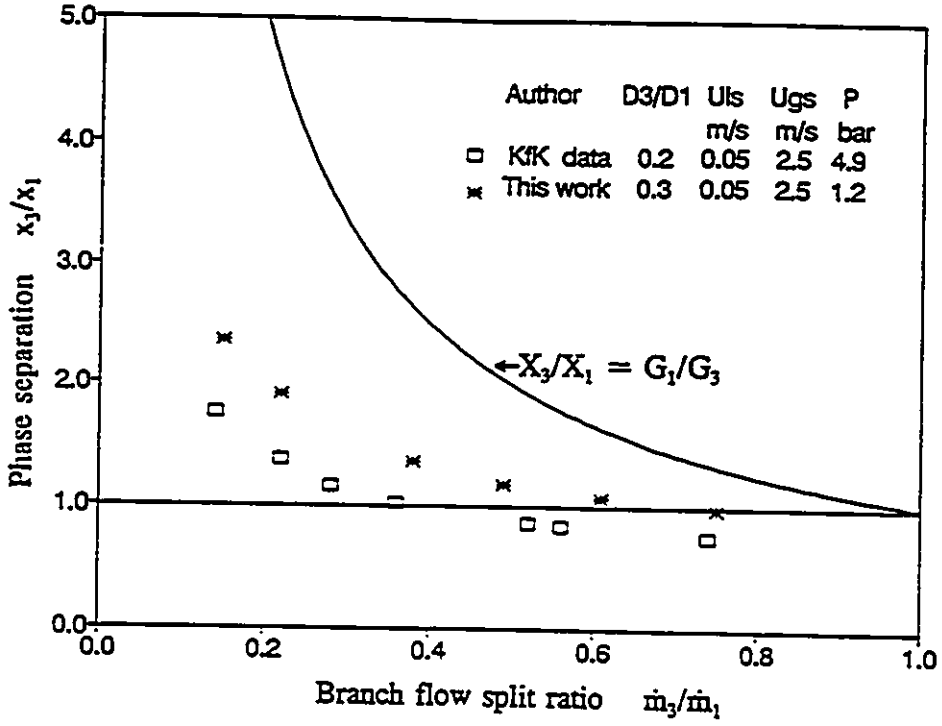

Fig.5.22 Effect of system pressure (u_{Ls}=0.05 m/s, u_{gs}=2.5 m/s)

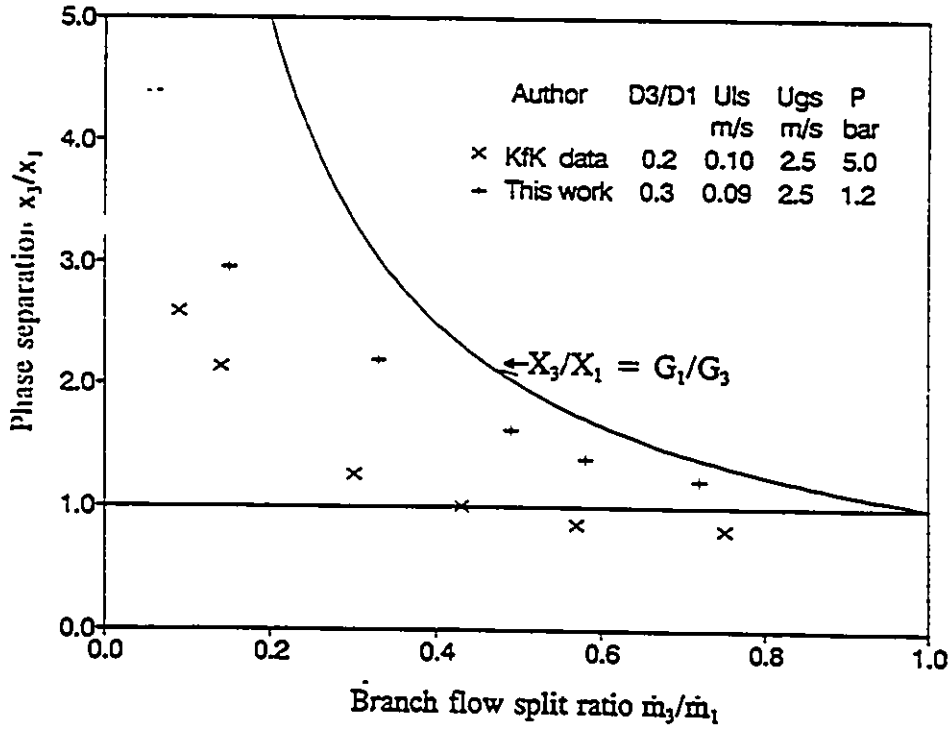

Fig.5.23 Effect of system pressure (u_{Ls}=0.09 m/s, u_{gs}=2.5 m/s)

a T-junction. The available data are mostly collected for high inlet mass flux conditions. To complement the existing data bank, the pressure changes in T-junctions were measured in this research. The experiments were first performed on single-phase flow to determine the empirical coefficients and then on two-phase flow to obtain the two-phase multipliers. This approach is commonly accepted in the study of pressure characteristics of two-phase flow.

5.3.2.1. Single-phase flow

In section 4.2.2.1, single phase water data on pressure changes in T-junctions were reported for the mass flux range of $G > 500$ kg/m^2.s. Similar to other investigators, the pressure rise in the run $\Delta P_{2\text{-}1}$ was modelled using an axial momentum balance, Equation (4.1), where the momentum correction factor K_{12} was defined. The pressure drop in the branch $\Delta P_{1\text{-}3}$ was modelled using a simple mechanical energy balance, Equation (4.2), where the loss coefficient K_{13} was defined. The data examined in section 4.2.2.1, showed that these empirical constants were well predicted by the correlations obtained by Ballyk et al. (1988).

As the experimental loop was modified to accommodate stratified flow, additional single-phase water experiments were carried out in the low mass flux range of $50 < G < 130$ kg/m^2.s. The results obtained are superimposed on the correlations of Ballyk et al. (1988) in Figures 5.24 and 5.25. Good agreement is shown for the data

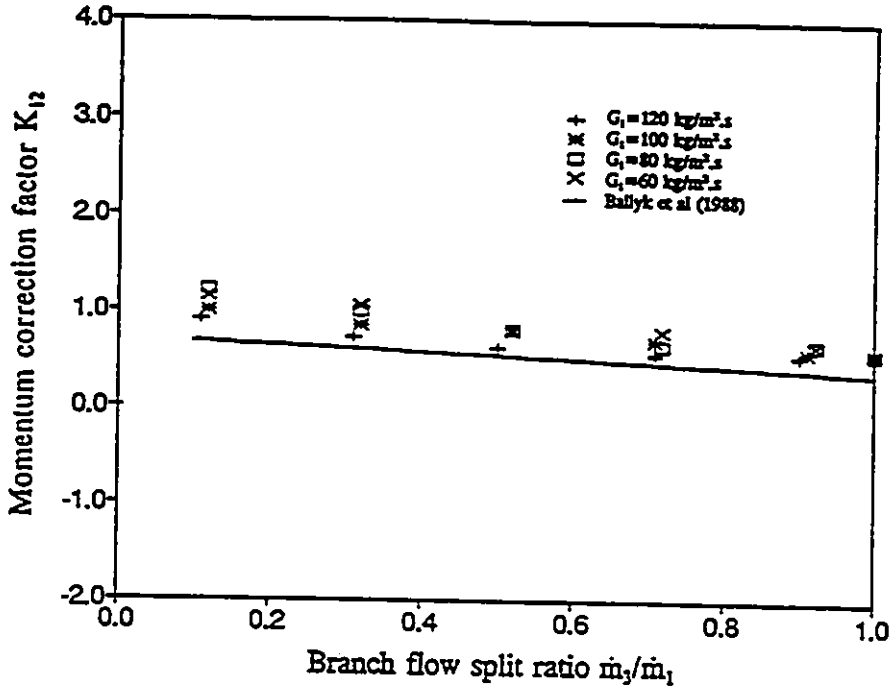

Fig.5.24 . Single-phase run momentum correction factor (D_3/D_1=1.0)

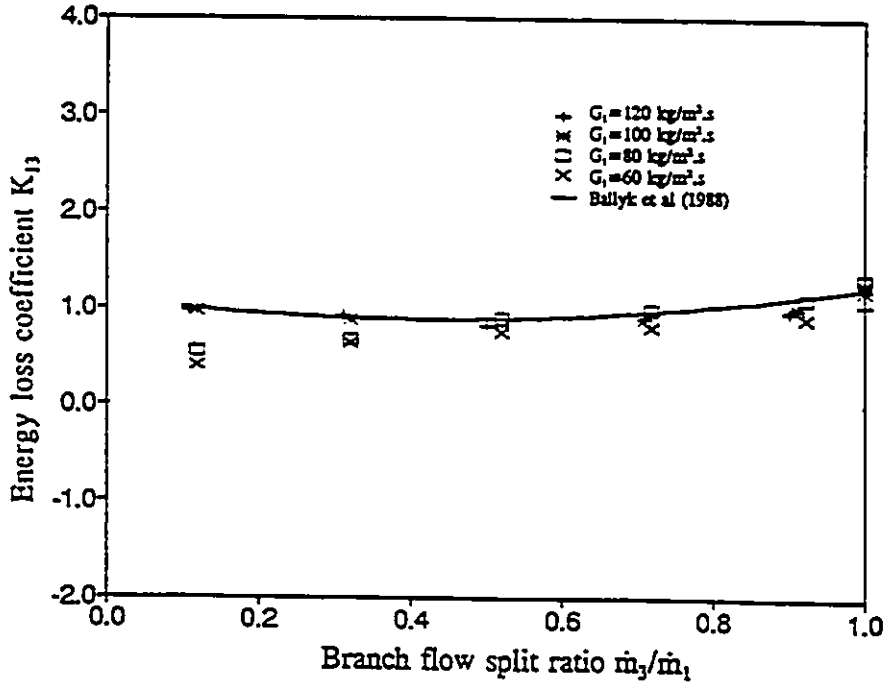

Fig.5.25 Single-phase branch energy loss coefficient (D_3/D_1=1.0)

obtained with $D_3/D_1 = 1.0$. As one may expect, since the correlations proposed by Ballyk et al (1988) do not include the effect of D_3/D_1, they are not applicable for the data obtained in the present work for $D_3/D_1 = 0.33$.

The single phase water data obtained for T-junction with reduced branch diameter was used to obtain the run momentum correction factor K_{12} and branch loss coefficient K_{13} for $D_3/D_1 = 0.33$ in terms of branch split ratio. The results are shown in Figures 5.26 and 5.27. The coefficients were correlated by

$$K_{12} = 1.00 - 0.83\left(\frac{\dot{m}_3}{\dot{m}_1}\right) + 0.33\left(\frac{\dot{m}_3}{\dot{m}_1}\right)^2 \qquad (5.4)$$

$$K_{13} = 1.00 + 12.17\left(\frac{\dot{m}_3}{\dot{m}_1}\right) + 26.91\left(\frac{\dot{m}_3}{\dot{m}_1}\right)^2 \qquad (5.5)$$

5.3.2.2. Two-phase flow

Various methods to model two-phase pressure changes suggested in the literature and described earlier are, in general, direct extensions of the approaches used in single-phase flow. The accepted procedure is to use the empirical coefficients determined in single-phase flow and modify the correlations by two-phase multiplier determined by two-phase flow experiments. The pressure changes of dividing two-phase flow in T-junctions are extremely complicated. The local fluid mechanics, for example, the momentum transfer between the two flow streams which enter through the run and the branch, the flow recirculation in the downstream of the junction, the velocity profiles immediately

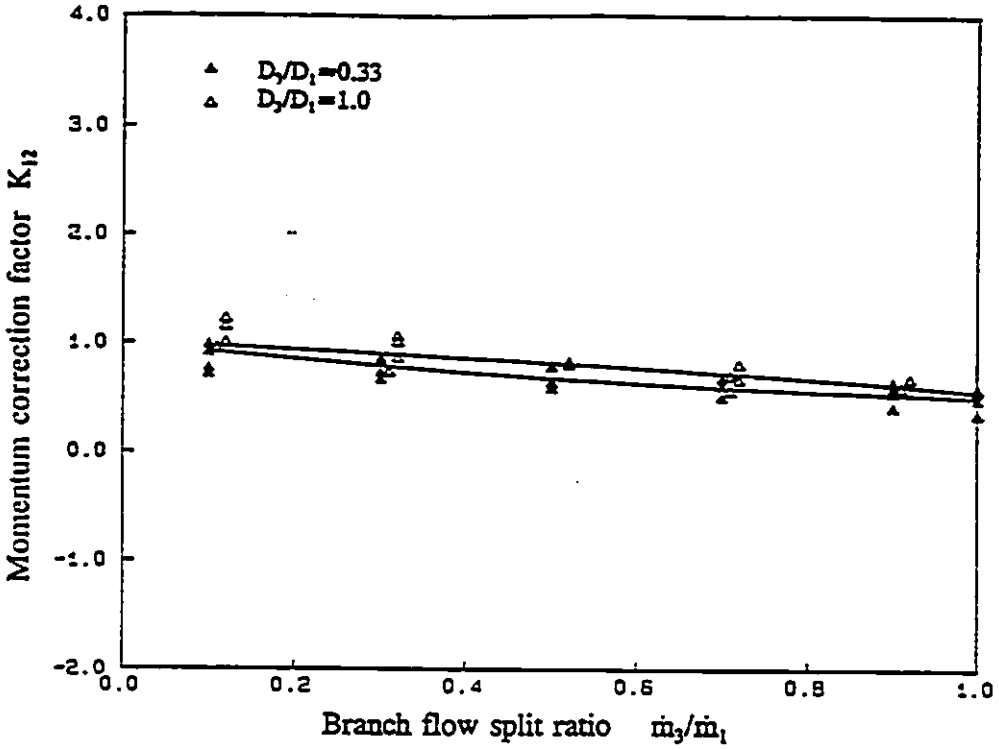

Fig.5.26 Single-phase run momentum correction factor ($D_3/D_1=0.33$)

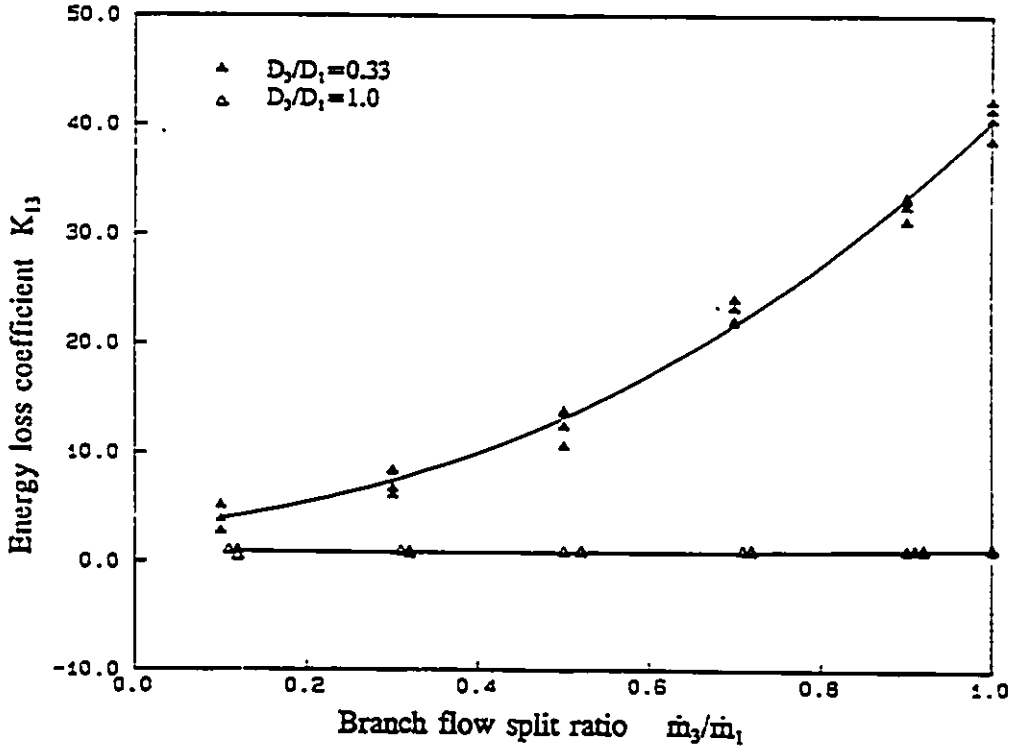

Fig.5.27 Single-phase branch energy loss coefficient ($D_3/D_1=0.33$)

upstream and downstream of the junction are poorly understood. Moreover, due to the significant difference of axial momentum flux between liquid and vapour, the two phases are redistributed in the junction. This phase redistribution is closely correlated with inlet flow and junction geometric parameters and is far from being understood. The phenomenon of phase separation makes the pressure changes in the T-junction even more complicated due to the variation of the flow qualities in the run and the branch. In the following, the pressure changes of dividing stratified flow in T-junctions are experimentally studied and the approach suggested by Ballyk et al. (1988) is followed to obtain the two-phase multipliers.

5.3.2.2.1. Run pressure recovery

Momentum balance was used to correlate run pressure recovery in this study. For a control volume in the junction the axial momentum balance yields:

$$\Delta P_{2-1}=K_{12s}\left(\frac{G_1^2}{\rho_{m1}}-\frac{G_2^2}{\rho_{m2}}\right) \tag{5.6}$$

where the momentum densities ρ_{m1} and ρ_{m2} are evaluated with the measured void fractions in the inlet and run respectively. The separated flow momentum correction factor K_{12s} reduced from Eqn.(5.6) is shown in Fig.5.28 as a function of branch flow split ratio. The data collected in the present study shows an averaged value of K_{12s} is

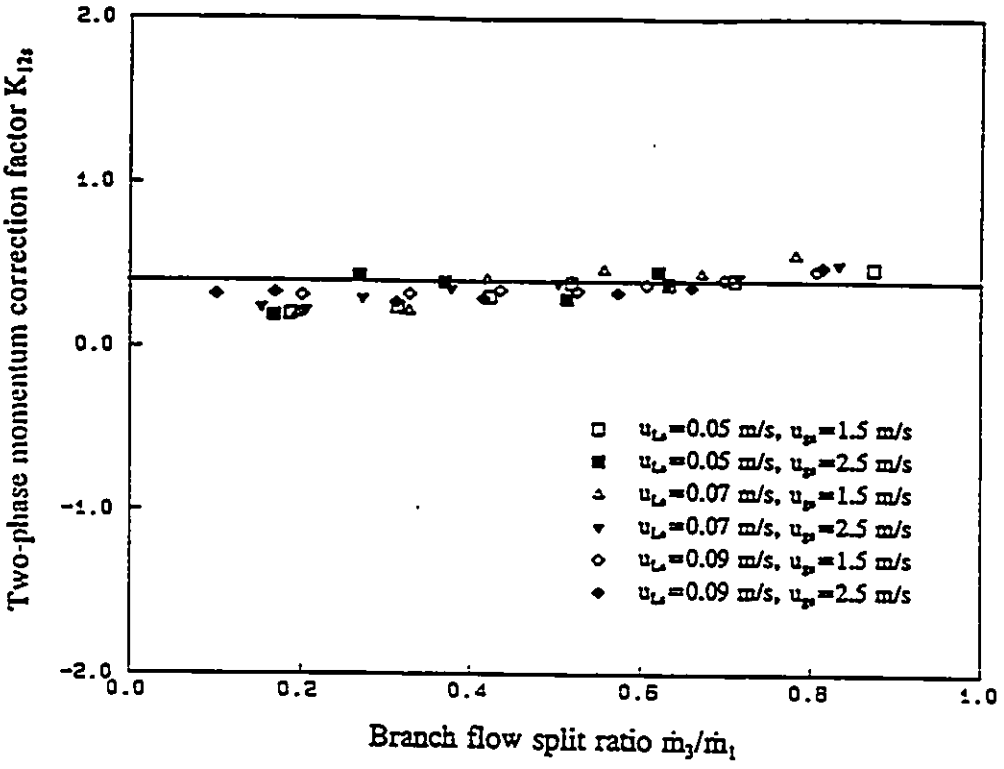

Fig.5.28 Two-phase run momentum correction factor K_{12s} (D_3/D_1=1.0)

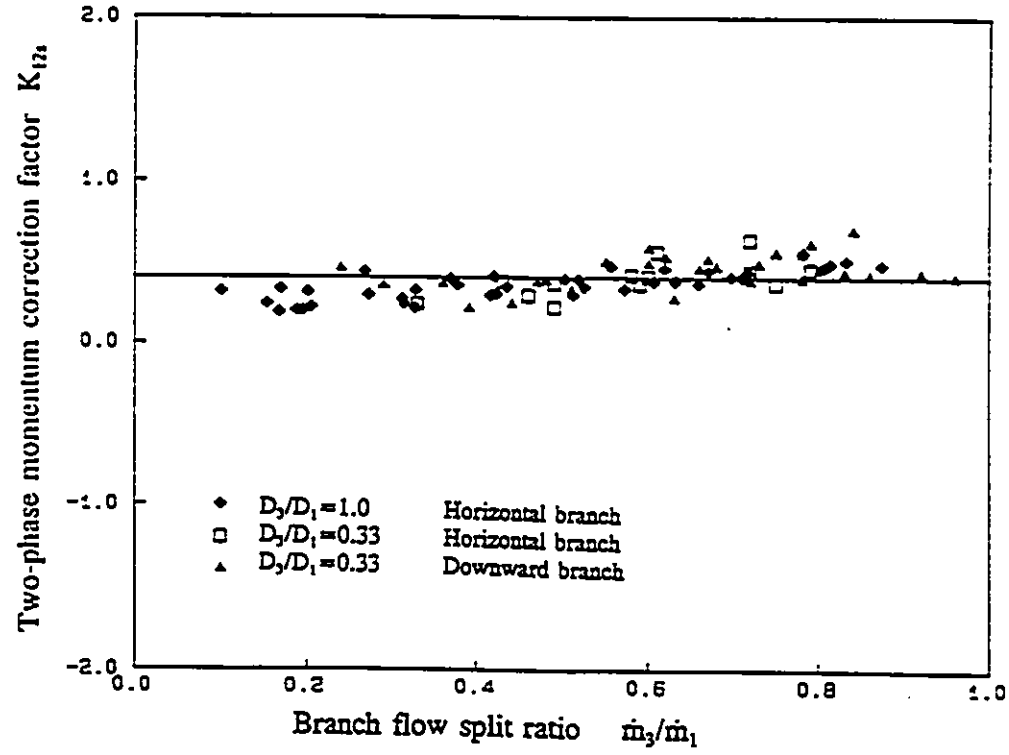

Fig.5.29 Effect of branch diameter and orientation on K_{12s}

0.45. Fig.5.29 presents the effects of branch diameter and branch orientation on run momentum correction factor K_{12s}, as shown, these geometrical parameter are not significant under the present stratified flow conditions.

5.3.2.2.2. Branch pressure drop

The mechanical energy equation was used to correlate the branch pressure drop, whereby the pressure change consists of two parts, i.e. reversible pressure change due to the Bernoulli effect, and irreversible pressure loss due to mechanical energy dissipation. Based on mechanical energy balance there are several simple models available to evaluate the branch pressure drop as outlined in Chapter 4. Among these models the separated flow model developed by Saba and Lahey model (1984) and the homogeneous flow model recommended by Reimann and Seeger (1986) are compared with the present stratified flow data in horizontal equal diameter T-junction. The results of the comparison are shown in Figs.5.30 and 5.31. As can be seen, that none of the models is satisfactory in the present stratified flow conditions. Both of the two models are based on the simple 1-D analysis no empirical coefficients are involved in the models.

Ballyk et al. (1988) suggested that the mechanical energy based model can be expressed as:

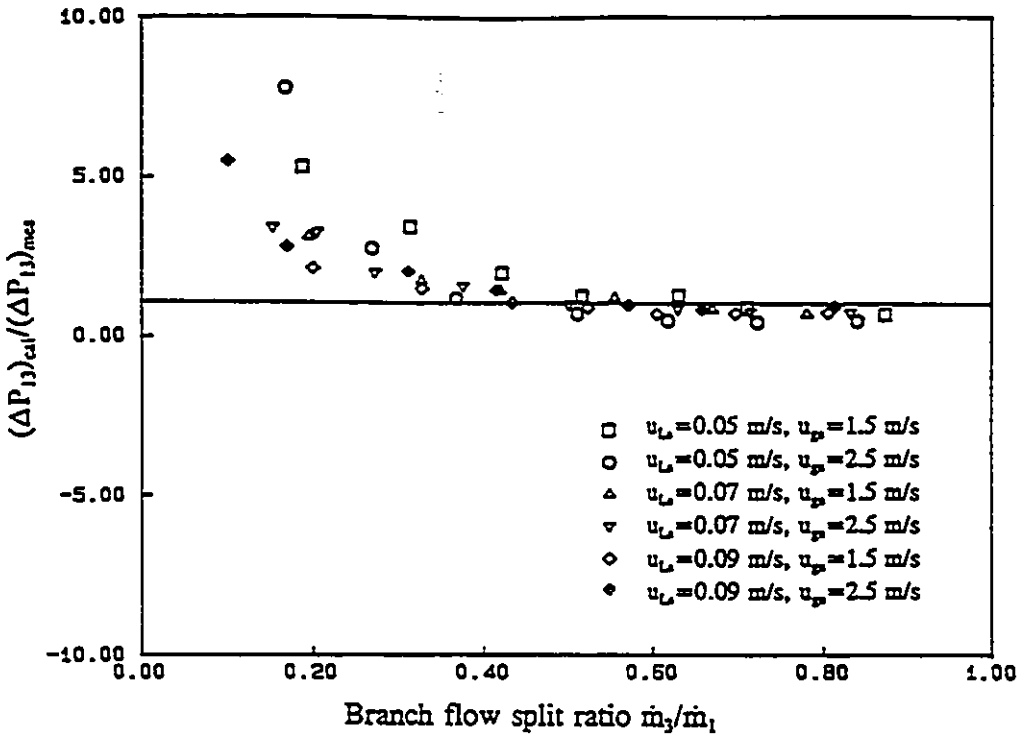

Fig.5.30 Comparison of the measured branch pressure drop with the prediction of Saba and Lahey model (1984)

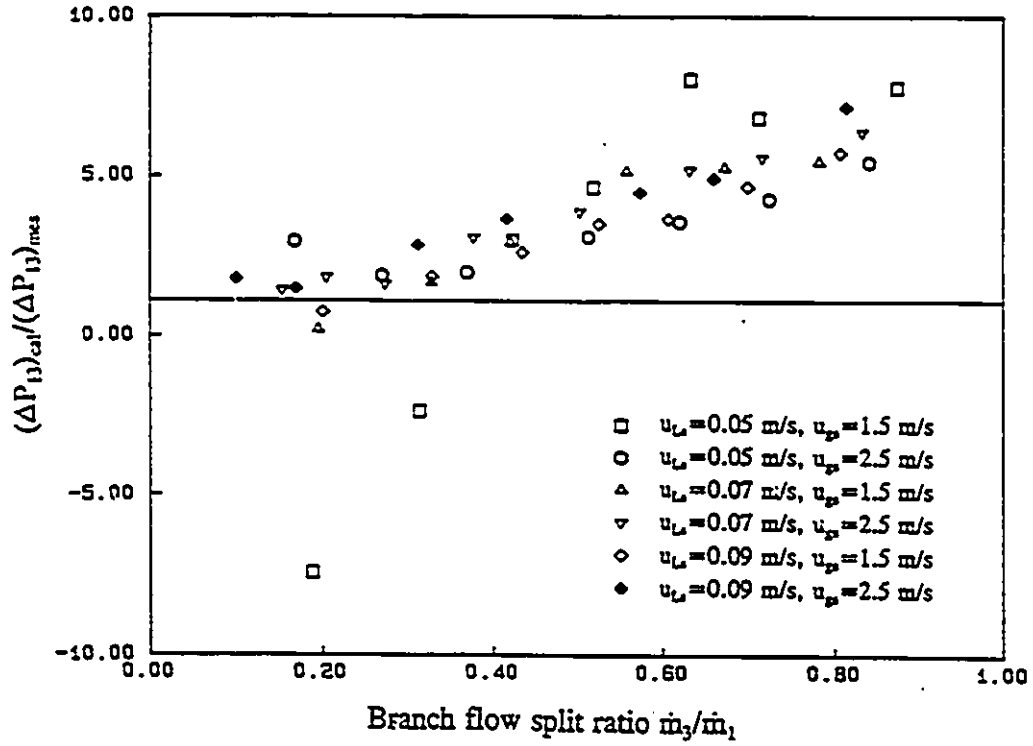

Fig.5.31 Comparison of the measured branch pressure drop with the prediction of Reimann and Seeger model (1986)

$$\Delta P_{1\text{-}3} = \frac{\rho_{h3}}{2}\left(\frac{G_3^2}{\rho_{e3}^2} - \frac{G_1^2}{\rho_1^{*2}}\right) + K_{13}\frac{\rho_{h3}G_1^2}{2\rho_1^{*2}}\phi_{tp} \qquad (5.7)$$

where ρ_{h3} and ρ_{e3} are homogeneous and energy densities of the branch and ρ_1^* is the equivalent inlet density. The densities are evaluated based on the measured void fractions. The two-phase multiplier Φ_{tp} in Eqn.(5.7) thus can be determined from the experiments. Using the present stratified flow data on the horizontal equal diameter T-junction the two-phase multiplier Φ_{tp} was obtained as shown in Fig.5.32. For the present stratified flow data the best fitted correlation was found as:

$$\phi_{tp} = 0.85 + 2.69\left(\frac{\dot{m}_3}{\dot{m}_1}\right) - 1.79\left(\frac{\dot{m}_3}{\dot{m}_1}\right)^2 \qquad (5.8)$$

For a smaller diameter branch T-junction (D_3/D_1=0.33) the two-phase multiplier Φ_{tp} is much larger than that of regular T-junction as shown in Fig.5.33 and can be correlated as:

$$\phi_{tp} = -0.87 + 17.36\left(\frac{\dot{m}_3}{\dot{m}_1}\right) - 10.46\left(\frac{\dot{m}_3}{\dot{m}_1}\right)^2 \qquad (5.9)$$

It can be seen that the two-phase multiplier Φ_{tp} increases as branch flow split ratio increases and is greatly affected by the branch diameter. The influences of inlet flow parameters, however, are less significant in horizontal branch T-junctions.

Fig.5.34 shows two-phase multiplier Φ_{tp} in downwardly orientated branch. The influence of the inlet superficial vapour velocity in this configuration is too large to fit

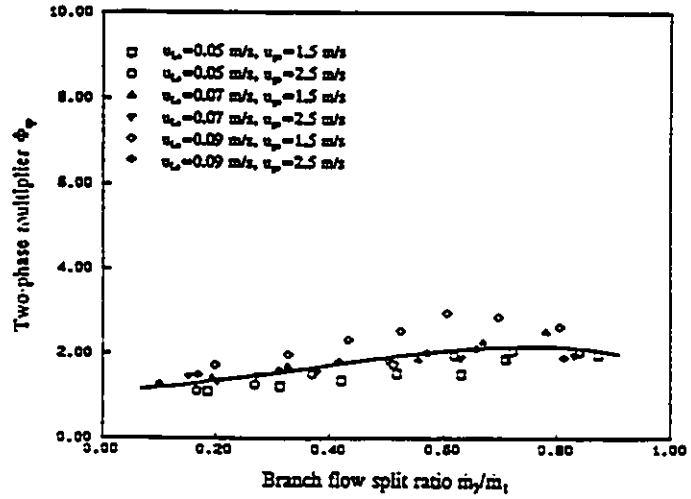

Fig.5.32 Stratified flow two-phase multiplier (horizontal branch $D_3/D_1=1.0$)

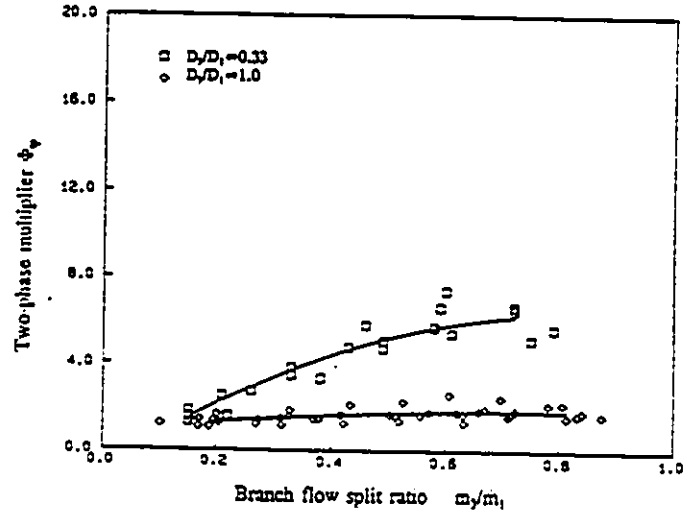

Fig.5.33 Stratified flow two-phase multiplier (horizontal branch $D_3/D_1=0.33$)

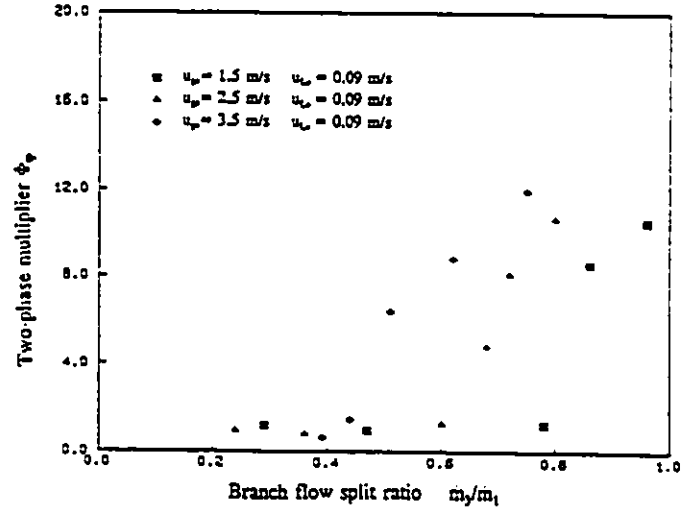

Fig.5.34 Stratified flow two-phase multiplier (90° downward branch $D_3/D_1=0.33$)

two-phase multiplier Φ_{tp} in one correlation. Moreover, the effect of the phase redistribution on branch pressure drop can be observed. It clearly makes sense that the onset of the vapour extraction will rapidly increase two-phase multiplier Φ_{tp} due to the dramatic increase of the branch pressure drop. Prior to the vapour pull-through only water is extracted into the branch, therefore the two-phase multiplier Φ_{tp} is not influenced by inlet flow condition. Since the onset of vapour extraction greatly depends on inlet flow conditions and junction geometries, the branch pressure drop is expected to be affected significantly by these parameters. Accordingly, it is difficult to correlate these variables in a single empirical correlation using the limited experimental data. More experiments is needed to further study the onset of vapour pull-through phenomenon.

Using the model represented by equation (5.7) and the two-phase multiplies predicted by equations (5.8) and (5.9) for the two horizontal branch sizes, the predicted branch pressure drop and the measured values are compared for horizontal branches under stratified flow conditions. Figure (5.35) shows good agreement.

5.4. Conclusion

Detailed experimental data on dividing steam-water stratified flow in T-junctions were obtained. The degree of the phase separation depends on inlet flow rates, densities of the two phases and the resulting liquid level in the inlet tube. It is also significantly affected by the junction geometry. Increasing vapour or liquid superficial velocities will

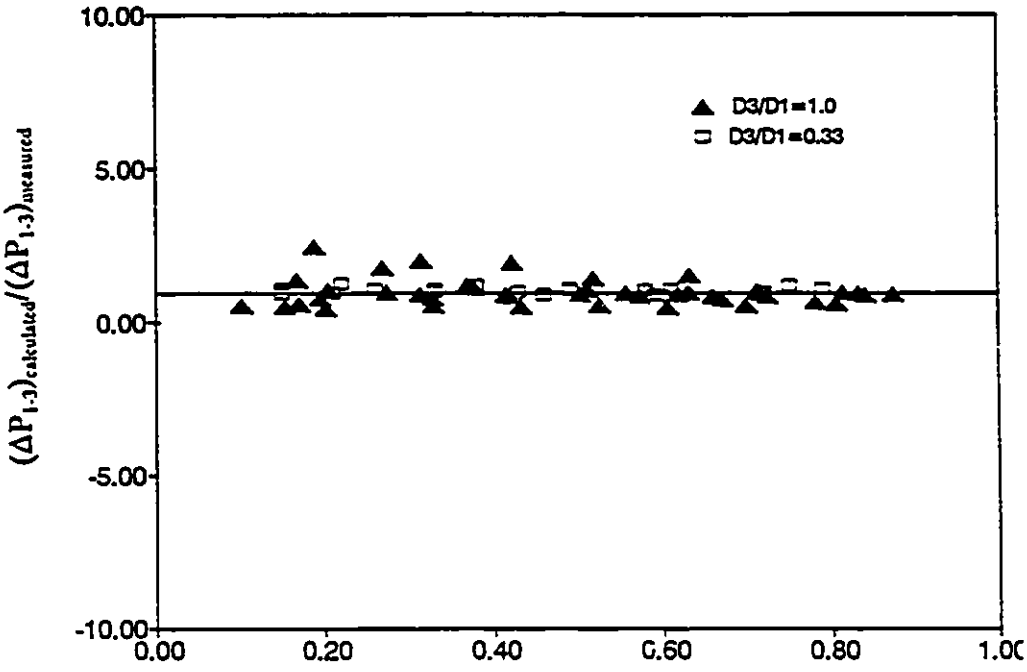

Fig.5.35 Comparison of Ballyk and Shoukri (1988) correlation with present horizontal branch data

increase the extent of phase separation under the present stratified flow conditions. Higher system pressure corresponding to a higher vapour density results in reducing the degree of the phase separation. In a reduced size branch T-junction, a higher level of phase separation will be experienced. A variation of branch orientation will greatly affect the phase redistribution and downwardly orientated branch will reduce the branch flow quality significantly.

The data on pressure changes through the junction were correlated using simple models based on momentum and mechanical energy balances. The momentum correction factor was found to be less influenced by the inlet flow rates of the two phases and is also independent of the branch diameter and orientation. However, the two-phase multiplier used to evaluate branch pressure drop greatly depends on branch diameter and branch orientation. It was found that the two-phase multiplier was less affected by the inlet flow conditions in horizontal branch T-junctions but was greatly influenced by the inlet flow parameters in downward branch configurations due to vapour pull-through phenomenon.

CHAPTER 6

MODELLING THE PHASE REDISTRIBUTION PHENOMENA

6.1. Introduction

When two-phase flow is divided in a T-junction, the original distribution of the phases will change at the junction. The phase redistribution in the junction is affected by the relative axial momentum of the two phases, inlet phase distribution, i.e. flow regime, and junction geometry. This phase redistribution phenomenon is very complicated by virtue of the large number of variables involved in the process.

Experimental investigations of the phenomenon indicated that phase redistribution in the junction depended greatly on phase distribution in the inlet tube. Therefore, a model of inlet phase distribution is a prerequisite for the modelling of the junction phase redistribution. Currently there is no model available to account for phase distribution in all flow regimes. Several phase distribution models of specific flow regimes can be found in the literature and most of the models are based on very simplified analysis. Phase distribution models are still a challenge to two-phase flow modelling techniques especially for complex flow regimes such as annular and slug flow.

In modelling phase redistribution phenomenon in T-junctions three approaches have been used by previous researchers. They are: (1) completely empirical correlations

e.g. Henry (1981) and Seeger et al. (1986); (2) phenomenological analysis e.g. Azzopardi and Whalley (1982), Shoham et al. (1987), Hwang et al. (1988), Ballyk and Shoukri (1990), McCreery and Banerjee (1990) and Lemonnier and Hervieu (1991); (3) two-fluid model numerical simulations, e.g. Lahey (1990) and Issa and Oliveira (1991). The current state-of-the-art of modelling techniques are far from obtaining accurate prediction of two-phase redistribution in T-junctions. There is no model available with general applicability to all inlet flows and junction geometries.

The empirical correlations are typically valid in the range of conditions within which the experimental data used for their development was obtained. The accuracy of the prediction of the empirical correlations also depends greatly on the size of the data bank from which they were developed. When these correlations are extended to conditions outside the range of their validity great care should be taken. The empirical correlations are easy to use and the predicted results are usually reasonable if they are used in their appropriate range of conditions. However, like a black box, the empirical correlations cannot help us to improve the understanding of the physical phenomenon. Using empirical correlations one can predict what may happen at the given inlet flow and junction geometry but cannot explain why it happens.

The phenomenological models were developed by expressing the physical phenomenon in conjunction with mathematical models. Based on physical understanding of a complex process some assumptions can be made to simplify the mathematical models, otherwise it may be impossible to express the phenomenon completely by a

mathematical model, or may not be solved due to its complexity even if the appropriate mathematic expressions can be achieved. Phenomenological models provide a simple and practical approach to analyze the complex physical phenomenon. The terminology of "phenomenological model" indicates that these models are based on a specific physical background, if the physical background is far from reality large deviation may occur. Consequently, phenomenological models are still flow regime and junction geometry dependent. However, they are helpful to improve the understanding of the physical phenomenon. Since they are based on physical understanding and the conservation laws are used, in a global sense at least, the applicable range of the model is wider than the empirical models. With the improvement of the knowledge of the physical phenomenon these models can be updated to become more sophisticated and more accurate predictions could be expected. The phenomenological models of dividing two-phase flow in T-junctions are based on two main observations believed to have first order effect on the phenomenon. These are: (i) geometrical effects concerning the inlet distribution of the phases in the inlet tube, i.e. inlet regime characteristics, and geometry of the branching conduit, and (ii) the fact that the phenomenon is dominated by the relative inertia of the phases. The first observation lead to the development of models based on the existence of "zones of influence" from which the liquid and gas phases are extracted through the branch. The early models considered geometrical effects only, i.e. Azzopardi and Whalley (1982). The second observation was utilized in later models where the boundaries of the zones of influence were defined by the "dividing stream lines" obtained

by assuming inertia dominated flow in the junction. These dividing streamlines separate the inlet flow into branch and run flows. If the inlet phase distribution and dividing streamlines in the junction are appropriately modelled the flow qualities in the branch and run can be easily determined.

Two-fluid models are based on the solution of the conservation equations of mass, momentum and energy for each phase. The equations are obtained by averaging the instantaneous conservation equations of each phase and the interfacial (jump) conditions at the interfaces. The averaging process introduces loss of information of the physical phenomenon and, as a result, interfacial transport terms are reintroduced in the conservation equations of the two phases to account for the interfacial transport phenomenon. The interfacial transfer terms require additional modelling. The accuracy of two-fluid models depends significantly on the appropriate interfacial constitutive correlations. Unfortunately, it is hard to find such constitutive correlations, in many cases, as in dividing two-phase flow in the T-junctions, no such correlations are available. With advances in computational fluid dynamics (CFD), solution methods are now available for dealing with multi-dimensional two-fluid modelling. The difficulty, however, remains in the interfacial equations required for closure.

In the following sections a general phenomenological phase redistribution model based on a survey of the available models is derived; a 2-D single-phase numerical simulation is performed to verify the hypothesis of the concept of dividing streamline; new models for annular and stratified flows are developed and the predictions of phase

redistribution by some available empirical and phenomenological models including the newly developed models are compared with experimental data.

6.2. A General Phenomenological Phase Redistribution Model

Phenomenological models are based on the assumption that there are "zones of influence" from which liquid and gas are diverted into the branch. These "zones of influence" are bounded by the dividing streamlines and the interface of the liquid and gas in the inlet tube as shown in Fig.6.1. The inlet flow is assumed to be separated by the dividing streamlines into two parts as branch and run flows. By superimposing the inlet flow distribution on the dividing streamlines in the inlet tube, the areas from which the two phases are diverted into the branch are determined. The concept of "zones of influence" came from experimental observations of single-phase flow by McNown (1954) and was extended to two-phase flow by Azzopardi and Whalley (1982). The concept of dividing streamline was widely accepted and further developed by other researchers and reasonable results were obtained, e.g. McCreery and Banerjee (1990) and Lemonnier and Hervieu (1991) for dispersed flow regimes and Shoham et al. (1987), Hwang et al. (1988) and Ballyk and Shoukri (1990) for separated flow regimes.

For separated two-phase flows, the phase redistribution models developed by Azzopardi and his colleagues (1982, 1984), Shoham et al. (1987), Hwang et al. (1988) and Ballyk and Shoukri (1990) were only different in the approaches used to determine

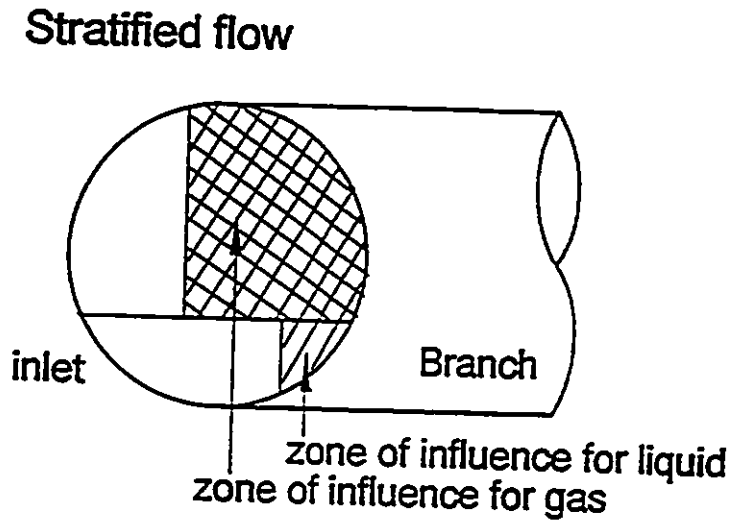

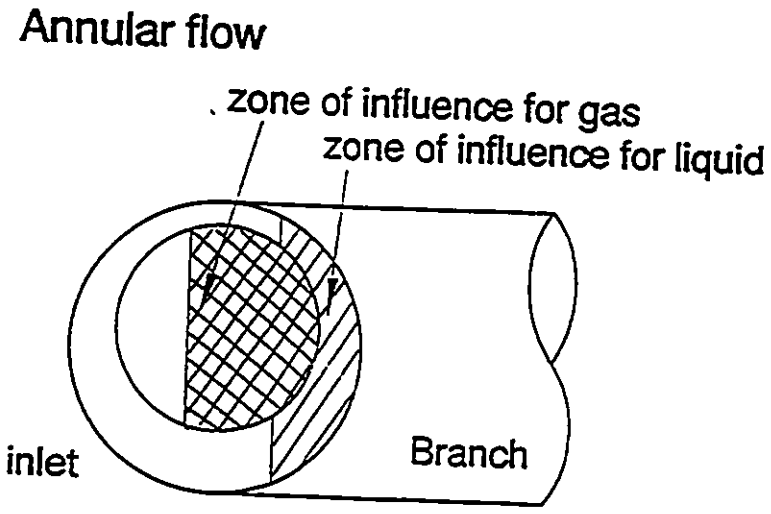

Fig.6.1 The zones of influence

the dividing streamlines in the junction. Azzopardi and Whalley (1982) developed a simple geometrical model for uniform liquid film annular flow. In this model the authors assumed that the liquid and gas diverted into the branch came from the same "zone of influence", i.e. the dividing streamlines for liquid and gas were co-incident. The "zone of influence" was defined based on geometrical considerations only. It was defined by the angle θ as shown in Fig.6.2a. It is a completely geometrical model and no fluid mechanics is involved in the model. Intuitively it makes sense that due to the significant difference in the axial momentum fluxes of the two phases, the inlet gas and liquid have different dividing streamlines. The locations of the gas and liquid dividing streamlines are governed by the momentum conservation law, therefore, fluid dynamics principles should be introduced into the modelling process.

Shoham et al. (1987) and Hwang et al. (1988) developed phase redistribution models based on the hypothesis that different gas and liquid dividing streamlines separated the inlet gas and liquid flows into the branch and run flows as show in Fig.6.2b. The relationship of the paths between the gas and liquid dividing streamlines can be determined either by simplified force balance (Shoham et al. 1987) or empirical correlations (Hwang et al. 1988). For simplification, these authors assumed two-dimensional flow and accordingly the locations of the dividing gas and liquid streamlines were independent of the location across the junction opening, i.e. constant δ_L and δ_g in Fig. 6.2b.

Ballyk and Shoukri (1990) further developed the idea of two dividing streamlines.

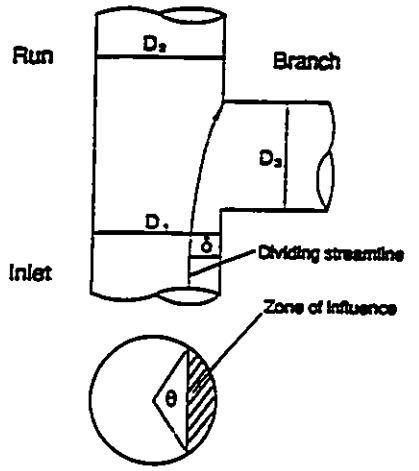

(a) Azzopardi and Whalley (1982)

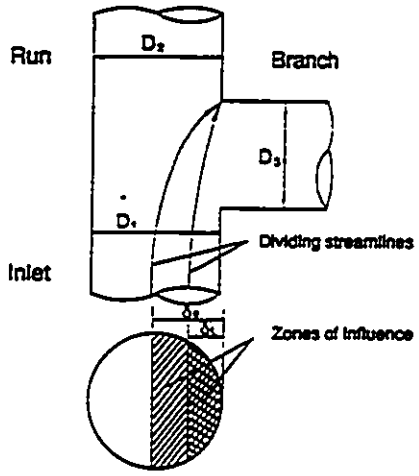

(b) Shoham et al. (1987) and Hwang et al. (1988)

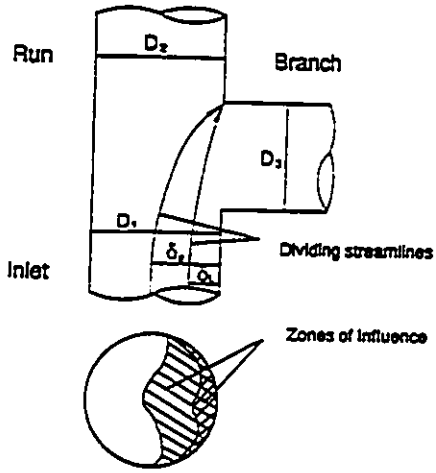

(c) Ballyk and Shoukri (1990)

Fig.6.2 Different definitions of dividing streamlines

They determined the positions of liquid and gas dividing streamlines separately by tracing the path of fluid particles via the free streamline theory of potential flow. The unique feature of this approach is that the locations of the dividing streamlines varied across the cross-sectional area of the main inlet tube in the direction normal to the branch as show in Fig.6.2c. Realizing the interdependence of the phase redistribution and pressure changes in the junction, the authors applied momentum balances, in which the empirical correlations for pressure changes were used, to close the set of equations used. This model is further developed in the following sections to predict phase redistribution in annular and stratified flows.

A general phenomenological model can be derived from the above discussion. In the phenomenological models two basic assumptions are made:

i. There are "zones of influence" from which gas and liquid are extracted into the branch.

ii. The velocity distribution of gas and liquid phases are uniform in the cross section of the main inlet tube.

The fractions of inlet gas and liquid phase removed to branch can be written as:

$$\frac{\dot{m}_{3g}}{\dot{m}_{1g}} = \frac{A_{gb}}{A_g} \tag{6.1}$$

$$\frac{\dot{m}_{3L}}{\dot{m}_{1L}} = \frac{A_{lb}}{A_L} \tag{6.2}$$

where $\dot{m}_{3g}$, $\dot{m}_{3L}$, $\dot{m}_{1g}$ and $\dot{m}_{1L}$ are the mass flow rates of the gas and liquid in the branch

and the inlet respectively. A_g and A_L are the areas of the inlet cross section occupied by gas and liquid respectively. A_{gb} and A_{Lb} are the influenced areas of gas and liquid phase from which two phases are diverted into the branch as shown in Fig.6.3.

Eqns.(6.1) and (6.2) can be rewritten as:

$$\dot{m}_{3g} = \dot{m}_1 x_1 \frac{A_{gb}}{A_g} \tag{6.3}$$

$$\dot{m}_{3L} = \dot{m}_1 (1-x_1)(1-E)\frac{A_{Lb}}{A_L} \tag{6.4}$$

where E is the fraction of the liquid phase entrained as droplets in the gas core in the case of annular flow. E is set to zero for stratified flow. Eqn.(6.4) indicates that only liquid film is extracted into the branch whilst the liquid droplets in the gas core are flowing through the run due to its high momentum flux.

The branch quality ratio can be expressed by:

$$\frac{x_3}{x_1} = \frac{A_{gb}}{A_g}\left(\frac{\dot{m}_1}{\dot{m}_3}\right) \tag{6.5}$$

Using Eqns.(6.3) and (6.4), the branch quality ratio can be written as:

$$\frac{x_3}{x_1} = \frac{A_{gb}A_L}{A_L A_{gb}x_1 + (1-x_1)(1-E)A_{Lb}A_g} \tag{6.6}$$

Eqn.(6.6) indicates that in phenomenological models the extent of phase separation x_3/x_1 can be evaluated by the geometrical relations of A_g, A_L, A_{gb}, A_{Lb} at known inlet flow parameters of x_1 and E. All phenomenological models available in the

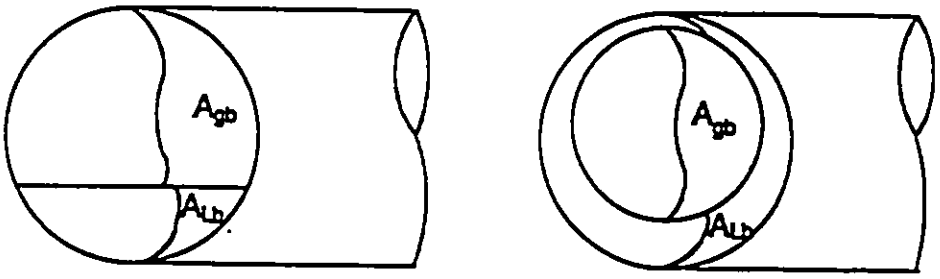

Fig.6.3 Definitions of general phenomenological models

literature are based on these fundamental equations. The differences among these models are the various approaches used to determine the areas of A_{gb} and A_{Lb}. To determine the areas of A_{gb} and A_{Lb}, a model of phase distribution in the inlet and a model of dividing streamlines in the junction have to be developed separately and then superimposed on each other. Since the most basic hypothesis of phenomenological model is that there are dividing streamlines to separate the inlet flow, a single-phase 2-D numerical simulation is performed in the next section to verify the validity of this fundamental assumption.

6.3. Single-Phase Numerical Simulation

The mechanics of dividing flow in a T-junction is governed by the mass and momentum conservation for the fluid. This numerical work is performed using FLUENT, a well known commercial CFD code.

For steady incompressible turbulent flow the mass and momentum conservation yield:

$$\frac{\partial}{\partial x_i}(\rho u_i) = 0 \tag{6.7}$$

$$\frac{\partial}{\partial x_i}(\rho u_i u_j) = \frac{\partial}{\partial x_i}[\mu(\frac{\partial u_i}{\partial x_j}+\frac{\partial u_j}{\partial x_i})]-\frac{\partial p}{\partial x_j}+\rho g_i+\frac{\partial}{\partial x_i}(\rho\overline{u_i' u_j'}) \tag{6.8}$$

The k-ϵ turbulence model is an eddy-viscosity model in which the Reynolds stresses are assumed to be proportional to the mean velocity gradients, with the constant

of proportionality being the turbulent eddy viscosity μ_t. This assumption, known as the Boussinesq hypothesis, provides the following expression for the Reynolds stresses:

$$\overline{\rho u_i' u_j'} = \mu_t\left(\frac{\partial u_i}{\partial x_j}+\frac{\partial u_j}{\partial x_i}\right) \tag{6.9}$$

The turbulent viscosity μ_t is obtained by assuming that it is proportional to the product of a turbulent velocity scale and a length scale. In the k-ϵ model these velocity and length scales are obtained from two parameters k, the turbulent kinetics energy, and ϵ, the dissipation rate of k as:

$$\mu_t = \rho C_\mu \frac{k^2}{\epsilon} \tag{6.10}$$

where C_μ is an empirical constant. The values of k and ϵ required in Eqn.(6.10) are obtained by solving the following conservation equations:

$$\frac{\partial}{\partial x_i}(\rho u_i k) = \frac{\partial}{\partial x_i}\left(\frac{\mu}{\sigma_k}\frac{\partial k}{\partial x_i}\right)+G_k-\rho\epsilon \tag{6.11}$$

$$\frac{\partial}{\partial x_i}(\rho u_i \epsilon) = \frac{\partial}{\partial x_i}\left(\frac{\mu}{\sigma_\epsilon}\frac{\partial \epsilon}{\partial x_i}\right)+C_1\frac{\epsilon}{k}G_k-C_2\rho\frac{\epsilon^2}{k} \tag{6.12}$$

where C_1 and C_2 are empirical constants, σ_k and σ_ϵ are "Prandtl" numbers governing the turbulent diffusion of k and ϵ, and G_k is the rate of production of turbulent kinetic energy:

$$G_k = \mu_t\left(\frac{\partial u_i}{\partial x_j}+\frac{\partial u_j}{\partial x_i}\right)\frac{\partial u_i}{\partial x_i} \qquad (6.13)$$

The empirical constants in this numerical simulation were C_μ=0.09, C_1=1.44, C_2=1.92, σ_k =1.0 and σ_ϵ=1.3 as recommended by FLUENT User's Manual.

Control volume based technique was used in FLUENT to convert the differential conservation equations to algebraic equations which can be numerically solved. This control volume technique consists of integrating the differential equations about each control volume, yielding a set of finite-difference equations that conserve each quantity on a control-volume basis. Power law scheme developed by Patankar (1980) is used in this discretization procedures. The distretized finite-difference equations are then numerically solved by SIMPLE algorithm on a calculation domain with 50x60 grid. Since the objective of this analysis is to validate the assumption that a dividing streamline does actually exist, no grid independence convergence tests were performed. The simulations were carried out for water flow in a 2-D junction. At the inlet of the T-junction a uniform axial velocity and fully developed turbulence quantities are specified. At the exit of the branch the uniform velocity was determined by the branch flow split ratio and inlet velocity. At the exit of the run the overall continuity was satisfied. Flows at both exits of the branch and run were assumed fully developed flow conditions (zero gradient conditions were prescribed). For the wall, a wall-function treatment is used in FLUENT to account for the steep variation of flow properties in that region. Log-law of the wall is employed to compute the wall stress for turbulent flow.

Fig.6.4 shows the resulting velocity vectors of the simulation for branch flow split ratio $\dot{m}_3/\dot{m}_1=0.7$. The velocity profiles in the horizontal and vertical directions are shown in Figs.6.5 and 6.6. A recirculation region in the branch is predicted by this model. The velocity profile of single-phase water divided in a T-junction has been experimentally studied by Popp and Sallet (1983) and Lamonnier and Hervieu (1991). The results of the model simulation in this study are consistent with their experimental observations. A lower branch flow split ratio case, $\dot{m}_3/\dot{m}_1=0.2$, at the same inlet velocity u=9 m/s was also performed and the velocity vectors is presented in Fig.6.7. A larger recirculation zone was observed when compared with that of the higher branch flow split case. Experimental observations by Popp and Sallet (1983) have shown a similar trend. In model simulation recirculation zones in the run were not observed. The pressure distribution predicted by the model is illustrated in Fig.6.8 at branch split ratio $\dot{m}_3/\dot{m}_1=0.7$. Generally speaking, the single-phase numerical simulation results were consistent with the single-phase data trends reported by Ballyk (1986). However, direct comparisons cannot be made because of the 2-D assumptions of the model and other simplifications.

Figs.6.9 and 6.10 show the stream function contours at branch flow split ratios $\dot{m}_3/\dot{m}_1=0.7$ and $\dot{m}_3/\dot{m}_1=0.2$ respectively. In both cases a dividing streamline which separates inlet flow into two parts forming the branch and run flows is clearly exhibited. Furthermore, with increase of branch flow split ratio, as expected, the "zone of influence" becomes larger. This single-phase simulation may serve as a confirmation for

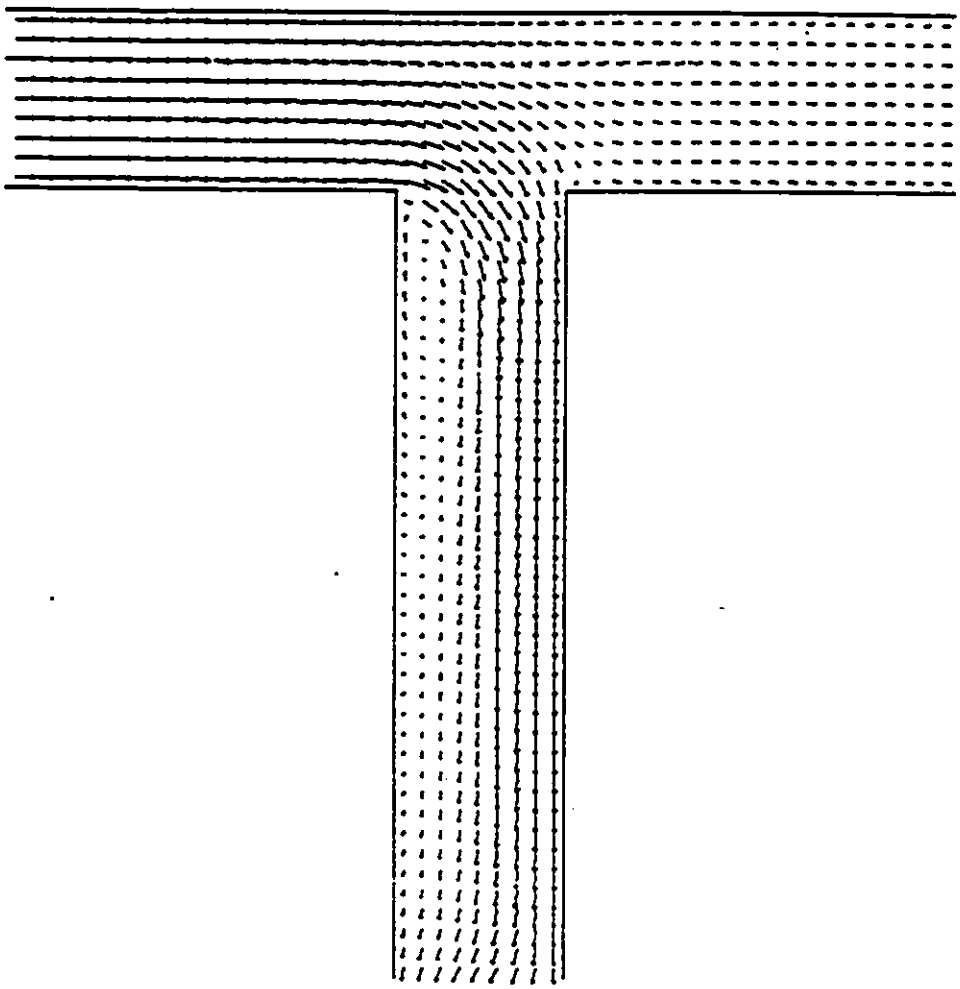

Fig.6.4 Velocity vectors of single-phase flow ($\dot{m}_2/\dot{m}_1=0.7$)

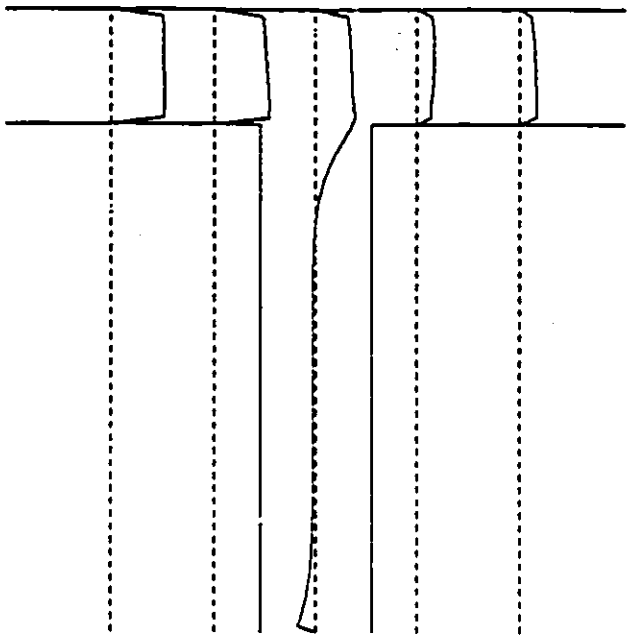

Fig.6.5 Profiles of velocity u in x-direction

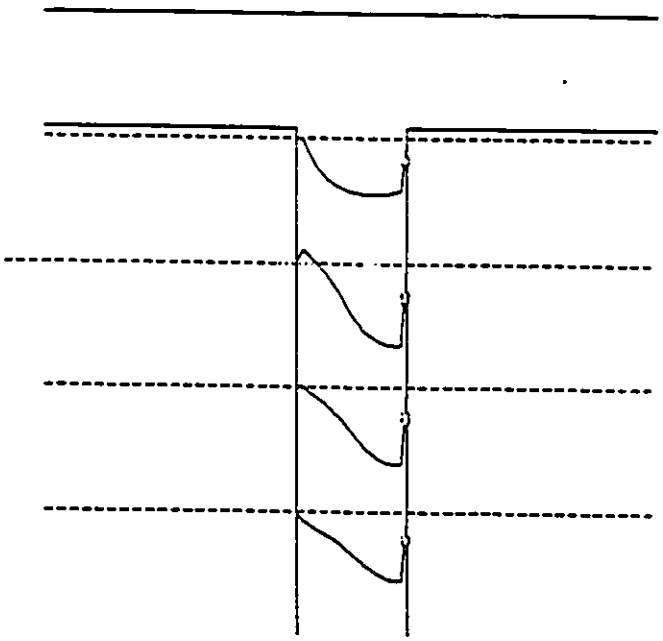

Fig.6.6 Profiles of velocity v in y-direction

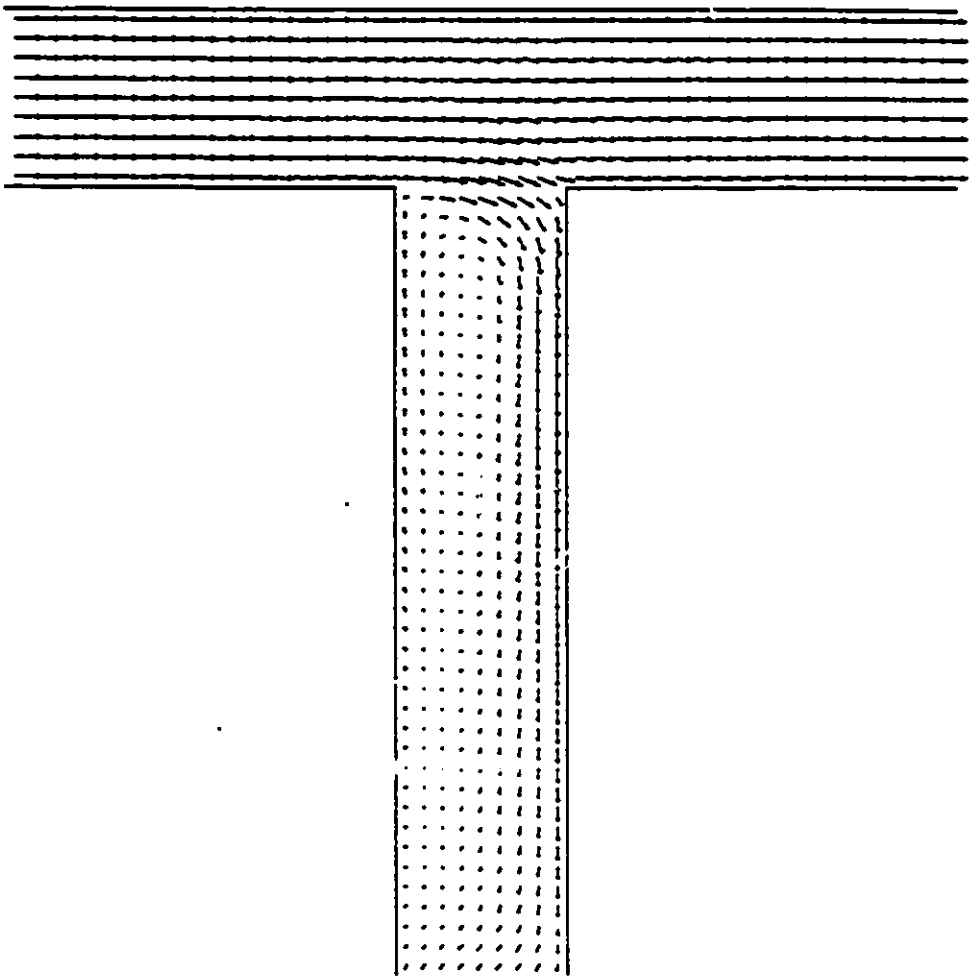

Fig.6.7 Velocity vectors of single-phase flow ($\dot{m}_3/\dot{m}_1=0.2$)

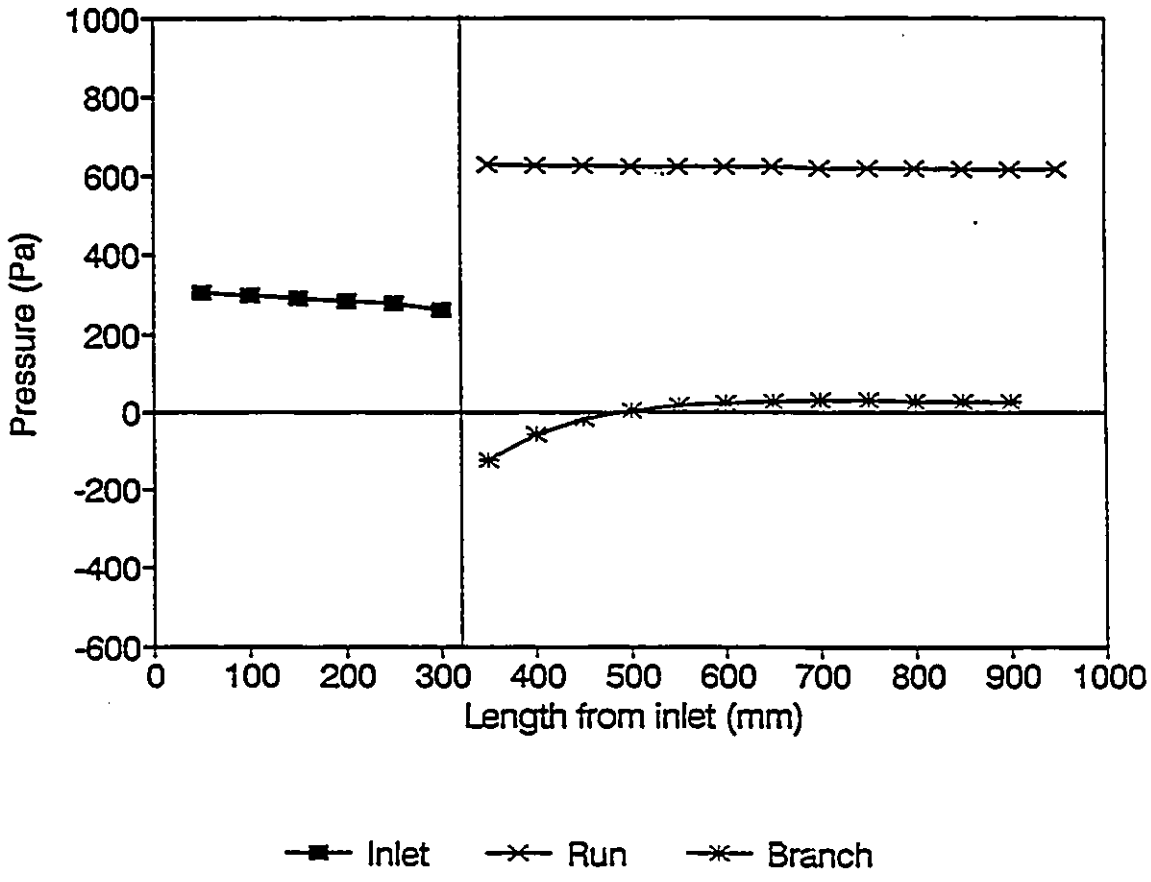

Fig.6.8 Pressure distribution of single-phase flow

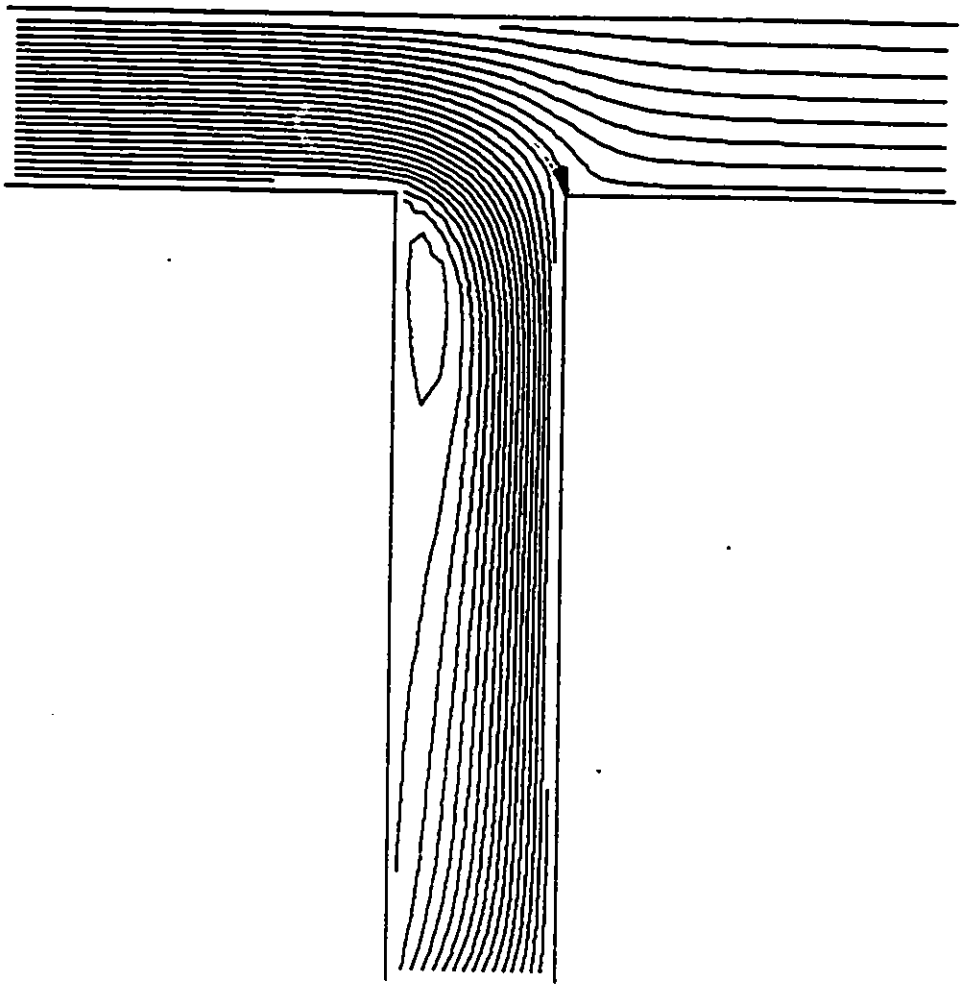

Fig.6.9 Stream function contours ($\dot{m}_2/\dot{m}_1=0.7$)

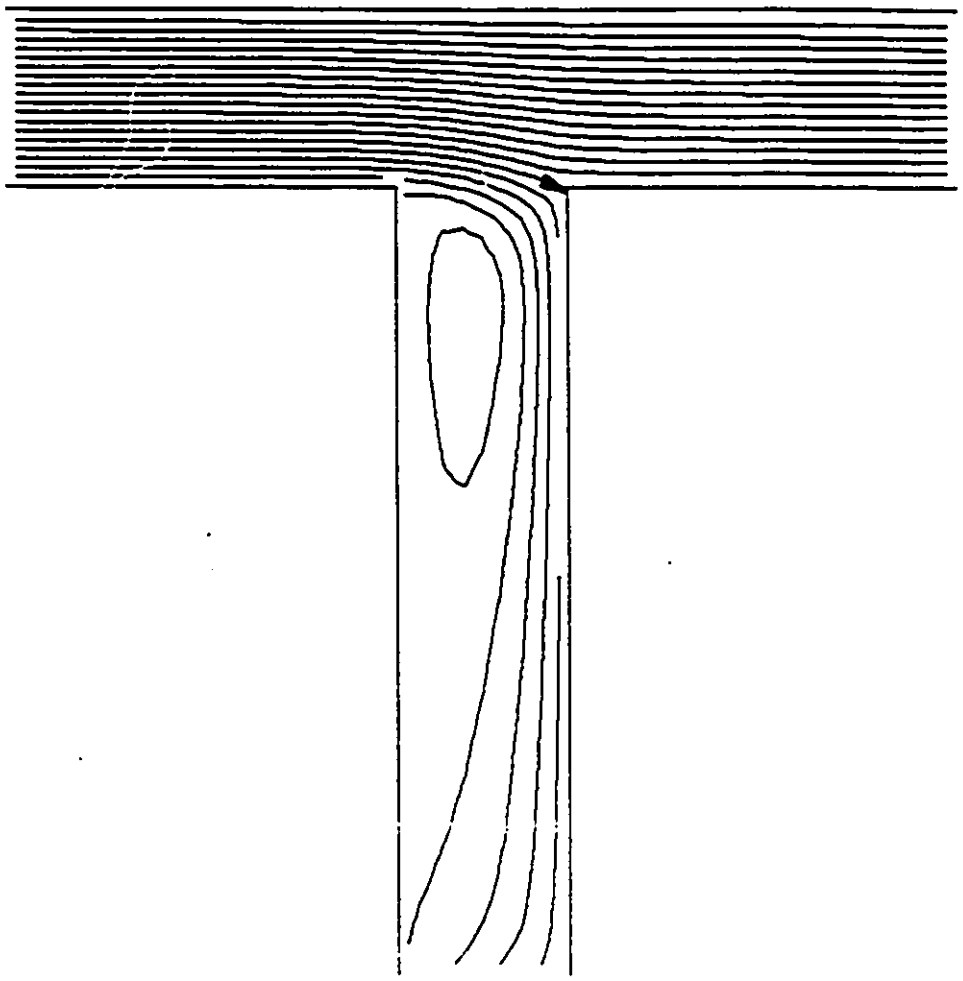

Fig.6.10 Stream function contours ($\dot{m}_2/\dot{m}_1=0.2$)

the use of dividing streamlines in the phenomenological models.

A better simulation result may be obtained by increasing the L/D ratio of branch and run and using larger number of grids in the calculation domain. Since the purpose of this single-phase simulation is mainly to verify the existence of dividing streamline and the satisfactory results have been obtained so far, the numerical study of single-phase flow is not expanded further in this study.

6.4. Development of Annular Flow Phase Redistribution Model

A phenomenological annular flow model capable of predicting phase redistribution in horizontal equal diameter T-junctions has been developed by Ballyk and Shoukri (1990). This model is further developed in this section to a more general one which accounts for the effect of branch orientation on phase redistribution and in which a more accurate inlet annular flow model is incorporated. Up to now there is no phenomenological model available to predict the effect of branch orientation on phase redistribution in T-junctions. The available models are all flow regime dependent models to predict phase redistribution in T-junctions with a horizontal branch. For simplification, in available phenomenological models, the liquid film was assumed to be uniform in the horizontal inlet tube. Under this assumption the effect of branch orientation has no effect on phase redistribution in downstream T-junctions.

As discussed above, the phenomenological models consists of two sub-models

describing the structure of inlet flow and the separation effect of the junction respectively. The gravity has significant effect on both phase distribution in the horizontal inlet and phase redistribution in the downward branches. Consequently, the effect of gravity should be included in the models of annular flow in the inlet and dividing streamlines in the junction.

For simplification, in Ballyk and Shoukri's model (1990) the experimental data from RPI, see Lin et al. (1985) were normalized and used to determine the angular distribution of the liquid film and, therefore, it cannot account for the effect of inlet flow conditions on the variation of liquid film. As an improvement a more detailed annular flow model was used in this work. This model is based on further development of the earlier work of Butterworth (1972 and 1974). Furthermore, the approach to determine dividing streamlines developed by Ballyk and Shoukri (1990) is further developed to account for the gravity effect on phase redistribution in T-junctions. A more general annular phase redistribution model which accounts for the effect of branch orientation is thus developed.

6.4.1. Inlet annular flow model

Considerable progress has been made in the analysis of vertical annular two-phase flow over the past two decades. Since the direction of gravity is parallel to that of the main flow, the angular liquid film distribution is assumed to be uniform along the

circumference of the vertical main inlet tube. The average thickness of the liquid film can be evaluated based on the knowledge of liquid film flow rate and interfacial shear stress. This relationship is usually called "triangular relationship" (Hewitt and Taylor 1970). However, the uniform distribution of the liquid film does not exist in horizontal annular flow. The liquid film thickness is much thicker at the bottom of the tube than at the top due to gravity effect. Consequently, the application of the triangular relationship in horizontal annular flow is much more complicated than in vertical flow. Complications arise both in describing the flow in the presence of gravity and in the solution of the governing equations once they are obtained. In horizontal annular flow, gravity acts in a direction normal to the main flow and produces a circumferential drainage flow in the liquid film. In addition to this gravitational drainage, Butterworth (1972) proposed that there were four mechanisms contributing to the angular distribution of the liquid film in horizontal annular flow:

(i) Transfer of liquid by entrainment and deposition of the liquid droplets.

(ii) Secondary flow of the gas which introduces additional circumferential shear forces.

(iii) Spreading of film by wave motion.

(iv) Surface tension forces.

In view of the complexity of the problem, a simple horizontal annular flow model is employed in the present phase redistribution model, namely the "entrainment-deposition model" which was mainly developed by Butterworth (1972 and 1974).

Fig.6.11 shows diagrammatic representation of the mass balance on a control volume in the liquid film. For a steady flow system, mass conservation yields:

$$\frac{d\Gamma}{d\theta}+R(M_e-M_d) = 0 \qquad (6.14)$$

where Γ is circumferential flow rate per unit length of the tube, M_e and M_d are the entrainment and deposition fluxes of liquid droplet. The thickness of the liquid film can be related to the circumferential flow rate and velocity u_x using the relationship:

$$\Gamma = \int_0^h \rho u_x dy \qquad (6.15)$$

where h is the local thickness of liquid film. Accordingly Eqn.(6.14) can be used to determine the angular distribution of the liquid film thickness provided the circumferential velocity u_x and the fluxes of entrainment and deposition are known. The circumferential velocity u_x can be determined by the momentum equation in the circumferential direction and the fluxes of entrainment and deposition can be evaluated using available empirical correlations.

Fig.6.12 shows a typical fully developed annular flow, the draining liquid film, the coordinate system and the forces acting on the control volume. For the thin films encountered in annular two-phase flow it is more convenient to work with the following coordinates,

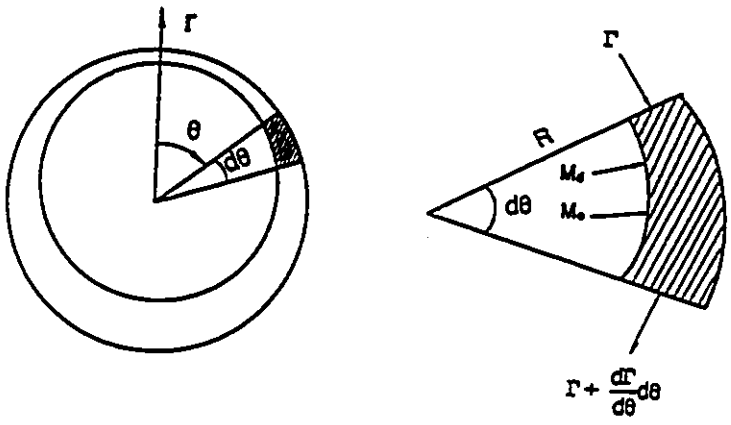

Fig.6.11 Mass balance of liquid film

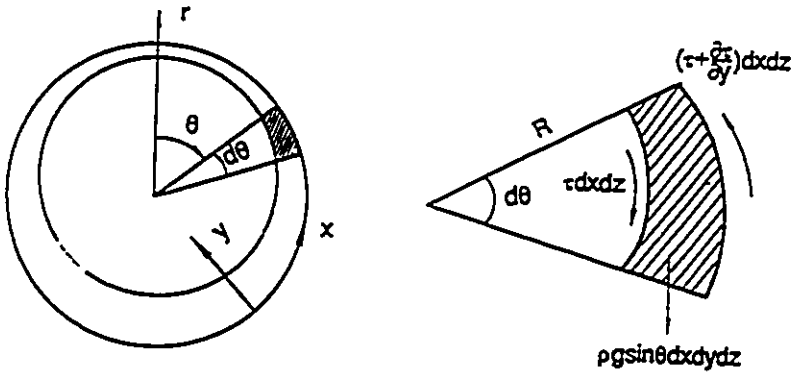

Fig.6.12 Momentum balance of liquid film

$$x = R\theta \tag{6.16}$$

$$y = R-r \tag{6.17}$$

The circumferential momentum equation can be expressed as:

$$u_x\frac{\partial u_x}{\partial x}+u_y\frac{\partial u_x}{\partial y} = \frac{\partial \tau}{\partial y}+\rho g\sin\theta \tag{6.18}$$

For simplification of this non-linear equation, Butterworth (1974) performed an order of magnitude analysis where he showed that the inertial terms in Eqn.(6.18) may be neglected. The simplified circumferential momentum equation has the form of:

$$\frac{\partial \tau}{\partial y}+\rho g\sin\theta = 0 \tag{6.19}$$

In the present study both the cases of laminar flow and turbulent flow for the integration of Eqn.(6.19) have been examined.

6.4.1.1. Laminar circumferential flow

If the circumferential flow is laminar the shear stress can be written as:

$$\tau = \mu\frac{\partial u_x}{\partial y} \tag{6.20}$$

Substituting Eqn.(6.20) into Eqn.(6.19) yields:

$$\mu\frac{\partial^2 u_x}{\partial y^2}+\rho g\sin\theta = 0 \qquad (6.21)$$

The boundary conditions to be satisfied are:

$u_x = 0$ at $y = 0$

$\tau_i = 0$ at $y = h$

The vapour-water interfacial shear stress τ_i is assumed to be zero here, in other words the secondary circumferential flows in the gas phase are ignored. Integration of Eqn.(6.21) with the boundary conditions gives:

$$u_x = \frac{y\rho g\sin\theta}{\mu} - \frac{y^2\rho g\sin\theta}{2\mu} \qquad (6.22)$$

the mean circumferential flow rate can be expressed as:

$$\Gamma = \int_o^h \rho u_x dy = \frac{\rho^2 h^3 g\sin\theta}{3\mu} \qquad (6.23)$$

Combining Eqns.(6.14) and (6.23) yields:

$$\frac{d}{d\theta}\left(\frac{\rho^2 h^3 g\sin\theta}{3\mu}\right)+R(M_e-M_d)= 0 \qquad (6.24)$$

Eqn.(6.24) is a simple ordinary differential equation which can be solved by Runge-Kutta method provided that the initial value of h at the top of the pipe and the correlations for evaluating the fluxes of deposition and entrainment are given.

6.4.1.2. Turbulent circumferential flow

Von Karman's universal axial velocity profile has been successfully used to describe axial liquid film flow (Hewitt 1970).

$$u_z^+ = y^+ \qquad y^+ \leq 5 \tag{6.25}$$

$$u_z^+ = 5.0 \ln y^+ - 3.05 \qquad 5 < y^+ \leq 30 \tag{6.26}$$

$$u_z^+ = 2.5 \ln y^+ + 5.5 \qquad y^+ > 30 \tag{6.27}$$

The dimensionless parameters are defined as:

$$u_z^+ = \frac{u_z}{u^*} \tag{6.28}$$

$$y^+ = \frac{u^* \rho y}{\mu} \tag{6.29}$$

where u^* is the friction velocity,

$$u^* = \sqrt{\frac{\tau_w}{\rho}} \tag{6.30}$$

For turbulent circumferential flow, the momentum Eqn.(6.19) can be written as:

$$(\nu+\varepsilon)\frac{\partial^2 u_x}{\partial y^2}+g\sin\theta = 0 \qquad (6.31)$$

where ϵ is turbulent diffusivity which is assumed to be consistent with the following profile if the axial flow velocity u_z^+ is expressed as Eqns.(6.25) to (6.27):

$$\frac{\varepsilon}{\nu} = 0 \qquad y^+ \le 5 \qquad (6.32)$$

$$\frac{\varepsilon}{\nu} = \frac{y^+}{5.0} - 1 \qquad 5 < y^+ \le 30 \qquad (6.33)$$

$$\frac{\varepsilon}{\nu} = \frac{y^+}{2.5} - 1 \qquad y^+ > 30 \qquad (6.34)$$

If the turbulent diffusivity is assumed to be isotropic, Eqns.(6.32) to (6.34) can be used as the profile of turbulent diffusivity in circumferential flow (Butterworth, 1974). Integrating Eqn.(6.31) with Eqns.(6.32) to (6.34), using the same boundary conditions in laminar flow, yields circumferential velocity profile as:

$$u_x^+ = B\left[h^+ y^+ - \frac{1}{2}(y^+)^2\right] \qquad y^+ \le 5 \qquad (6.35)$$

$$u_x^+ = 5B\left[h^+ - y^+ + h^+ \ln\frac{y^+}{5} + \frac{5}{2}\right] \qquad 5 < y^+ \le 30 \qquad (6.36)$$

$$u_x^* = 5B\,[h^*(1+\ln 6) + \frac{h^*}{2}\ln\frac{y^*}{30} - \frac{y^*}{2} - \frac{25}{2}] \qquad y^*>30 \qquad (6.37)$$

where

$$B = \frac{\nu g \sin\theta}{(u^*)^3} \qquad (6.38)$$

$$h^* = \frac{hu^*}{\nu} \qquad (6.39)$$

The dimensionless circumferential flow rate is integrated as:

$$\Gamma_x^* = \int_0^{h^*} u_x^* dy^* = \beta\phi(h^*)\sin\theta \qquad (6.40)$$

where

$$\beta = \frac{B}{\sin\theta} \qquad (6.41)$$

$$\phi = \frac{1}{3}(h^*)^3 \qquad h^*\le 5 \qquad (6.42)$$

$$\phi = 5\,[5h^* + (h^*)^2(\ln\frac{h^*}{5} - \frac{1}{2}) - \frac{25}{6}] \qquad 5<h^*\le 30 \qquad (6.43)$$

$$\phi = 5\,[(h^*)^2(\frac{1}{4} + \ln 6 + \frac{1}{2}\ln\frac{y^*}{30}) - 25h^* + \frac{1325}{6}] \qquad h^*>30 \qquad (6.44)$$

The dimensionless mass conservation of liquid film can be expressed as:

$$\frac{d\Gamma_x^+}{d\theta} = M_d^+ - M_e^+ \tag{6.45}$$

where

$$M_d^+ = \frac{M_d R}{\mu} \qquad M_e^+ = \frac{M_e R}{\mu} \tag{6.46}$$

Combining Eqns.(6.40) to (6.46) results in:

$$\frac{dh^+}{d\theta} = \frac{M_d^+ - M_e^+}{\beta\dot{\phi}\sin\theta} - \frac{\phi\cos\theta}{\dot{\phi}\sin\theta} \tag{6.47}$$

where

$$\dot{\phi} = \frac{d\phi}{dh^+} \tag{6.48}$$

Eqn.(6.47) was derived earlier by Lin et al. (1985). It is an initial value ordinary differential equation as Eqn.(6.24). If the initial value of film thickness at the top of the tube and the correlations for evaluating M_e and M_d are available these two equations can be numerically integrated with well known Runge-Kutta method.

6.4.1.3. Entrainment and deposition

There are no theoretical models available for liquid droplet entrainment and

deposition fluxes, in order to perform the numerical solution for Eqns.(6.24) and (6.47), empirical correlations of the entrainment and deposition fluxes of liquid droplets were used in the present study as the earlier treatment by Fisher and Pearce (1978) and Lin et al. (1985). The deposition flux of liquid droplets is assumed to depend on its concentration in the gas core:

$$M_d = K\frac{E\dot{m}_L}{\frac{E\dot{m}_L}{\rho_L}+\frac{\dot{m}_g}{\rho_g}} \tag{6.49}$$

The dimensional constant K, in this study, was evaluated using Eqn.(6.47) at the initial value of film thickness and the condition of zero film thickness gradient at the top of the tube.

An entrainment flux correlation of liquid droplets was developed for vertical annular flow by Hutchinson and Whalley (1973). This correlation gives the entrainment flux as a function of the dimensionless group:

$$S = \frac{\tau_i h}{\sigma} \tag{6.50}$$

where τ_i is the interfacial shear stress. As a first approximation the interfacial shear stress was assumed to be the same as the axial wall shear stress τ_w which was evaluated by the Blasius equation. In the absence of information for horizontal annular flow it was assumed that Hutchinson and Whalley's correlation (1973) was valid in horizontal flows:

$$M_e = 0.15e^{(5.76-\frac{2.303}{S^{0.33}})} \tag{6.51}$$

6.4.1.4. Results

Results of the numerical solution of Eqn.(6.24) for laminar flow and Eqn.(6.47) for turbulent flow are shown in Fig.6.13. The experimental measurements by Fisher and Pearce (1978) are also presented. The measurements were taken in air-water horizontal annular flow in a 19.1 mm diameter tube under inlet mass flux G=530 kg/m^2.s and inlet quality x=5.5%. As shown in Fig.6.13 this simple entrainment-deposition model can predict the data reasonably well. The comparisons of the model prediction with the measurements of Butterworth (1972) are shown in Fig.6.14. Butterworth performed the measurement in a 31.8 mm diameter tube at G=342 kg/m^2.s, x=7.2%. In this lower mass flux and higher quality flow, the predicted results can generally capture the data trend but significantly underpredicts the value of the data. The deviation of model prediction from the measurements, especially in the lower part of the tube, is clearly shown in Fig.6.14. Comparison of the different circumference liquid film flows shows that, in any case, the turbulent flow model works better than the laminar flow model. A further modification of this simple model was not performed since there is no film thickness measurement data available for the present steam-water flow conditions.

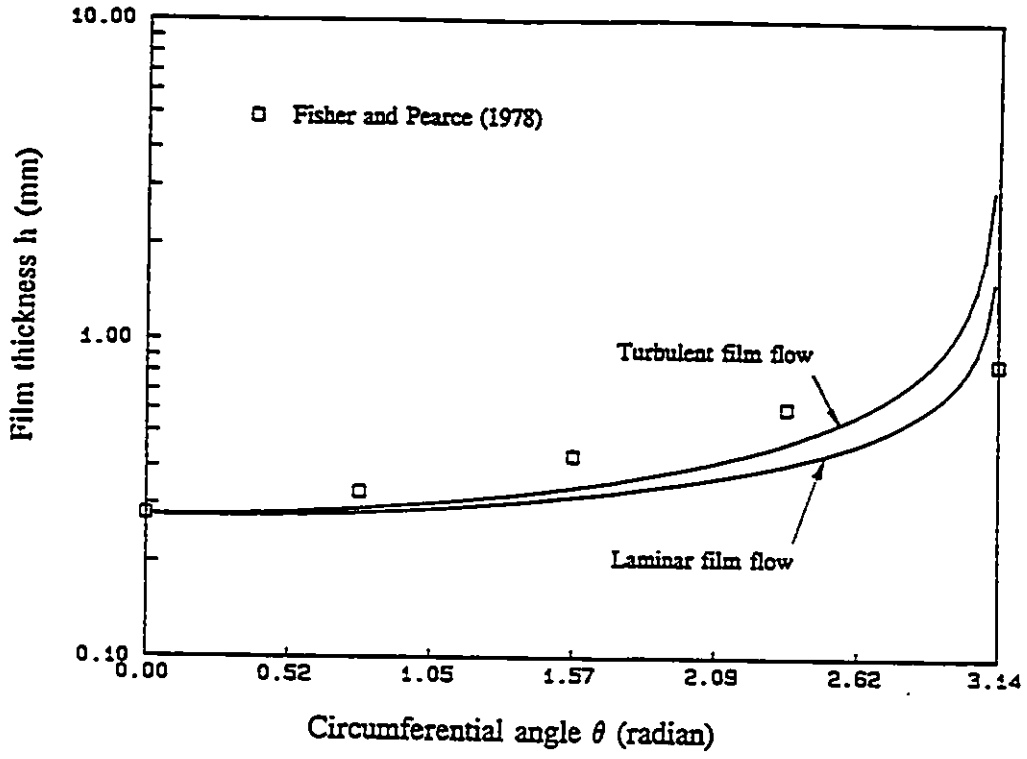

Fig.6.13 Model prediction with Fisher and Pearce data (1978)

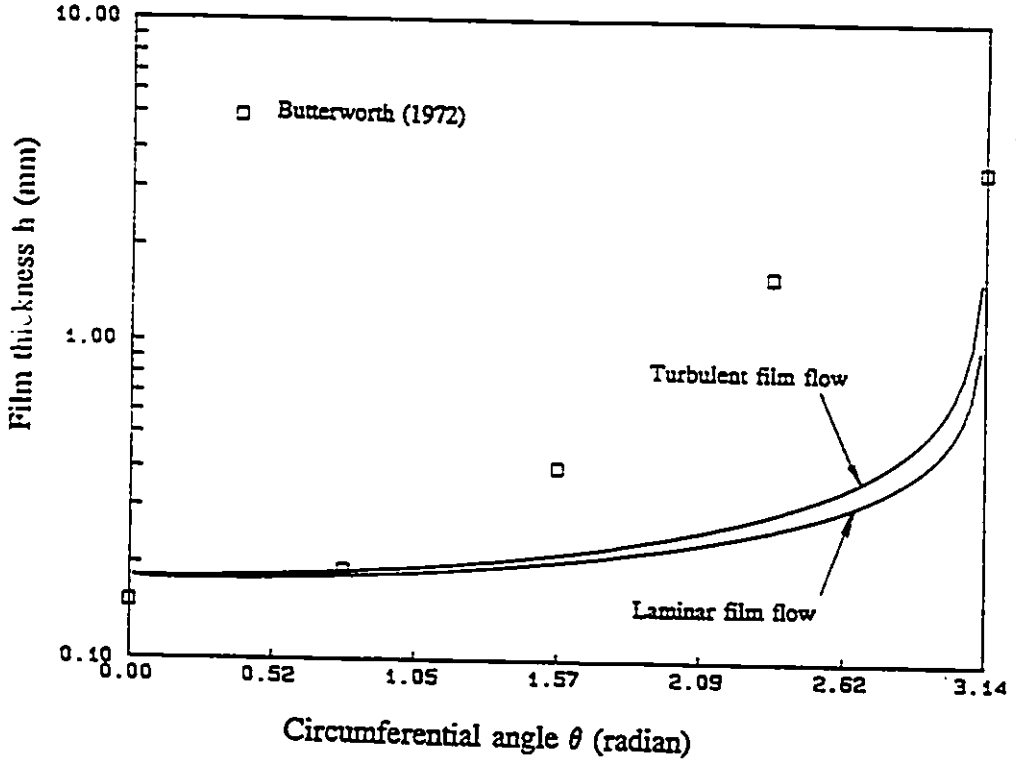

Fig.6.14 Model prediction with Butterworth et al. data (1972)

A more sophisticated model of liquid film thickness could be obtained by adding the effect of vapour secondary flow into the momentum equation (Laurinat et al. 1985) or performing more advanced numerical simulation using multi-fluid model (Tso and Sugawara, 1990). As a first approximation, the simple turbulent entrainment-deposition model was used in the development of the present model of phase redistribution.

6.4.2. Dividing streamline model

Generally speaking, the phenomenological models are based on the physical understanding that there is a dividing streamline in the junction. The amount of vapour flowing to the branch conduit comes from the area bounded by the vapour dividing streamline and the liquid film boundary.

Ballyk & Shoukri (1990) developed a simple approach to determine the liquid and vapour dividing streamlines in horizontal branch using free streamline theory of potential flow. The streamline equations, rather than the detailed field equations, were numerically integrated to determine the positions of the dividing streamline of each phase. The approach is now extended to determine the dividing streamlines in T-junction with downward branch in which the gravity effect is included in the model.

As shown in Fig.6.15 the path of the dividing streamline within the junction in a plane parallel to the branch can be determined from a shooting solution of the streamline equation:

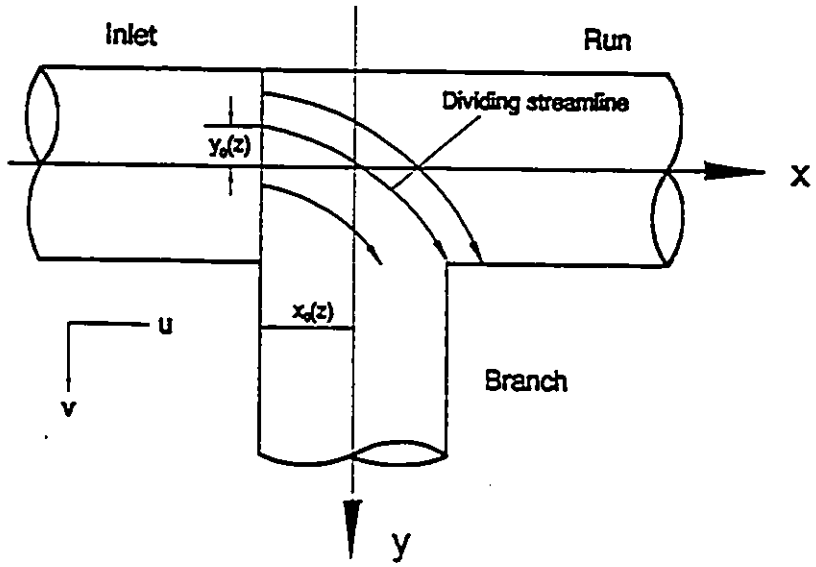

Fig.6.15 Dividing streamline defined by Baliyk and Shoukri (1990)

$$\frac{\Delta x}{u_{ij}} = \frac{\Delta y}{v_{ij}} \tag{6.52}$$

The velocities are expressed by the fist order of Taylor series as:

$$u_{i+1,j+1} = u_{i,j} + \frac{\partial u}{\partial x}\Delta x + \frac{\partial u}{\partial y}\Delta y \tag{6.53}$$

$$v_{i+1,j+1} = v_{i,j} + \frac{\partial v}{\partial x}\Delta x + \frac{\partial v}{\partial y}\Delta y \tag{6.54}$$

The derivatives in Eqns.(6.53) and (6.54) can be obtained from continuity and momentum equations as well as the irrotational flow relation:

$$\frac{\partial u}{\partial x} + \frac{\partial v}{\partial y} = 0 \tag{6.55}$$

$$u\frac{\partial u}{\partial x} + v\frac{\partial u}{\partial y} = -\frac{1}{\rho}\frac{\partial p}{\partial x} \tag{6.56}$$

$$u\frac{\partial v}{\partial x} + v\frac{\partial v}{\partial y} = -\frac{1}{\rho}\frac{\partial p}{\partial y} + \rho g\sin\theta \tag{6.57}$$

$$\frac{\partial v}{\partial x} - \frac{\partial u}{\partial y} = 0 \tag{6.58}$$

Rearranging Eqns.(6.55) to (6.58) yields:

$$\frac{\partial v}{\partial y} = -\frac{\partial u}{\partial x} \tag{6.60}$$

$$\frac{\partial u}{\partial x} = \frac{u}{u^2+v^2}\left[\frac{v}{u\rho}\frac{\partial p}{\partial y} - \frac{1}{\rho}\frac{\partial p}{\partial x} - \frac{v\rho\sin\theta}{u}\right] \tag{6.59}$$

$$\frac{\partial u}{\partial y} = \frac{\partial v}{\partial x} \tag{6.61}$$

$$\frac{\partial v}{\partial x} = \left[-\frac{1}{\rho}\frac{\partial p}{\partial y} + \rho g\sin\theta - v\frac{\partial v}{\partial y}\right]\frac{1}{u} \tag{6.62}$$

Before substituting these derivative into Eqns.(6.53) and (6.54) the pressure gradients $\partial p/\partial x$ and $\partial p/\partial y$ have to be determined. At present there is no report on the pressure gradients $\partial p/\partial x$ and $\partial p/\partial y$ in the T-junction. However, experimental observations have shown that, (i) the value of $\partial p/\partial x$ is positive while the value of $\partial p/\partial y$ is negative and, (ii) the absolute value of $\partial p/\partial y$ (the slope of the branch pressure profile) is much larger than that of $\partial p/\partial x$ (the slop of the run pressure profile). As a first approximation, the pressure in x-direction through the run and in y-direction through the branch are assumed to increase and decrease linearly respectively:

$$\frac{\partial p}{\partial x} = \frac{\Delta P_{2\text{-}1}}{(DLX+R)} \tag{6.63}$$

$$\frac{\partial p}{\partial y} = -\frac{\Delta P_{1\text{-}3}}{(DLY+R)^4} \tag{6.64}$$

The pressure changes $\Delta P_{2\text{-}1}$ and $\Delta P_{1\text{-}3}$ were experimentally determined as shown in the previous section. It should be noted that in a complete mechanistic model, the pressure distribution should be obtained as part of the solution. However, since the

current state-of-the-art does not permit that, the problem is incomplete and the empirical correlations for pressure changes are used to calculate the flow field. Using the development lengths DLX and DLY in Eqns.(6.63) and (6.64) to correlate the pressure gradients is such an assumption which depends on the experimental observations and closely correlates with the slopes of the pressure profiles.

The initial velocity of the y-component v_0 in Eqns.(6.53) and (6.54) is prescribed to zero for both liquid and vapour phases since the flow is assumed to be 1-D flow in the inlet conduit. The initial velocity of the x-component for the vapour and liquid is determined by considering the presence of liquid entrainment in the gas core. The mean velocities of vapour, liquid film and liquid droplets can be expressed as:

$$u_g = \frac{Gx}{\alpha \rho_g} \tag{6.65}$$

$$u_f = \frac{G(1-x)(1-E)}{\alpha_f \rho_L} \tag{6.66}$$

$$u_e = \frac{G(1-x)E}{\alpha_e \rho_L} \tag{6.67}$$

where α, α_f and α_e are the inlet volumetric concentrations of the vapour (void fraction), liquid film and entrained droplets respectively.

It is reasonable to assume that the droplets in the gas core are travelling at the same velocity as the gas phase, i.e.

$$u_e = u_g \tag{6.68}$$

Combining Eqns.(6.65) and (6.67) gives:

$$\alpha_f = 1-\alpha-\frac{\alpha(1-x)E\rho_g}{x\rho_L} \tag{6.69}$$

where the relation

$$\alpha+\alpha_f+\alpha_e=1 \tag{6.70}$$

is used. The average film velocity is obtained by substituting Eqn.(6.69) into Eqn.(6.66) as:

$$u_f = \frac{\rho_g u_g(1-x)(1-E)}{\rho_L x}\left[\frac{1}{\alpha}-1-\frac{E(1-x)\rho_g}{x\rho_L}\right]^{-1} \tag{6.71}$$

Finally the initial conditions of the x-component vapour and liquid velocities are assumed to be:

$$u_{go} = u_g \tag{6.72}$$

$$u_{Lo} = u_f \tag{6.73}$$

An any height of z in the junction, the initial position of the dividing streamline in x-direction x_0 (Fig.6.15) can be geometrically determined as:

$$x_o = -\sqrt{(R^2-Z^2)} \tag{6.74}$$

With an initially guessed value the shooting solution is performed. If the

determined dividing streamline fails to end at the corner of tube intersection, as shown in Fig.6.15, the initial value is modified and the shooting process restarts until the correct dividing streamline is obtained.

6.4.3. Model predictions

The position of dividing streamlines at different heights of the inlet cross section are determined to form surfaces y_{oL} and y_{og}, separating the inlet water and vapour flows as the branch and run flows as shown in Fig.6.16. Flows of each phase entering the shaded areas are assumed to be extracted to the branch and the remaining flow to the run. The shaded areas of each phase A_{Lb} and A_{gb} are bounded by the dividing streamline surfaces and the interface of liquid-vapour as well as the inlet tube wall. As shown earlier, the phase separation ratio x_3/x_1 is evaluated by the knowledge of geometrical relationships of the areas A_{Lb}, A_{gb}, A_L and A_g as:

$$\frac{x_3}{x_1} = \frac{A_{gb}A_f}{A_f A_{gb}x_1 + (1-x_1)(1-E)A_{Lb}A_g} \qquad (6.75)$$

In annular flow a part of the liquid is entrained in the vapour core as liquid droplets and it is assumed that this part of liquid, due to the high axial momentum fluxes, are not diverted into the branch until the entire liquid film is extracted. It is assumed that only the liquid film, having lower momentum flux, can be extracted to the branch. As a result, in annular flow the area occupied by liquid A_L in above equations are assumed

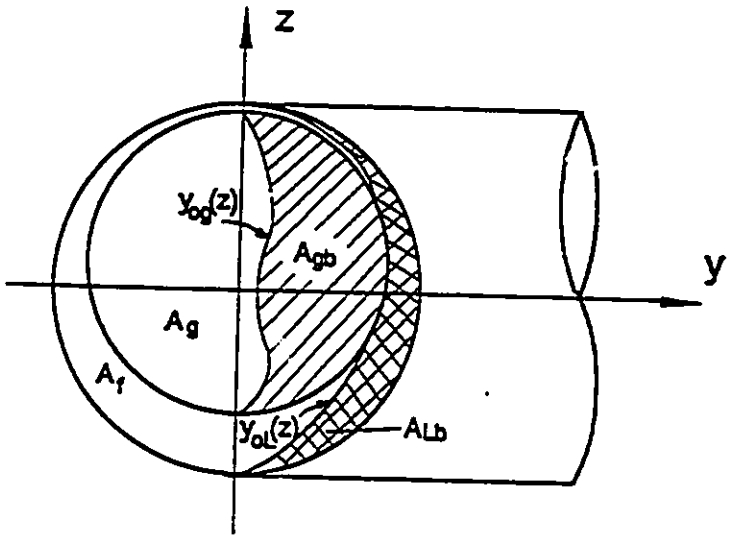

Fig.6.16 Definitions of annular flow phase separation model

to be equal to the area occupied by the liquid film A_f which is expressed as:

$$A_f = \int_0^{2\pi}\int_{R-h}^{R} r dr d\theta = 2R\int_0^{\pi} h d\theta - \int_0^{\pi} h^2 d\theta \qquad (6.76)$$

The integration of the liquid film thickness $h(\theta)$ in Eqn.(6.76) can be performed using the Simpson method with the information of the angular distribution of liquid film discussed in previous section. Several empirical correlations are available to evaluate the entrainment fraction E in Eqns.(6.75). As the result of comparison of a few correlations, E was estimated by the correlation recommended by Dallman et al. (1984):

$$E = \left(1-\frac{W_{LFC}}{W_F}\right)\cdot\frac{3.6\cdot10^{-5}[(D_1-2h)\rho_g^{\frac{1}{2}}\rho_L^{\frac{1}{2}}u_g^3]^{1.5}}{1+3.6\cdot10^{-5}[(D_1-2h)\rho_g^{\frac{1}{2}}\rho_L^{\frac{1}{2}}u_g^3]^{1.5}} \qquad (6.77)$$

where W_{LFC} is the critical film flow rate at which the process of droplet entrainment takes place. This critical film flow rate was fixed as 0.175 kg/s in this analysis. W_F is averaged film flow rate calculated from the inlet flow condition. The inlet tube diameter D_1 and the averaged liquid film thickness h can be correlated with the inlet vapour void fraction α measured in the present investigation:

$$D_1 - 2h = D_1\sqrt{\alpha} \qquad (6.78)$$

The two-phase properties, e.g. densities ρ_g and ρ_L, viscosity μ_g and μ_L and surface tension σ were evaluated using the regressive equations obtained from standard saturated water-vapour table (Ballyk, 1992).

The model developed in this analysis is an improved version of that developed by Ballyk (1992) as it incorporates a general film thickness distribution model and is capable of predicting the effect of branch orientation on phase redistribution. It is the first phenomenological model which accounts for the effect of branch orientation. The models available so far are only valid for the junctions with a horizontal branch.

Fig.6.17 presents the predictions of this model under different branch orientations. The results are based on the inlet mass flux G_1=600 kg/m^2.s, inlet quality x_1=5.0% and inlet pressure P_1=1.5 bar. The development length DLX in the run was fixed at 20 diameters and DLY were fixed at 10, 15 and 20 diameters for the horizontal, 45^0 downward and 90^0 downward branches respectively. The entrainment fraction E under such an inlet condition was calculated as 6.1% using Eqn.(6.78). As shown, the model predicts the levels of phase separation in different branch orientations fairly well. In horizontal annular inlet flow the thickness of liquid film at the bottom of the tube is much thicker than that in the other locations of the circumference of the inlet tube due to the gravity effect. Consequently, there is much more liquid available for extraction through the downward branch and the level of phase separation should be much lower than that of horizontal branch. As shown in Fig.6.17, the model is capable of capturing the correct trend of the data.

Figs.6.18 and 6.19 show the predicted results of the same inlet quality x_1 = 2.0%, but different inlet mass flux G_1=600 kg/m^2.s and G_1=900 kg/m^2.s, respectively. The inlet pressure P_1 in these two cases was 1.2 bar and 1.3 bar respectively. The

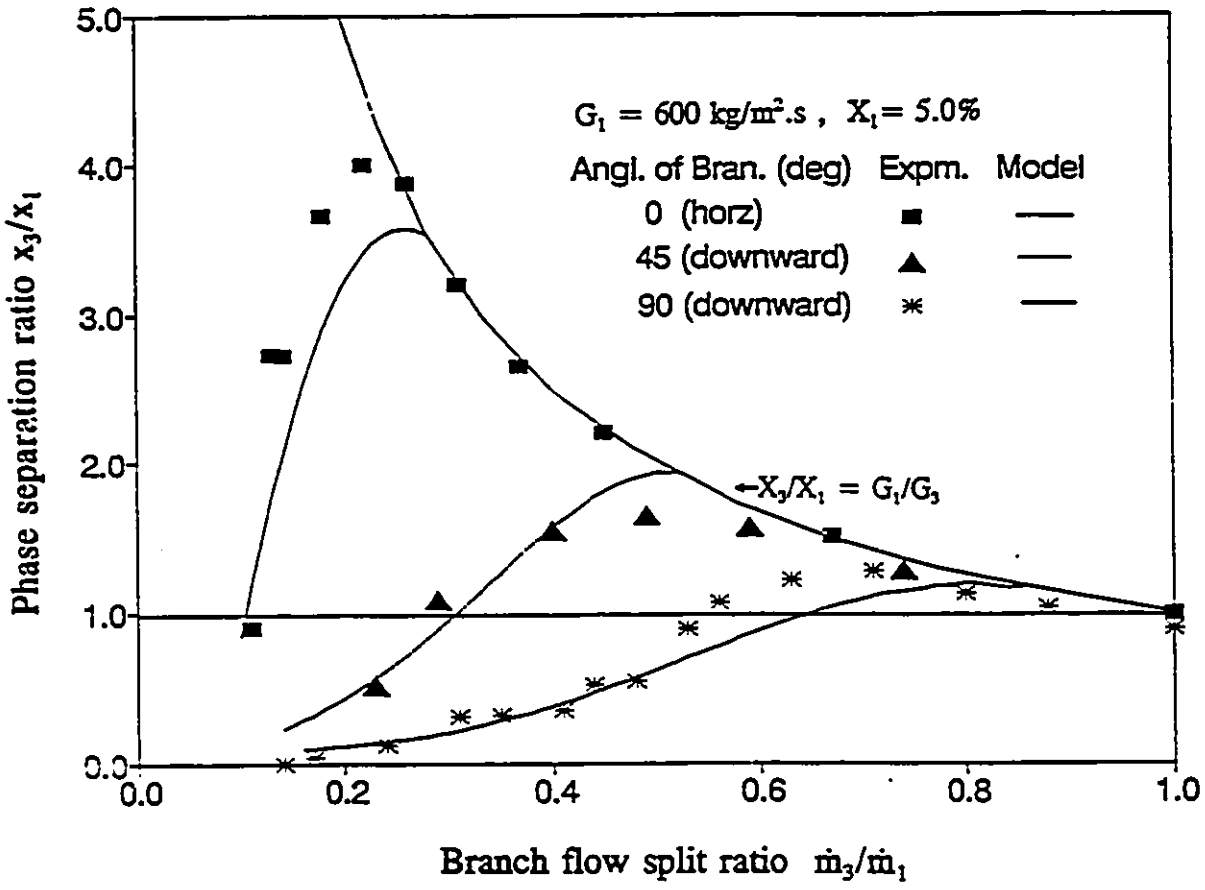

Fig.6.17 Model prediction of the effect of the branch orientation in annular flow (G_1=600 kg/m².s, x_1=0.05)

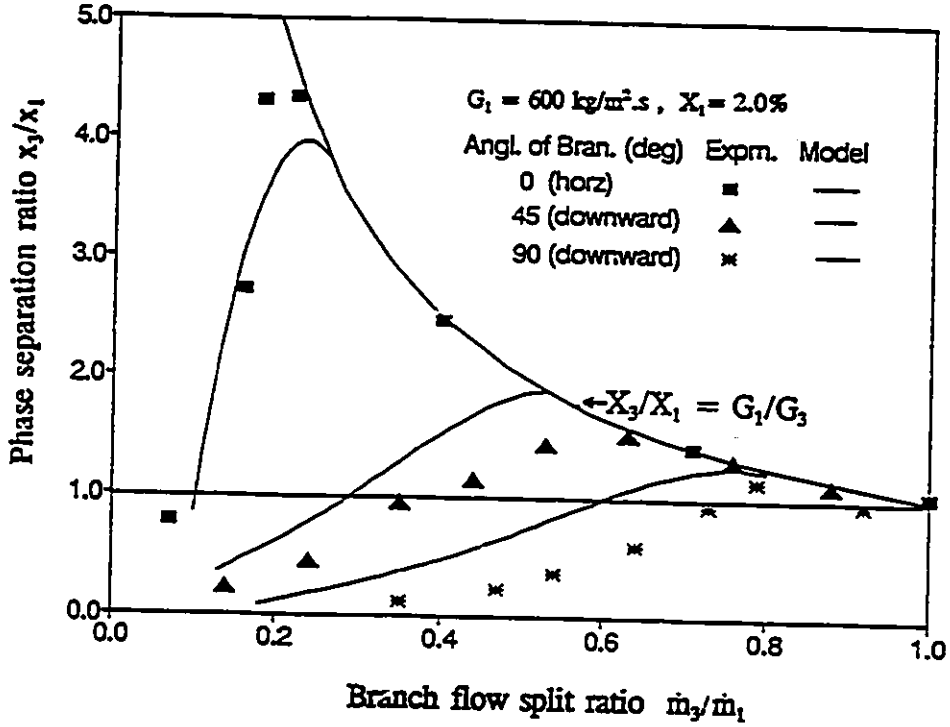

Fig.6.18 Model prediction of the effect of the branch orientation in annular flow (G_1=600 kg/m².s, x_1=0.02)

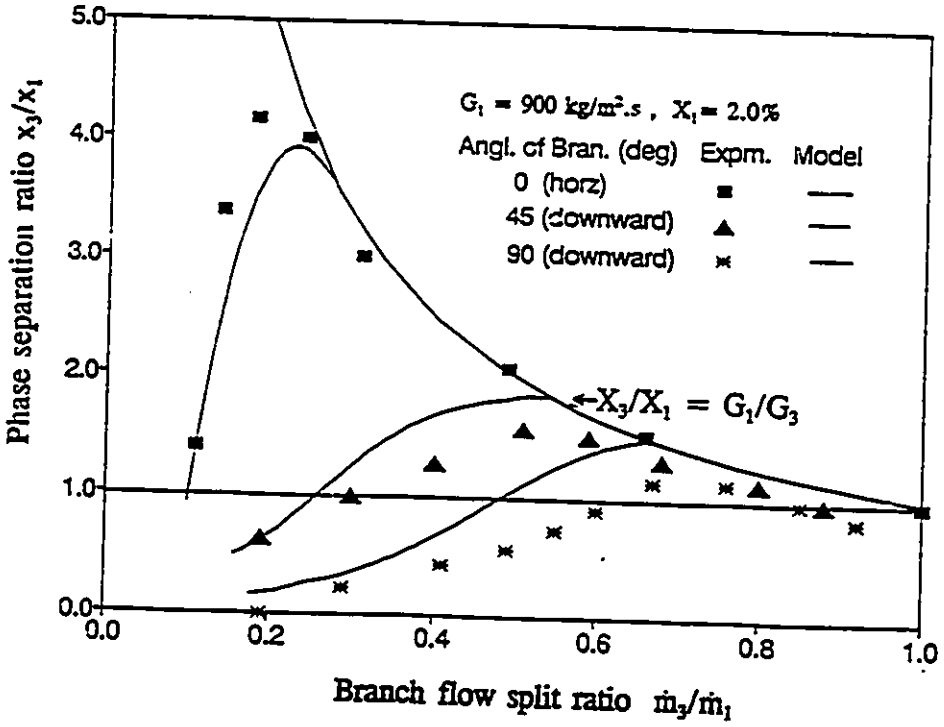

Fig.6.19 Model prediction of the effect of the branch orientation in annular flow (G_1=900 kg/m².s, x_1=0.02)

entrainment fraction E in these two inlet conditions were predicted as 0.25% for the inlet mass flux of 600 kg/m^2.s and 1.63% for the inlet mass flux of 900 kg/m^2.s. The phase redistribution data in different branch orientations are predicted reasonably well in these two conditions.

Fig.6.20 shows the predicted results for inlet mass flux G_1=600 kg/m^2.s, inlet quality x_1=8.0% and inlet pressure P_1=1.65 bar. As shown, the model fails to predict the phase redistribution for the downward branches under this inlet flow condition. The value of the phase separation ratio x_3/x_1 is clearly underpredicted in the downward branches. It is believed that a higher inlet flow quality results in a more uniform liquid film distribution, probably due to the existence of vapour secondary flow. However, the simple analysis of the angular distribution of liquid film used in this study are incapable of modelling the variation of liquid film. The distribution of the film in the entrainment-deposition model is based on the mass balance of liquid entrainment and deposition fluxes and circumferential drainage flow. The effect of vapour secondary flow is ignored. As the inlet quality increases, the effect of the secondary flow may lift up some of the liquid from the bottom of the tube, as a result, more liquid is ready to be extracted for horizontal branch and less liquid is available for downwardly oriented branches. The phase separation ratio x_3/x_1, accordingly, is reduced in the horizontal branch and is increased in the downward branches under a higher inlet quality condition. A correct prediction of this trend in horizontal and downward branches requires that the model can predict the variation of liquid film distribution accurately and, therefore, a more

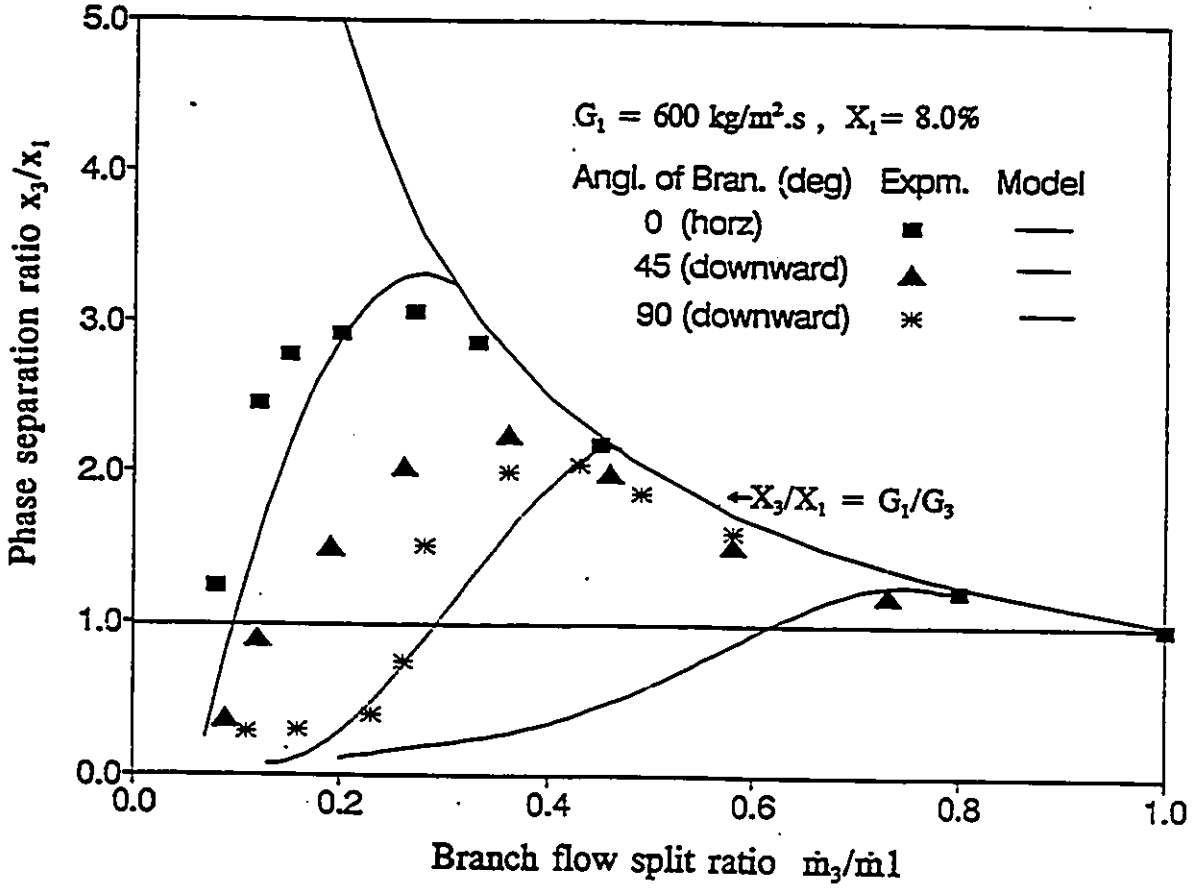

Fig.6.20 Model prediction of the effect of the branch orientation in annular flow (G_1=600 kg/m².s, x_1=0.08)

sophisticated model for inlet annular flow is needed to account for the effect of vapour secondary flow.

Advancing the modelling of phase redistribution in annular flow in T-junctions appear to be limited by the lack of an accurate model of film thickness distribution in the inlet tube. It might not be realistic to expect that a satisfactory prediction of phase redistribution can be achieved without obtaining an accurate knowledge of phase distribution of the inlet flow. Studies on the liquid entrainment and deposition of liquid droplet are also critical to model annular flow. These fundamental research works on annular two-phase flow are all potential subjects for future studies.

6.5. Development of Stratified Flow Phase Redistribution Model

For low velocities of vapour and liquid flow in a horizontal pipe, a stratified flow regime exits whereby the liquid moves along the bottom of the pipe and the vapour concurrently flows above it. In stratified flow in T-junctions, the phenomenological model of phase redistribution also requires two sub-models to account for the different effects of phase distribution in the inlet and phase redistribution in the junction separately. The inlet stratified flow is characterized by the height of liquid level, or the liquid holdup; a terminology usually used in the literature. Several models are available for modelling stratified flow. Among these models, Taitel-Dukler's model has the feature of being simple, therefore, is employed in this study to develop a new phenomenological

phase redistribution model for stratified flow in T-junctions. The analysis given in section 5.2.3. showed that the Taitel-Dukler model is capable of predicting the liquid level accurately within the range of smooth stratified flow but underpredicts the liquid level when large amplitude roll waves were generated. The dividing streamline model developed by Ballyk and Shoukri (1990) is again further developed to be applicable in stratified flow.

6.5.1. Inlet stratified flow model

The first widely used correlation for predicting liquid holdup (the fraction of the pipe cross section occupied by liquid) in stratified flow was developed by Lockhart and Martinelli (1949). More than 20 years later, Johannessen (1972) theoretically analyzed Lockhart and Martinelli's experiments and developed a model in which the shear stress at the liquid-gas interface was neglected and it was assumed that liquid and gas were both turbulent flows. Agrawal et al. (1973) and Russel et al. (1974) studied stratified flow in a more adequate fashion but did not reach a generalized dimensionless correlation. The most widely used model in stratified flow came from Taitel and Dukler (1976), in which a simple momentum balance was applied on the two phases. In this model, the liquid-gas interfacial frictional factor f_i was assumed to be equal to the gas friction factor f_g. Cheremisinoff and Davis (1979) attempted to account for the effect of interfacial waves on the interfacial friction factor f_i. They recommended different correlations to evaluate

f_i for small amplitude waves and roll waves. Andritsos and Hanratty (1987) recommended a new approach to calculate the interfacial stresses from their measurement for fully developed stratified flow. Good agreement was achieved by these improvements on the evaluation of the interfacial frictional factor. However, both the methods of Andritsos and Hanratty (1987) and Cheremisinoff and Davis (1979) need an iterative procedure to solve. In the present study of modelling phase redistribution for stratified flow, Taitel and Dukler's model (1976) was used to evaluate the liquid level in the inlet tube. Andritsos and Hanratty model (1987) was used when the superficial velocity was higher than 3 m/s.

In Taitel and Dukler's model the liquid holdup was obtained by considering the momentum balance for fully developed flow for the two phases separately:

$$-A_g\left(\frac{dp}{dx}\right)-\tau_{wg}S_g-\tau_i S_i=0 \qquad (6.79)$$

$$-A_L\left(\frac{dp}{dx}\right)-\tau_{wL}S_L+\tau_i S_i=0 \qquad (6.80)$$

Eqn.(6.79) represents a balance between the pressure forces on the gas space and the resisting stresses at the gas-solid boundary τ_{wg} and at the gas-liquid interface τ_i; Eqn.(6.80) is a balance between the forces due to pressure, the drag of the gas on the liquid and the resisting stress at the liquid-solid boundary τ_{wL}, as show in Fig.6.21. By eliminating the pressure gradient between Eqns.(6.79) and (6.80), which is the basic postulation of Lockhart-Martinelli type approach, one can get:

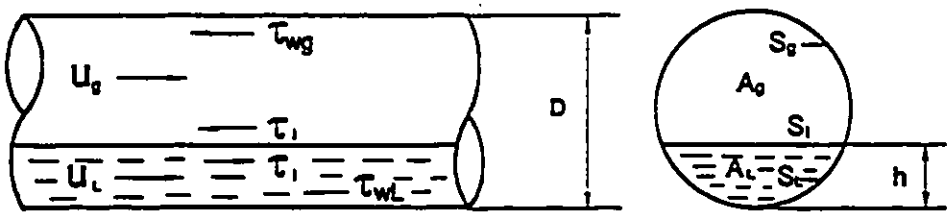

Fig.6.21 Definitions of inlet stratified flow

$$\frac{\tau_{wg}S_g}{A_g}+\frac{\tau_{wL}S_L}{A_L}+\tau_i S_i(\frac{1}{A_L}+\frac{1}{A_g})=0 \qquad (6.81)$$

The shear stresses are evaluated in a conventional manner:

$$\tau_{wL}=f_i\frac{\rho_L u_L^2}{2}, \quad \tau_{wg}=f_g\frac{\rho_g u_g^2}{2}, \quad \tau_i=f_i\frac{\rho_g(u_g-u_L)^2}{2} \qquad (6.82)$$

Normally for stratified flow, u_g is much higher than u_L, thus u_L can be neglected in the expression of τ_i in Eqn.(6.82). Equation (6.81) can be conveniently written in a dimensionless form. The reference variables are chosen as D for length, D^2 for area, the superficial velocities u_{Ls} and u_{gs} for the liquid and gas velocities, respectively:

$$-\frac{f_L}{f_g}\frac{\rho_L u_{Ls}^2}{\rho_g u_{gs}^2}\frac{\bar{S}_L}{\bar{A}_L}\bar{U}_L^2+[\frac{\bar{S}_g}{\bar{A}_g}+\frac{f_i}{f_g}(\frac{\bar{S}_i}{\bar{A}_L}+\frac{\bar{S}_i}{\bar{A}_g})]\bar{U}_g^2=0 \qquad (6.83)$$

where the over-bar of the capital letters denote dimensionless variables.

The Blasius equation is used to evaluate the frictional factors f_L and f_g:

$$f_L=c_L(\frac{D_L u_L}{\nu_L})^{-m}, \qquad f_g=c_g(\frac{D_g u_g}{\nu_g})^{-n} \qquad (6.84)$$

where D_L and D_g are hydraulic diameters. The liquid is visualized as if it is flowing in an open channel and the gas is visualized as flowing in a closed duct.

Substituting Eqn.(6.84) into Eqn.(6.83) gives:

$$-X^2\frac{(\bar{U}_L\bar{D}_L)^{-n}}{(\bar{U}_g\bar{D}_g)^{-m}}\frac{\bar{S}_L}{\bar{A}_L}\bar{U}_L^2+[\frac{\bar{S}_g}{\bar{A}_g}+\frac{f_i}{f_g}(\frac{\bar{S}_i}{\bar{A}_L}+\frac{\bar{S}_i}{\bar{A}_g})]\bar{U}_g^2=0 \qquad (6.85)$$

where the Martinelli parameter is defined as:

$$X^2=\frac{\frac{4c_L}{D}\left(\frac{u_{Ls}D}{\nu_L}\right)^{-n}\left(\frac{\rho_L u_{Ls}^2}{2}\right)\left(\frac{dp}{dx}\right)_{Ls}}{\frac{4c_g}{D}\left(\frac{u_{gs}D}{\nu_g}\right)^{-m}\left(\frac{\rho_g u_{gs}^2}{2}\right)\left(\frac{dp}{dx}\right)_{gs}} \tag{6.86}$$

Eqn.(6.85) can be used to evaluate the dimensionless equilibrium liquid elevation H=h/D since all variables in the equation depend on H from the following relations:

$$\bar{A}_L=0.25\{\pi-\cos^{-1}(2H-1)+(2H-1)\sqrt{[1-(2H-1)^2]}\} \tag{6.87}$$

$$\bar{A}_g=0.25\{\cos^{-1}(2H-1)-(2H-1)\sqrt{[1-(2H-1)^2]}\} \tag{6.88}$$

$$\bar{S}_L=\pi-\cos^{-1}(2H-1) \tag{6.89}$$

$$\bar{S}_g=\cos^{-1}(2H-1) \tag{6.90}$$

$$\bar{U}_L=\frac{A}{A_L} \tag{6.91}$$

$$\bar{U}_g=\frac{A}{A_g} \tag{6.92}$$

Eqn.(6.85) indicates that the dimensionless liquid level H depends on two parameters, i.e. X and f_i/f_g. In the absence of the information on interfacial momentum transfer, Taitel and Dukler assumed that $f_i/f_g=1.0$, i.e. the interfacial friction factor was

the same as that of gas phase. Consequently, the solution of the height of liquid level H in Eqn.(6.85) depends only on the Lockhart-Martinelli parameter X. A comparison of the prediction of this stratified flow model and the present measurement data has shown satisfactory results in the previous section for the Martinelli parameter higher than 1.0. After the evaluation of liquid level H the areas occupied by the liquid and vapour phases A_g and A_L in Eqn. (6.6) can be easily determined, which is the basic information for evaluating phase redistribution in the general phenomenological model.

6.5.2. Dividing streamline model

As shown in the previous section, the basic formulations for the prediction of phase redistribution not only requires the knowledge of A_g and A_L determined from the inlet stratified flow model but also needs the knowledge of A_{gb} and A_{Lb} which have to be determined by the boundary of the dividing streamlines and the inlet tube wall. The model of dividing streamline, which accounts for the redistribution of the two phases in T-junction, is then needed to evaluate areas A_{gb} and A_{Lb}. For a horizontal T-junction (horizontal inlet and horizontal branch) Ballyk and Shoukri's approach (1990) can be directly employed. However, this approach requires the information of the pressure changes in the T-junction. In the development of the phase redistribution model for stratified flow, the empirical pressure correlations obtained from stratified flow experiments were used. The detailed description of the model is not repeated here. It

should be noted, however, since there is no report on pressure gradients in the junction, a linear changes in both run pressure rise and branch pressure drop were assumed in the analysis of annular flow and such pressure profiles are also assumed to be valid in stratified flow. The basic knowledge of pressure gradients in the junction remains the same as in annular flow, originated from experimental observation, i.e. firstly the value of the run pressure gradient is positive whereas the branch pressure gradient is negative; secondly the absolute value of the branch pressure gradient is usually much larger than that of the run pressure gradient. Consequently, the same pressure gradient expressions in annular flow analysis are used in stratified flow.

6.5.3. Results of model predictions

The areas A_g and A_L, occupied by vapour and liquid in the inlet tube respectively, are evaluated using Taitel-Dukler stratified flow model; the areas of A_{gb} and A_{Lb} (the zones of influence) from which the two-phase flow is diverted into the branch are determined separately for the liquid and vapour phases using the dividing streamline model; thus the general phenomenological model is used to determine the phase separation ratio x_3/x_1:

$$\frac{x_3}{x_1} = \frac{A_{gb}A_L}{A_L A_{gb}x_1 + (1-x_1)(1-E)A_{Lb}A_g} \qquad (6.93)$$

In stratified flow no entrainment occurs, or the fraction of entrainment of liquid

phase E is prescribed to zero in the above equations. A comparison of the model prediction of Taitel and Dukler with measured data of liquid level has showed satisfactory results under the present stratified flow conditions for the Martinelli parameter higher than 1.0. At lower values of the Martinelli parameter, which corresponds to $u_{gs}>3.0$ m/s, the Taitel-Dukler model overpredicts the liquid level. In this range, the deviation is believed to be due to the onset of the large amplitude roll waves and the liquid level is better predicted by the Andritsos and Hanratty's model (1987).

In the analysis of stratified flow, the development lengths, DLX and DLY, were assumed to be independent of the superficial vapour velocity u_{gs}. For different superficial liquid velocities u_{Ls}=0.05, 0.07 and 0.09 m/s, the development lengths DLX and DLY were fixed at 2, 2.5 and 3.5 diameters respectively.

Figs.6.22, 6.23 and 6.24 show the predicted effect of the superficial vapour velocity on phase redistribution at fixed superficial liquid velocities of 0.05, 0.07 and 0.09 m/s respectively. The system pressures in the three cases are the averaged pressures at varied branch flow split conditions. In the predictions shown in the figures, the liquid level is calculated using Taitel-Dukler model for $u_{gs}<3$ m/s. For the case of u_{gs}=5 m/s the liquid level is calculated using both models of Taitel-Dukler (T-D) and Andritsos-Hanratty model (A-H) respectively. The model predicts the data trend and the level of phase redistribution well. The predicted trend of phase redistribution is consistent with the measurements, i.e. at very low branch flow split high level of phase separation occurs, with increasing the flow split ratio the branch flow quality decreases and tends

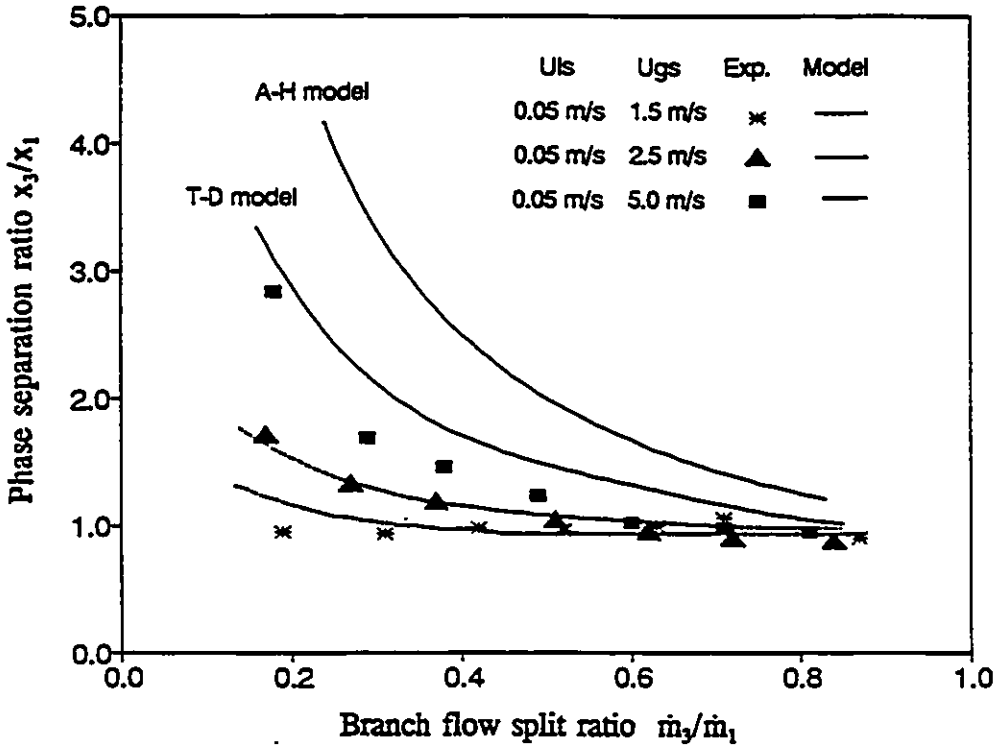

Fig.6.22 Model prediction of the effect of the u_{gs} in stratified flow (u_{Ls}=0.05 m/s)

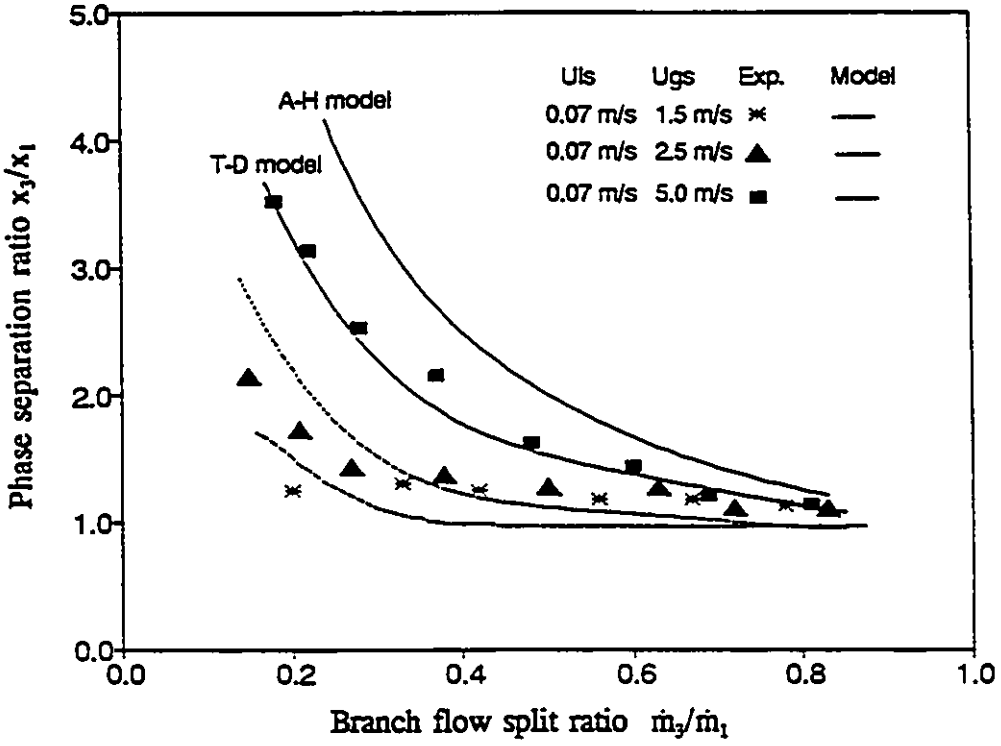

Fig.6.23 Model prediction of the effect of the u_{gs} in stratified flow (u_{Ls}=0.07 m/s)

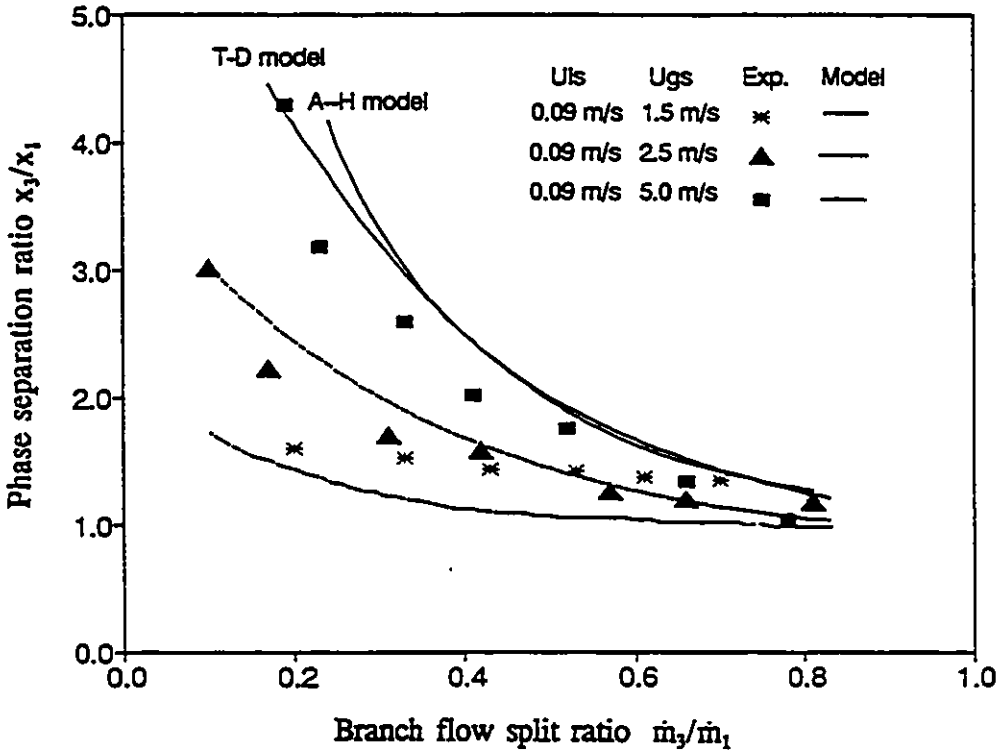

Fig.6.24 Model prediction of the effect of the u_{gs} in stratified flow (u_{Ls}=0.09 m/s)

to become equal to the inlet flow quality after all inlet flow being extracted through the branch. In stratified flow, the branch flow quality may be as high as 1.0 if only vapour phase is extracted into the branch and the maximum level of the phase separation ratio may reach $1/x_1$. The high level of phase separation occurs only for low liquid level in the inlet tube at low branch flow split ratio, as increasing the branch flow split, liquid begins to be diverted into the branch and the level of phase separation decreases. The model, as shown in these figures, is capable of predicting the appropriate trend of this physical phenomenon. The model can also predict the correct trend of the effect of inlet superficial vapour velocity. A higher superficial vapour velocity will reduce the height of liquid level in the inlet tube and, therefore, increases the inertia of liquid phase forcing it passing though the run conduit. As a result the branch flow quality x_3 increases.

It is interesting to note that although, as shown earlier, Andritsos and Hanratty's model was better able to predict the liquid level for the high vapour velocities, i.e. $u_{gs}>3$ m/s, the use of Taitel and Dukler's model predicted better agreement with the phase redistribution results shown in Figs. 6.22 and 6.23. Using Andritsos and Hanratty's model as inlet flow model overpredicted the present phase redistribution data for the $u_{gs}=5.0$ m/s test conditions. Under these test conditions large roll waves were generated. The liquid-gas surface was no longer smooth as in lower gas velocity conditions. The present phase redistribution model, however, does not account for the wave effect on the phase redistribution in the junction. This apparent agreement between the model prediction and the data, when Taitel-Dukler model is used for high u_{gs}, can be

explained in terms of the model assumptions and the nature of the flow regime. The existence of wavy interface may allow more liquid to be diverted into the branch which implies that the liquid level is effectively higher than the measured mean value predicted by Andritsos-Hanratty model (1987). However, it is clear that the applicability of the present model should be limited to smooth stratified flows.

The effect of the inlet superficial liquid velocity on phase redistribution as predicted by the model is illustrated in Figs.6.25 and 6.26 in which the results are compared at different superficial liquid velocities u_{L_s}=0.05 and 0.09 m/s with fixed superficial vapour velocities (1.5 m/s in Fig.6.25 and 2.5 m/s in Fig.6.26). Again, both the data trends and level of phase separation are reasonably predicted by the model. The height of liquid level, in the model, is a unique function of the Martinelli parameter. If assume $c_L=c_g$ and m=n=0.2, Martinelli parameter in Eqn.(6.86) can be rewritten as:

$$X_{tt}^2 = \left(\frac{\nu_L}{\nu_g}\right)^{0.2}\left(\frac{\rho_g}{\rho_L}\right)^{0.8}\left(\frac{1-x}{x}\right)^{1.8} \qquad (6.94)$$

It indicates that the Martinelli parameter depends on the inlet flow quality. Under the present test conditions a variation of the inlet liquid velocity has less effect on the inlet flow quality and, therefore, is insignificant to Martinelli parameter. As a result, Taitel-Dukler's model predicts little difference in the liquid level as the inlet liquid superficial velocity is changed. The good results of prediction can then be attributed to Ballyk-Shoukri's model of dividing streamline to be capable of evaluating the correct zones of influence when the inlet liquid velocity is changed.

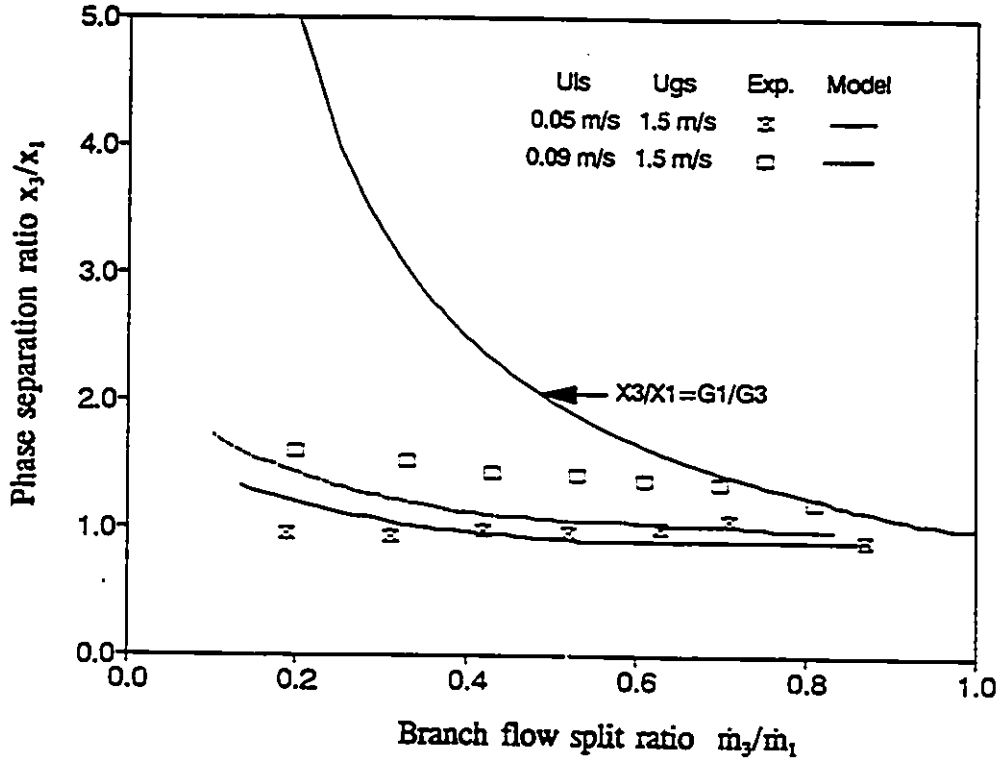

Fig.6.25 Model prediction of the effect of the u_{L_s} in stratified flow (u_{gs}=1.5 m/s)

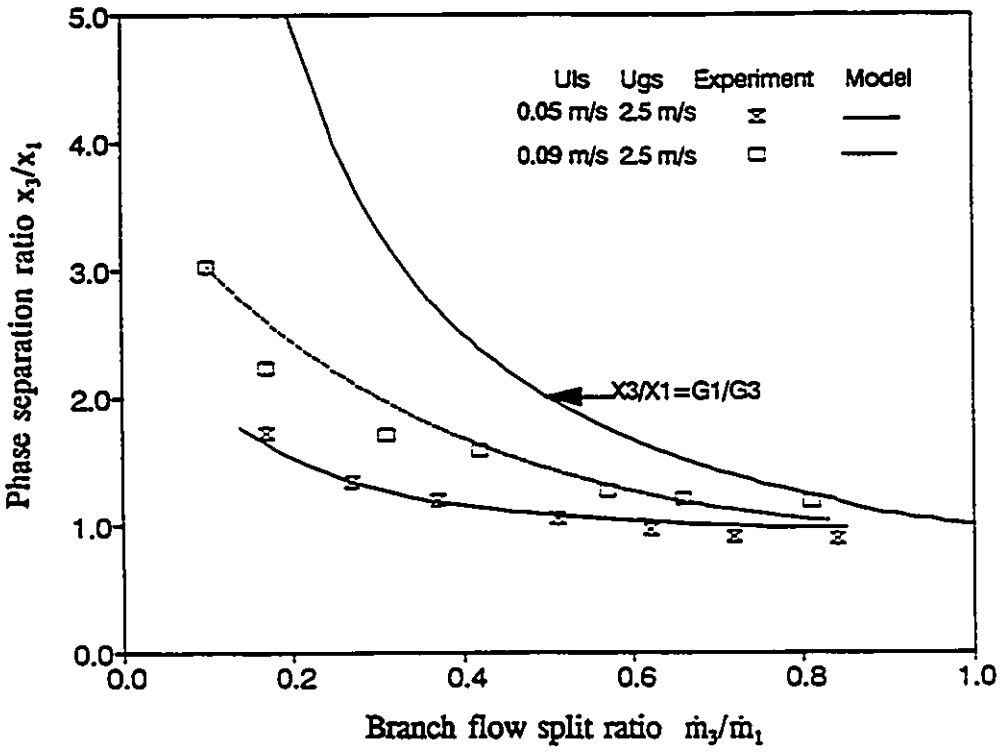

Fig.6.26 Model prediction of the effect of the u_{Ls} in stratified flow (u_{gs}=2.5 m/s)

The predictions of the model were also compared with the experimental data obtained by other researchers. A comparison with the work of Azzopardi et al. (1988) is presented in Fig.6.27. The experiments were performed at a fixed superficial liquid velocity u_{Ls}= 0.06 m/s with different superficial vapour velocity u_{gs}=11, and 15 m/s in a 35 mm diameter T-junction under the system pressure of 1.5 bar. Since the superficial velocity of liquid is close to one of our experimental conditions (u_{Ls}=0.05 m/s), the same development lengths of DLX=DLY=2D were used as before. As shown in Fig.6.27 the model can predict the data of Azzopardi et al. quite well.

A comparison of the model predictions with the work of Reimann et al. (1988) is shown in Fig.6.28. The experiments were performed at a fixed superficial liquid velocity u_{Ls}=0.05 m/s with superficial vapour velocities u_{gs}=5, and 10 m/s in a 50 mm diameter T-junction under high system pressure, P_1= 6.86 bar. Again, the development lengths of DLX and DLY were assumed to be 2D. As shown in Fig.6.28, the model predicts the case in lower vapour velocity (u_{gs}=5 m/s) pretty well but fails to predict the case in higher vapour velocity (u_{gs}=10 m/s). It should be noted that the data of Reimann et al. (1988) was collected at high system pressure. Under this condition a 10 m/s superficial vapour velocity may cause flow regime transition from stratified flow to semi-annular flow, or a curved liquid-gas interface may be formed. Unfortunately, there is no flow map available for such a high pressure two-phase flow conditions.

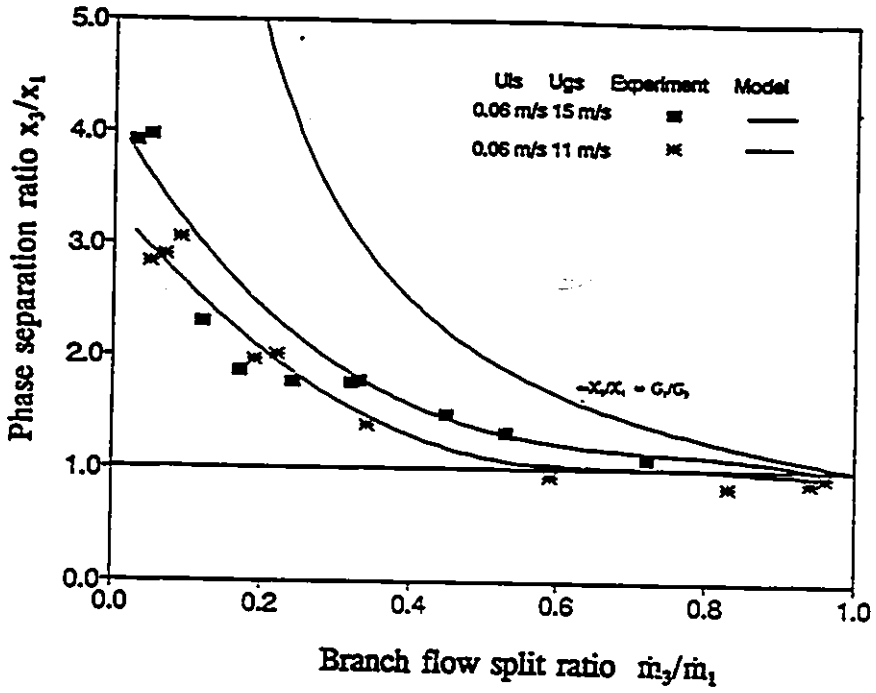

Fig 6.27 Model prediction compared with the data of Azzopardi et al. (1988) (u_{Ls}=0.06 m/s, u_{gs}=11, 15 m/s, P_1=1.5 bar)

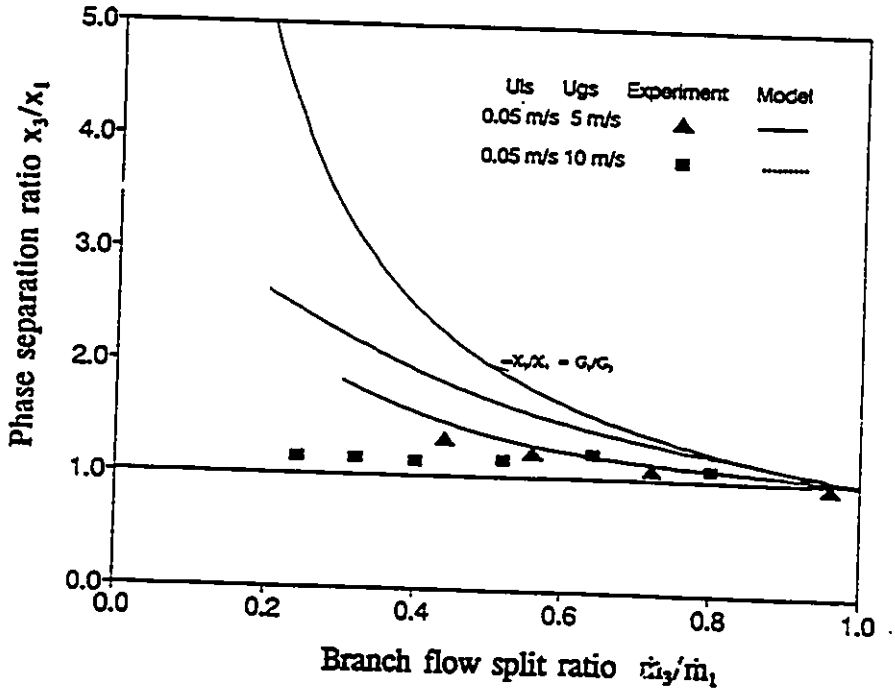

Fig.6.28 Model prediction compared with the data of Reimann et al. (1988) (u_{Ls}=0.05 m/s, u_{gs}=5, 10 m/s, P_1=6.68 bar)

6.6. Comparison with Available Models

The ability of the models presented in this work in predicting phase redistribution data in horizontal T-junction were compared with other available models. In this comparison, the data obtained in the present work for stratified flow and the data of Ballyk et al. (1988) for annular flow were used. It should be noted that all available models are only valid for the prediction of phase redistribution in T-junctions with horizontal branch of equal diameter to the inlet tube. The empirical model of Seeger et al. (1986) and the newly developed annular flow model in this study, howeve:, can be applicable in the junctions with different branch orientations.

It should be also noted that a uniform distribution of the liquid film in the horizontal inlet tube was assumed in all available annular phase redistribution models, therefore, a correlation to determine the mean liquid film thickness developed by Laurinat et al. (1984) was used in the following comparison. For the stratified flow, Taitel and Dukler (1976) model was used to evaluated the liquid level in the inlet tube. By using these inlet flow models and different dividing streamline models in each of the available models the areas of A_g, A_L, A_{gb} and A_{Lb} were determined and the branch flow split ratio $\dot{m}_3/\dot{m}_1$ and phase separation ratios x_3/x_1 were evaluated using the general phenomenological model Eqns.(6.5) and (6.6).

6.6.1. Comparison of annular flow models

The predictions of the data of Ballyk et al. (1988) in annular flow by the empirical model of Seeger et al. (1986) are presented in Fig.6.29. This empirical model was based on a large data bank of air-water ($P_1 < 1$ MPa) and steam-water ($P_1 < 10$ MPa) flows. The inlet mass flux and inlet flow quality covered the range of $500 < G_1 < 7000$ kg/m^2.s and $0.02 < x_1 < 0.40$, led to the observation of different inlet flow patterns. As shown 70% of the predictions are within $\pm 40\%$ of the data.

The predictions by Azzopardi and Whalley's model (1982) are shown in Fig.6.30. This model was developed for vertical inlet tubes and, therefore, a uniform liquid film thickness distribution was assumed. Azzopardi and Whalley's model was able to predict their low inlet mass flux annular data in vertical pipes quite well but is not satisfactory in predicting Ballyk's data on high inlet mass flux in horizontal pipes. This is probably caused by the assumption that the film thickness is uniform and the fact that much higher liquid entrainment occurs under the high inlet mass flux conditions. The liquid droplets are barely extracted through the branch due to their much higher axial momentum fluxes. Azzopardi and Whalley's model is a completely geometrical model since the authors assumed that the liquid and gas phases have the same "zone of influence". Generally, due to the lower axial momentum flux, the gas phase is much easier to be diverted into the branch than the liquid film and, therefore, the zone of influence of the gas may be larger than that of liquid phase. The predicted level of phase separation by Azzopardi and

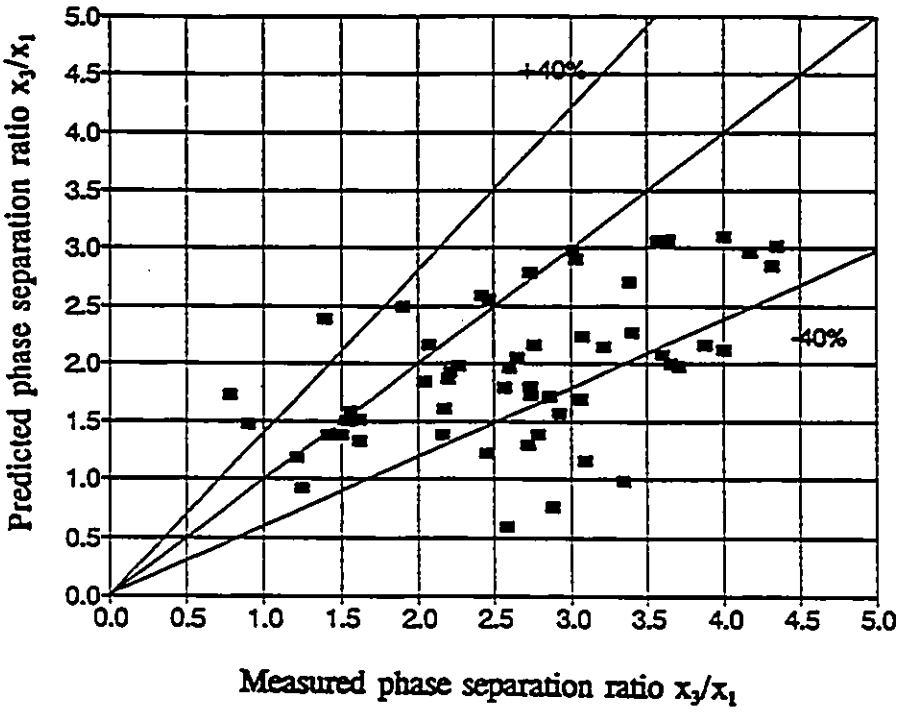

Fig.6.29 Comparison of annular flow data with the model of Seeger et al. (1986)

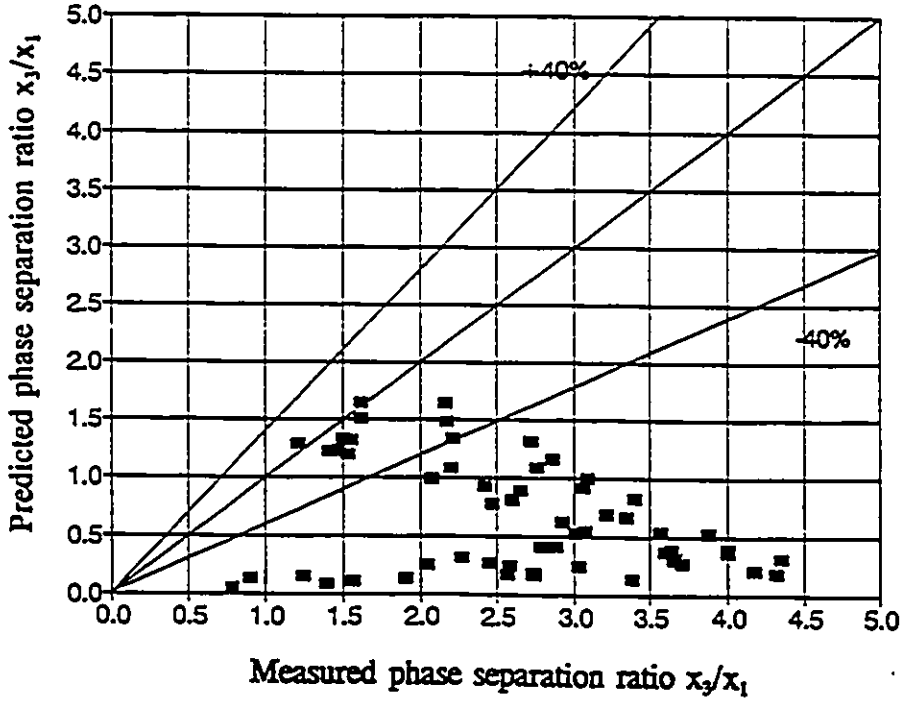

Fig.6.30 Comparison of annular flow data with the model of Azzopardi and Whalley (1982)

Whalley's model is lower than the measured data. As shown in Fig.6.30, only 19% predictions are within ±40% of the data obtained in high inlet mass flux annular flow conditions.

Hwang et al. (1988) defined two zones of influence for the two phases in their model. An empirical correlation was used to connect the relationship between the locations of the dividing streamlines of the liquid and gas:

$$\frac{(\frac{\delta_L}{D_1})^{n_L}}{(\frac{\delta_g}{D_1})^{n_g}} = (\frac{1-\alpha_1}{\alpha_1})^2(\frac{x_1}{1-x_1})^2(\frac{\rho_g}{\rho_L}) \qquad (6.95)$$

The exponent of n_k in the equation was determined empirically as:

$$n_k = 5.0+20\exp[-53(\frac{\delta_k}{D_1})] \qquad k=g, L \qquad (6.96)$$

The comparison of the predictions by the model of Hwang et al. (1988) with the measured data is illustrated in Fig.6.31. Defining a different zone of influence for each phase seems to improve the predictions over those of Azzopardi and Whalley's model. The zones of influence for the liquid phase, as expected, is much smaller than that of gas phase in most of the flow conditions. 70% of the predictions are within ±40% of the data.

Shoham et al. (1987) also defined two dividing streamlines. The relationship of the two dividing streamlines was expressed as:

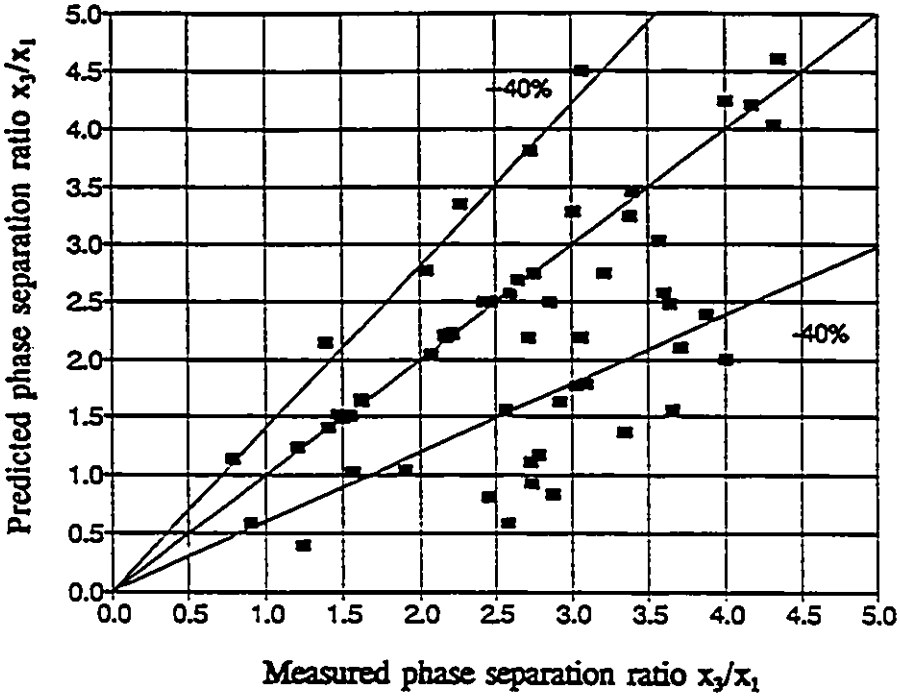

Fig.6.31 Comparison of annular flow data with the model of Hwang et al. (1988)

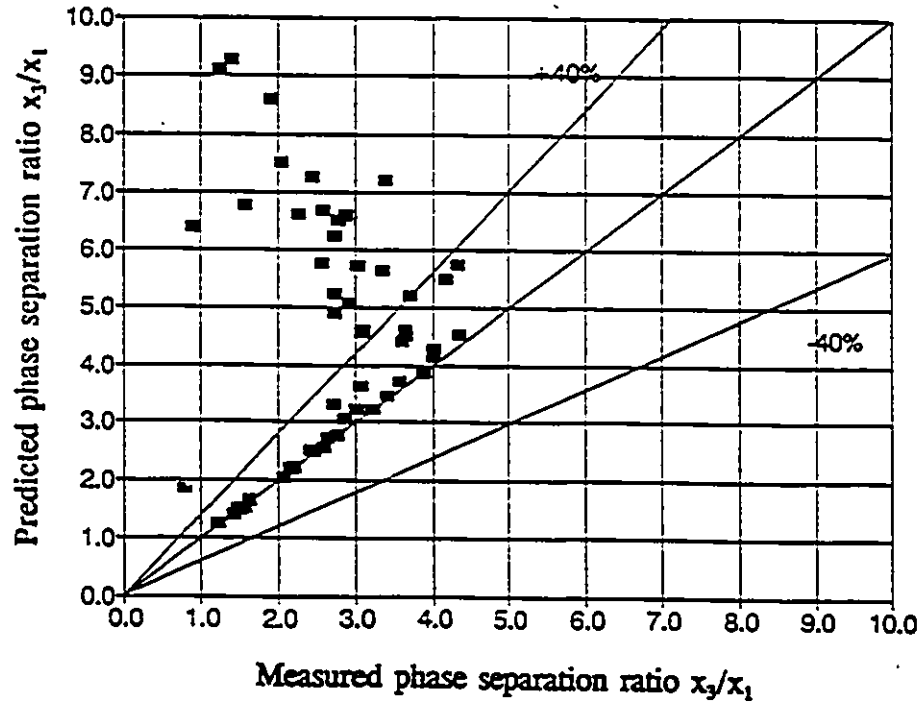

Fig.6.32 Comparison of annular flow data with the model of Shoham et al. (1987)

$$\delta_L = \delta_g - \Delta r \qquad (6.97)$$

where the distance between the liquid and gas dividing streamline Δr was evaluated by solving an ordinary differential equation based on the force balance of the liquid film. The predicted results are shown in Fig.6.32. This model can predict 63% of the data within $\pm 40\%$ of the measurement. Some of the predictions are pretty good whereas some of them significantly overpredict the data, indicating the approach of this model to determine the dividing streamlines needs to be improved.

The comparison of the predictions by the present annular flow model with the experimental data is presented in Fig.6.33. As shown in the figure, 93% of the predictions are within $\pm 40\%$ of the data. This may be contributed by the fact that the model both accounted for the effect of asymmetrical liquid film distribution and used a better model to determine the "zones of influence". A more attractive feature of the new model is its capability to predict phase redistribution in T-junctions with different branch orientations, which cannot be achieved by other available models and, therefore, the direct comparison cannot be made at the present time.

6.6.2. Comparison of stratified flow models

Fig.6.34 shows the comparison between the predictions of Seeger et al. model (1986) with the present stratified flow experimental data. 64% of the predictions are

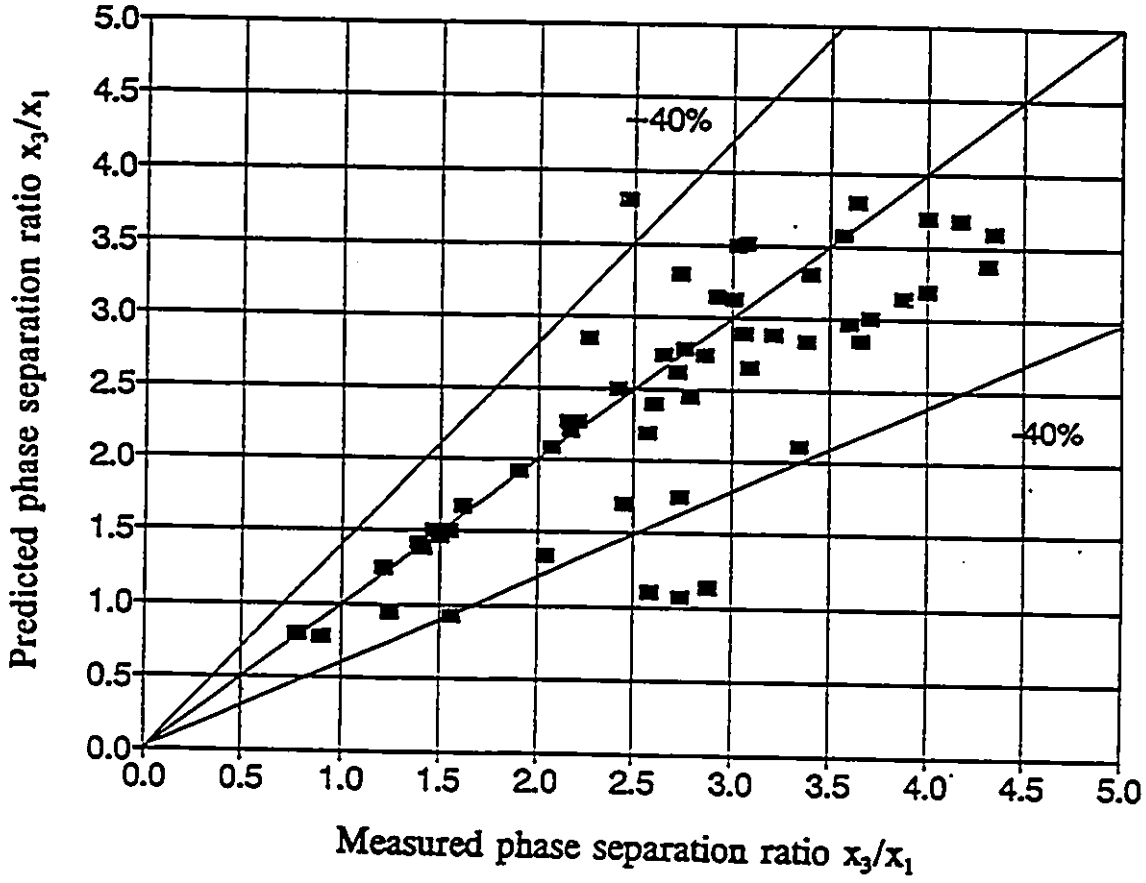

Fig.6.33 Comparison of annular flow data with the new developed model

within the range of ±40% of the measurement. It can be seen that Seeger et al.'s model worked better in annular flow than in stratified flow. It is believed that this was caused by the fact that the data used to develop the correlations were collected mainly in slug and annular flow.

A completely geometrical model, following the approach of Azzopardi and Whalley for annular flow, was developed for stratified flow in this study by assuming that A_{zb} and A_{Lb} had the same dividing streamline in the general phenomenological model of Eqn.(6.6). A comparison of the prediction of this model with the stratified data is presented in Fig.6.35. Again, similar to the annular flow, the data were underpredicted by this model. However, the model worked much better in stratified flow than in annular flow conditions with high inlet mass flux. 80% of the predictions are within the range of ±40% of the measurement.

Fig.6.36 shows the results of the predictions of the model of Hwang et al. (1988). The model also can predict the stratified flow data quite well, 89% of the data are predicted within ±40% of the measurement. It should be noted that the model developed by Hwang et al. (1988) was examined by other researchers, e.g. Rubel et at. (1988) and Timmenrman et al. (1992) in different flow conditions and good results were obtained. This model has achieved satisfactory results for most of the data examined.

The results of the prediction by Shoham et al. model (1987) are illustrated in Fig.6.37. As in annular flow this model overpredicts most of the stratified flow data, 63% of the predictions are within ±40% of the measurement. In the analysis to evaluate

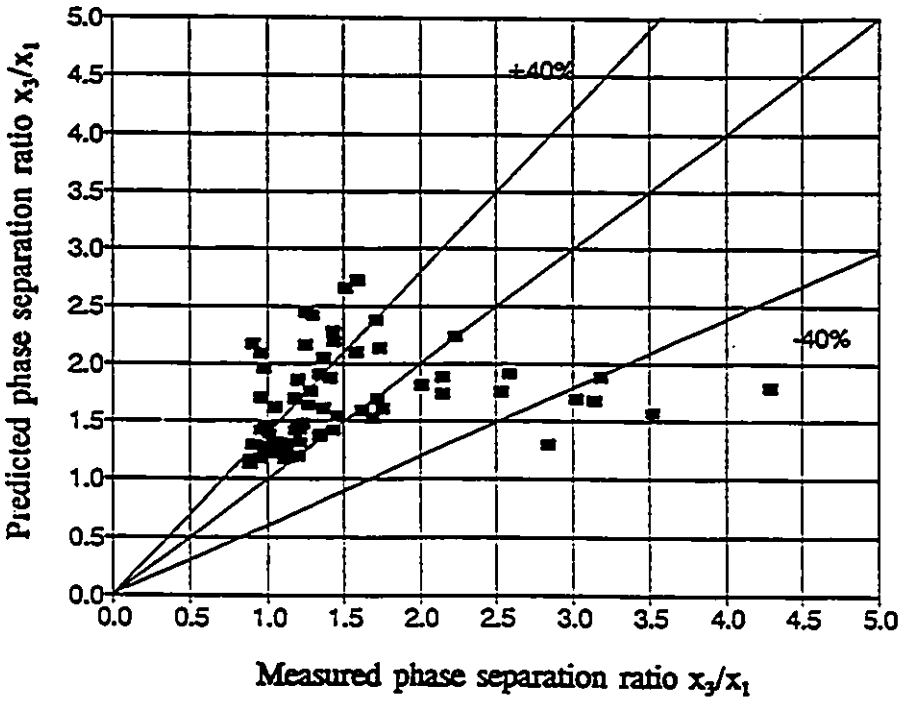

Fig.6.34 Comparison of stratified flow data with the model of Seeger et al. (1986)

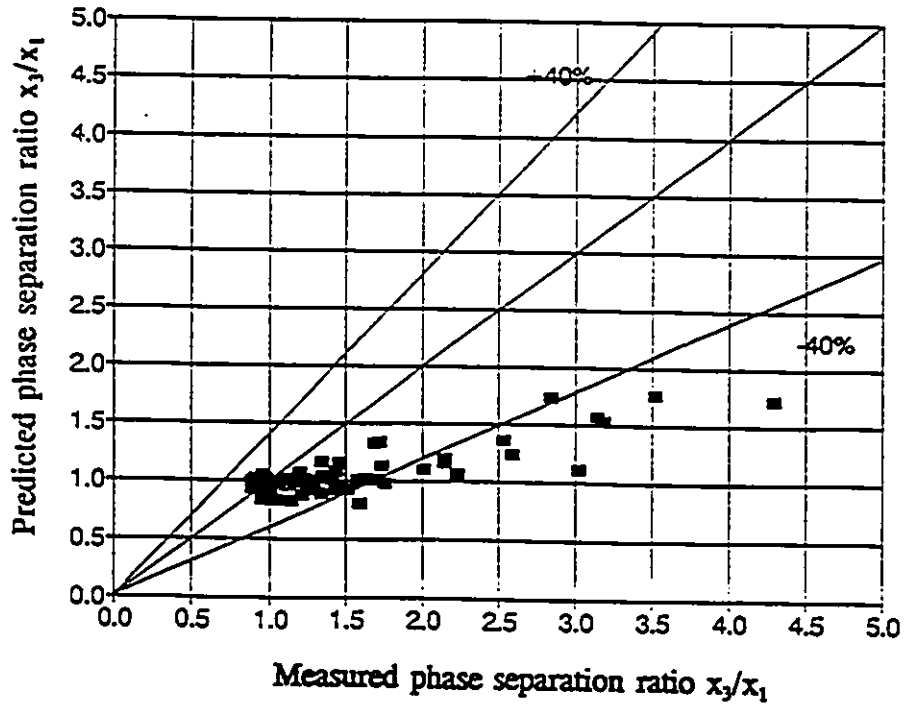

Fig.6.35 Comparison of stratified flow data with completely geometric model

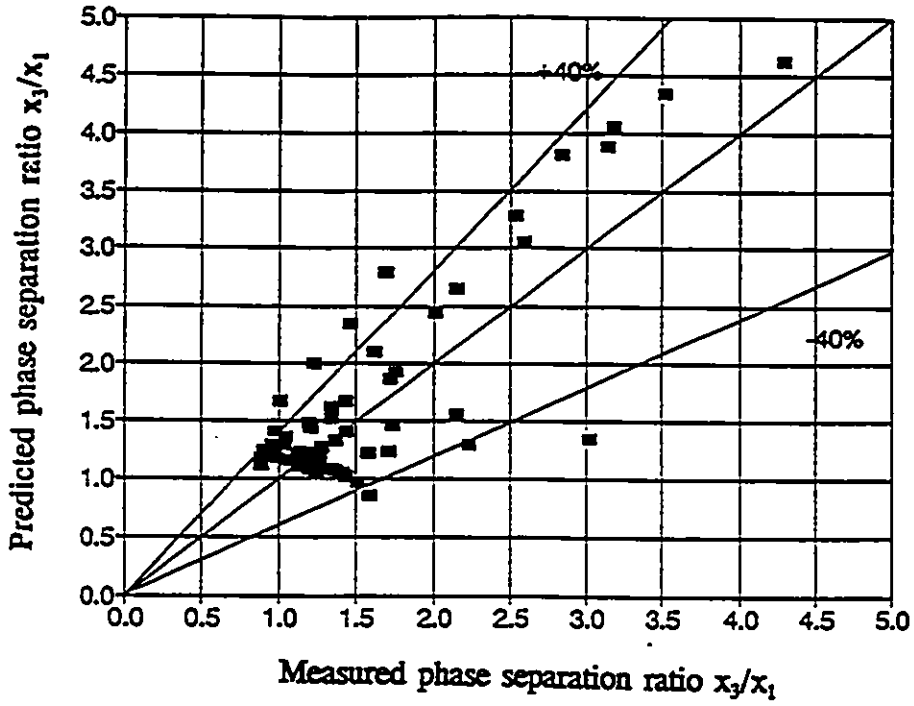

Fig.6.36 Comparison of stratified flow data with the model of Hwang et al. (1988)

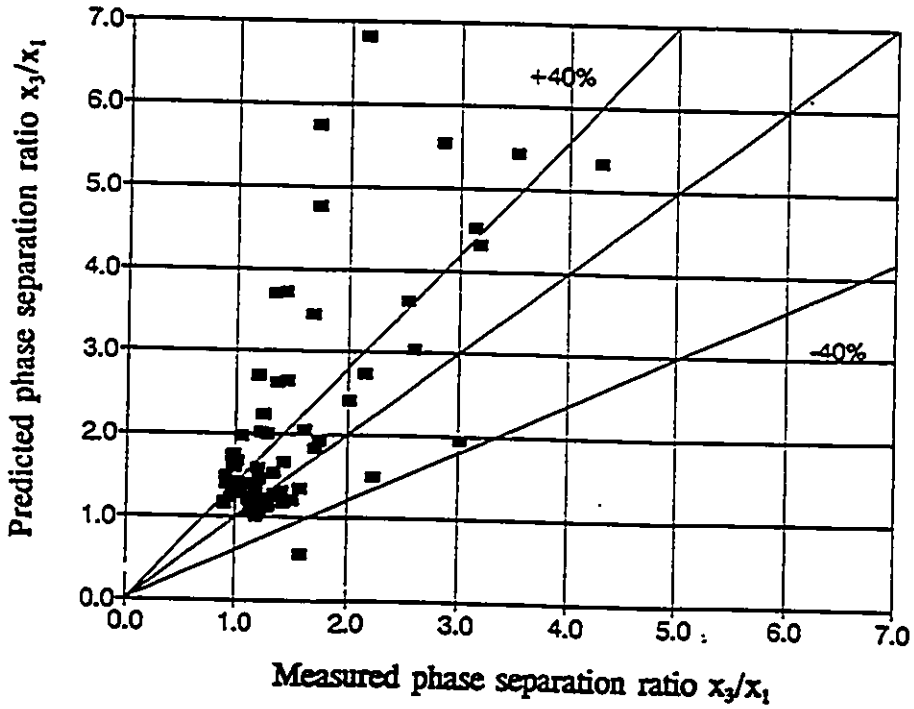

Fig.6.37 Comparison of stratified flow data with the model of Shoham et al. (1987)

dividing streamline the authors argued that the centripetal and inertial forces were dominant in the junction. This assumption is probably too simple and is not valid in the whole range of the branch flow split. The pressure gradients may play an important role on phase redistribution in the T-junction, however, the effect of the pressure gradients was ignored in Shoham et al. model .

A comparison of the available models and the present stratified flow model is presented in Fig.6.38. The experimental data were collected at the superficial liquid velocity of 0.09 m/s and the superficial vapour velocity of 2.5 m/s. As shown, the models of Shoham et al., Hwang et al., the geometrical stratified flow model and the present stratified flow model can predict the correct trend of the data. Seeger et al.'s empirical model fails to predict the correct data trend. The geometric model significantly underpredicts the data. Hwang et al.'s model improved geometrical model by predicting a larger influenced gas area A_{gb}. Shoham et al. also attempted to refine the geometric model by enlarging the area A_{gb} but went too far, it significantly overpredicts the measurement data. The present stratified flow model obtains the best results by using a different approach to evaluate liquid and gas dividing streamline separately.

Fig.6.39 shows the predictions by the present model. As shown, 95% of the predictions are within $\pm 40\%$. Generally speaking, good prediction results are easier to obtain in stratified flow than in annular flow. This success is caused by the simplicity of the inlet stratified flow model, where no entrainment and deposition occur and, therefore, less empirical correlations were used, making the model more accurate and reliable.

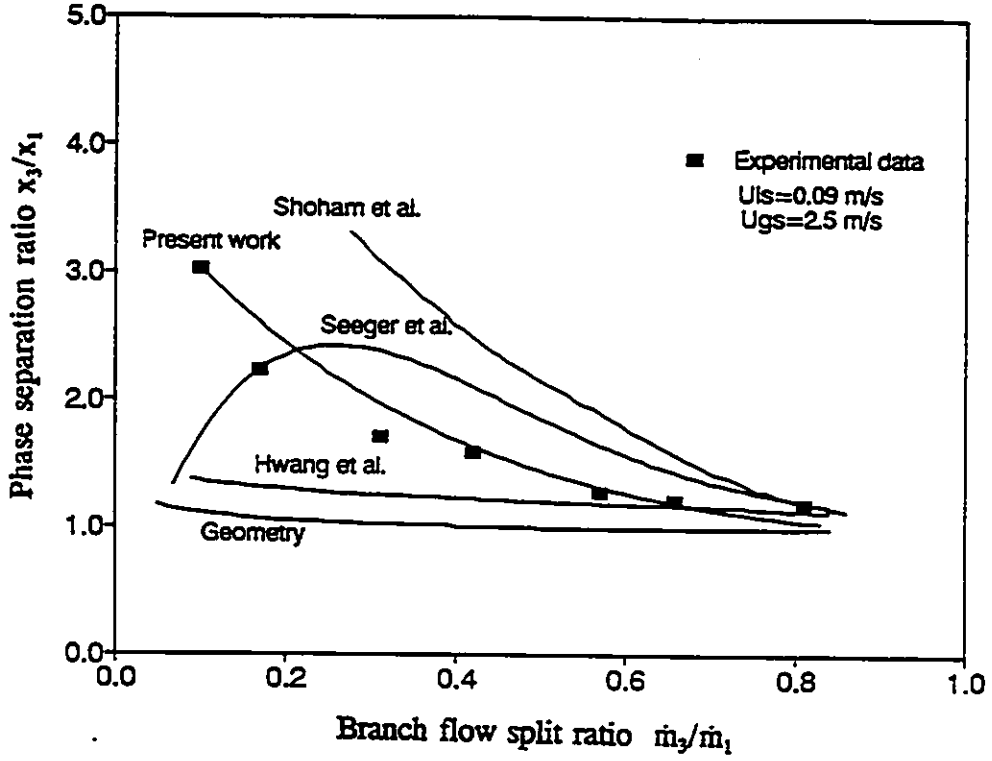

Fig.6.38 Comparison of different models in stratified flow (u_{Ls}=0.07 m/s, u_g=2.5 m/s, P_1=1.35 bar)

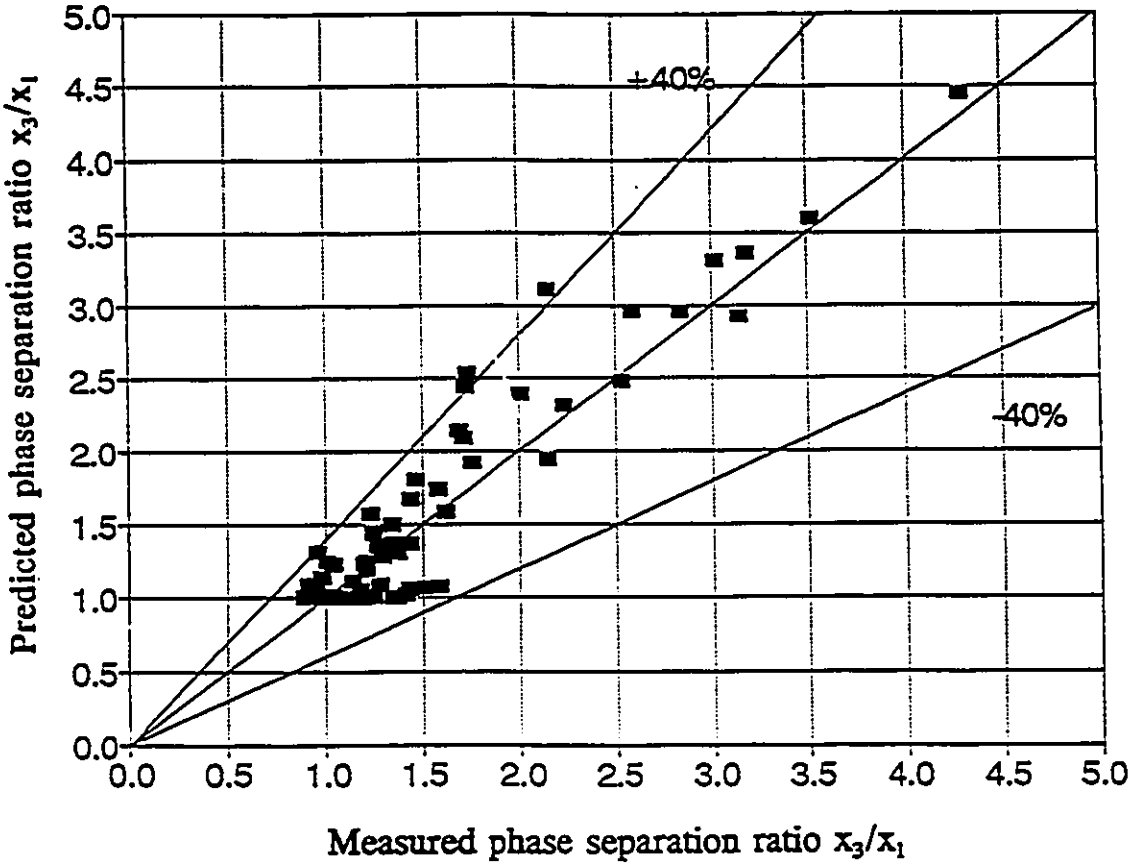

Fig.6.39 Comparison of stratified flow data with the new developed model

CHAPTER 7

CONCLUSIONS AND RECOMMENDATIONS

Detailed experimental data of phase redistribution and pressure changes of dividing steam-water two-phase flow in T-junctions were obtained. Most of the data were collected in the ranges which were not examined before. The data covered stratified and annular flows. A unique feature of the experiments was the measurements of void fractions in the three legs of T-junction and the liquid level in the inlet tube in stratified flow conditions.The following are the major findings and conclusions of the experimental and analytical studies.

In annular flow, It was found that the branch orientation was a significant parameter affecting phase redistribution in horizontal inlet T-junctions. The effect of branch orientation on phase redistribution is mainly caused by the non-uniform thickness distribution of the liquid film in the inlet tube.The results showed that, in general, downward rotation of the branch results in less vapour extraction as the liquid film available for extraction is thicker.The inlet mass flux was found not to have significant effect on the phase redistribution phenomenon under the present test conditions. However, the inlet quality has a pronounced effect. Changing the inlet quality affects the liquid film thickness distribution and accordingly affects the phase redistribution in the junction.

In stratified flow, the degree of the phase separation depends on inlet flow rates, densities of the two phases and the resulting liquid level in the inlet tube. It is also significantly affected by the junction geometry. Increasing vapour or liquid superficial velocities will increase the extent of phase separation under the present stratified flow conditions. Higher system pressure corresponding to a higher vapour density results in reducing the degree of the phase separation. In a reduced size branch T-junction, a higher level of phase separation will be experienced. A variation of branch orientation will greatly affect the phase redistribution and downwardly orientated branch will reduce the branch flow quality significantly.

The pressure changes in T-junctions were less studied by previous researchers. The data on pressure changes in the present study were correlated using simple momentum and energy balances for the run and branch respectively. Measured void fractions in the inlet, branch and run were used to evaluate the two-phase densities. In stratified flow, the inlet flow conditions and junction geometries were insignificant in terms of the run momentum correction factor. In annular flow, however, it was observed that the run momentum correction factor was independent of inlet flow conditions and branch diameter (Ballyk, 1992) but was influenced by branch orientation. The branch two-phase multiplier was found to depend on both inlet flow conditions and junction geometry in stratified flow, while in annular flow it only depended on branch diameter. Comparison of the present data with available correlations indicated that those models

which account for phase redistribution effect in calculating the two-phase multiplier worked better. However, there is no model available to predict the present data satisfactorily. Up to now, most of the available models of junction pressure changes are simple 1-D models based on the momentum or energy balances. Due to the poor understanding of the local flow mechanism and phase redistribution phenomenon, there is no pressure model available which is applicable to any inlet flow conditions and junction geometries.

A general phase redistribution model was derived based on the analysis of the available models. This general model was extended to two phenomenological models to predict phase redistribution for annular and stratified flows in T-junctions. The phase redistribution model consisted of two sub-models to account for phase distribution in the inlet tube and phase redistribution in the junction separately. Due to a simple phase distribution in the inlet tube, the stratified flow model worked more effectively than the annular flow model. A comparison of some available models with the experimental data showed that most models can predict 70% of the annular flow data and 80% of the stratified flow data within $\pm 40\%$ of the experimental data. The present models can predict 90% of the data within $\pm 40\%$ in both annular and stratified flows.

Some of the recommendations for future research in the subject are:

1. Experimental data of phase redistribution are needed in the transition ranges, e.g. the ranges from stratified to annular flow and the ranges from stratified to slug flow.

Experimental evidence has shown that the data trend may reverse in different flow regimes. Therefore, the criteria for the flow regime transition are important to improve the understanding of phase redistribution in T-junctions.

2. In stratified flow, the vapour pull-through or water pull-through phenomena occur in downward or upward branch junctions. In downward branch, the flow split ratio at which vapour pull-through occurred was found to depend on the inlet flow conditions and junction geometry. The same effects are expected to exist in water pull-through phenomenon in upward branch junctions. When these phenomena occur, the branch flow pattern abruptly changes from single phase flow into two-phase flow. The knowledge of these phenomena is important to improve the understanding of phase redistribution and the associated pressure changes in T-junctions.

3. Seeger et al. empirical phase redistribution model (1986) predicted the present experimental data well. Nowadays the size of the data bank of phase redistribution is much larger than that available in eight years ago when Seeger et al. developed their empirical correlations. Empirical models are suitable for engineering design due to its simplicity, therefore, studies on the latest version of empirical phase redistribution models in different flow regimes and different junction geometry is a very attractive work in the future.

4. As shown in the present study, the development of phase redistribution model in annular flow has been limited by the lack of an accurate inlet flow model. Both the measurement and the analysis of asymmetrical liquid film in horizontal annular flow are

great challenges to the researchers. Without the solid knowledge of the liquid film and the entrainment and deposition of the liquid droplets it is impossible to fully understand the mechanisms of phase redistribution in annular flow. The studies on modelling annular flow directly contribute to the improvement of the understanding in phase redistribution phenomenon.

5. Two-fluid model formulation is the most sophisticated modelling technique to study two-phase flow phenomenon. Although the two-fluid model greatly depends on the constitutive relations of the two phases, encouraging results have been shown recently. In some flow conditions in which the interfacial momentum transfer may be insignificant, i.e. in bubbly and smooth stratified flows, the two-fluid model may be a very attractive approach to model phase redistribution in T-junctions in such flow conditions. The three-dimensional numerical simulation can be performed by using the commercial CFD codes simultaneously on two-phase distribution in the inlet tube and two-phase redistribution in the junction. Moreover, the pressure distributions in the inlet, branch and run can be obtained as well.

REFERENCES

Agrawal, S.S., Gregory, G.A. and Govier, G.W. 1973 "An analysis of horizontal stratified two phase flow in pipes", Can. J. Chem. Engng. 51, 280-286.

Andritsos, N. and Hanratty, T.J., 1987 "Influence of interfacial waves in stratified gas-liquid flows", AIChE J. 33, 444-454.

Azzopardi, B.J. and Whalley, P.B. 1982 "The effect of flow patterns on two-phase flow in a T-junction", Int. J. Multiphase Flow 8, 491-507.

Azzopardi, B.J. 1986 "Two-phase flows in junctions", in "Encyclopedia of Fluid Mechanics", Vol. 3, Chapter 25, (ed. by N. Cheremisinoff)

Azzopardi, B.J., Wagstaff, D., Patrick, L., Memory, S.B. and Dowling J. 1988 "The split of two-phase flow at a horizontal T-annular and stratified flow", Harwell, UK. AERE R 13059.

Azzopardi, B.J. and Smith, P.A. 1992 "Two-phase flow split at T junctions: effect of side arm orientation and downstream geometry", Int. J. Multiphase flow, 18, 861-875.

Ballyk, J.D., Shoukri, M. and Chan, A.M.C. 1987 "Experimental investigation of steam-water annular flow in piping junctions", Presented at the ASME Winter Annular Meeting, Boston, Mass., Dec. 13-18, 1987 (87-WA/NE-8)

Ballyk, J.D. Shoukri, M and Chan, A.M.C. 1988 "Steam-water annular flow in a horizontal dividing T-junction", Int. J. Multiphase Flow, 14, 265-285.

Ballyk, J.D. and Shoukri, M. 1990 "On the development of a model for predicting phase separation phenomena in dividing two-phase flow", Nuclear Engineering and Design, 123, 67-75.

Ballyk, J.D. 1992 "Dividing annular two-phase flow in horizontal T junctions" Ph.D Thesis, McMaster University.

Boulanger, F. and Lemonnier, H. 1992 "Analysis of two-phase pressure drops at a tee junction by two-dimensional modelling and experiments", ANS Proceedings 1992 National Heat Transfer Conference, 109-117.

Buell, J.R., Soliman, H.M. and Sims, G. 1993 "Two-phase pressure drop and phase distribution at a horizontal Tee junction", ASME FED-Vol. 165, Gas-Liquid Flows, 25-37.

Butterworth, D. 1972 "Air-water annular flow in a horizontal tube", Progress in Heat and Mass Transfer, 6, 235

Butterworth, D. 1974 "An analysis of film flow and its application to condensation in a horizontal tube", Int. J. Multiphase Flow, 1, 671-682.

Butterworth, D. 1975 "A comparison of some void-fraction relationships for co-current gas-liquid flow", Int. J. Multiphase Flow, 1, 845-850.

Chang, J. S. and Morala, E. C. 1990 "Determination of two-phase interfacial areas by an ultrasonic technique", Nuclear Engineering and Design, 122, 143-156.

Cheremisinoff, N.P. and Davis, E.J. 1979 "Stratified turbulent-turbulent gas liquid flows", AIChE J., 25, 48-57.

Coleman, H.W. and Steele Jr. W.G. 1989 "Experimentation and uncertainty analysis for engineers", John Wiley and Sons, New York.

Collier, J.G. 1976 "Single-phase and two-phase flow behaviour in primary circuit components", In Proceedings of NATO Advanced Institute on Two-phase Flow and Heat Transfer, 1, 313-365, Hemisphere, Washington, D.C.

Davis, M.R. and Fungtamasan, B. 1990 "Two-phase flow through pipe branch junctions", Int. J. Multiphase Flow, 16, 799-817.

Dallman, J.C., Laurinat, J.E. and Hanratty, T.J 1984 "Entrainment for horizontal annular gas-liquid flow", Int. J. Multiphase Flow, 10, 677-690.

Fisher, S.A. and Pearce, D.L. 1978 "A theoretical model for describing horizontal annular flows", Presented at Int. Semin. on Momentum, Heat and Mass Transfer in Two-Phase Energy and Chemical System, Dubrovnik, Yugoslavia.

Fouda, A.E. and Rhodes, E. 1974 "Two-phase annular flow stream division in a simple tee", Tran. Instn. Chem. Engrs. 52, 354-360.

Henry, J.A.R. 1981 "Dividing annular flow in a horizontal Tee", Int. J. Multiphase Flow, 7, 342-355.

Hewitt, G.F. and Hall-Taylor, N.S. 1970 "Annular two-phase flow", Pergamon Press Ltd., Oxford.

Hong, K.C. 1978 "Two-phase flow splitting at a pipe tee", J. Petrol. Technol. 290-296.

Hutchinson, P., Butterworth, D, and Owen, R.G. 1974 "Development of a model for horizontal annular flow", AERE-R7789.

Hwang, S.T., Soliman, H.M. and Lahey, R.T. Jr., 1988 "Phase separation in dividing two-phase flows", Int. J. Multiphase Flow, 14, 439-458.

Issa, R.I. and Oliveira, P.J. 1991 "Three dimensional predictions of phase separation in T-junctions", Multiphase Flows 91-Tsukuba, Japan, 3-6.

Johannessen, T. 1972 "A theoretical solution of the Lockhart and Martinelli flow model for calculating two-phase flow pressure drop and hold up", Int. J. Heat Mass Transfer, 15, 1443-1449.

Lahey, R.J.Jr. 1986 "Current understanding of phase separation mechanisms in branching conduits", Nuclear Engineering and Design, 95, 145-161.

Lahey, R.T. Jr. 1990 "The analysis of phase separation and phase distribution phenomena using two-fluid models", Nuclear Engineering and Design, 122, 17-40.

Laurinat, J.E. and Hanratty, T.J. 1984 "Pressure drop and film height measurements for annular gas-liquid flow", Int. J. Multiphase Flow, 10, 341-356.

Laurinat, J.E. 1982 "Studies of the effects of pipe size on horizontal annular two-phase flows", Ph.D. Thesis, University of Illinois, Urbana.

Lemonnier, H. and Hervieu, E. 1991 "Theoretical modelling and experimental investigation of single-phase and two-phase flow division at a tee-junction", Nuclear Engineering and Design, 125, 201-213.

Lin, T.F., Jones, O.C., Lahey, R.T. Jr., Block, R.C. and Murase, M. 1985 "Film thickness measurements and modelling in horizontal annular flows", PhysicoChemical Hydrodynamics, 6, 197-206.

Lockhart, R.W. and Martinelli, R.C. 1949 "Proposed correlation of data for isothermal two-phase, two-component flow in pipes", Chem. Engng. Prog. 45, 39-48.

Mandhane, J.M., Gregory, G.A. and Aziz, K. 1974"A flow pattern map for gas-liquid flow in horizontal pipes", Int. J. Multiphase Flow, 1, 537-553.

Madden, J.M. and St. Piere, C.C. 1969 "Two-Phase Flow in a Slot-type Distributor", Proc. B. Inst. M.E., 184, Part 3C.

McCreery, G.E. and Banerjee, S. 1990 "Phase separation of dispersed mist and dispersed annular (rivulet or thin film) flow in a Tee - I , Experiments", Int. J. Multiphase Flow, 16, 429-445.

McCreery, G.E. and Banerjee, S. 1990 "Phase separation of dispersed mist and dispersed annular (rivulet or thin film) flow in a Tee - II, Analysis", Int. J. Multiphase Flow, 17, 309-325.

McNown, J.S. 1954 "Mechanics of manifold flow", Trans. of ASCE, 119, 1103-1142.

Müller, U. and Reimann, J. 1991 "Redistribution of two-phase flow in branching conduits: A survey", Proceedings of the International Conference on Multiphase Flows, 91-TSUKUBA, Vol. 3, pp. 85-107, Sept. 24-27, 1991, Tsukuba, Japan.

Patanker, S.V. 1980 "Numerical heat transfer and fluid flow", Washington, D.C., Hemisphere Publishing Corp.

Popp, M. and Sallet, D.W. 1983 "Experimental investigation of one and two phase flow through a Tee junction", Int. Conf. on the Physical Modelling of Multi-Phase Flow, Coventry, England, 67-88.

Reimann, J. and Seeger, W. 1986 "Two-phase flow in a T-junction with a horizontal inlet Part II: Pressure differences", Int. J. Multiphase Flow, 12, 587-608.

Reimann, J., Brinkmann, H.J. and Domanski, R. 1988 "Gas-liquid flow in dividing Tee-junctions with a horizontal inlet and different branch orientations and diameters", Karlsruhe, Report KfK 4399.

Rubel, M.T. Soliman, H.M. and Sims, G.E. 1988 "Phase distribution during steam-water flow in a horizontal T-junction", Int. J. Multiphase Flow, 14, 425-438.

Russel, T.W.F., Etchells, A.W., Jensen, R. H. and Arruda, P.J. 1974 "Pressure drop and holdup in stratified gas-liquid flow", AIChE J. 20, 664-669.

Saba, N. and Lahey, R.T. Jr. 1984 "The analysis of phase separation phenomena in branching conduits," Int. J. Multiphase Flow, 10, 1-20

Seeger, W. Reimann, J. and Müller, U. 1986 "Two-phase flow in a T-junction with a horizontal inlet Part I: Phase separation", Int. J. Multiphase Flow, 12, 575-585.

Shi, J. and Kocamustafaogullari, G. 1993 "Interficial characteristic measurements in horizontal stratified flow", Proceedings of the Sixth International Topical Meeting on Nuclear Reactor Thermalhydraulics, Oct. 5-8, 1993, Grenoble, France.

Shohm, O., Brill J.P. and Taitel, Y. 1987 "Two-phase flow splitting in a T-junction, Experiment and modelling", Chem. Eng. Sci. 42, 2667-2676.

Shohm, O., Airachakaran, S. and Brill, J.P. 1989 "Two-phase flow splitting in a horizontal reduced pipe tee", Chem. Eng. Sci. 44, 2388-2391.

Taitel, Y. and Dukler, A.E. 1976 "A theoretical approach to the Lockhart-Martinelli correlation for stratified flow", Int. J. Multiphase Flow, 2, 591-595.

Tso, C.P. and Sugawara, S. 1990 "Film thickness prediction in a horizontal annular two-phase flow", Int. J. Multiphase Flow, 16, 867-884.

APPENDIX A
EXPERIMENTAL DATA

Table A1. SINGLE-PHASE EXPERIMENTAL RESULTS

G_1 kg/s.m^2	G_2/G_1	D_2/D_1	ΔP_{21} Pa	K_{12}	ΔP_{13} Pa	K_{13}
1200	0.00	1.0	-240	-	56	1.08
1200	0.20	1.0	271	0.54	16	0.98
1200	0.40	1.0	438	0.47	56	0.92
1200	0.60	1.0	502	0.41	212	0.93
1200	0.80	1.0	488	0.35	505	1.06
900	0.00	1.0	-150	-	30	1.07
900	0.20	1.0	154	0.53	10	0.99
900	0.40	1.0	247	0.47	35	0.95
900	0.60	1.0	281	0.41	128	0.95
900	0.80	1.0	293	0.37	269	1.02
900	1.00	1.0	271	0.33	465	1.15
600	0.00	1.0	-7	-	13	1.07
600	0.20	1.0	73	0.55	4	0.98
600	0.40	1.0	113	0.48	15	0.92
600	0.60	1.0	130	0.42	55	0.95
600	0.80	1.0	131	0.38	122	1.03
600	1.00	1.0	119	0.33	212	1.17
450	0.00	1.0	-3	-	7	1.07
450	0.20	1.0	42	0.59	0	0.96
450	0.40	1.0	67	0.51	7	0.91
450	0.60	1.0	79	0.45	32	0.95
450	0.80	1.0	78	0.40	67	1.02
450	1.00	1.0	71	0.35	120	1.15
120	0.11	1.0	2.81	0.94	-0.14	0.96
120	0.31	1.0	5.43	0.72	0.13	0.92
120	0.50	1.0	6.75	0.62	0.52	0.82
120	0.71	1.0	7.17	0.55	2.93	0.90
120	0.90	1.0	7.71	0.54	5.51	0.96
120	1.00	1.0	8.34	0.58	6.06	1.04
100	0.12	1.0	2.49	0.99	-0.13	0.96
100	0.32	1.0	5.48	0.85	-0.07	0.88
100	0.52	1.0	6.26	0.82	0 05	0.83
100	0.71	1.0	6.41	0.69	1.99	0.89
100	0.91	1.0	5.78	0.58	4.22	1.01
100	1.00	1.0	5.77	0.57	6.00	1.19
80	0.12	1.0	1.71	1.21	-1.43	0.54
80	0.32	1.0	3.49	1.00	-0.74	0.67

G_1, kg/s.m^2	G_2/G_1	D_2/D_1	ΔP_{21}, Pa	K_{12}	ΔP_{13}, Pa	K_{13}
80	0.52	1.0	3.99	0.81	0.53	0.90
80	0.72	1.0	3.80	0.65	1.61	0.98
80	0.92	1.0	4.15	0.66	3.04	1.10
80	1.00	1.0	4.72	0.57	4.24	1.31
60	0.12	1.0	1.36	1.14	-1.08	0.39
60	0.32	1.0	2.45	1.05	-0.48	0.64
60	0.52	1.0	2.20	0.79	0.02	0.75
60	0.72	1.0	2.61	0.79	0.58	0.81
60	0.92	1.0	2.35	0.66	1.17	0.90
60	1.00	1.0	2.12	0.58	2.30	1.26
120	0.10	0.33	1.92	0.70	26	3.78
120	0.30	0.33	4.78	0.65	93	6.69
120	0.50	0.33	6.17	0.57	228	12.39
120	0.70	0.33	6.43	0.49	438	22.06
120	0.90	0.33	5.71	0.40	691	31.11
120	1.00	0.33	4.91	0.34	855	38.56
100	0.10	0.33	1.43	0.75	12	2.67
100	0.30	0.33	3.63	0.71	62	6.03
100	0.50	0.33	4.81	0.64	149	10.54
100	0.70	0.33	5.38	0.59	303	21.88
100	0.90	0.33	5.56	0.56	487	32.52
100	1.00	0.33	4.81	0.48	604	40.49
80	0.10	0.33	1.10	0.90	16	5.02
80	0.30	0.33	2.65	0.81	47	8.32
80	0.50	0.33	3.75	0.78	105	13.55
80	0.70	0.33	3.85	0.66	199	23.23
80	0.90	0.33	4.00	0.63	313	33.02
80	1.00	0.33	3.72	0.58	389	41.39
60	0.10	0.33	0.66	0.97	10	5.98
60	0.30	0.33	1.55	0.84	28	9.21
60	0.50	0.33	2.06	0.76	61	14.79
60	0.70	0.33	2.13	0.65	115	25.05
60	0.90	0.33	2.07	0.58	178	34.32
60	1.00	0.33	1.95	0.54	222	43.22

Table A2. ANNULAR FLOW EXPERIMENTAL RESULTS

G_1 kg/s.m^2	G_2/G_1	X_1 %	X_2 %	X_3 %	X_2/X_1	α_1	α_2	α_3	θ degree	$\Delta P_{2\phi}$ kPa	$\Delta P_{1\phi}$ kPa
608	0.346	1.929	2.500	0.199	0.103	0.786	0.790	0.761	90	-0.089	-0.153
614	0.470	2.058	2.684	0.447	0.217	0.812	0.841	0.579	90	0.027	0.911
598	0.538	1.834	2.952	0.649	0.354	0.791	0.845	0.635	90	0.034	0.567
602	0.637	2.020	3.111	1.186	0.587	0.797	0.845	0.724	90	0.135	0.945
593	0.725	2.316	2.589	2.145	0.926	0.803	0.816	0.795	90	0.186	2.836
593	0.787	2.391	1.957	2.689	1.125	0.800	0.775	0.814	90	0.624	3.541
608	0.918	1.929	4.937	1.829	0.948	0.768	0.978	0.761	90	0.694	3.625
599	0.137	4.761	5.289	0.000	0.000	0.870	0.879	0.000	90	-0.062	0.569
599	0.167	4.647	5.385	0.186	0.040	0.871	0.883	0.374	90	0.045	-0.116
604	0.241	4.699	5.896	0.944	0.201	0.873	0.891	0.686	90	0.123	0.764
596	0.307	4.607	6.118	1.433	0.311	0.876	0.898	0.776	90	0.175	0.869
606	0.347	4.583	6.256	1.457	0.318	0.876	0.900	0.747	90	0.289	1.014
604	0.410	4.525	6.286	1.567	0.346	0.872	0.901	0.753	90	0.454	1.351
602	0.436	4.866	6.572	2.540	0.522	0.885	0.907	0.824	90	0.728	1.701
606	0.484	4.358	5.611	2.353	0.540	0.882	0.927	0.807	90	0.734	1.814
601	0.530	4.584	4.949	4.080	0.890	0.878	0.884	0.868	90	1.419	2.951
602	0.562	4.684	4.119	4.951	1.057	0.875	0.863	0.879	90	1.699	3.737
607	0.630	4.531	2.734	5.496	1.213	0.865	0.813	0.882	90	2.115	4.820
594	0.709	4.860	0.544	6.182	1.272	0.864	0.548	0.885	90	3.002	6.242
593	0.797	4.808	1.031	5.385	1.120	0.859	0.655	0.870	90	3.848	6.537
593	0.884	4.937	0.000	5.070	1.027	0.858	0.000	0.861	90	3.910	7.270
593	1.000	4.897	0.000	4.353	0.889	0.852	0.000	0.840	90	3.324	7.923
589	0.108	8.072	8.945	2.219	0.275	0.900	0.907	0.767	90	-0.548	0.548
606	0.159	7.798	9.330	2.285	0.293	0.897	0.910	0.771	90	-0.256	0.702
601	0.226	7.891	8.949	3.109	0.394	0.903	0.911	0.818	90	0.234	0.439
606	0.262	7.496	8.257	5.517	0.736	0.903	0.910	0.880	90	0.708	0.826
595	0.284	8.051	6 460	12.08	1.500	0.915	0.900	0.918	90	4.488	2.003
602	0.356	8.161	4.270	16.26	1.993	0.908	0.856	0.946	90	5.714	6.317
601	0.427	8.079	2.638	16.51	2.043	0.901	0.792	0.943	90	6.123	8.707
601	0.491	8.094	1.479	14.97	1.849	0.900	0.707	0.934	90	5.654	9.366
598	0.581	7.882	0.624	12.56	1.593	0.894	0.549	0.925	90	6.650	10.19
894	0.192	2.096	2.579	0.000	0.000	0.780	0.806	0.000	90	-0.005	1.019
904	0.288	2.069	2.601	0.463	0.224	0.785	0.813	0.544	90	0.045	1.271
905	0.406	2.005	2.761	0.854	0.426	0.791	0.828	0.666	90	0.306	1.745
905	0.487	1.952	2.676	1.085	0.556	0.794	0.830	0.682	90	0.315	2.475
899	0.555	2.114	2.641	1.537	0.727	0.796	0.822	0.734	90	0.454	3.288
909	0.598	1.885	2.103	1.693	0.898	0.778	0.792	0.727	90	0.653	3.612

G_1 kg/s.m^2	G_2/G_1	X_1 %	X_2 %	X_3 %	X_2/X_1	α_1	α_2	α_3	θ degree	ΔP_{21} kPa	ΔP_{13} kPa	P_1 bar
907	0.666	2.081	0.927	2.377	1.142	0.772	0.649	0.789	90	0.706	5.440	1.71
900	0.763	2.178	0.844	2.461	1.130	0.765	0.615	0.782	90	2.446	6.477	1.95
895	0.849	2.148	1.424	2.077	0.967	0.757	0.696	0.753	90	2.475	6.633	2.05
900	0.929	2.322	4.000	1 923	0.828	0.767	0.961	0.740	90	2.143	6.998	2.14
579	0.144	2.121	3.519	0.492	0.232	0.800	0.855	0.574	45	0.232	-0.678	1.37
617	0.235	1.661	2.245	0.747	0.450	0.773	0.810	0.608	45	0.279	0.264	1.31
623	0.347	1.869	1.973	1.779	0.952	0.801	0.807	0.829	45	0.478	0.674	1.14
604	0.442	2.682	2.334	3.055	1.139	0.836	0.821	0.849	45	0.541	2.304	1.20
589	0.527	2.767	1.887	3.979	1.438	0.834	0.790	0.869	45	0.642	2.961	1.27
602	0.630	2.146	0.878	3.292	1.534	0.800	0.671	0.853	45	2.033	2.468	1.36
603	0.758	2.382	2.734	3.116	1.308	0.804	0.820	0.842	45	2.244	3.484	1.48
612	0.880	2.404	4.136	2.656	1.105	0.801	0.992	0.822	45	1.699	4.313	1.59
584	0.232	4.991	5.383	2.580	0.517	0.883	0.889	0.819	45	0.394	0.254	1.50
587	0.291	4.801	5.074	5.233	1.090	0.885	0.889	0.892	45	0.888	0.685	1.34
613	0.402	4.313	2.895	6.646	1.541	0.875	0.838	0.908	45	1.779	1.131	1.29
607	0.494	4.532	1.332	7.409	1.635	0.872	0.728	0.909	45	2.473	2.230	1.46
602	0.587	4.364	0.782	6.817	1.562	0.865	0.636	0.896	45	2.873	4.169	1.53
592	0.752	4.858	0.863	6.218	1.280	0.865	0.647	0.880	45	4.680	5.803	1.83
582	0.087	8.452	9.026	3.119	0.369	0.902	0.906	0.808	45	-0.455	-0.031	2.08
605	0.121	8.145	9.032	7.339	0.901	0.900	0.907	0.892	45	-0.024	0.159	2.04
589	0.194	8.581	7.380	12.84	1.496	0.913	0.902	0.936	45	2.632	-0.016	1.67
611	0.262	7.867	4.627	16.01	2.035	0.915	0.876	0.951	45	6.046	0.384	1.46
606	0.361	7.850	2.940	17.64	2.247	0.906	0.817	0.946	45	5.841	2.571	1.71
599	0.462	7.940	1.148	15.83	1.994	0.900	0.670	0.941	45	11.55	5.417	1.91
594	0.578	8.159	1.352	12.39	1.518	0.898	0.688	0.925	45	11.04	7.749	2.05
588	0.726	7.718	1.091	9.292	1.204	0.891	0.648	0.905	45	9.608	8.201	2.14
902	0.192	2.530	2.512	1.584	0.626	0.803	0.802	0.741	45	0.227	1.319	1.64
926	0.305	1.942	1.911	1.921	0.989	0.787	0.785	0.786	45	0.238	1.345	1.37
892	0.402	2.285	1.638	2.904	1.271	0.806	0.764	0.833	45	0.952	1.981	1.37
913	0.511	1.985	0.447	3.112	1.568	0.774	0.530	0.828	45	2.546	3.602	1.59
898	0.587	2.298	0.591	3.477	1.513	0.784	0.567	0.825	45	3.334	4.676	1.75
903	0.684	1.993	1.993	2.637	1.323	0.760	0.709	0.776	45	3.548	5.930	1.84
913	0.800	1.942	2.397	2.163	1.114	0.756	0.784	0.758	45	3.786	6.823	1.86
922	0.889	1.695	3.874	1.668	0.984	0.733	0.921	0.719	45	3.036	7.724	1.94

Table A3. STRATIFIED FLOW EXPERIMENTAL RESULTS

u_{sg} m/s	u_{sl} m/s	m_g/m_t	x_1 %	x_2 %	x_3 %	α_1	α_2	α_3	θ degree	D_g/D_t	ΔP_{21} Pa	ΔP_{32} Pa	P_t bar
0.05	1.49	0.19	2.12	2.14	2.02	0.56	0.57	0.56	0	1.0	0.55	0.11	1.19
0.05	1.50	0.31	2.11	2.20	1.91	0.57	0.58	0.55	0	1.0	1.03	0.34	1.18
0.05	1.50	0.42	2.15	2.19	2.10	0.57	0.58	0.57	0	1.0	1.68	0.72	1.20
0.05	1.51	0.52	2.20	2.28	2.12	0.57	0.58	0.57	0	1.0	2.51	1.23	1.22
0.05	1.48	0.63	2.22	2.26	2.22	0.57	0.58	0.57	0	1.0	2.78	1.51	1.26
0.05	1.52	0.71	2.32	1.97	2.46	0.58	0.55	0.59	0	1.0	3.27	2.87	1.28
0.05	1.50	0.87	2.34	4.16	2.08	0.58	0.69	0.56	0	1.0	4.03	3.86	1.31
0.05	2.50	0.17	3.61	3.09	6.20	0.67	0.64	0.76	0	1.0	1.07	0.52	1.23
0.05	2.53	0.27	3.66	3.19	4.91	0.67	0.65	0.73	0	1.0	3.29	1.14	1.23
0.05	2.52	0.37	3.73	3.30	4.45	0.67	0.65	0.71	0	1.0	3.67	2.38	1.26
0.05	2.49	0.51	3.63	3.43	3.82	0.67	0.66	0.68	0	1.0	3.18	3.63	1.24
0.05	2.51	0.62	3.74	3.97	3.60	0.67	0.68	0.67	0	1.0	5.52	5.27	1.27
0.05	2.50	0.72	3.90	4.77	3.56	0.68	0.71	0.66	0	1.0	12.3	6.84	1.33
0.05	2.53	0.84	4.08	6.35	3.65	0.68	0.76	0.66	0	1.0	13.8	8.43	1.38
0.05	4.88	0.18	7.03	4.19	19.9	-	-	-	0	1.0	-	-	1.27
0.05	5.05	0.29	7.46	5.36	12.6	-	-	-	0	1.0	-	-	1.31
0.05	4.96	0.38	7.49	5.38	10.9	-	-	-	0	1.0	-	-	1.34
0.05	5.32	0.49	8.05	6.27	9.90	-	-	-	0	1.0	-	-	1.35
0.05	4.84	0.60	7.48	7.36	7.55	-	-	-	0	1.0	-	-	1.37
0.05	5.08	0.71	7.87	8.26	7.71	-	-	-	0	1.0	-	-	1.38
0.05	5.12	0.81	8.19	9.94	7.78	-	-	-	0	1.0	-	-	1.43
0.07	1.50	0.20	1.58	1.49	1.98	0.51	0.50	0.55	0	1.0	0.95	1.08	1.23
0.07	1.51	0.33	1.59	1.37	2.06	0.51	0.48	0.56	0	1.0	1.63	1.93	1.23
0.07	1.49	0.42	1.58	1.30	1.98	0.51	0.47	0.55	0	1.0	3.65	2.32	1.24
0.07	1.50	0.56	1.68	1.30	1.99	0.51	0.46	0.54	0	1.0	5.05	2.94	1.31
0.07	1.53	0.67	1.80	1.15	2.12	0.52	0.43	0.56	0	1.0	5.44	5.05	1.38
0.07	1.48	0.78	1.87	1.00	2.12	0.52	0.40	0.55	0	1.0	7.23	6.87	1.48
0.07	2.52	0.15	1.65	1.31	3.56	0.51	0.47	0.66	0	1.0	1.20	1.40	1.27
0.07	2.49	0.21	2.70	2.20	4.66	0.61	0.57	0.71	0	1.0	2.05	1.84	1.28
0.07	2.50	0.27	2.71	2.27	3.90	0.61	0.58	0.68	0	1.0	3.18	2.59	1.28
0.07	2.51	0.38	2.74	2.13	3.75	0.61	0.56	0.67	0	1.0	4.86	3.27	1.29
0.07	2.51	0.50	2.78	2.00	3.56	0.61	0.55	0.66	0	1.0	6.36	5.43	1.31
0.07	2.50	0.63	3.00	1.96	3.60	0.62	0.54	0.66	0	1.0	7.07	7.17	1.42
0.07	2.49	0.72	3.21	2.28	3.58	0.63	0.56	0.65	0	1.0	8.54	8.64	1.53
0.07	2.48	0.83	3.36	1.53	3.72	0.63	0.47	0.65	0	1.0	10.9	11.3	1.61
0.07	5.25	0.18	5.41	2.42	19.0	-	-	-	0	1.0	-	-	1.25
0.07	5.10	0.22	5.46	2.16	17.1	-	-	-	0	1.0	-	-	1.30

u_m m/s	$u_{s,2}$ m/s	m_2/m_1	x_1 %	x_2 %	x_3 %	α_1	α_2	α_3	θ degree	D_2/D_1	ΔP_{21} Pa	ΔP_{12} Pa	P_1 bar
0.07	4.96	0.28	5.39	2.18	13.7	-	-	-	0	1.0	-	-	1.32
0.07	4.88	0.37	5.54	1.80	11.9	-	-	-	0	1.0	-	-	1.38
0.07	5.02	0.48	5.84	2.50	9.46	-	-	-	0	1.0	-	-	1.42
0.07	4.89	0.60	5.81	2.06	8.31	-	-	-	0	1.0	-	-	1.45
0.07	5.24	0.69	6.48	3.45	7.84	-	-	-	0	1.0	-	-	1.52
0.07	5.15	0.81	6.49	2.62	7.40	-	-	-	0	1.0	-	-	1.55
0.09	1.50	0.20	1.26	1.08	2.01	0.46	0.43	0.55	0	1.0	2.32	2.62	1.26
0.09	1.51	0.33	1.28	0.96	1.94	0.46	0.41	0.55	0	1.0	3.58	3.55	1.27
0.09	1.52	0.43	1.29	0.87	1.85	0.46	0.39	0.54	0	1.0	4.64	5.06	1.27
0.09	1.50	0.53	1.29	0.71	1.83	0.46	0.35	0.53	0	1.0	5.16	6.16	1.29
0.09	1.50	0.61	1.31	0.56	1.80	0.46	0.31	0.53	0	1.0	6.15	8.37	1.31
0.09	1.49	0.70	1.42	0.28	1.92	0.47	0.20	0.53	0	1.0	7.19	9.21	1.43
0.09	1.52	0.81	1.54	0.24	1.85	0.48	0.18	0.52	0	1.0	8.73	9.88	1.52
0.09	2.51	0.10	2.19	1.70	6.63	0.57	0.51	0.77	0	1.0	2.78	2.01	1.32
0.09	2.50	0.17	2.23	1.67	4.97	0.57	0.51	0.72	0	1.0	3.88	3.54	1.35
0.09	2.51	0.31	2.26	1.54	3.85	0.57	0.49	0.67	0	1.0	4.65	4.26	1.36
0.09	2.49	0.42	2.31	1.36	3.64	0.57	0.46	0.66	0	1.0	6.02	6.07	1.40
0.09	2.48	0.57	2.34	1.49	2.99	0.57	0.48	0.62	0	1.0	7.74	8.59	1.43
0.09	2.51	0.66	2.55	1.50	3.09	0.58	0.47	0.62	0	1.0	9.46	11.1	1.54
0.09	2.50	0.81	2.76	0.59	3.26	0.59	0.30	0.62	0	1.0	13.9	12.8	1.68
0.09	4.86	0.19	4.25	0.97	18.3	-	-	-	0	1.0	-	-	1.35
0.09	4.98	0.23	4.45	1.55	14.1	-	-	-	0	1.0	-	-	1.38
0.09	5.06	0.33	4.67	1.01	12.1	-	-	-	0	1.0	-	-	1.43
0.09	5.01	0.41	4.78	1.42	9.60	-	-	-	0	1.0	-	-	1.48
0.09	5.10	0.52	5.11	0.96	8.94	-	-	-	0	1.0	-	-	1.56
0.09	4.96	0.66	5.27	1.79	7.07	-	-	-	0	1.0	-	-	1.66
0.09	5.20	0.78	5.67	4.87	5.90	-	-	-	0	1.0	-	-	1.71
0.05	1.48	0.15	1.95	1.79	2.84	0.56	0.57	0.72	0	0.33	0.09	17	1.10
0.05	1.58	0.26	2.04	1.80	2.71	0.57	0.58	0.63	0	0.33	0.47	58	1.08
0.05	1.34	0.43	1.77	1.63	1.91	0.54	0.52	0.56	0	0.33	1.92	143	1.10
0.05	1.46	0.59	2.01	1.80	2.15	0.56	0.64	0.58	0	0.33	2.45	345	1.15
0.05	1.55	0.79	2.29	1.69	2.45	0.58	0.21	0.74	0	0.33	3.81	555	1.24
0.05	2.72	0.15	3.58	2.72	8.46	0.68	0.64	0.81	0	0.33	0.24	55	1.12
0.05	2.53	0.22	3.28	2.44	6.27	0.66	0.63	0.73	0	0.33	0.53	81	1.10
0.05	2.82	0.38	3.58	2.79	4.87	0.68	0.66	0.72	0	0.33	1.02	269	1.08
0.05	2.78	0.49	3.72	3.08	4.39	0.68	0.68	0.71	0	0.33	2.63	483	1.14
0.05	2.25	0.61	3.14	2.79	3.36	0.65	0.70	0.66	0	0.33	5.89	558	1.18
0.05	2.57	0.75	3.68	3.90	3.61	0.68	0.24	0.61	0	0.33	4.91	902	1.22
0.05	4.87	0.18	6.54	4.55	25.51	-	-	-	0	0.33	-	-	1.21

u_{sl} m/s	u_{sg} m/s	m_g/m_l	x_1 %	x_2 %	x_3 %	α_1	α_2	α_3	θ degree	D_j/D_1	ΔP_{21} Pa	ΔP_{32} Pa	P_1 bar
0.05	4.51	0.26	6.01	5.54	14.78	-	-	-	0	0.33	-	-	1.20
0.05	4.97	0.49	7.22	4.53	9.96	-	-	-	0	0.33	-	-	1.31
0.05	4.65	0.64	6.79	8.42	8.15	-	-	-	0	0.33	-	-	1.34
0.05	4.36	0.78	6.75	8.45	6.68	-	-	-	0	0.33	-	-	1.38
0.09	1.52	0.21	1.22	0.89	2.45	0.48	0.47	0.65	0	0.33	0.58	78	1.20
0.09	1.56	0.33	1.19	0.71	2.17	0.47	0.45	0.63	0	0.33	2.78	193	1.14
0.09	1.59	0.46	1.31	0.68	2.04	0.49	0.44	0.55	0	0.33	4.24	436	1.23
0.09	1.51	0.60	1.23	0.46	1.75	0.48	0.45	0.48	0	0.33	6.51	736	1.22
0.09	1.55	0.72	1.35	0.24	1.78	0.49	0.43	0.49	0	0.33	7.78	963	1.30
0.09	2.57	0.15	2.11	1.38	6.26	0.53	0.50	0.78	0	0.33	0.04	105	1.24
0.09	2.47	0.33	1.90	0.78	4.19	0.50	0.48	0.72	0	0.33	1.15	364	1.16
0.09	2.38	0.49	1.87	0.74	3.04	0.54	0.48	0.55	0	0.33	7.49	699	1.18
0.09	2.45	0.58	1.98	0.92	2.76	0.56	0.52	0.56	0	0.33	9.29	993	1.22
0.09	2.38	0.72	2.11	0.97	2.56	0.56	0.49	0.56	0	0.33	15.4	1528	1.34
0.09	5.51	0.18	4.24	0.50	21.12	-	-	-	0	0.33	-	-	1.38
0.09	5.26	0.23	4.12	0.76	15.57	-	-	-	0	0.33	-	-	1.36
0.09	5.11	0.26	4.06	0.85	13.85	-	-	-	0	0.33	-	-	1.38
0.09	5.03	0.41	4.01	1.12	8.78	-	-	-	0	0.33	-	-	1.45
0.09	5.52	0.56	4.14	2.35	6.58	-	-	-	0	0.33	-	-	1.58
0.09	5.15	0.68	4.00	1.07	5.08	-	-	-	0	0.33	-	-	1.69
0.05	1.39	0.48	1.83	3.52	0.00	0.54	0.70	0.00	90	0.33	1.38	153	1.10
0.05	1.22	0.63	1.65	4.47	0.00	0.59	0.78	0.00	90	0.33	1.30	206	1.13
0.05	1.69	0.83	2.37	11.9	0.43	0.56	0.88	0.79	90	0.33	2.95	314	1.18
0.05	1.58	0.92	2.37	10.3	1.68	0.55	0.95	0.89	90	0.33	3.45	2269	1.26
0.05	2.55	0.55	3.37	7.48	0.00	0.64	0.81	0.00	90	0.33	2.81	180	1.12
0.05	2.59	0.66	3.48	10.2	0.00	0.63	0.84	0.00	90	0.33	3.03	258	1.14
0.05	2.67	0.72	3.67	10.8	0.88	0.67	0.89	0.74	90	0.33	3.53	281	1.17
0.05	2.63	0.79	3.82	10.7	1.99	0.65	0.92	0.85	90	0.33	7.00	1250	1.24
0.05	2.85	0.84	4.32	7.72	3.67	0.66	0.98	0.93	90	0.33	8.96	2221	1.30
0.05	3.45	0.60	4.62	11.5	0.00	0.73	0.90	0.00	90	0.33	4.42	155	1.15
0.05	3.61	0.67	4.94	12.7	1.14	0.73	0.92	0.72	90	0.33	5.82	207	1.18
0.05	3.64	0.73	5.06	10.9	2.88	0.74	0.95	0.85	90	0.33	7.35	1406	1.20
0.05	3.52	0.78	5.21	9.08	4.11	0.75	0.98	0.94	90	0.33	8.32	2560	1.28
0.09	1.27	0.29	1.01	1.42	0.00	0.40	0.46	0.00	90	0.33	2.13	133	1.18
0.09	1.31	0.47	1.00	1.89	0.00	0.46	0.54	0.00	90	0.33	3.72	222	1.14
0.09	1.32	0.78	1.07	4.52	0.10	0.44	0.76	0.62	90	0.33	5.36	317	1.21
0.09	1.40	0.86	1.17	5.42	0.48	0.48	0.78	0.75	90	0.33	6.74	1273	1.25
0.09	1.69	0.96	1.59	3.49	1.51	0.47	0.87	0.87	90	0.33	7.76	2284	1.41
0.09	2.47	0.24	2.13	2.80	0.00	0.54	0.61	0.00	90	0.33	2.92	96	1.30

u_m m/s	u_c m/s	m_2/m_1	x_1 %	x_2 %	x_3 %	α_1	α_2	α_3	θ degree	D_2/D_1	ΔP_{21} Pa	ΔP_{13} Pa	P_1 bar
0.09	2.48	0.36	2.02	3.16	0.00	0.53	0.65	0.00	90	0.33	3.29	153	1.23
0.09	2.54	0.60	1.96	4.66	0.16	0.54	0.73	0.69	90	0.33	7.27	274	1.16
0.09	2.15	0.68	1.70	4.56	0.36	0.56	0.75	0.74	90	0.33	7.98	810	1.19
0.09	2.10	0.72	1.69	4.35	0.66	0.55	0.77	0.83	90	0.33	8.02	1262	1.21
0.09	2.10	0.80	1.80	3.82	1.30	0.54	0.83	0.88	90	0.33	9.16	1914	1.29
0.09	3.55	0.39	3.05	5.01	0.00	0.62	0.72	0.00	90	0.33	2.65	195	1.31
0.09	3.73	0.44	3.16	5.36	0.35	0.61	0.74	0.61	90	0.33	3.60	270	1.29
0.09	3.69	0.51	3.05	5.44	0.76	0.62	0.78	0.78	90	0.33	5.97	1282	1.26
0.09	3.63	0.62	3.01	5.06	1.74	0.62	0.83	0.82	90	0.33	12.9	2180	1.26
0.09	3.68	0.75	3.23	4.69	2.75	0.63	0.85	0.95	90	0.33	29.3	3368	1.34

APPENDIX B

EXPERIMENTAL UNCERTAINTIES

Consider a general case in which an experimental result R is a function of variables X_i:

$$R = R\ (\ X_1,\ X_2,\ \cdots\cdots\ X_i\ ) \qquad \text{B.1}$$

Eqn.(B.1) is the data reduction equation used for determining R from the measured values of variables X_i. The uncertainty in the result is given as:

$$\frac{dR}{R} = \left[\left(\frac{\partial R}{\partial X_1}\frac{dX_1}{R}\right)^2 + \left(\frac{\partial R}{\partial X_2}\frac{dX_2}{R}\right)^2 + \cdots\cdots \left(\frac{\partial R}{\partial X_i}\frac{dX_i}{R}\right)^2 \right]^{\frac{1}{2}} \qquad \text{B.2}$$

B.1. Uncertainties of mass flow rates

The inlet mass flow rate $\dot{m}_1$ was reduced as:

$$\dot{m}_1 = \dot{m}_{gm} + \dot{m}_{Lm} \qquad \text{B.3}$$

the uncertainty of $\dot{m}_1$ was defined as:

$$\begin{aligned} \frac{d\dot{m}_1}{\dot{m}_1} &= \left[\left(\frac{\partial \dot{m}_1}{\partial \dot{m}_{gm}}\frac{d\dot{m}_{gm}}{\dot{m}_1}\right)^2 + \left(\frac{\partial \dot{m}_1}{\partial \dot{m}_{Lm}}\frac{d\dot{m}_{Lm}}{\dot{m}_1}\right)^2 \right]^{\frac{1}{2}} \\ &= \left[\left(\frac{d\dot{m}_{gm}}{\dot{m}_1}\right)^2 + \left(\frac{d\dot{m}_{Lm}}{\dot{m}_1}\right)^2 \right]^{\frac{1}{2}} \end{aligned} \qquad \text{B.4}$$

The mass flow rates of run and branch condensates were measured directly by the turbine flow meters. The uncertainties of the turbine flow meters were provided by the manufacturer as $\pm 1\%$. The uncertainty of the branch flow split ratio was expressed as:

$$\frac{d(\frac{\dot{m}_3}{\dot{m}_1})}{(\frac{\dot{m}_3}{\dot{m}_1})} = [(\frac{d\dot{m}_3}{\dot{m}_3})^2+(\frac{d\dot{m}_1}{\dot{m}_1})^2]^{\frac{1}{2}} \qquad \text{B.5}$$

B.2. Uncertainties of qualities

The inlet quality x_1 was determined based on the energy balance of two-phase mixer and was reduced as:

$$x_1 = \frac{\dot{m}_{gm}h_{gm}+\dot{m}_{Lm}h_{Lm}-\dot{m}_1h_{Lti}}{\dot{m}_1(h_{gti}-h_{Lti})} = \frac{H_{gm}+H_{Lm}-H_{Lti}}{H_{gLti}} \qquad \text{B.6}$$

The uncertainty of x_1 was defined as:

$$\frac{dx_1}{x_1} = [(\frac{dH_{gm}}{(H_{gm}+H_{Lm}-H_{Lti})})^2+(\frac{dH_{Lm}}{(H_{gm}+H_{Lm}-H_{Lti})})^2 + (\frac{dH_{Lti}}{(H_{gm}+H_{Lm}-H_{Lti})})^2+(\frac{dH_{gLti}}{H_{gLti}})^2]^{\frac{1}{2}} \qquad \text{B.7}$$

The run quality x_2 was determined based on the run condenser and was reduced as:

$$x_2 = \frac{\dot{m}_2h_{ci}+\dot{m}_{cw}h_{cwo}-\dot{m}_{cw}h_{cwi}-\dot{m}_2h_{Ltb}}{\dot{m}_2(h_{gb}-h_{Lb})} = \frac{H_{2c}+H_{cwo}-H_{cwi}-H_{Ltb}}{H_{gLtb}} \qquad \text{B.8}$$

The uncertainty of x_2 was defined as:

$$\frac{dx_2}{x_2} = \left[\left(\frac{dH_{2c}}{(H_{2c}+H_{cwo}-H_{cwi}-H_{Ltb})}\right)^2+\left(\frac{dH_{cwo}}{(H_{2c}+H_{cwo}-H_{cwi}-H_{Ltb})}\right)^2 + \left(\frac{dH_{cwi}}{(H_{2c}+H_{cwo}-H_{cwi}-H_{Ltb})}\right)^2+\left(\frac{dH_{Ltb}}{(H_{2c}+H_{cwo}-H_{cwi}-H_{Ltb})}\right)^2 + \left(\frac{dH_{gLtb}}{H_{gLtb}}\right)^2\right]^{\frac{1}{2}} \qquad \text{B.9}$$

The branch quality x_3 was determined based on the branch condenser and was reduced as:

$$x_3 = \frac{\dot{m}_3 h_{ci}+\dot{m}_{cw}h_{cwo}-\dot{m}_{cw}h_{cwi}-\dot{m}_3 h_{Ltb}}{\dot{m}_3 (h_{gb}-h_{Lb})} = \frac{H_{3c}+H_{cwo}-H_{cwi}-H_{Ltb}}{H_{gLtb}} \qquad \text{B.10}$$

The uncertainty of x_3 was defined as:

$$\frac{dx_3}{x_3} = \left[\left(\frac{dH_{3c}}{(H_{3c}+H_{cwo}-H_{cwi}-H_{Ltb})}\right)^2+\left(\frac{dH_{cwo}}{(H_{3c}+H_{cwo}-H_{cwi}-H_{Ltb})}\right)^2 + \left(\frac{dH_{cwi}}{(H_{3c}+H_{cwo}-H_{cwi}-H_{Ltb})}\right)^2+\left(\frac{dH_{Ltb}}{(H_{3c}+H_{cwo}-H_{cwi}-H_{Ltb})}\right)^2 + \left(\frac{dH_{gLtb}}{H_{gLtb}}\right)^2\right]^{\frac{1}{2}} \qquad \text{B.11}$$

The uncertainty of the phase separation was defined as:

$$\frac{d\left(\frac{x_3}{x_1}\right)}{\left(\frac{x_3}{x_1}\right)} = \left[\left(\frac{dx_3}{x_3}\right)^2+\left(\frac{dx_1}{x_1}\right)^2\right]^{\frac{1}{2}} \qquad \text{B.12}$$

B.3. Uncertainties of pressure changes

The pressure changes were obtained by extrapolating the fully developed pressure gradients in the inlet, run and branch to the centre of the T-junction,

$$\Delta P_{2-1} = P_2 - P_1 \qquad \text{B.13}$$

$$\Delta P_{1-3} = P_1 - P_3 \qquad \text{B.14}$$

where P_1, P_2 and P_3 were obtained by the linear regression equations in the inlet, run and branch. The uncertainties of the pressure changes were defined as:

$$\left[\frac{d(\Delta P_{2-1})}{\Delta P_{2-1}}\right] = \left[\left(\frac{dP_1}{\Delta P_{2-1}}\right)^2 + \left(\frac{dP_2}{\Delta P_{2-1}}\right)^2\right]^{\frac{1}{2}} \qquad \text{B.15}$$

$$\left[\frac{d(\Delta P_{1-3})}{\Delta P_{1-3}}\right] = \left[\left(\frac{dP_1}{\Delta P_{1-3}}\right)^2 + \left(\frac{dP_3}{\Delta P_{1-3}}\right)^2\right]^{\frac{1}{2}} \qquad \text{B.16}$$

The uncertainties of P_1, P_2 and P_3 consist of the measurement uncertainties of the differential pressure transducers and the linear regression uncertainties due to the scatter of the pressure data about the regression line.

B.4. Uncertainty of void fraction

The uncertainty of the measured void fraction by using gamma densitometer was given by Banerjee and Lahey (1981) as:

$$\frac{d\alpha}{\alpha} = \frac{\frac{\Delta N}{N}}{\alpha Ln(\frac{N_g}{N_L})} [1+(\alpha-1)^2+\alpha^2]^{\frac{1}{2}} \qquad \text{B.17}$$

B.5. Evaluation of experimental uncertainties

A typical test operating condition was used to evaluate the experimental uncertainties: Water and steam entered two-phase mixer at 0.28 kg/s, 90 °C and 0.025 kg/s, 110 °C respectively, the steam-water flow at the saturated temperature of 104 °C was divided into branch flow of 0.162 kg/s and run flow of 0.143 kg/s at 90 °C, the cooling water enter the condenser at 0.198 kg/s and 10 °C and exit at 65 °C. The pressure changes of the T-junction determined by the regression equations were 1.42 kPa and 2.95 kPa for $\Delta P_{2\text{-}1}$ and $\Delta P_{1\text{-}3}$ respectively.

The uncertainty of the temperature was determined as $\pm 1\%$. The uncertainty of the flow meters were provided by the manufacturer as $\pm 1\%$. The enthalpies of the fluids were determined by the correlations generated from steam-water tables, the uncertainty of the correlations were evaluated as $\pm 1\%$. The uncertainty of the pressure changes consist of the uncertainty of pressure transducer which provided by the manufacturer as $\pm 0.5\%$ and the uncertainty of regression equation which was evaluated as 5%. The uncertainty of void fraction determined by Eqn.(B.16) was 2.3%, however the calibration results showed that the typical error was about 5%. The experimental uncertainties determined using the above equations were summarized as Table 3.1 in Chapter 3.